ASSESSMENTS OF THE THORIUM AND URANIUM FUEL CYCLE IN FAST BREEDER REACTORS AND HIGH TEMPERATURE REACTORS

W. Michael Schikorr

Editor:
Maria Bacher-Helm

December 1979
CP-79-19

INTERNATIONAL INSTITUTE FOR APPLIED SYSTEMS ANALYSIS
A-2361 Laxenburg, Austria

W.M. Schikorr was formerly with the Nuclear Research Center, Karlsruhe, FRG. Now he is with Science Applications, Inc., Palo Alto, Calif., USA.

PREFACE

This assessment was performed between 1973 and 1977 at the Nuclear Research Center Karlsruhe (KFK), F.R.G., and is in line with research work going on at the Energy Systems Program of the International Institute for Applied Systems Analysis (IIASA) at Laxenburg, Austria.

The point of interest was to understand in some detail the capability of a Fast Breeder Reactor (FBR) of a design considered and explored today in producing U233 in the radial blanket, with a view to using this U233 in High Temperature Reactors (HTRs). More specifically, the problem was to look at design changes of FBR cores that would or would not be necessary if a thorium blanket were installed instead of a UO_2 blanket. This investigation was to be complemented by identification of the features of the reactor strategy scenarios that should become possible in this way.

The operation of an FBR/HTR compound based on the breeding capabilities of the FBR can serve to generate not only electricity but also high temperature process heat, under practically no resource supply constraints and thus for a virtually unlimited period of time. Such process heat could facilitate the production of hydrogen or other chemical processes used for energy supply.

The energy studies at IIASA clearly point to the medium- and long-range necessity to apply nuclear power to purposes other than solely electricity. Therefore, the present report should be seen in conjunction with the forthcoming book on "Energy in a Finite World--A Global Systems Analysis" by IIASA's Energy Systems Program reporting in greater depth on the energy systems analysis it has performed. The present study by its very nature equally relates to the work of the Fast Breeder Project of the Nuclear Research Center Karlsruhe.

ACKNOWLEDGMENT

The author wishes to thank Wolf Häfele[1] for his continuous support and patience which made this study possible. Special appreciation is extended to Peter McGrath[2] while at Karlsruhe and Peter Jansen[3] for their corroboration in implementing the nuclear data and computer code systems, E. Teuchert[4] for making available results of burnup calculations on which the HTR assessments in Chapter III are based, and U. Seele[3] for assisting in the performance of the reactor strategy calculations. The task could not have been completed without the editorial effort of M. Bacher-Helm.[1]

[1] International Institute for Applied Systems Analysis, Laxenburg, Austria

[2] formerly Kernforschungszentrum Karlsruhe and now at the Nuclear Regulatory Commission, U.S.A.

[3] Kernforschungszentrum Karlsruhe (KFK), F.R.G.

[4] Kernforschungsanlage Jülich (KFA), F.R.G.

SUMMARY

This assessment focuses on the optimal use of the uranium and thorium nuclear fuel resources in the advanced nuclear reactor types currently under development in several countries, the Fast Breeder Reactor (FBR) and the High Temperature Reactor (HTR). The study has been motivated by the increased need for nuclear power anticipated for the coming decades, and by the apparently limited reserves of nuclear fuels, that is, of economically viable uranium ore (U_3O_8) resources.

The need for nuclear power as a major long-term energy source can be justified by several arguments. Above all, it is absolutely necessary to reduce the world's reliance on fossil fuels (oil), which are not only limited but also confined to a few politically unstable regions. Furthermore, the world's--and especially the third world's--demand for primary and electric energy is foreseen to increase substantially within the next 50 years, making it mandatory for industrialized societies to develop new energy sources besides continuing to exploit fossil fuels. At the present time, nuclear energy seems to be the only technologically viable alternative capable of meeting these large-scale and long-term challenges.

Reliance on uranium ore is currently ascribed to Light Water Reactors (LWRs). These require considerable amounts of U_3O_8 for utilizing the U235 isotope, on which this reactor type relies as fissile fuel. Since uranium ore resources--and thus U235--seem to be finite like fossil fuels, it appears prudent to determine to what extent these resources are used more efficiently in FBRs and HTRs than in LWRs. It is a main goal of this study to show that the development of nuclear power, if continued along the current lines of FBR and HTR development, can lead to a practically self-sustaining large-scale energy supply system offering

the following advantages: this system (1) relies on an essentially inexhaustible fuel resource base, and (2) has the potential of meeting a very significant fraction of all primary and electrical needs for many centuries. Underlying is the assumption that the available U_3O_8 resources are invested expediently in the next few decades, and the fuel logistics between FBRs and HTRs is properly chosen.

This study assesses in detail the fuel utilization characteristics of the uranium ore-*independent* U238/Pu239 and Th232/U233 nuclear fuel cycles in the FBR and in the HTR, both by means of extensive burnup calculations and analytical one-group models. In the case of the HTR, the analysis is extended to the fuel utilization of the U238/U235 and Th232/U235 fuel cycles, which are currently viable but uranium-ore dependent; these serve as reference cases for the U_3O_8-independent U238/Pu239 and Th232/U233 fuel cycles.

The optimal fuel cycle logistics of a symbiotic reactor system consisting of FBRs and HTRs is specified and analyzed. The results obtained are also applicable, in principle, to any other fast-thermal reactor system with either LWRs or CANDUs as thermal reactors. The incentive to analyze the fuel economy of such a fast-thermal reactor system lies in its capability of supporting a large-scale energy supply system for several centuries on the basis of the abounding U238 and Th232 fertile isotopes. In the case of an FBR/HTR system, the FBRs could meet future electricity requirements and the HTRs future process heat requirements. In the case of an FBR/LWR system on the other hand, FBRs, located on socalled energy islands or fuel cycle parks, could supply regionally operating LWRs with denatured fissile fuel. Within the frame of these perspectives, such a fast-thermal reactor system can be compared to other essentially inexhaustible energy sources, solar energy and nuclear fusion.

None of these practically resource-independent energy systems can be expected to be fully established and deployed on a large scale earlier than several decades after the turn of the century. In the case of nuclear power, the interim period, referred to as the transition phase, thus necessarily relies on LWRs presently deployable, which consume large quantities of U_3O_8. But the availability and accessibility of this economically viable uranium resource seems limited. This nonrenewable resource of nuclear fuel, which can be considered a one-time endowment, should therefore be invested expediently, namely in the establishment of a self-sustaining energy system. It is thus appropriate to assess the uranium ore requirements of such a system for the case of a typical industrialized country which is most likely to increasingly rely on nuclear power.

For the purpose of comparison, an assessment is made of three different reactor strategy scenarios focusing on different reactor tpyes, in order to determine their long-range U_3O_8 commitments. One scenario relies predominantly on LWRs, another on HTRs, and a third, considered the reference scenario, emphasizes FBRs in conjunction with HTRs and LWRs. In this scenario, the

reactor system converges into a symbiotic FBR/HTR system near the end of the transition period. The influence on U_3O_8 demand of various fast breeder designs, such as (Liquid-Metal) Sodium-Cooled Fast Breeder Reactors (LMFBRs) with oxide or carbide fuel, or Gas-Cooled Fast Breeder Reactors (GCFBRs), is also addressed within the FBR/HTR scenario. The potential of HTR designs with high conversion ratios (i.e. CR = 0.85) is also analyzed.

The uranium ore demands associated with these scenarios are determined and discussed for a wide range of possible nuclear energy demand forecasts for an industrialized region such as the DeBeNeLux countries.

The results of the reactor physics and reactor strategy calculations are described in *Chapters II* to *V*. *Chapter I* summarizes the mathematical background of the FBR breeding ratios as well as HTR conversion ratios, which are derived in the appendix to that chapter. The rest of the appendices elaborate on FBR reaction rates, the fissile fission fraction distribution in the HTR, fissile fuel utilization in various fissile fuel cycles, FBR self-supply in an FBR/HTR system in steady state and the growth rate of such an expanding system, as well as the LWR/FBR fissile fuel balance in the transition phase.

According to the fast breeder reactor physics assessments in *Chapter II*, utilization of the Th232/U233 fuel cycle is limited to the FBR blanket regions, and preferably to the radial blanket. Using Th232 in the FBR core region--as has been suggested for the socalled proliferation resistant fuel cycles--reduces the fertile fission contribution such that the global breeding ratio BR_N (for all regions n) of present oxide-fueled LMFBR designs ($BR_N \simeq 1.20$) decreases to less than 1.0, which would make these LMFBRs nonbreeding reactors. By contrast, Th232 causes only minor changes in the relevant FBR parameters if it is used as fertile breeding fuel in the blanket regions. The most pronounced effect is a noticeable redistribution of the region-dependent breeding ratios BR_n and breeding gains g_n as well as as slight decrease in the global breeding ratio.

Compared to the reference UO_2 radial blanket, the breeding characteristics of a Th-metal (Th^m) radial blanket as well as of a ThO_2 radial blanket are found to be superior. The U232 and Pa233 isotopes associated with the thorium cycle do not have any significant effect on the performance of the FBR if thorium is used in the blanket region. The sodium void coefficient is somewhat ($\sim 10\%$) increased for the thorium blankets. This can be ascribed to the larger fissile fuel enrichment in the core zone adjacent to the radial blanket (i.e. a fissile fuel inventory larger by 1.2% for ThO_2 and by 2.37% for Th^m).

There is, however, no particular incentive to recycle the U233 bred in the radial blanket into the FBR core region, where U233 has slightly less favorable nuclear characteristics than Pu239. The use of Th232 as fertile radial blanket fuel is thus contingent on the efficient utilization of U233 bred in other reactor types.

In the context of this FBR assessment, an analysis is made, involving considerable detail, of the effects of various FBR designs on parameters determining the global breeding ratio. The intrinsic difference between oxide- or carbide-fueled, and sodium- or gas-cooled designs, and large or small reactor units is demonstrated to be primarily due to their widely differing fast-fission contributions. BR_N is thus adversely affected by either a decrease in fast fission by way of spectrum softening, shifting breeding into the blanket regions (FBRs with small cores, i.e. small power units), or substitution of Th232 for U238 as fertile isotope in the core region. Only by use of the U238/Pu239 cycle in the core region can breeding ratios larger than 1.0 be assured for current LMFBR designs.

The fissile fuel cycle assessments of the HTR in *Chapter III* demonstrate that the HTR attains its full potential for high conversion ratios (CR $\geq$ 0.90) when it is supplied with FBR-bred U233. In this context, it is also shown extensively why the thorium cycle exhibits a better fuel utilization (i.e. CR is larger by about 0.20 than for the uranium cycle) under the assumption that the U233 converted in the HTR can be recycled, i.e. if the corresponding thorium reprocessing facilities are available.

Without reprocessing, fuel utilization in the thorium cycle is only insignificantly better than in the uranium cycle. About equal amounts of U_3O_8 are required as makeup fuel in both cycles, and the U_3O_8 demand of HTRs is similar to that of LWRs. Under these constraints, there is no incentive to decrease the fuel burnup in HTRs since this would result in a larger annual U_3O_8 demand. The HTR conversion ratio is limited to about 0.65 in this case without reprocessing.

If reprocessing facilities are assumed to be available, the thorium cycle is clearly advantageous over the uranium cycle. In addition, the U_3O_8 demand can be reduced significantly (by $\sim$ 50% or more) if the HTR fuel burnup is decreased to approximately 30,000 MWd/t. Conversion ratios as high as 0.85 seem attainable with U235 as makeup fuel.

Optimal thermal reactor fuel utilization is achieved if this U235 makeup in the thorium cycle can be replaced by U233 makeup. Only very small quantities of U233 are necessary if the fuel burnup is kept low ($\sim$30,000 MWd/t). This, of course, presupposes fuel processing. Conversion ratios of up to 0.95 seem attainable under these circumstances.

The highest HTR conversion ratios are therefore attained under the following conditions:

-- utilization of the thorium cycle;
-- recycling of U233 converted in the HTR; this requires Th reprocessing and fabrication facilities;
-- decreasing the fuel burnups currently optimized in terms of fuel cycle costs from 100,000 MWd/t to values of 20,000-30,000 MWd/t, to be optimized in terms of fissile fuel utilization;

-- use of U233 makeup supplied by an external source (e.g. FBR).

Good HTR fuel utilization thus depends also on the availability of Th reprocessing facilities.

These reactor physics assessments lead to the discussion in *Chapters IV* and *V* on fuel utilization of reactor systems.

Chapter IV demonstrates that the by far most favorable fuel utilization of a symbiotic fast-thermal (FBR/HTR) reactor system with a closed fissile fuel balance (i.e. a system independent of U235 requirements) is achieved by utilizing both the uranium cycle and the thorium cycle. For the FBR/HTR system, this is identified as the mixed fuel cycle /U-Th/, which assumes the use of the thorium cycle in the thermal reactor (HTR) and in the FBR radial blanket region, and the uranium cycle in the FBR core and axial blanket regions. In the other feasible system fuel cycle, called the uranium cycle /U/, the thorium cycle is not used at all, and both reactor types exclusively rely on the uranium cycle. The advantage of the /U-Th/ cycle over the /U/ cycle is significant, the difference in fuel utilization being a factor of 2 to 4, depending on HTR fuel burnup and FBR design.

In a nonexpanding or no-growth FBR/HTR system, the FBR and HTR fissile inventories are of little significance. Instead, high breeding ratios and/or low HTR burnups are important. An FBR with a high breeding ratio (BR_N = 1.4) can, for example, supply up to three equivalent HTRs with fissile fuel.

In an expanding FBR/HTR system, a system growth rate α_S of up to 5%/yr is possible with appropriate FBR and HTR designs. The influence of fissile fuel inventories is considerable. FBRs with medium size inventories and average breeding ratios are generally to be preferred over FBRs with high breeding ratios and high inventories.

Chapter V assesses the U_3O_8 requirements during the transition phase for three different reactor strategy scenarios, each focusing on a particular reactor type. The reference scenario relies on FBRs, with both LWRs and HTRs being deployed in the transition phase. This LWR/HTR//FBR reactor system converges into the U_3O_8-independent FBR/HTR system in the asymptotic phase. The second scenario is primarily based on LWRs and has some HTRs, and the third almost exclusively uses HTRs and some LWRs in the transition phase; both of these scenarios are without FBRs.

In the context of the HTR scenario, the influence of optimal HTR fuel utilization (use of the thorium cycle, availability of thorium reprocessing facilities, low fuel burnup at 30,000 MWd/t, i.e. CR $\simeq$ 0.85) on U_3O_8 requirements is assessed in order to compare it with the FBR scenario.

In the FBR scenario, different FBR strategies are also analyzed in order to assess the influence of different FBR designs on future U_3O_8 requirements. These FBR strategies are determined in terms of FBR fissile fuel cycle inventory and breeding gains.

Future uranium ore requirements for these three reactor strategy scenarios were calculated for a high, a medium, and a low nuclear energy demand forecast. The U_3O_8 requirements for the various scenarios and strategies within the scenarios are observed to differ only quantitatively but *not* qualitatively for the various demand forecasts.

During the early period of the transition phase, 1970-2000, all three scenarios exhibit substantial and very similar uranium ore demands. These requirements, cumulative as well as annual, do not differ significantly before 2000-2010, until the reactor type under consideration assumes a significant fraction of the total reactor capacity. Since the market penetration of any new energy system or reactor type takes on the order of several decades, the differences between the reactor scenarios and reactor types cannot be expected to become significant before 2010-2020. This is especially demonstrated by a comparison of the U_3O_8 requirements associated with some FBR designs in the FBR scenario with the HTR scenario with optimal fuel utilization. Accordingly, no significant difference is to be expected between the FBR and HTR scenarios with respect to their U_3O_8 demands if the time horizon is limited to about 2020. Under these constraints, even the LWR scenario shows comparable results.

The differences in U_3O_8 requirements between the scenarios and between the strategies within the scenarios become transparent if the time horizon is extended to 2050, or to about 40 to 50 years after commercial introduction of the advanced reactor types.

The salient, and intrinsic, difference between the FBR and HTR scenarios is made clear by comparison of their *annual* uranium ore demands.

Between 2020-2050, the annual U_3O_8 demand of most FBR strategies, depending on the reactor design-specific fissile fuel cycle inventory and breeding gains, decreases to zero, thus limiting the cumulative U_3O_8 requirements of this strategy to a finite value. In contrast, the annual U_3O_8 demand does not decrease to zero even for the the most optimal HTR strategy. In the HTR scenario, the annual demand *never* approaches zero. This is indicative of a continuous reliance and dependence on the availability of U_3O_8 resources in this scenario until the time when FBRs are introduced to replace some HTRs. Any scenario relying exclusively on HTRs or, for that matter, any thermal reactor type, therefore requires a practically *unlimited* U_3O_8 supply or resource base. Adopting an HTR strategy would therefore merely imply substitution of a long-term U_3O_8 dependence for the current oil dependence.

The largest U_3O_8 resources are clearly required for the LWR scenario. Exclusive reliance on LWRs would deplete present nonrenewable U_3O_8 reserves within a few decades. Adopting such a strategy forecloses the use of nuclear power as a long-range option, since by then the nuclear fuel base necessary for establishing a self-sustaining reactor system will have been consumed.

The deployment of FBRs with socalled proliferation resistant fuel cycles, i.e. with Th232 in the core region, exhibits characteristics very similar to those of the HTR scenario, in that a continuous annual U_3O_8 demand would be needed to sustain the system beyond the year 2050. The only feasible fuel logistics between fast and thermal reactors is to use the U238/Pu239 cycle in the FBR core region and Th232 in the radial blanket. Only in this manner can the cumulative uranium ore requirement be held finite.

In principle, the cumulative U_3O_8 demand can only be limited by the deployment of FBRs. Different FBR designs have different uranium ore requirements. It is shown in this context that the FBR doubling time is not the dominant parameter during the FBR introduction phase, when the deployment of FBRs is coupled to the fissile plutonium production in LWRs. Rather, it is the FBR fissile inventory. The breeding ratio or breeding gain becomes relevant 10 to 20 years after FBR introduction. Generally, FBRs of low fissile inventories and high breeding gains allow considerable savings in U_3O_8 (in this case 0.5-1.0 million tons). In comparison to FBRs with high breeding ratios and high inventories, FBRs with medium breeding ratios but medium inventories are preferable.

These reactor strategy assessments confirm that the complementary deployment of FBRs and HTRs in the transition phase can lead to a self-sustaining FBR/HTR reactor system within a period of 40 to 60 years. The quantities of U_3O_8 necessary for such a system to become operational (referred to as the *critical mass* of the FBR/HTR system) essentially depend on the choice of FBR design (gas-cooled fast breeder reactor, carbide-fueled LMFBR, etc.), the fuel or fissile fuel cycle logistics between FBRs and HTRs (uranium or thorium cycles, recycling or nonrecycling of the bred fissile isotopes), and HTR fuel burnup. The U_3O_8 reserves currently available are not sufficient to allow a significant delay in establishing such a self-sustaining reactor system, lest the option of using nuclear energy as a long-range energy supply system should be foreclosed. Considerable quantities of uranium ore can be saved by strategically favorable designs of both FBRs and HTRs. Large-scale deployment of both reactor types assures optimum utilization of the thorium and uranium reserves available, provided the reactors have a closed fissile fuel balance and provided their fissile fuel cycle logistics is coupled in the manner assessed in this investigation.

CONTENTS

CHAPTER I. EQUATIONS FOR THE BREEDING RATIOS OF FBRs AND FOR THE CONVERSION RATIOS OF HTRs AND OTHER THERMAL REACTORS

I.1. INTRODUCTION

The breeding ratio BR of the FBR and the conversion ratio CR of the HTR are by far the most important parameters as regards the fuel utilization of these reactors. These two parameters are indicative of the fissile fuel requirements of these reactor types, reflecting their needs for nuclear fuel, e.g. uranium ore. Since BR and CR are viewed as the major parameters of this study, they are discussed beforehand in some detail.

In this chapter relations are derived which are frequently referred to in the subsequent chapters. Some of them can be found in similar form in the literature (Adkins 1972), but most of the derivations are developed and introduced here to meet the special requirements of this assessment.

In the derivations of the relevant equations, a clear distinction is made between equations pertaining to multiregion reactors whose contribution of fast fission is significant, and equations for single-region reactors without significant fast fission. The former types can be associated with FBRs, and the latter with thermal reactors, such as HTRs, LWRs, etc.

Differentiation is also made between incore and excore relations. The incore relations, limited to basic nuclear parameters, are useful for reactor physics assessments. The excore (or out-of-core) relations also include parameters taking into consideration the characteristics of excore fuel cycle activities, such as reprocessing and fabrication of reactor fuel.

The incore relations are used in the reactor physics analyses of Chapters II and III, and the excore relations in Chapters III to V.

Some further relations of the breeding ratio BR_N and the conversion ratio CR are introduced that are based on parameters of a more universal applicability. These equations are particularly suitable for comparisons of different reactor designs as well as for parametric sensitivity studies.

I.2. INCORE PARAMETERS OF A MULTIREGION REACTOR WITH FAST FISSION (e.g. FBR)

Assessment of the impact of different fertile and fissile isotopes in the various reactor regions[1] of an FBR requires a detailed description of the breeding characteristics of each region. This is usually accomplished by consideration of the reaction rates of each region.

I.2.a. The Global Breeding Ratio BR_N and the Region Breeding Ratio BR_n

In FBRs of current design, the core region is surrounded by both an axial blanket region and a radial blanket region. The core region is fueled with enriched fuel[2], and the axial and radial blanket regions are fueled with fertile fuel. Such reactors made up of distinctly different fuel regions are referred to as multiregion reactors. The global breeding ratio BR_N of such a multiregion reactor is normally given by

$$BR_N = \frac{\sum_{n}^{N}\sum_{j}^{J}\sum_{g}^{G} N^j(n)\sigma_c^j(g,n)\,\phi(g,n)\cdot V_n}{\sum_{n}^{N}\sum_{i}^{I}\sum_{g}^{G} N^i(n)\sigma_a^i(g,n)\,\phi(g,n)\cdot V_n}\ ; \qquad \text{(I-1)}$$

---

[1] The following designations are adopted here: reactor regions are global regions of similar nuclear characteristics. The core, the axial blanket, and the radial blanket of an FBR are referred to as regions. Each region can be subdivided into zones; the core region is usually partitioned into two or more zones.

[2] enriched fuel is a mixture of fertile and fissile fuels.

N represents the total number of regions n, G the total number of energy-groups g into which the continuous neutron spectrum is partitioned, J the total number of fertile isotopes j, and I the total number of fissile isotopes i. The following isotopes are usually referred to as fissile and fertile isotopes:

$$i = \{U233,\ U235,\ Pu239,\ Pu241\}$$

$$j = \{Th232,\ U234,\ U238,\ Pu240\}\ .$$

$\sigma_x^j(g,n)$ are few-group neutron capture (c) and absorption (a) cross sections of energy group g in region n, $\phi(g,n)$ is the corresponding neutron flux, N^y the particle density of isotopes i or j, and V_n the total volume of region n. Equation (I-1) is utilized in multidimensional burnup calculations as were performed for the assessments in Chapter II.

Equation (I-1) can be reduced by collapsing the G energy groups into a one-energy group, such that

$$BR_N = \frac{c_N^J}{a_N^I} = \frac{\sum_n^N \sum_j^J c_n^j}{\sum_n^N \sum_i^I a_n^i}\ , \qquad \text{(I-2)}$$

where a_N^i is the *absolute* absorption reaction rates defined as

$$a_n^i \equiv \sum_g^G N^i(n) \cdot \sigma_a^i(g,n)\ \phi(g,n) \cdot V_n\ , \qquad \text{(I-3)}$$

with c_N^j being similarly defined.

Equations (I-1) and (I-2) describe the ratio of fissile fuel generated due to neutron capture c^j in the fertile fuel to the fissile fuel lost due to neutron absorption a^i in fissile isotopes i.

It is usually more convenient to consider *normalized* reaction rates instead of the absolute reaction rates used in Equation (I-3). Normalization is accomplished by equating all neutron losses throughout the reactor to unity, i.e.

$$A_N^I + A_N^J + P_N \equiv 1.0 \quad , \tag{I-4}$$

where A_N^I represents the normalized total absorption rate of all I fissile isotopes in all N reactor regions. Likewise, A_N^J represents the corresponding normalized total absorption rate of all J fertile isotopes, and P_N is defined as the sum of all fractional parasitic neutron losses, such that

$$P_N = L + FP + St + M + C + R \quad ; \tag{I-5}$$

L is the parasitic neutron leakage loss (reflector leakage); FP the parasitic neutron absorption in the fission products, St stands for losses in the structural materials, M in the moderator, and C in the control rods; R represents a remainder of absorptions in parasitic actinides, such as Np237, Pu242, Pa233, etc. A_N^I, A_N^J, and P_N are all normalized in the following manner:

$$A_N^I = \frac{a_N^I}{a_N^I + a_N^J + p_N} \quad , \tag{I-6}$$

p_N being the nonnormalized parasitic neutron losses. The pertinent Equation (I-2) can now be expressed in terms of normalized reaction rates as

$$BR_N = \frac{C_N^J}{A_N^J} = \frac{\sum_n^N \sum_j^J C_n^j}{\sum_n^N \sum_i^I A_n^i} \quad . \tag{I-7}$$

In order to maintain criticality of the reactor, Equation (I-4), describing the sum of all neutron losses, must be equated to the neutron generation. For an exactly critical reactor, in this case an FBR, the equation describing the production of neutrons is then

$$(\nu F)_N^I + (\nu F)_N^J \equiv 1.0 \quad , \tag{I-8}$$

where $(\nu F)_N^I$ represents the normalized neutron production rate as a result of all fissile fissions, and $(\nu F)_N^J$ the neutron production due to all fertile fissions (fertile fissions are also referred to as fast fissions).

Equations (I-2) and (I-7), which are of importance for burnup calculations, can be used either as *point-in-time* relations, which describe the ratio of reaction rates at any given time in any burnup cycle, or as burnup cycle-*averaged* relations that describe the reaction rates averaged over one or more burnup cycles.

The breeding ratio of a given reactor region n [3] can then be written as

$$BR_n = \frac{C_n^J}{A_N^I} = \frac{\sum_j^J C_n^j}{\sum_n^N \sum_i^I A_n^i} \quad . \tag{I-9}$$

Other than in Equation (I-7), the capture rate in Equation (I-9) is limited to region n. It can be shown, of course, that the global breeding ratio BR_N is the sum of the region breeding ratios BR_n, such that

---

[3] n can also be any zone of a region.

$$BR_N = \sum_n^N BR_n \quad . \tag{I-10}$$

I.2.b. The Region Conversion Ratio KR_n

Analogously to the region breeding ratio BR_n, a region conversion ratio KR_n can be defined for each individual region as

$$KR_n = \frac{C_n^J}{A_n^I} = \frac{\sum_j^J C_n^i}{\sum_i^I A_n^i} \quad . \tag{I-11}$$

The difference between Equation (I-11) and Equation (I-9) is in the fissile absorption rate, which in Equation (I-11) is restricted to the particular region n.

The relationship between KR_n and BR_N can be easily shown to be the following:

$$BR_n = \frac{A_n^I}{A_N^I} KR_n \quad , \tag{I-12}$$

$$BR_N = \sum_n^N \left[\frac{A_n^I}{A_N^I} KR_n \right] \quad . \tag{I-13}$$

I.2.c. The Global Breeding Ratio BR_N Expressed in Terms of Global Nuclear Parameters

The previous equations are given in terms of reaction rates, which are normally determined by detailed criticality and/or burnup calculations. Since such calculations cannot always be performed, it is desirable to develop an equation of the global breeding ratio BR_N in terms of more fundamental and universal parameters. Okrent (1964) has suggested such an equation, given as

$$BR_N = \frac{(\nu-1) - \alpha - P - L + (\nu'-1)F}{1+\alpha} \quad , \qquad (I\text{-}14)$$

with α as the capture-to-fission ratio of the fissile fuel, and ν and ν' as the neutrons released per fission in the fissile and fertile materials, respectively. From a physics point of view, this equation provides more information about the influence of the relevant nuclear parameters on BR_N, assuming the behavior of the parameters to be known. The applicability of this equation is, however, limited by the unfavorable normalization of the variables P, L, etc., which in this case are normalized to the neutron absorption in the fissile fuel.

A similar equation is derived in Appendix I.A:

$$BR_N = \left(\eta_N^I + \frac{(\nu F)_N^J}{A_N^I}\right)\left[1-(P_N+F_N^J)\right] - 1 \quad , \qquad (I\text{-}15)$$

with $\eta_N^I = (\nu F)_N^I / A_N^I$. The parameters in this equation are normalized according to Equations (I-4) and (I-8); they are referred to as *global nuclear parameters*. These parameters, which are more widely applicable than those in Equation (I-14), can be used as reference parameters for comparing FBRs of different designs. Equation (I-15) is convenient for parametric sensitivity studies because it allows one to assess the effect of design changes on these parameters, and thus on BR_N. For example, the influence on BR_N of increasing the radial blanket thickness can be easily determined, since an additional row of blanket elements can be shown to affect primarily P. A reliable estimate of BR_N can be obtained this way without detailed burnup calculations. A region-dependent equation similar to Equation (I-15) is derived in Appendix I.A.2.

I.2.d. The Global Breeding Gain G_N and the Region Breeding Gain G_n

The breeding ratios defined above refer to the ratio of fissile fuel produced by means of fertile capture to the fissile

fuel lost as a result of neutron absorption. A more relevant parameter as regards the fissile fuel utilization of the reactor (FBR) is the breeding gain G that describes the actual surplus of fissile fuel produced.

Two definitions of the breeding gain should be differentiated. According to the standard definition, the breeding gain is normalized to the total fissile fuel consumed, i.e.

$$BG = \frac{\text{Excess fissile material produced}}{\text{Total fissile material consumed}} \quad .$$

The definition more relevant in this context (Adkins 1972) is the breeding gain normalized to the fission rate, or the total power produced:

$$G = \frac{\text{Excess fissile material produced}}{\text{Power of reactor produced (fission rate)}} \quad .$$

In terms of reaction rates, BG_N is given by

$$BG_N = \frac{C_N^J - A_N^I}{A_N^I} = (BR_N - 1) \quad , \tag{I-16}$$

and the global breeding gain relevant in this context as

$$G_N = \frac{C_N^J - A_N^I}{F_N^{IJ}} \quad , \tag{I-17}$$

with

$$F_N^{IJ} \equiv F_N^I + F_N^J \quad . \tag{I-18}$$

In general, reference to a surplus, or breeding gain, of fissile fuel is only made if $G_N > 0$, or $C_N^J > A_N^I$. A more explicit derivation of G_N is derived in Appendix I.B.1:

$$G_N = (BR_N - 1) \sum_n^N \sum_i^I \left(\frac{F_n^i}{F_N^{IJ}} \right) (1+\alpha)_n^i \quad . \tag{I-19}$$

This equation can be expressed in the more useful form in terms of the fundamental *global neutron parameters*.

$$G_N = (BR_N - 1)\ (1-\varepsilon_N)\ (1+\alpha)_N^I \quad ; \tag{I-20}$$

ε_N and $(1+\alpha)_N^I$ are derived in Appendix I.B, Equations (I.B-9) to (I.B-11).

Analogously to the region-related breeding ratio BR_n and the conversion ratio KR_n, a region-related breeding gain G_n can be derived (Appendix I.B.3) such that

$$G_n = BR_n \sum_n^N \sum_i^I \frac{F_n^i}{F_n^{IJ}} (1+\alpha)_n^i - \sum_i^I \frac{F_n^i}{F_n^{IJ}} (1+\alpha)_n^i \quad , \tag{I-21}$$

or in the more useful form as

$$G_n = BR_n\ (1-\varepsilon_N)\ (1+\alpha)_N^I - (1-\varepsilon_n)\,\delta_n (1+\alpha)_n^I \quad ; \tag{I-22}$$

ε_n, δ_n, and $(1+\alpha)_n^I$ are defined in Appendix I.B.2. Equation (I-22) is particularly significant for the radial blanket assessments in Chapter II. Moreover, it can be shown that

$$G_N = \sum_n^N G_n \quad . \tag{I-23}$$

The breeding gain g_m of several regions m can be derived similarly as g_n, see Appendix I.B.2.

I.3. INCORE PARAMETERS OF A SINGLE-REGION REACTOR WITHOUT FAST FISSION (e.g. HTR, LWR)

The equations referred to in Section I.2 relate to multi-region reactors with fast fission, e.g. the FBR. Similar relations can be derived for the HTR and/or the LWR. These reactor types differ from the FBR in the following two ways:

-- Both the HTR and the LWR can be described by means of single-region equations, i.e. $N = 1$.
-- Fast fission in the HTR and/or LWR does not make any significant contribution to the overall neutron production, i.e. $(\nu F)^J \simeq 0$.

If these properties are taken into account, the relations in Section I.2 can be reduced to the equations discussed in the following. Reactor types with such properties normally exhibit breeding or conversion ratios of less than 1.0. Therefore, it is convenient to introduce the designation CR for the conversion ratios of such reactor types, in order to differentiate them clearly from the region dependent FBR conversion ratios KR_n, which were defined in Equation (I-11).

I.3.a. The Conversion Ratio CR

The conversion ratio is expressed in terms of reaction rates, in a similar way as is the global breeeding ratio in Equations (I-2) and (I-7):

$$CR = \frac{c_N^J}{a_N^I} = \frac{C_N^J}{A_N^I} \quad ; \qquad \text{(I-24)}$$

in the case of thermal reactors C_N^J is usually smaller than A_N^I. CR may again be interpreted as a point-in-time or burnup cycle-averaged relation.

A more universal equation of CR in terms of the fundamental global nuclear parameters, similar to Equation (I-15) for the FBR, is independently derived in Appendix I.C.1:

$$CR = \eta^I (1-P) - 1 \quad , \tag{I-25}$$

with

$$\eta^I = \frac{\nu^I}{(1+\alpha)^I} \quad , \tag{I-26}$$

$$(1+\alpha)^I = \sum_i^I \left(\frac{F^i}{F^I}\right) (1+\alpha)^i \quad , \tag{I-27}$$

$$\nu^I = \sum_i^I \left(\frac{F^i}{F^I}\right) \nu^i \quad . \tag{I-28}$$

P is the total parasitic neutron loss defined in Equation (I-5). One could also have derived Equation (I-25) from Equation (I-15) setting $F^J = 0$. Equation (I-25) is essential to the HTR fuel cycle assessments described in Chapter III.

I.3.b. The Fissile Fuel Demand D

In general, one only speaks of a breeding gain or surplus of fissile fuel if BR_N or CR is larger than 1.0. In HTRs or LWRs, the conversion ratio is normally less than 1.0 and, therefore, a demand for fissile fuel is associated with these reactors. This demand D, defined similarly as gain G_N, is normalized with respect to the total fission rate:

Demand D:

$$D = \frac{\text{Demand for fissile fuel}}{\text{Total fission rate in the reactor}} \quad ,$$

or, as is shown in greater detail in Appendix I.C.2, as

$$D = \frac{A^I - C^J}{F^I} \quad , \tag{I-29}$$

or

$$D = (1 - CR) \cdot (1 + \alpha)^{I} \quad , \qquad (I\text{-}30)$$

with $(1 + \alpha)^{I}$ defined in Equation (I-27).

I.4. FBR AND HTR EXCORE PARAMETERS

So far the relevant relations have been derived in terms of neutron reaction rates and global nuclear and neutron parameters. These equations are generally used to assess the nuclear characteristics of different reactor types.

In order to determine the actual mass flow of fissile fuel into and out of the reactor, the relevant equations of the previous sections must be multiplied by a factor W, the fissile mass fissioned per unit energy released. The above equations are thereby transformed into mass balance equations. In addition, the losses of fissile fuel incurred in the reprocessing and fabrication steps of the excore reactor fuel cycle must also be taken into account.

I.4.a. The Breeding Gains g_N, g_n, g_N^V, and g_n^V of the FBR

The incore breeding gain, expressed in terms of excess fissile fuel mass per unit energy g_N, is obtained by multiplying G_N by W_N^F, such that:

$$g_N = G_N W_N^F = (BR_N - 1)\ (1-\varepsilon_N)\ (1+\alpha)_N^I\ W_N^F \quad . \qquad (I\text{-}31)$$

W_N^F is given by

$$W_N^F = \{\sum_n^N Q_n^{IJ} \cdot \delta_n\}^{-1}, \text{ and } Q_n^{IJ} = \frac{Q_n^I F_n^I + Q_n^J F_n^J}{F_n^I + F_n^J} \quad , \qquad (I\text{-}32)$$

where Q_n^I is the energy released per unit weight of the fissile isotopes I in region n, and δ_n is defined in Appendix I.B.2 as the power fraction of region n.

In order to account for the fissile fuel losses incurred in the excore activities one must consider the fissile fuel incore inventories I and the fuel residence time T. If the FBR excore loss fraction is designated V^F, the global excore breeding gain g_N^V becomes

$$g_N^V = g_N(1-V^F) - V^F \sum_n^N \left(\frac{I_n}{T_n}\right) \quad , \tag{I-33}$$

with I_n being the fissile inventory in region n, and T_n the corresponding residence time.

The excore breeding gain of a single region n or of several regions m can be shown to be

$$g_n^V = g_n(1-V^F) - \frac{I_n V^F}{T_n} \quad , \tag{I-34}$$

with g_n given by Equation (I-22) and the corresponding form of Equation (I-31). Likewise,

$$g_m^V = g_m(1-V^F) - \sum_n^m \left(\frac{I_n V^F}{T_n}\right) \quad , \tag{I-35}$$

where $g_m = \sum_n^m g_n$.

I.4.b. The Fissile Fuel Demands d and d^V of the HTR

As with the FBR, the influence of the (reprocessing, refabrication) losses in the excore cycle must also be taken into consideration in the case of the HTR. The incore demand for fissile fuel normalized to the power generated is given by

$$d = D \cdot W_H = (1 - CR)(1 + \alpha)^I W_H^I \quad , \tag{I-36}$$

where W_H is given similarly as in Equation (I-32) for N = 1, and D by Equation (I-30). If excore losses V^H are considered, the result is

$$d^V = (1 - CR)\ (1 + \alpha)^I\ W_H^I + \frac{I_H \cdot V^H}{T_H} \quad , \qquad \text{(I-37)}$$

where d^V is the *excore fissile fuel* demand of the HTR after deduction of reprocessing and other losses.

These mass balance equations are particularly important in Chapter IV, in which the fuel utilization of a symbiotic FBR/HTR system is analysed, and for Chapter V, determining the uranium ore demand for various reactor strategy scenarios.

CHAPTER II. THORIUM IN THE FBR

II.1. INTRODUCTION

The goal of fast breeder reactor (FBR) development is the implementation of an economic, safe, and environmentally acceptable energy source that provides a practically inexhaustible energy supply by optimum utilization of the uranium resources available. Among all the fission reactors currently under development and consideration, only the FBR offers the prospect of serving as a long-range, inexhaustible energy supply system. By means of the breeding process, the FBR produces more fissile fuel than it consumes while generating power. This excess fissile fuel can then be used either as initial fissile fuel inventory for starting up additional FBRs, or as fissile fuel supply for other, nonbreeding, reactor types.

Early in the development of FBRs it was recognized that the use of the uranium cycle (U238/Pu239) in the FBR is clearly superior to that of the thorium cycle (Th232/U233) as regards fissile and fertile fuel utilization. Such considerations have led to the present FBR design whose core region is fueled with the (fertile) U238 and (fissile) Pu239 isotopes and whose axial and radial blanket regions are both fueled with U238. The fuel materials chosen are PuO_2/UO_2 and UO_2, respectively.

This chapter serves to assess the performance of an FBR in which the fertile isotope U238 in the radial blanket is replaced by the fertile isotope Th232. The fuels in the core region (PuO_2/UO_2) and in the axial blanket region (UO_2) are assumed to remain unchanged, and the fuel material for the radial blanket is assumed to be either ThO_2 or Th^m (thorium metal). The differences between these radial blanket configurations are compared to the UO_2 blanket, and their impact on the performance of the FBR is examined with respect to the global breeding ratio, the

breeding characteristics of the radial blankets, the fissile fuel inventory, the sodium void coefficient, and other parameters pertaining to reactor operation.

The relative merits of using either the U238/Pu239 cycle or the Th232/U233 cycle in the FBR were assessed in a number of earlier investigations. (They include studies by Loewenstein and Okrent 1958, Okrent et al. 1965, Hankel et al. 1962, Loewenstein and Blumenthal 1965, Allen et al. 1966, and Sofer et al. 1963.) Their main focus was on the use of the Th232/U233 cycle in the core zones. One of the earliest studies on this topic by Loewenstein and Okrent (1958) considered small metallic spherical reactor cores, and the breeding ratios calculated were 1.2 to 1.4 for the thorium cycle and 1.4 to 1.7 for the uranium cycle. In a later study with revised cross sections Okrent et.al. (1965) showed that, with regard to the breeding ratio, the thorium cycle was even more disadvantageous than the uranium cycle.

Hankel et al. (1962) conducted an extensive investigation into the use of Th232/U233 in the FBR. It became clear from this study that the shortest doubling time and the lowest fuel cycle costs were to be achieved with carbide fuel. The results, among others, were the following:

-- Shorter doubling times are obtained with the U238/Pu239 cycle.
-- The fuel cycle costs are lower with the U238/Pu239 cycle.
-- The sodium void coefficient is negative for the Th232/U233 cycle, but positive for the U238/Pu239 cycle.
-- The Th232/U233 cycle requires at least 50% more excess reactivity than the uranium cycle.

Loewenstein and Blumenthal (1965) and Allen et al. (1966) emphasized the improved safety coefficients arising from the use of thorium in the central zones of the core of large LMFBRs. This advantage was ascribed to the lower sodium void coefficient with thorium in the core zones.

Sofer et al. (1963) conducted a detailed study stressing the safety aspects of the thorium cycle for a carbide-fueled system. They pointed out the following problems:

-- the increase in reactivity in the core after shutdown due to the decay of Pa233 to U233,
-- the smaller fraction of delayed neutrons for the thorium system (0.003 as compared to 0.004 for the U238/Pu239 cycle), which is explained by the significantly lower contribution of fast fission in Th232,
-- the larger excess reactivity requirement in the core region, which is due to the delay of U233 formation (the half-life of Pa233 is 27.4 days).

All these assessments of the use of the Th232/U233 cycle in the FBR core region led to the conclusion that, due to its higher fissile inventory and much lower breeding ratio, the thorium cycle is considerably less attractive for the FBR than the uranium cycle. For current LMFBR designs, the global breeding ratio BR_N would become less than 1.0. These studies had been mainly motivated by the lower sodium void coefficient attainable with the thorium cycle.

A number of Soviet investigations (Leipunskii et al. 1965 and 1971, Batyrebekov et al. 1964) considered a mixed uranium/thorium cycle in FBR core zones. Leipunskii et al. (1965) optimized an LMFBR using Th232 as fertile fuel in the radial blanket and a mixture of Pu239, U233, and U238 in the core zones. In the authors' opinion, the breeding ratio of such a system approaches that of a U238/Pu239 system. Their calculations also showed a relatively low U232 buildup in the blanket region. (U232 is an undesired by-product since it leads to considerable shielding problems in U233 refabrication.)

Batyrebekov et al. (1964) used BR-1 experiments to study the contribution of an infinitely thick thorium-metal blanket to the breeding ratio. Calculations showed that the breeding ratio for the Th^m blanket was approximately 20% less than that for an infinitely thick uranium-metal blanket. This difference was ascribed to the different fast fission contributions in the radial blankets. The report did not provide any other details about the capture and fission rates obtained.

In a more recent study, Leipunskii et al. (1971) examined a number of different configurations with thorium blankets

only. The work centered around the influence of the isotopic composition in the core on the safety and on the power density distribution in the core zones. Here, too, combinations of U238, U233, and Pu239 cycles proved to be optimal systems. An optimal Pu239 and U233 isotope distribution was shown to reduce the maximum radial form factors in the core zones from approximately 1.8 to approximately 1.2. These studies demonstrated the Soviet interest in using Th232 in the FBR radial blanket.

More recent studies have dealt with the coupling of the fissile fuel cycles of two reactor types, the crossed-progeny cycle (for example, Lang 1968 and 1969, Wenzel 1971, and Brogli and Schultz 1974). The considerations were based on two or more reactors that mutually exchange fissile material. Lang (1968 and 1969) investigated coupling the fissile cycles of an LMFBR and of a PWR with a hard neutron spectrum. In the PWR, U238/U233 is used as fuel, and the converted Pu239 is transferred to the LMFBR. The LMFBR breeds U233 in the radial blanket and in the internal breeding zone (LMFBR design by Allis Chalmer, 1964). Lang was of the opinion that because of this reactor configuration LWRs might be phased out early in the next century.

Wenzel (1971) investigated a similar PWR and LMFBR reactor configuration. His results can be summarized as follows:

-- The fuel cycle costs of the PWR can be reduced by approximately 10% to 30%, with the FBR fuel cycle costs remaining approximately the same.
-- The PWR-LMFBR reactor configuration can slightly reduce the separative work requirements expected for the 1980s.

Brogli and Schultz (1974) studied the economic aspects of coupling the cycles of a GCFBR-HTGR system. They concluded that the fuel cycle costs of such a configuration are little influenced by uranium and plutonium prices.

Wood and Discroll (1973) conducted an extensive investigation into the economic aspects of radial and axial thorium oxide blankets. They calculated an advantage in fuel cycle costs of up to 30% for a radial thorium blanket as compared to a uranium blanket, assuming a favorable U233 price (16.7 dollars/gram) as compared

to the Pu239 price (10.0 dollars/gram). Their burnup calculations, like those in the preceding studies, were based on relatively old cross-section sets, such as the ABBN nuclear data set (Abagjan 1964).

This chapter is meant to provide a comprehensive and detailed comparison of fissile fuel utilization in different radial thorium (ThO_2 and Th^m) blankets and a uranium blanket (UO_2), on the basis of revised cross sections. Since uncertainties in the various cost assumptions still prevail, the economic aspects have been viewed as subordinate to the fuel economic aspects and are therefore not considered here.

II.2. GENERAL REMARKS ON THE PROPERTIES OF A RADIAL BLANKET

The blankets (axial or radial) of an FBR have two principal functions. They primarily serve as efficient neutron reflectors, backscattering into the core region the neutrons escaping from it, their secondary function is to breed fissile fuel by absorbing the nonbackscattered neutrons in the fertile fuel of the blankets.

The effectiveness of a blanket in fulfilling these two functions depends largely on the nuclear and, to some extent, material properties of the nuclear fuel employed, i.e. on the types of fissile and fertile isotopes and on the chemical composition of the fuel material (oxide, carbide, or metal, etc.). The fissile and fertile isotopes relevant to this study are U233 and Pu239, and Th232 and U238, respectively, and the relevant fuel materials are UO_2, ThO_2, and Th^m.

This investigation focuses on the breeding characteristics of the various radial blankets. Such an assessment requires analysis of the various factors that influence and govern radial breeding. These factors can be made translucent if the *buildup* of fissile fuel in the radial blanket region is understood in terms of the neutron economy of the blanket. (The *gain*, or *buildup*, of fissile fuel is here defined as the difference between the *production* of fissile fuel due to neutron capture by fertile fuel minus the *loss* of fissile fuel due to neutron absorption by fissile fuel.)

One can do this, for example, by looking at the number of neutrons available for absorption in the blanket, and where these neutrons originate. There are two sources of neutrons for the blanket region: the leakage neutrons scattering into the blanket region from the core region (these are the nonbackscattered neutrons referred to above), and the fission-induced self-generated neutrons originating in the blanket. Their total makes up the sum of neutrons available in the blanket. Under the assumption that all these neutrons are captured in the fertile fuel of the blanket, the *production* of fissile fuel is clearly directly proportional to the total number of neutrons available.

Not all of the neutrons available in the blanket are utilized in the breeding process, however. Some of them are lost by parasitic processes. (The neutrons absorbed by the structural material of the blanket and of the neutrons leaking into the radial reflector are referred to as parasitic neutron losses.) The extent of fissile fuel *buildup* is thus also, to some degree, influenced by such parasitic losses.

The discussion has concentrated on the FBR radial blanket thus far. As the radial blanket region is only one in three reactor regions, it is also interesting to compare its importance relative to the other reactor regions, the core and the axial blanket.

Table II.1, listing the condensed neutron balance distribution of the FBR design investigated here, illustrates on the one hand the relative significance of the core leakage neutrons, the fission-induced self-generated radial blanket neutrons, and the parasitic neutron losses in the blanket, and on the other hand the role of the radial blanket with respect to the other reactor regions.

In the equilibrium burnup condition of the core and the blankets, 100 neutrons are produced throughout the reactor due to fission; 85 of them are generated in the core region, and 15 in the blanket regions; 10 of the latter originate in the axial blanket, and 5 in the radial blanket.

Table II.1. Distribution of neutron production and neutron losses in the various FBR regions (equilibrium burnup condition).

FBR regions	Losses	Production
Core zones	69	85
Axial blanket	18	10
Radial blanket	9	5
Reflector	1	-
Leakage (total)	3	-

The greatest majority of these 100 neutrons is absorbed in the reactor, and only a small fraction (3) is lost due to leakage from the reactor (reflector leakage). 69 of the total 100 are absorbed in the core region, leaving a net surplus of 16 core neutrons (85-69) that scatter into the blanket regions[1]. These neutrons, representing about 19% of the neutrons generated in the core region, are referred to as core leakage neutrons, or leakage neutrons.

Ten of the 16 leakage neutrons (62%) diffuse into the axial blanket, and only six (38%) leak into the radial blanket. (This axial leak preference can be ascribed to the low H/D[2] ratio of this FBR[3].) Thus a total of 11 neutrons remains for absorption in the radial blanket, six of which (55%) are core leakage neutrons, and five (45%) originate in the blanket itself. For a radial blanket in equilibrium burnup condition, this implies about equal contributions of core leakage neutrons and self-generated neutrons. This distribution, of course, changes with the burnup condition of the radial blanket.

---

[1] In the actual case, more than 16 neutrons leak into the blankets. Most of them, however, are backscattered into the core region (about 70-80%, see discussion in Section II.7.a). The 16 neutrons referred to above represent a net leakage.

[2] Height to diameter ratio.

[3] A more detailed discussion of the influence of the H/D ratio follows in Section II.7.a.

Of the 11 neutrons available for absorption in the radial blanket, only nine (80-85%) are actually absorbed there; the remaining two are permanently lost into the radial reflector, where they are either absorbed or lost due to reflector leakage. These two neutrons are representative of the parasitic neutron losses of the radial blanket.

The importance of the radial blanket with respect to the other reactor regions can be inferred from the fact that only nine out of a total of 100 neutrons are absorbed there. As far as neutron absorption is concerned, the radial blanket is thus of only limited significance. It can therefore be expected that different fertile or fissile fuels and fuel materials in the radial blanket region will have no major impact on the overall reactor performance.

The buildup of fissile fuel in the radial blanket has been shown to be governed primarily by the neutron leakage into and the neutron generation in the blanket. At a later point, neutron leakage will be shown to be primarily determined by the geometric FBR design expressed by the H/D ratio, and by the neutron reflective property, or albedo β, of the radial blanket fuel material. A favorable H/D ratio and a small β generally imply a large neutron leakage into the radial blanket.

The extent of neutron generation in the blanket is determined by its fertile fission and fissile fission. Both fission processes release excess neutrons, which are again utilized in the breeding process. A large fast-fission contribution in the radial blanket will therefore enhance its breeding potential.

A large *production* of fissile fuel, governed by these parameters, however, does not necessarily correspond to a large *buildup*, or *gain*, of fissile fuel since part of the fissile fuel built up in the blanket is consumed, or lost due to fissile neutron absorption. A large *loss* of fissile fuel will therefore keep the buildup low.

A radial blanket with the following properties would exhibit a large buildup of fissile fuel:

-- small albedo β,
-- high η_r^i of bred fissile fuel,
-- small absorption cross section of bred fissile fuel $(\sigma_a^{fiss})_r$,
-- large capture cross section of fertile fuel $(\sigma_c^{fert})_r$.

The last condition assures that most of the neutrons available in the radial blanket are actually utilized in the breeding process and not lost by some parasitic neutron loss process.

Not all of these properties, which are favorable to a large buildup of fissile material in the radial blanket, are actually advantageous to the reactor as a whole.

For example, a high η_r^i, a small $(\sigma_a^{fiss})_r$, and a large $(\sigma_c^{fert})_r$ generally improve the global reactor performance. A small blanket albedo β, however, implies an enhanced neutron leakage from a region of high reactivity worth into one of relatively low reactivity worth, resulting in a net decrease in reactivity. This reactivity loss must be compensated for by an increase in the fissile fuel enrichment in the core region, so that sufficient burnup reactivity is maintained. The resulting higher fissile fuel inventory, on the other hand, is not a desirable feature since it tends to increase the doubling time of the reactor.

Blanket characteristics apparently conducive to breeding in the blanket, therefore, do not necessarily exert a favorable influence on the reactor as a whole.

Therefore, in order to assess the impact of the various radial blankets, i.e. UO_2, ThO_2, or Th^m, on FBR performance, it is necessary to compare not only the parameters governing the breeding characteristics of a radial blanket but also the global reactor parameters. Both groups of parameters depend on the radial blanket fuel materials. For an overall assessment, one must examine in particular the following reactor characteristics:

-- changes in reactivity k_{eff},
-- changes in fissile fuel enrichment and fissile fuel inventory I,
-- changes in radial breeding ratio BR_r and radial breeding gain G_r,
-- changes in global breeding ratio BR_N and global breeding gain G_N,
-- changes in the distribution of region breeding ratios BR_n and region breeding gains G_n,
-- the effective buildup of fissile fuel in a given blanket,
-- the power contribution of radial blankets,
-- the maximum linear rod power χ^{max},
-- the buildup of U232 in the thorium blankets,
-- the reactivity worth of Pa233 in the thorium blankets,
-- the influence of the various blankets on the Na void coefficient.

Such an analysis requires detailed nuclear burnup calculations, focusing on the radial blanket of a representative power reactor. This is the objective of the following sections.

II.3. MATERIAL PROPERTIES OF UO_2, ThO_2, and Th METAL

The basic material data of some nuclear fuels are compiled in Table II.2. Of interest here is a comparison between UO_2, ThO_2, and Th metal. Regarding its heavy-metal density, ThO_2 has a slight disadvantage of 8.7% with respect to UO_2; yet, on account of its higher melting temperature (3290°C for ThO_2, and 2750°C for UO_2) and its somewhat better thermal conductivity, higher maximum linear rod powers with theoretical upper limits of 1000 W/cm are attainable for ThO_2, as compared to approximately 650 W/cm for UO_2. ThO_2 irradiation properties in FBR neutron spectra are expected to be similar to those of UO_2.

Because of its high density, U metal would be a good reflector or the ideal FBR blanket material. However, due to anisotropic expansion under neutron irradiation, U metal exhibits a very unfavorable burnup behavior, which is attributed to its

Table II.2. Properties of nuclear fuel materials.

		Th	U	Pu	ThO_2	UO_2	PuO_2	ThC	UC	PuC
Theoretical density	(g/cm^3)	11.6	19.0	19.0	10.04	10.96	11.46	10.6	13.63	13.60
Metal density	(g/cm^3)	11.6	19.0	19.0	9.14	9.68	10.12	10.08	12.97	13.0
Melting point	(^oC)	1749	1132	650	3290	2750	2280	2625	2350	1650
Thermal conductivity (600^oC)	(W/cm^oC)	0.45	0.37	0.04	0.04	0.035	0.02	0.25	0.23	
Phase transition	(^oC)	1375	665 775							
Lattice structure		FCC	orthorhombic							

orthorhombic lattice structure. It is mainly for this reason that U metal is not a suitable fuel material in power reactors.

Th metal, on the other hand, does not have these unfavorable properties. Because of its body-centered cubic lattice structure, it expands isotropically under irradiation and (as reported in Olsen 1966 and Bundschuh 1972) has very good irradiation properties for the burnup range (up to 10,000 MWd/t) relevant to radial blankets. In addition, its melting point is much higher than that of U metal. More important, however, is the considerably higher temperature at which Th metal undergoes a phase change. It is 1375°C, as compared to 665°C for U metal. On the basis of the very high thermal conductivity K(T) of Th metal, which differs by a factor of 10 compared to UO_2 and ThO_2, a very high linear rod power[4] of approximately 800 W/cm, and thus high power densities can be achieved. This makes Th metal an interesting fuel for FBRs requiring high power densities.

These few points serve to illustrate that ThO_2 and Th metal have material properties that are as favorable as, and in some respects even superior to, those of UO_2. The use of ThO_2 or Th metal as FBR blanket material is therefore not expected to be restricted on account of their material properties.

II.4. DESCRIPTION OF THE FBR INVESTIGATED

General Electric's design of a 1000 MW(e) oxide LMFBR is used as reference reactor (General Electric 1968). It was selected because of the extensive documentation available on results of detailed burnup calculations, which helped the author check the computer codes and nuclear cross-section libraries used.

The basic reactor data of this LMFBR are compiled in Table II.3. Figure II.1 indicates the reactor dimensions, the partitioning of the various reactor regions into burnup zones, and

---

[4] linear rod power $\chi = 4\pi \int_{T_S}^{T_{max}} K(T)\, dt$; T_{max} = maximum central temperature; T_S = surface temperature.

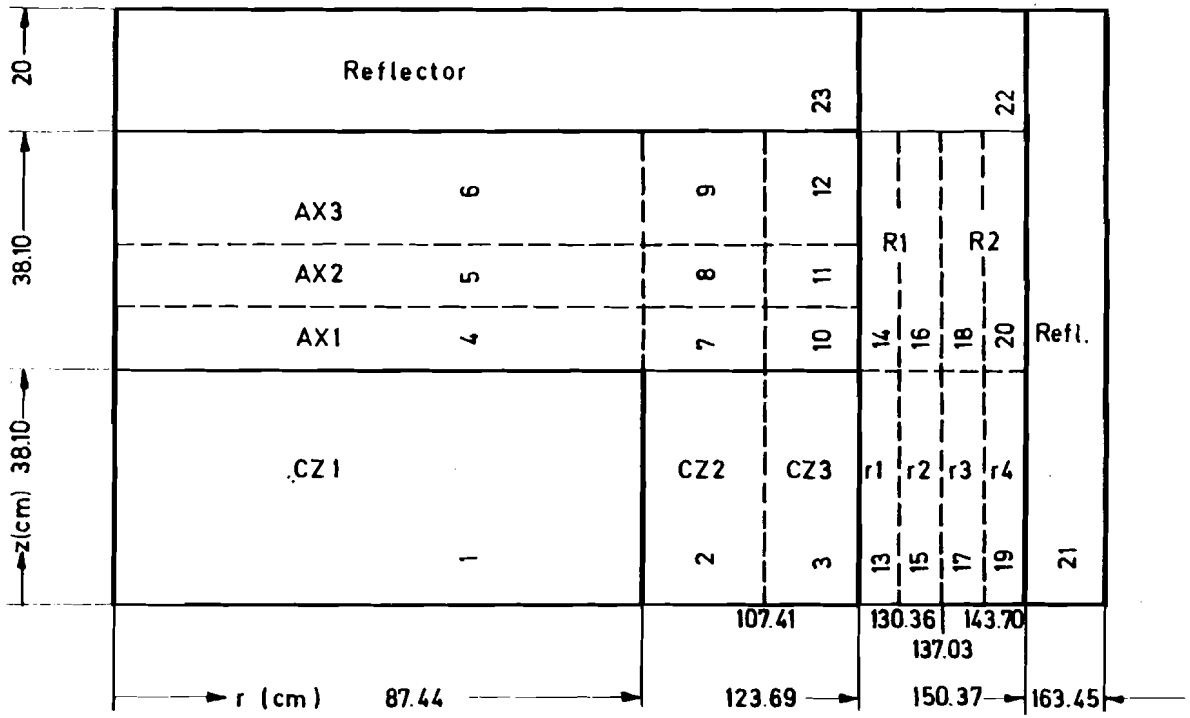

Volume Fractions	(%)	Core and Axial Blanket	Radial Blanket
Fuel	(ω)	46.74	54.55
Structural Material	(β)	14.90	17.76
Sodium	(α)	35.14	27.69
Control Rod		3.23	0.00

Figure II.1. Schematic of the 1000 MW(e) LMFBR reactor regions used for burnup calculations. Source: General Electric (1968).

Table II.3. Reactor Data.

Parameter	Symbol	Unit	
Core: height	H	cm	76.20
diameter	D	cm	247.40
volume	V	liter	3662
H/D	H/D		0.308
Axial blanket	ax	cm	38.10
Radial blanket	r	cm	26.68
Power density (core)	q	kW(th)/ liter	580
Core zones 1-3:	CZ1-CZ3		
CZ1, o.d.		cm	174.88
CZ1, volume		liter	1831
CZ1+CZ3, o.d.		cm	247.38
CZ2+CZ3, volume		liter	1831
Power (equilibrium burnup condition):	P	MW(th)	
Core	P_c		2120
Axial blanket	P_{ax}		180
Radial blanket	P_r		120
Total		MW(th)	2420
Enrichment (equilibrium burnup condition):			
CZ1/CZ2+CZ3	e		10.73/13.45
Fissile fuel Pu239, Pu241, Pu235:			
Core	I_c	kg	1624
Blankets	$I_{r,ax}$	kg	611
Breeding ratio	BR_N		1.42

Fuel rod diameter		mm	6.30
Fertile rod diameter		mm	10.62
Cladding material thickness		mm	0.266
Maximum rod power	χ^{max}	W/cm	546
Average rod power	χ^{av}	W/cm	239
Average discharge burnup (core)	A	MWd/t*	100000
Heavy metal inventory:			
Core		kg	13450
Axial blanket		kg	15030
Radial blanket		kg	16700
Total		kg	45180
Theoretical fuel density:		%	
CZ1, CZ2, CZ3			90
Axial blanket			95
Radial blanket			95
Smear density:		%	
CZ1, CZ2, CZ3			85
Axial blanket			90
Radial blanket			90

* t for metric ton is used throughout this paper.

the corresponding volume fractions of fuel ω, structural material β, and coolant α. Reference is to be made here in advance to the volume fraction of structural and cladding material in the core region which, in the light of the present state of the art, appears too low. The General Electric results, especially with regard to the breeding ratio, should not thus be compared to representative values of more recent LMFBR designs, in which the volume fraction of structural material in the core region is 20-22%, instead of the 15% assumed here. The breeding ratio calculated here is, therefore, higher than the values obtained for large oxide-fueled LMFBRs of current design of $BR_N \approx 1.20$. Since the prime purpose of this investigation is to compare the influence of different radial blankets on FBR performance, emphasis should be on the relative results--especially as regards the global breeding ratio BR_N--rather than on the absolute values calculated. It should be expected that the relative results are also applicable to FBRs of a more recent design with comparable H/D ratios.

Furthermore, mention should be made of the rather optimistic maximum linear rod power of 550 W/cm assumed here, which is a technological goal of the future. This high value explains the relatively high power density of 580 kW(th) per liter, and thus the very low fissile inventory of the oxide-fueled LMFBR design considered here.

II.5. NUCLEAR CROSS SECTIONS

This is a short description of the nuclear cross-section library and the procedure used to generate the few-group cross-section sets for the burnup calculations in this study.

II.5.a. Comparisons of Multigroup Cross Sections Based on the ENDF/B-III File

The ENDF/B-III 29 group constant set (Kidman and Scheuter 1971) has been used as nuclear library for the burnup calculations. First, the 29 groups were collapsed into 26 groups, so that the data set became compatible with the NUSYS computer code system (Höbel and Huschke 1966) for fast breeder calculations, available at the Nuclear Research Center Karlsruhe (KFK), F.R.G. Then,

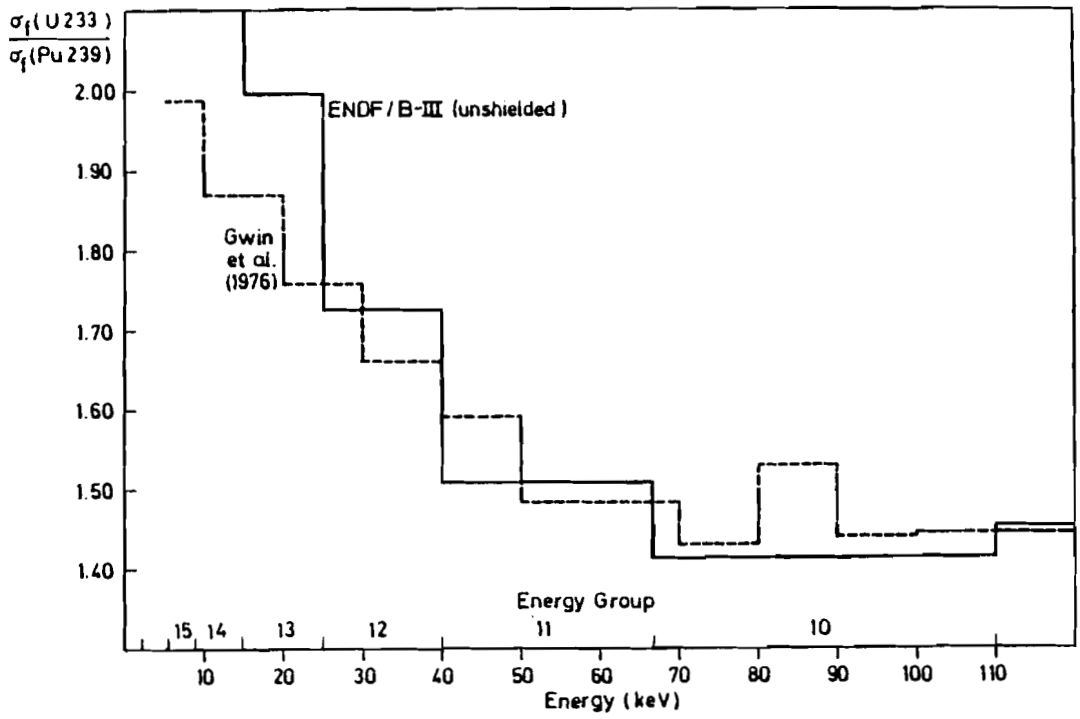

Figure II.2. Comparison of σ_f(U233)/σ_f(Pu239) from the ENDF/B-III group constant set (Kidman and Scheuter 1971) and values measured by Gwin et al. (1976).

the ENDF/B-III and KFK-INR (Kiefhaber 1972) cross-section sets were compared by way of criticality calculations on a UO_2-PuO_2 fueled fast critical assembly (SNEAK) (P.McGrath, personal communication, KFK, 1973). The results showed good agreement between the cross-section sets with respect to the U238 and Pu isotopes. This was to be expected since the cross sections of these isotopes had continually been revised and updated for the past decade. The reliability of the Th232 and U233 cross sections in ENDF/B-III could not be verified in a similar manner since, for these isotopes, the KFK-INR set contains data from the original ABBN set (Abagjan 1964). It was felt, however, that the reliability of the thorium cross-section data in ENDF/B-III is comparable to that of the U238 and Pu data of ten years ago, in particular as regards the inelastic scattering cross section of Th232.

More recent data on U233 and Pu239 published by Gwin et al. (1976) show generally good agreement with the U233 absorption data from ENDF/B-III (see Figure II.2) in the relevant energy

range. More recent Th232 foil irradiations performed in the radial blanket of SNEAK (W. Scholtyssek, personal communication, KFK, 1975) also show good agreement (5%) between the Th232 capture rates calculated with ENDF/B-III and the values measured, whereas a deviation of 15% to 20% was found with the ABBN set. This satisfactory agreement allows the conjecture that the Th232 and U233 data contained in ENDF/B-III are sufficiently accurate for the present investigation. This in particular applies to the present assessment, where the Th232 and U233 isotopes are located in a reactor region of only moderate importance (see Section II.2). However, the reliability of the cross sections of these isotopes becomes more significant if the radial blanket region assumes a more important role (e.g. in gas-cooled FBRs, see discussion in Section II.7.a), or if these isotopes are used as fuel in the FBR core region.

In evaluating the breeding properties of different radial blankets, it is imperative to compare the relevant cross sections of the fertile isotopes Th232 and U238 and the fissile isotopes U233 and Pu239. Table II.4 contains such an energy group-dependent comparison for the unshielded microscopic capture and fission cross sections of Th232 and U238, and Table II.5 lists the corresponding shielded cross sections of the oxide blankets investigated here. Table II.6 compares the unshielded U233 data with the corresponding Pu239 data. The effect of self-shielding of the fissile isotope is shown to be negligible in the blankets. Table II.7 shows the differences between the shielded Th232 cross sections of a ThO_2 and of a Th-metal radial blanket. Some of these data are plotted in Figures II.3 and II.4. Comparing the data leads one to observe the following:

-- Th232 has a considerably higher capture cross section than U238 (by $\sim 30\%$) in the energy region above 60 keV.
-- The fast-fission cross section of U238 is larger, by approximately a factor of 4, than that of Th232.
-- The fission cross section of U233 is decisively above that of Pu239 for the energy range below 1 MeV, increasing quite considerably with decreasing energy.

Table II.4. Comparison between *unshielded* microscopic capture and fission cross sections of Th232 and U238 (ENDF/B-III).

Energy group	Upper Energy	$\langle\sigma_c\rangle$ (barns)		$\frac{Th232}{U238}$	$\langle\sigma_f\rangle$ (barns)		$\frac{U238}{Th232}$
		Th232	U238		Th232	U238	
1	10.00 MeV	.0115	.0064	1.80	.2862	.8772	3.07
2	6.05	.0209	.0116	1.80	.1424	.5467	3.84
3	3.68	.0401	.0272	1.47	.1237	.5471	4.42
4	2.23	.0787	.0632	1.245	.0918	.4268	4.65
5	1.35	.1418	.1208	1.174	.002	.0270	13.5
6	.821	.1774	.1258	1.410	-	.0013	-
7	.498	.1784	.1169	1.526	-	-	-
8	.302	.1837	.1346	1.365			
9	.183	.2184	.1698	1.286			
10	.111	.2903	.2155	1.347			
11	67.4 keV	.3829	.3386	1.131			
12	40.8	.4525	.4444	1.018			
13	25.5	.5716	.5671	1.008			
14	15.0	.7047	.7034	1.002			
15	9.11	.8633	.8624	1.001			
16	5.53	1.073	1.065	1.007			
17	3.35	1.388	1.296	1.071			
18	2.84	1.527	1.385	1.102			
19	2.40	1.602	1.492	1.074			
20	2.03	2.154	1.777	1.212			
21	1.23	2.163	2.916	0.742			
22	748 eV	4.353	3.606	1.207			
23	454	7.10	20.31	0.350			
24	275	18.56	52.96	0.350			
25	61	10.22	29.16	0.351			
26	thermal						

Table II.5. Comparison between *shielded* microscopic capture and fission cross sections of Th232 and U238 in oxide radial blankets (ENDF/B-III).

Energy group	Upper energy	$f_c\langle\sigma_c\rangle$ (barns)		Th232/U238	$f_f\langle\sigma_f\rangle$ (barns)		U238/Th232
		Th232	U238		Th232	U238	
1	10.00 MeV	.0114	.0064	1.781	.2862	.8772	3.067
2	6.05	.0207	.0117	1.769	.1424	.5466	3.831
3	3.68	.0399	.0270	1.478	.1237	.5470	4.428
4	2.23	.0780	.0627	1.244	.0918	.4268	4.652
5	1.35	.1418	.1208	1.174	.0020	.0270	13.51
6	.821	.1774	.1259	1.409	-	.013	-
7	.498	.1787	.1168	1.530	-	.001	-
8	.302	.1837	.1345	1.366	-	-	-
9	.183	.2184	.1698	1.286			
10	.111	.2903	.2155	1.347			
11	67.4 keV	.3774	.3343	1.129			
12	40.8	.4478	.4342	1.031			
13	25.5	.5413	.5280	1.025			
14	15.0	.6424	.6271	1.024			
15	9.11	.7576	.7370	1.028			
16	5.53	.8790	.8173	1.076			
17	3.35	1.1677	1.0907	1.071			
18	2.84	1.1279	1.0171	1.109			
19	2.40	1.0947	0.9559	1.145			
20	2.03	1.0930	0.8756	1.248			
21	1.23	0.9962	1.0980	0.907			
22	748 eV	1.1604	1.0931	1.062			
23	454	1.2380	0.9515	1.301			
24	275	1.6435	1.7628	0.932			
25	61	1.0151	2.6356	0.385			
26	thermal						

f_c, f_f are energy group dependent shielding factors

Table II.6. Comparison between *unshielded* microscopic capture and fission cross sections of U233 and Pu239 (ENDF/B-III).

Energy group	Upper energy	$\langle\sigma_c\rangle$ (barns)		$\frac{U233}{Pu239}$	$\langle\sigma_f\rangle$ (barns)		$\frac{U233}{Pu239}$
		U233	Pu239		U233	Pu239	
1	10.00 MeV	.0008	.0653	0.012	2.1292	2.0247	1.052
2	6.05	.0017	.0018	0.944	1.6703	1.7082	0.978
3	3.68	.0069	.0038	1.816	1.9012	1.9452	0.977
4	2.23	.0218	.0097	2.247	1.9222	2.0084	0.957
5	1.35	.0590	.0243	2.428	1.8550	1.7517	1.059
6	.821	.1183	.0762	1.553	1.9187	1.6308	1.177
7	.498	.1669	.1399	1.193	2.0742	1.5551	1.334
8	.302	.2024	.1957	1.034	2.1806	1.4933	1.460
9	.183	.2258	.2275	0.993	2.2462	1.5405	1.458
10	.111	.2424	.2697	0.899	2.3126	1.6323	1.417
11	67.4 keV	.2752	.3629	0.758	2.5668	1.7021	1.508
12	40.8	.3258	.5507	0.592	3.0032	1.7413	1.725
13	25.5	.3943	.7676	0.514	3.6187	1.8154	1.993
14	15.0	.4918	1.0670	0.461	4.3703	1.9820	2.205
15	9.11	.6391	1.5951	0.401	5.2419	2.2489	2.331
16	5.53	.8925	2.2416	0.398	6.2375	2.6585	2.346
17	3.35	1.1760	2.7015	0.435	7.1640	3.3635	2.130
18	2.84	1.3910	2.9281	0.475	7.8160	3.6319	2.152
19	2.40	1.6360	3.7320	0.438	8.6440	2.7830	3.106
20	2.03	2.3160	3.5729	0.648	10.0440	4.6701	2.151
21	1.23	3.5360	4.6767	0.756	11.3840	6.3333	1.798
22	748 eV	4.8440	7.3763	0.657	14.2960	10.3438	1.382
23	454	3.9900	9.6917	0.412	18.0200	10.7083	1.683
24	275	6.0160	21.2288	0.283	28.4440	29.7813	0.955
25	61	26.3200	29.4039	0.895	140.0800	41.7361	3.356
26	thermal	10.9400	0.6276	17.432	93.3600	7.2604	12.859

Table II.7. Comparison between *shielded* microscopic capture cross sections of Th232 in ThO_2 and Th^m radial blankets (ENDF/B-III).

Energy group	Upper energy	$f_c\langle\sigma_c\rangle$ (barns)		$\frac{ThO_2}{Th^m}$
		ThO_2	Th^m	
1	10.00 MeV	0.0114	.0114	1.000
2	6.05	.0207	.0207	1.000
3	3.68	.0399	.0400	0.998
4	2.23	.0780	.0781	0.999
5	1.35	.1418	.1418	1.000
6	.821	.1774	.1774	1.000
7	.498	.1787	.1787	1.000
8	.302	.1837	.1835	1.001
9	.183	.2184	.2181	1.001
10	.111	.2903	.2900	1.001
11	67.4 keV	.3774	.3766	1.002
12	40.8	.4478	.4415	1.014
13	25.5	.5413	.5283	1.025
14	15.0	.6424	.6212	1.034
15	9.11	.7576	.7284	1.040
16	5.53	.8790	.8329	1.055
17	3.35	1.1677	1.1164	1.046
18	2.84	1.1279	1.0524	1.072
19	2.40	1.0947	0.9989	1.096
20	2.03	1.0930	0.9578	1.141
21	1.23	0.9962	0.8755	1.138
22	748 eV	1.1604	0.9384	1.237
23	454	1.2380	0.9600	1.290
24	275	1.6435	1.3200	1.245
25	61	1.0151	0.8560	1.186
26	thermal			

f_c energy group dependent shielding factor

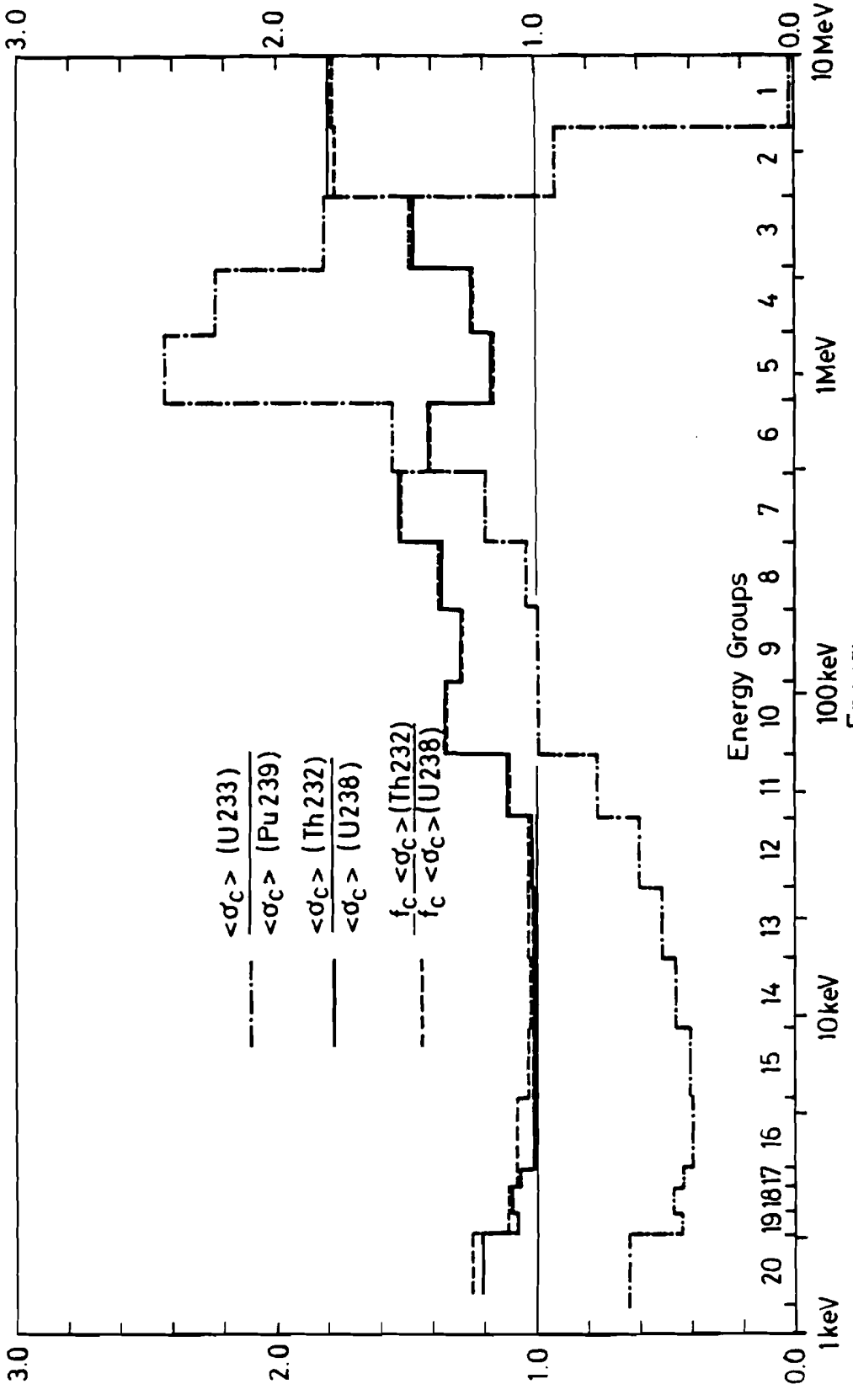

Figure II.3. Ratio of unshielded and shielded microscopic capture cross sections of fertile and fissile isotopes in oxide radial blankets (ENDF/B-III).

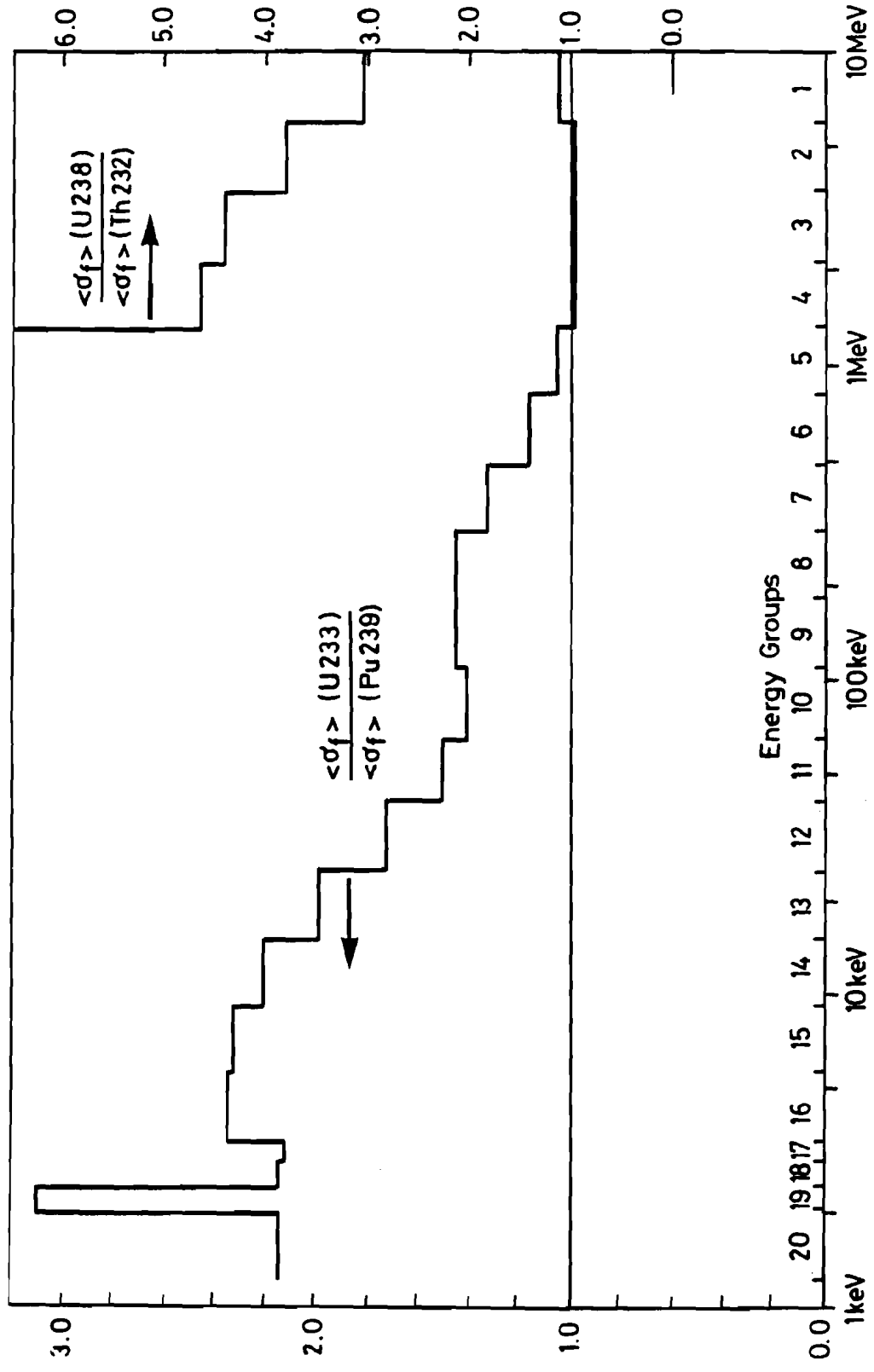

Figure II.4. Ratio of unshielded microscopic fission cross sections of fertile and fissile isotopes in oxide radial blankets (ENDF/B-III).

-- The capture cross section of U233 is larger (by ~60%) than that of Pu239 in the 200 keV-6 MeV energy range.
-- There is no significant difference between the ratios of the shielded and unshielded cross sections of Th232 to U238.

These considerable differences between the basic cross sections of the respective isotopes in thorium- and uranium-fueled blankets lead one to expect rather significant dissimilarities between their breeding as well as neutron reflective properties.

II.5.b. Generation of Few-Group Cross Sections for the Burnup Calculations Performed

In order to reduce computer time for the burnup calculations, the 26-group constants were collapsed into four energy groups by means of the Karlsruhe NUSYS System. The reactor was partitioned into various burnup zones, as is indicated in Figure II.1. The core and axial blanket regions were divided into three zones each, and the radial blanket region into four zones, labeled:

Reactor Zone	Designation
Core zones 1, 2, and 3	CZ1, CZ2, and CZ3
Axial blanket zones 1, 2, and 3	AX1, AX2, and AX3
Radial blanket zones 1, 2, 3, and 4	r1, r2, r3, and r4, where R1 stands for r1 and r2 and corresponds to the first row of blanket elements; R2 stands for r3 and r4 and corresponds to the second row of blanket elements.

Table II.8. Spectrum-weighted four-group cross sections of the fertile and fissile isotopes in core zone CZ1 and in radial blanket zones r1 and r3 (oxide fuel).

Group	Energy group interval	Core zone CZ1				Radial blanket zone r1					
		U238	Th232	Pu239	U233	U238	Th232	Th232*	Pu239	U233	U233*
	$f_a\langle\sigma_a^g\rangle$ *Absorption (barns)*										
1	.820-10 MeV	.4000	.1695	1.8783	1.898	.3921	.1603	.1593	1.8774	1.8964	1.8977
2	40.8-820 keV	.1820	.2333	1.8015	2.4116	.1858	.2392	.2332	1.8090	2.4319	2.4163
3	.748-40.8 keV	.6818	.6474	3.4282	5.1607	.6262	.6499	.5928	3.6315	5.4187	4.9896
4	<.748 keV	1.7161	1.424	18.492	21.033	1.1784	1.2707	.9831	23.42	23.844	21.754
	$f_f\langle\sigma_f^g\rangle$ *Fission (barns)*										
1	.820-10 MeV	.3301	.0816	1.8653	1.8681	.3205	.0710	.0661	1.8639	1.8653	1.8659
2	40.8-820 keV	.0002	-	1.5887	2.2080	.0002	-	-	1.5913	2.224	2.2215
3	.748-40.8 keV	-	-	2.1956	4.5203	-	-	-	2.2871	4.723	4.387
4	<.748 keV	-	-	10.838	16.2970	-	-	-	13.478	18.862	16.963

*Th-metal blanket.

Group	Energy group interval	Core zone CZ1				Radial blanket zone r3					
		U238	Th232	Pu239	U233	U238	Th232	Th232*	Pu239	U233	U233*
	$f_a\langle\sigma_a^g\rangle$ *Absorption (barns)*										
1	.820-10 MeV	.4000	.1695	1.8783	1.898	.3778	.1589	.1556	1.884	1.9011	1.9043
2	40.8-820 keV	.1820	.2333	1.8015	2.4116	.1948	.2468	.2337	1.8255	2.4580	2.4221
3	.748-40.8 keV	.6818	.6474	3.4282	5.1607	.6496	.6766	.5962	3.9313	5.8185	5.0644
4	<.748 keV	1.7161	1.424	18.492	21.033	1.2396	1.298	1.0200	27.244	27.626	25.587
	$f_f\langle\sigma_f^g\rangle$ *Fission (barns)*										
1	.820-10 MeV	.3301	.0816	1.8653	1.8681	.3043	.06437	.0498	1.870	1.8675	1.8653
2	40.8-820 keV	.0002	-	1.5887	2.2080	.0002	-	-	1.5966	2.2452	2.2164
3	.748-40.8 keV	-	-	2.1956	4.5203	-	-	-	2.4212	5.0300	4.4385
4	<.748 keV	-	-	10.838	16.2970	-	-	-	15.671	22.2000	20.384

*Th-metal blanket.

By means of the 1-D diffusion program in the NUSYS system, the 26-group constants were neutron-flux weighted with the corresponding eigenspectrum for each individual zone, and collapsed into four energy groups. An isotopic composition-dependent four-group cross-section set was thus obtained for each reactor zone (Figure II.1). This resulted in three four-group cross-section sets for the core, three for the axial blanket, four for each of the UO_2, ThO_2, and Th-metal blankets, and one for the reflector. Changes in volume fraction, fuel type, or isotopic composition in any one of the zones made it necessary to generate new four-group cross-section sets. These sets were generated for isotopic compositions with the reactor in equilibrium burnup condition. Stored on tape in a retrievable manner, they served as input data for the multidimensional burnup code CITATION (Fowler 1971).

Table II.8 reproduces four-group cross sections of the most important isotopes in core zone CZ1 and radial blanket zones r1 and r3 (see Figure II.1). Table II.9 shows the corresponding one-group cross sections. The influence of the softer neutron spectrum in the blanket zones on the cross sections is clearly noticeable from the increase in the blanket cross sections, as compared to those in the core zones. Regarding the oxide blankets, for example, the absorption cross section of U238 in radial zones r1 and r2 is larger by 1.2% and 18%, respectively, than in core zone CZ1; for Pu239 the differences are 13.4% and 45.1%, and for U233 15.8% and 42.4%. Comparisons of fertile fuel cross sections show the same trend.

Comparing the fertile and fissile isotope cross sections for the UO_2 and ThO_2 blankets, one observes the following differences:

-- a 16% larger capture cross section σ_c [5] of Th232 than of U238 in r1, which decreases to 9.1% in r2,
-- a 35.6% larger absorption cross section σ_a of U233 than of Pu239 in r1, which decreases to 30.4% in r2;

---

[5] $\sigma_c = \sigma_a - \sigma_f$

Table II.9. Spectrum-weighted one-group cross sections of fertile and fissile isotopes in core zone CZ1 and in radial blanket zones r1 and r3 for various fuel materials.

Reactor zone	Fuel material	U238	Th232	Pu239	U233
	$\sigma_{a\,(barns)}$				
Core zone CZ1	UO_2	0.3460		2.3019	
	ThO_2		0.325	2.258	3.057
Radial blanket zone r1	UO_2	0.3504		2.6102	
	ThO_2		0.3740		3.5404
	Th^m		0.3050		2.9779
Radial blanket zone r3	UO_2	0.4083		3.3410	
	ThO_2		0.4304		4.3550
	Th^m		0.3173		3.1551
	$\sigma_{f\,(barns)}$				
Core zone CZ1	UO_2	0.0453		1.830	
	ThO_2		0.0116	1.811	2.759
Radial blanket zone r1	UO_2	0.0342		1.964	
	ThO_2		0.0067		3.1486
	Th^m		0.0082		2.6769
Radial blanket zone r3	UO_2	0.0175		2.319	
	ThO_2		0.0039		3.7987
	Th^m		0.0043		2.8301

and, comparing the cross sections of the Th^m blanket and the ThO_2 and UO_2 blankets:

-- In r1 of the metal blanket, Th232 shows capture cross sections that are smaller by 19.2% and 6.3% than such values for Th232 and U238 in the oxide blankets.
-- U233 in the metal blanket has an absorption cross section 14.1% larger than Pu239 but 16% smaller than U233 in the oxide blankets.
-- Th232 in the metal blanket has a fast-fission cross section 22.4% larger than Th232 and 4.17 times smaller than U238 in the oxide blankets.

From these cross-section differences, one may infer that the production, the loss, and thus the buildup of fissile fuel in the various radial blankets can be expected to show the following behavior:

-- a larger production of U233 in both the ThO_2 and Th^m blankets than of Pu239 in the UO_2 blanket,
-- higher losses of U233 due to neutron absorption in both thorium blankets than of Pu239 in the UO_2 blanket,
-- a higher loss of U233 in the ThO_2 blanket than in the Th^m blanket.

The buildup, i.e. the difference between production and losses, is difficult to assess offhand, since both the production and loss terms are larger for the thorium blankets than for the UO_2 blanket.

The above deductions are based on the supposition that an approximately equal number of neutrons is available for absorption in the three different blankets. Since the various fuel materials are most likely to have different albedos--and thus different core neutron leakages into the blankets--the above considerations are simply deductions based on the nuclear data. Only by detailed burnup calculations can the described behavior of the production and loss of fissile fuel in the various blankets be verified and determined exactly.

II.6. DESCRIPTION OF THE BURNUP CALCULATIONS PERFORMED

The aim of this investigation is to assess the influence of the different fuel materials UO_2, ThO_2, and Th^m in the radial blanket region on the blanket breeding properties and on the global reactor parameters of the LMFBR. Such an assessment requires two-dimensional burnup calculations.

II.6.a. Reference Conditions

For the burnup calculations, the reactor regions were partitioned as described above, and the mesh width selected was 5 cm in the core zones and 3 cm in the radial blanket zones. The burnup calculations were performed along the geometric R and Z axis of the reactor.

Among the first points to consider was the specification of a representative burnup reference condition for the core and the axial blanket. It was assumed to be the condition when the fuel isotopic compositions in the core and the axial blanket are in equilibrium. This condition was attained after repeated recycling and refueling of PuO_2/UO_2 fuel in the core and axial blanket regions, with UO_2 as reference fuel in the radial blanket region. At the end of each burnup cycle, the fuel of the inner core and axial blanket zones was unloaded, and the fuel in the outer core and axial blanket zones was shuffled into the adjacent inner zones; outer zone CZ3 and the corresponding axial blanket zones were supplied with fresh fuel. After three burnup cycles--each lasting for 292 full power days at 2420 MW(th)--the fuel was removed from the inner core and inner axial blanket zones, and the plutonium recovered from these two regions was subsequently mixed and recycled as fresh fuel into the outermost core zone CZ3. This procedure was continued until the composition Pu-vector of the fuel freshly charged into CZ3 attained equilibrium.

With the core and the axial blanket in equilibrium burnup condition, the radial blanket region was then supplied with fresh fuel: depleted UO_2, ThO_2, or Th^m. After sufficient burnup

reactivity was ensured for each of these reactor configurations, the core and the axial blanket were refueled after each burnup cycle as described above, while the fuel in the radial blanket remained in place for five burnup cycles.

Under these conditions, the radial breeding characteristics and the global reactor parameters were compared for the three blanket configurations. The results of these calculations are now being discussed.

II.6.b. Criticality Calculations

The influence on k_{eff} of the thorium blankets as compared to the UO_2 radial blanket is shown in Table II.10. A decrease in k_{eff} (from 1.0180 for the UO_2 blanket to 1.0147 for the ThO_2 blanket and to 1.0116 for the Th^m blanket) corresponds to a loss in k_{eff} of 0.324% and 0.629% for the two thorium blankets. In order to ensure sufficient burnup reactivity for the thorium blankets, the Pu enrichment in the core region was increased by iteration of k_{eff} for either blanket. Thus it was necessary to increase the fissile Pu inventory by 1.2% in the case of the ThO_2 blanket and by 2.43% for the Th^m blanket, as compared to the UO_2 blanket.

For maintaining a uniform power distribution in the core region, the increase in Pu enrichment was limited to CZ3, the core zone immediately adjacent to the radial blanket. For the ThO_2 blanket the enrichment of CZ3 had to be increased by 4.64%, and for the Th^m blanket by 9.63%.

Figure II.5 shows k_{eff} as a function of the blanket residence time for the three different radial blankets. A noticeable difference in k_{eff} between the blankets occurs after the fourth or fifth burnup cycle, but this can be easily compensated for by moving the control rods. For these burnup calculations, the control rods were assumed to be stationary. This accounts for the cyclic increase in k_{eff}, which can be ascribed to the continuous buildup of fissile fuel in the radial blankets.

Table II.10. Enrichments and fissile inventories of the core and axial blanket regions before and after k_{eff} iteration for various radial blankets.

Radial blanket configuration	Before k_{eff} iteration	After k_{eff} iteration					
	k_{eff} (t=0)	k_{eff} (t=0)	Pu^{fiss} enrichment (%)			Pu^{fiss*} inventory (core + ax) (kg)	
			CZ1	CZ2	CZ3		
UO_2	1.0180	1.0180	11.02	14.68	14.45	1855.0	
ThO_2	1.0147	1.0180	11.02	14.68	15.12	1877.0	
Th^m	1.0116	1.0180	11.02	14.68	15.84	1900.0	

*The axial blanket contains a small quantity of U235.

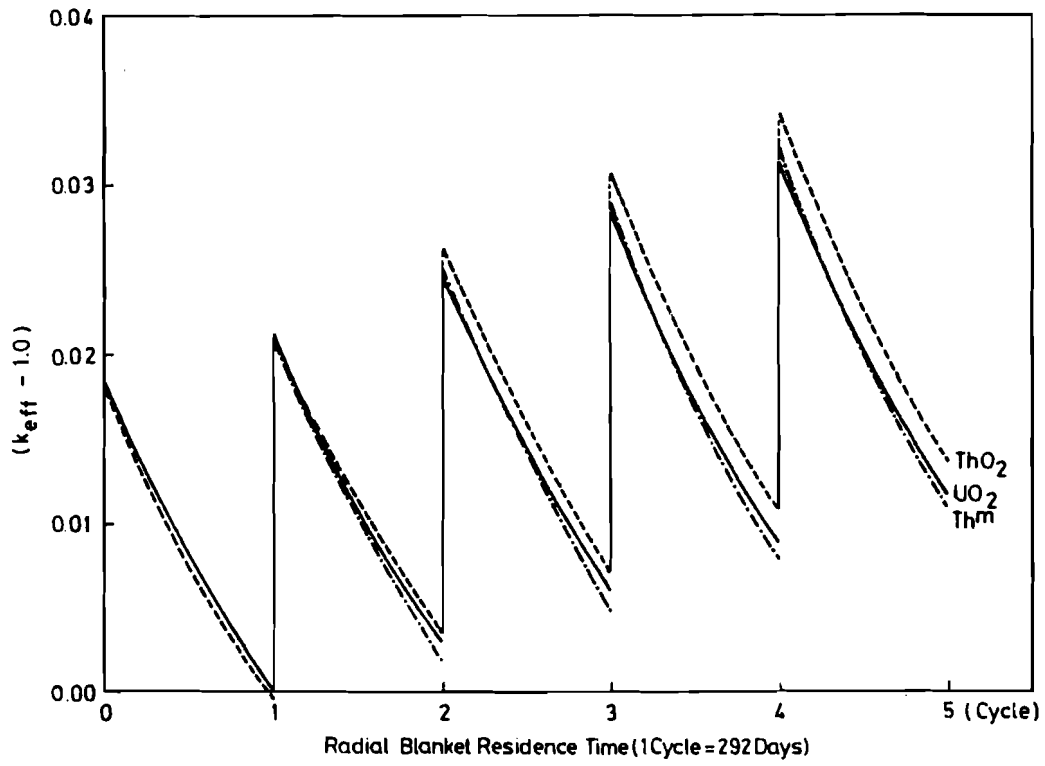

Figure II.5. k_{eff} as a function of the radial blanket residence time for an LMFBR with UO_2, ThO_2, and Th^m radial blankets (the core and the axial blanket are refueled after each cycle).

II.7. THE MAIN FACTORS INFLUENCING THE RADIAL BREEDING RATIO BR_r

Before the numerical results for the various radial blanket configurations are presented in Section II.8, it is useful to discuss in some more detail the various factors influencing the breeding characteristics of a radial blanket.

The breeding properties of a radial blanket are generally described by two parameters, the radial breeding ratio BR_r and the radial breeding gain G_r. Both are formally defined in Chapter I in terms of the cumbersome neutron reaction rates and the more useful global neutron parameters. Physically speaking, however, neither representation conveys a very clear understanding of how these factors influence the breeding characteristics of a blanket. The following discussion, therefore, focuses on neutron balances in a way similar to the approach taken in Section II.2.

The neutrons available for absorption in the blanket have been defined as the sum of the neutrons leaking into the radial blanket from the core region and of the neutrons generated in the blanket. There are basically four processes competing for these neutrons in the radial blanket: absorption by fertile fuel, absorption by self-bred fissile fuel, parasitic absorptions by structural material and other nonbreeding materials in the blanket, and leakage into the radial reflector. (Parasitic neutron absorptions and radial leakage losses are here defined as parasitic (neutron) losses.)

Assuming temporarily an ideal blanket condition, i.e. no neutrons are lost due to parasitic losses, and assuming that neutron absorption by self-bred fissile fuel is small, one can expect that practically all of the neutrons available are used for breeding, i.e. they are captured by fertile fuel. Since the radial breeding ratio BR_r is defined in terms of neutrons captured by fertile fuel in the radial blanket, BR_r is obviously directly proportional to the number of neutrons available, i.e. those leaking into the radial blanket from the core region and generated in the blanket. A larger neutron leakage and/or a larger neutron self-generation imply a larger BR_r. The

parameters determining leakage and self-generation are therefore relevant for comparing the radial breeding ratios BR_r of the various radial blankets.

How many neutrons leak into the radial blanket is determined by two factors independent of each other: the geometric design of a given FBR, and the neutron reflective properties of the particular radial blanket material. The geometric design is discussed in terms of the H/D ratio of the core design, and the neutron reflective properties are examined in terms of the blanket albedo β.

Self-generated neutrons result from fissions occuring in the fissile and fertile fuels[6]. The influence of fissile fission and fertile fission on the radial and global breeding ratios can be suitably illustrated in terms of two parameters, η_r^i, the number of neutrons released per radial fissile absorption, and $(\nu F)_r^J/A_N^I$, the contribution of radial fertile fission neutrons.

Since the latter parameter is shown to be a very sensitive function of the neutron spectrum prevailing in the radial blanket, its influence on BR_r is much more difficult to assess beforehand than that of η_r^i. A more convenient, but less concise, parameter representing the fast-fission component is the fast-fission cross section of the fertile isotope.

Thus the radial breeding ratio BR_r is determined by basically four parameters:

- -- the H/D ratio of the FBR core design,
- -- the albedo β of the blanket material,
- -- the neutron effectiveness of the bred fissile fuel, represented by η_r^i,
- -- the fertile-fission fission contribution of the radial blanket, represented by $(\nu F)_r^J/A_N^I$ or illustrated by cross section σ_f^J,

where the first two parameters determine the neutron leakage into, and the last two the neutron self-generation in the blanket.

---

[6] Fission in fertile fuel is referred to as fertile fission or fast fission; neutrons released by fertile fission are fertile-fission or fast-fission neutrons.

II.7.a. Neutron Leakage into the Radial Blanket: Influence of the H/D Ratio and the Albedo

Neutron leakage from the core region into the radial blanket is determined by the FBR core design, which is described by the H/D ratio, and by the neutron reflective properties of the radial blanket material.

Influence of the H/D Ratio on the Breeding Properties of the Radial Blanket

The geometric configuration or design of the FBR core determines essentially the directional leakage preference of neutrons originating in the core region and diffusing into the blanket regions that surround it. Safety- and thermohydraulic-related considerations require FBR designs with relatively flat, pancaked, cores. It can be shown that such designs with H/D ratios of 0.3 to 0.4 have a definite neutron leakage preference into the axial direction, or into the axial blanket, for that matter. This leakage preference was briefly demonstrated in Section II.2. There it was shown that 10 (or 62%) of a total of 16 core leakage neutrons scatter into the axial blanket, while only 6 (or 38%) scatter into the radial blanket region.

It has been argued that the radial breeding ratio BR_r is a direct function of the neutron leakage into the blanket. One should therefore expect a distinct correlation between the H/D ratio and BR_r. This is shown to be the case in Table II.11, in which H/D, BR_N, and BR_r are listed for some current FBR designs. BR_r clearly increases with increasing H/D, even though not all of the FBRs have the same blanket thickness[7]. In addition, the data demonstrate that there is a definite correlation between the H/D ratio and the BR_r/BR_N ratio (see last

---

[7] The radial blanket thickness determines the reflector leakage component of the parasitic neutron losses. In the case of a thick blanket, only a few neutrons are lost due to leakage into the reflector. Such leakage losses can be quite significant if the radial blankets are not sufficiently thick and in FBR designs with small cores (i.e. SNR 300), where the contribution of the blanket breeding ratios is very important. In the latter case, the reflector leakage losses must be kept small (see discussion in Section II.9.b).

Table II.11. Influence of the H/D_c ratio on the radial breeding ratio BR_r and on the ratio of radial and global breeding ratios (BR_r/BR_N).

FBR type	H/D_c	Breeding ratios BR_N	Breeding ratios BR_R	$\frac{BR_r}{BR_N}$ (%)
SNR-2*				
Carbide	0.240	1.35	0.20	15
Oxide	0.273	1.22	0.22	18
LMFBR**	0.31	1.36	0.24	17.6
GCFBR***				
GGA	0.40	1.43	0.32	22.4
KFK	0.40	1.32	0.33	25

*H. Spenke, personal communication, Interatom, Bensberg, F.R.G. (1974).

**Values based on General Electric, GEAP 5678 (1968).

***Kernforschungszentrum Karlsruhe, KFK 1375 (1971).

column in Table II.11). For example, BR_r/BR_N increases from 15-18% for designs with low H/D ratios of 0.24-0.31 to 22-25% for designs with high H/D ratios of 0.40, which indicates a larger neutron leakage component into the radial direction as the H/D ratio increases. Changing the H/D ratio will therefore change the contribution of the radial breeding ratio BR_r. This fact is relevant to the discussion in Chapter IV.

Currently, the H/D ratio of the FBR is limited to a narrow range by safety and thermohydraulic considerations. These considerations will most likely prevail in the coming decade of FBR development. A detailed assessment of the influence of the H/D ratio on FBR performance, especially as regards the radial breeding ratio in connection with different radial blanket materials, is therefore not attempted here. At this point, one observation is in order, however: the differences in the relevant reactor parameters, due to the different blanket fuel materials, are amplified as the H/D ratio increases. This should

be kept in mind when comparing numerical results of this investigation with those of similar assessments for FBRs with larger H/D ratios, e.g. gas-cooled FBRs with H/D ≃ 0.40.

The axial leakage preference due to the H/D ratio can partly be compensated for by changing the fissile fuel enrichment in the core zone adjacent to the radial blanket. Usually, the enrichment in this core zone is already increased for the purpose of power flattening. If the enrichment should be increased even further, enhanced neutron leakage into the radial blanket will result on account of the larger neutron flux gradient at the core-blanket interface. This is expected for the thorium blankets, since the enrichment in core zone CZ3 was increased in both cases.

The Albedos of UO_2, ThO_2, and Th^m Radial Blankets

Since the H/D ratio remains the same throughout this investigation, neutron leakage into the radial blanket is basically determined by the neutron reflective property, or albedo β, of the UO_2, ThO_2, and Th^m blanket fuel materials. The radial breeding ratios BR_r are thus expected to be inversely proportional to the β values of the radial blanket materials. According to diffusion theory, the albedo β of a reflector, which in this case is the radial blanket, can be derived for a slab in the one-group theory as follows:

$$\beta = \frac{1 - 2\,D_c/S}{1 + 2\,D_c/S} \quad , \qquad \text{(II-1)}$$

where S is the reflector saving, given by

$$S = (D_c/D_B)L_B \tanh(a/L_B) \quad ; \qquad \text{(II-2)}$$

D_B, D_C are the diffusion coefficients in the blanket and in the core, a is the blanket thickness, and L_B the diffusion length in the blanket, approximated by

$$L_B^2 = D_B/(\Sigma_a - \nu \Sigma_f) \quad . \tag{II-3}$$

L_B is corrected by the neutron production $\nu \Sigma_f$.

Using the one-group data listed in Table II.12 of the blanket mixtures investigated here, the albedo values can be calculated for fresh radial blankets of infinite and finite (e.g. 26.7 cm of the present blanket) thickness. These values are listed in Table II.13.

The UO_2 blanket is shown to have the highest albedo β of 0.742, and hence the best neutron reflective properties among the blankets considered. It is closely followed by the ThO_2 blanket with β = 0.729 and the Th^m blanket with β = 0.678. The reflectivity of the ThO_2 blanket is less by 1.8%, compared to that of the UO_2 blanket, and the β of the Th^m blanket is less by 8.6%. The superior reflective property of UO_2 is clearly due to the larger fast-fission contribution and the small U235 concentration remaining in depleted uranium, 0.25% in this study. (Compare the data with and without fast fission in Table II.13.) The considerably lower β for the Th^m blanket is principally due to the much harder neutron spectrum in a metal blanket. For this particular case, backscattering of neutrons is reduced on account of the larger neutron diffusion coefficient D_B.

Thus, on the basis of albedo comparisons, the following differences between the three radial blankets can be anticipated:

- -- a larger neutron leakage into the ThO_2 and Th^m blankets than into the UO_2 blanket, on account of the smaller β values,
- -- the necessity of increasing the fissile fuel enrichment of the core region in both thorium blankets,
- -- the largest enrichment increase in the case of the Th^m blanket due to its smallest β,
- -- a larger BR_r for both ThO_2 and Th^m blankets on account of their lower β values, with the Th^m blanket showing the largest increase,
- -- redistribution of the region breeding ratios BR_n.

Table II.12. One-group data of fresh radial blankets.

One-group data		Radial blanket		
		UO_2	ThO_2	Th^m
D_B	(cm)	1.327	1.189	1.500
Σ_a	(cm^{-1})	.00459	.00471	.00546
$\nu\Sigma_f$	(cm^{-1})	.00157	.000283	.000307

Table II.13. One-group albedos β of fresh radial blankets.

Radial blanket thickness = ∞			Radial blanket thickness = 26.7 cm		
Radial blanket	β		Radial blanket	β	
	with fast fission	without		with fast fission	without
UO_2	.755	.730	UO_2	.742	.709
ThO_2	.746	.740	ThO_2	.729	.723
Th^m	.701	.693	Th^m	.678	.672

II.7.b. Production of Neutrons in the Radial Blanket

There are two sources of neutron self-generation in the radial blanket: the neutrons released as a result of fission in the blanket-bred fissile fuel, and the neutrons released as result of fertile fission. Their influence on BR_r and BR_N can be illustrated in the case of the fissile-induced neutrons by the η_r^i value of the bred fissile isotope(s), and in the case of the fertile-induced neutrons by $(\nu F)_r^J/A_N^I$, the fertile-fission neutron contribution in the radial blanket.

The Energy-Dependent $\eta^i(e)$ for Various Fissile Isotopes in the LMFBR Neutron Spectrum

The number of neutrons released per fissile neutron absorption η is one of the most important parameters with regard to the breeding ratio of any reactor type. Figure II.6 shows the energy-dependent η^i of various fissile isotopes for the core neutron spectrum of the LMFBR investigated.

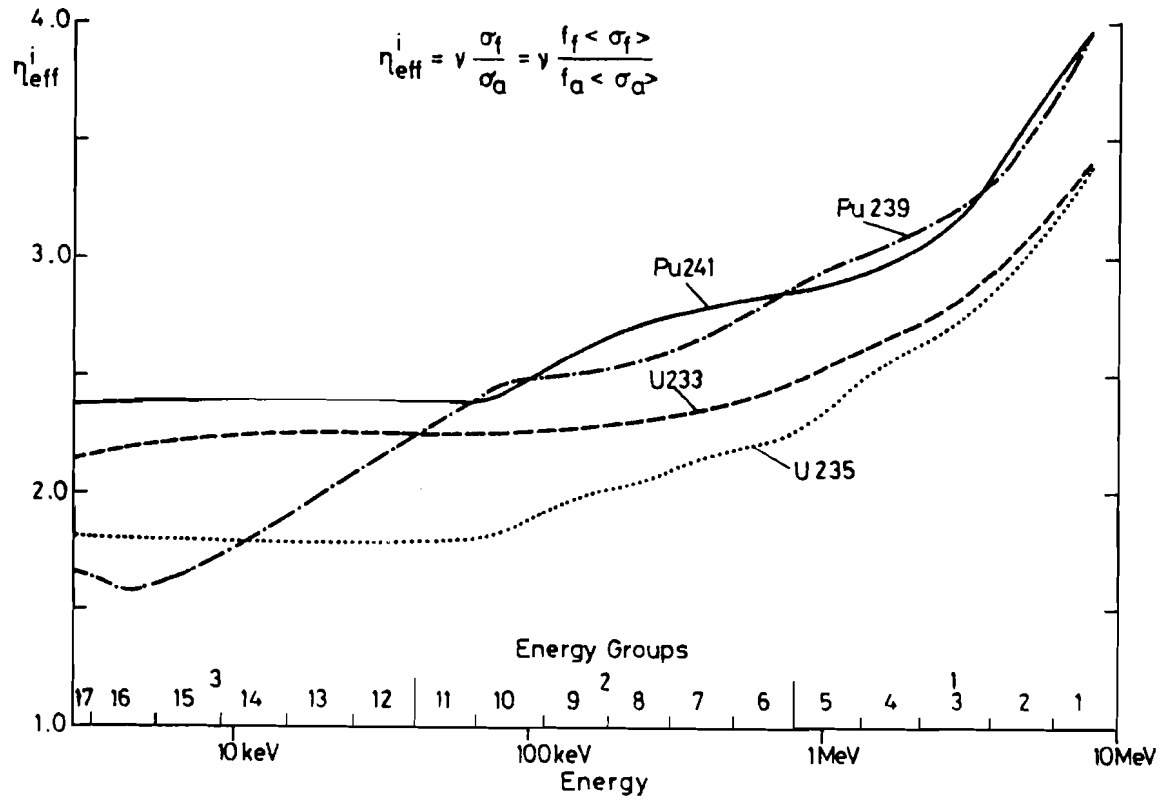

Figure II.6. η^i of different fissile isotopes for the LMFBR spectrum (ENDF/B-III data).

The average neutron energy in the core zones of an oxide-fueled LMFBR is about 80-100 keV. In this energy range, the fissile isotopes Pu239 and Pu241 have considerably larger η^i values than the corresponding uranium fissile isotopes U233 and U235. Much higher global breeding ratios BR_N are therefore attainable in FBRs with Pu as fissile fuel in the core region. This is partly why Pu239/Pu241 is chosen as fissile fuel for all FBR designs.

The neutron spectra in the blanket regions of an FBR are considerably softer than the spectrum in the core region. This is due to the fact that the core leakage neutrons are degraded in energy as they are diffusing into the blanket region.

In the mean neutron energy range of an oxide radial blanket (10-40 keV), U233 clearly has the larger η^i value than Pu239. This advantage of U233 increases as the neutron spectrum becomes even softer.

The U233 bred in a thorium blanket will therefore have a more positive influence on the radial and global breeding ratios than the Pu239 bred in a UO_2 blanket[8].

η_N^I, weighted over all N FBR regions and all I fissile isotopes, is therefore expected to be larger in the case of the thorium blankets than for the UO_2 blanket.

The Fast-Fission Effect in the Radial Blanket

The importance of fast fission for the global breeding ratio BR_N is discussed in detail in Section II.9.b, comparing the global nuclear parameters of Equation (I-15) for various FBR designs. Since the fast-fission contribution strongly depends on the prevailing neutron spectrum--as can be readily inferred from the threshold fast-fission cross sections of U238 and Th232 in Figure II.4--BR_N is also dependent on the neutron spectrum.

---

[8] The fissile fuel bred in the blankets is almost exclusively pure Pu239 or U233, e.g. the vector for a UO_2 radial blanket is Pu239/Pu240/Pu241/Pu242 = 92.36/7.32/0.30/0.02, and the vector for ThO_2 is U233/U234/U235/U236 = 96.17/3.55/0.27/0.

Most of the fast fissions occur in the core region of the FBR, where the neutron spectrum is hardest. The blanket regions supply only few fast-fission neutrons. In the FBR investigated, 21.45 out of 100 neutrons generated throughout the reactor are fast-fission neutrons, 18.42 (86%) of which are generated in the core region and 1.05 (only 5%) in the radial blanket region. This indicates that a change in the neutron spectrum of the core region, such as the use of a different fertile isotope, will have a profound impact on the total fast fission and thus on BR_N, whereas this impact will be considerably less if such change occurs in the radial blanket region. A different fertile fuel or neutron spectrum degradation in the radial blanket will affect the total fast fission only insignificantly and is expected to have little influence on BR_N.

The fast-fission cross section of Th232 has been shown to be about four to five times smaller than that of U238. Thus the fast-fission contribution of the radial blanket will still be even smaller if the U238 there is replaced by Th232.

This explains why a thorium blanket, in comparison with the UO_2 blanket, is expected to exhibit superior nuclear properties as regards the breeding of U233 as fissile fuel, but less favorable properties as regards the fast-fission contribution. Which of the two opposing trends come to dominate the total neutron production can only be determined by detailed burnup calculations.

II.8. COMPARISON OF THE BREEDING PROPERTIES OF UO_2, ThO_2, AND Th^m RADIAL BLANKETS

The breeding properties of radial blankets have been said to be described by two parameters, the radial breeding ratio BR_r and the radial breeding gain G_r. BR_r was discussed in the previous section, and this section focuses on the breeding gain G_r.

Table II.14. Region-dependent global neutron parameters for the LMFBR with various radial blankets as a function of the radial blanket residence time.

Radial blanket residence time (days)	Reactor averaged		Core					Axial blanket				
	$(1+\alpha)^I_N$	$(1-\epsilon_N)$	BR_c	$(1-\epsilon_c)$	δ_c	$(1+\alpha)^I_c$	G_c	BR_{ax}	$(1-\epsilon_{ax})$	δ_{ax}	$(1+\alpha)^I_{ax}$	G_{ax}
UO_2 blanket												
0	1.2436	.7870	.8528	.8055	.939	1.238	-.1022	.3705	.5736	.0458	1.363	.3268
219	1.2528	.7912	.8023	.8030	.893	1.243	-.0958	.3723	.7220	.0789	1.354	.2919
803	1.2575	.7934	.7654	.8030	.861	1.242	-.0951	.3552	.7140	.0743	1.356	.2820
1387	1.2609	.7960	.7347	.8035	.832	1.242	-.0928	.3403	.7088	.0700	1.366	.2740
ThO_2 blanket												
0	1.2428	.7930	.8498	.8056	.952	1.238	-.1114	.3690	.5716	.0459	1.3648	.3279
219	1.2478	.7970	.8000	.8028	.902	1.242	-.1031	.3713	.7190	.0794	1.3542	.2921
803	1.2400	.8060	.7540	.8032	.858	1.241	-.1011	.3494	.7123	.0731	1.3548	.2787
1387	1.2321	.8128	.7151	.8031	.819	1.240	-.0993	.3316	.7070	.0680	1.3545	.2670
Th^m blanket												
0	1.2398	.7921	.8400	.8054	.951	1.236	-.1216	.3667	.5714	.0456	1.3606	.3247
219	1.2456	.7959	.7958	.8026	.904	1.240	-.1106	.3712	.7182	.0792	1.3520	.2911
803	1.2283	.8039	.7569	.8026	.861	1.239	-.1090	.3530	.7113	.0753	1.3517	.2780
1387	1.2298	.8092	.7211	.8027	.831	1.238	-.1083	.3364	.7057	.0692	1.3520	.2687

$W^F_N(UO_2$ blanket) = 1.071 g/MW(th)d, $W^F_N(ThO_2$ blanket) = 1.070 g/MW(th)d.

Radial blanket residence time (days)	Reactor averaged		Radial blanket					Reactor			
	$(1+\alpha)_N^I$	$(1-\epsilon_N)$	BR_r	$(1-\epsilon_r)$	δ_r	$(1+\alpha)_r^I$	G_r	$\sum_n^N G_n$	G_N*	$\sum_n^N BR_n$	BR_N*
UO_2 blanket											
0	1.2436	.7870	.2280	.3086	.0151	1.3395	.2169	.4415	.4418	1.4513	1.4515
219	1.2528	.7912	.2180	.6102	.0285	1.3460	.1927	.3888	.3896	1.3926	1.3931
803	1.2575	.7934	.2310	.7546	.0647	1.3702	.1636	.3509	.3524	1.3516	1.3532
1387	1.2609	.7960	.2412	.7948	.0981	1.3560	.1365	.3176	.3176	1.3162	1.3164
ThO_2 blanket											
0	1.2428	.7930	.2357	0	.0025	-	.2323	.4488	.4481	1.4545	1.4547
219	1.2478	.7970	.2235	.8609	.0190	1.1385	.2037	.3927	.3913	1.3948	1.3933
803	1.2400	.8060	.2421	.9372	.0697	1.1323	.1681	.3457	.3437	1.3455	1.3439
1387	1.2321	.8128	.2537	.9460	.1133	1.1287	.1331	.3008	.2991	1.3004	1.2987
Th^m blanket											
0	1.2398	.7921	.2310	0	.0032	-	.2367	.4398	.4398	1.4477	1.4478
219	1.2456	.7959	.2283	.8000	.0166	1.1118	.2115	.3920	.3910	1.3953	1.3944
803	1.2283	.8039	.2455	.9172	.0593	1.1067	.1822	.3512	.3498	1.3554	1.3543
1387	1.2298	.8092	.2585	.9340	.0999	1.1062	.1540	.3144	.3136	1.3160	1.3151

*Results of burnup calculations.

II.8.a. Parameters Determining the Radial Breeding Gain G_r

The radial breeding gain G_r, or radial buildup, was derived in Chapter I in terms of global neutron parameters, such that

$$G_r = BR_r \, (1+\alpha)_N^I \, (1-\varepsilon_N) - (1+\alpha)_r^I \, \delta_r \, (1-\varepsilon_r) \quad . \qquad \text{(II-4)}$$

production of fissile fuel — loss of fissile fuel

The first term in the equation represents the production of fissile fuel, and the second term the consumption, or loss, of fissile fuel, in the radial blanket.

Regarding the first term, the global neutron parameters $(1+\alpha)_N^I$ and $(1-\varepsilon_N)$ primarily depend on the neutron characteristics of the core region. The fissile isotope production term is thus largely determined by the radial breeding ratio, which in turn is governed by the neutron leakage into and the neutron production in the blanket, as discussed previously.

The second term, or loss term, in the equation is primarily a function of the absorption cross section of the fissile fuel bred in the blanket. This loss term is expected to be larger for the thorium blankets than for the UO_2 blanket, on account of the larger absorption cross section of U233 than of Pu239.

Since the thorium blankets are expected to exhibit fissile fuel losses offsetting the larger fissile fuel production--both terms being larger than in the case of a UO_2 blanket--the trend of G_r for the thorium blankets is difficult to assess beforehand, especially without burnup calculations.

Burnup calculations are also needed to verify the negligible parasitic neutron losses previously assumed for all blankets.

II.8.b. G_r for the UO_2, ThO_2, and Th^m Blankets

The relevant global neutron parameters $(1+\alpha)_n^I$, $(1-\varepsilon_n)$, δ_n, BR_n, and G_n for the core, axial blanket, and radial blanket regions of the FBR investigated are listed in Table II.14. They

are given as functions of the residence times of the UO_2, ThO_2, and Th^m radial blankets. The neutron parameters $(1+\alpha)_n^I$, $(1-\varepsilon_n)$, and δ_n were calculated by means of the normalized, region- and isotope-dependent reaction rates extracted from the burnup calculations. The corresponding fertile and fissile isotope-dependent absorption, capture, and fission rates are found in Table II.A.1 in Appendix II.A.

On the basis of the data in Table II.14, the fissile fuel production and loss terms of the radial breeding gain G_r of Equation (II-4) can be calculated for each blanket configuration as a function of the blanket residence time. The numerical results in Table II.15 are illustrated by Figure II.7.

As has been expected, the production of fissile fuel is indeed larger for each thorium blanket than for the UO_2 blanket, and is highest for the Th^m blanket. The differences, in percent, between the thorium blankets with respect to the UO_2 blanket are plotted in Figure II.8: the ThO_2 fissile production appears to approach an asymptotic value of 5%, whereas that of the Th^m blanket increases from 4.5% to 6%.

The loss of bred fissile fuel due to absorption (Figure II.7) is shown to be largest for the ThO_2 blanket, less for the UO_2 blanket, and least for the Th^m blanket. The large loss in the ThO_2 blanket can be clearly ascribed to the absorption cross section of U233 (which has been shown to be 30-35% larger than that for Pu239). According to Figure II.8, the loss of U233 in the ThO_2 blanket approaches a value 16% higher than that of Pu239 in the UO_2 blanket, while that of the Th^m blanket is smaller throughout the full residence time.

The highest radial breeding gain G_r (Figure II.7) is obtained with the Th^m blanket, followed by the ThO_2 blanket, for residence times of less than four cycles. For longer residence times, G_r of the UO_2 blanket slightly increases, compared to the ThO_2 blanket. Since the residence time of a radial blanket is normally limited to between three and four cycles, a ThO_2 blanket can be expected to have a somewhat higher breeding gain than a UO_2 blanket.

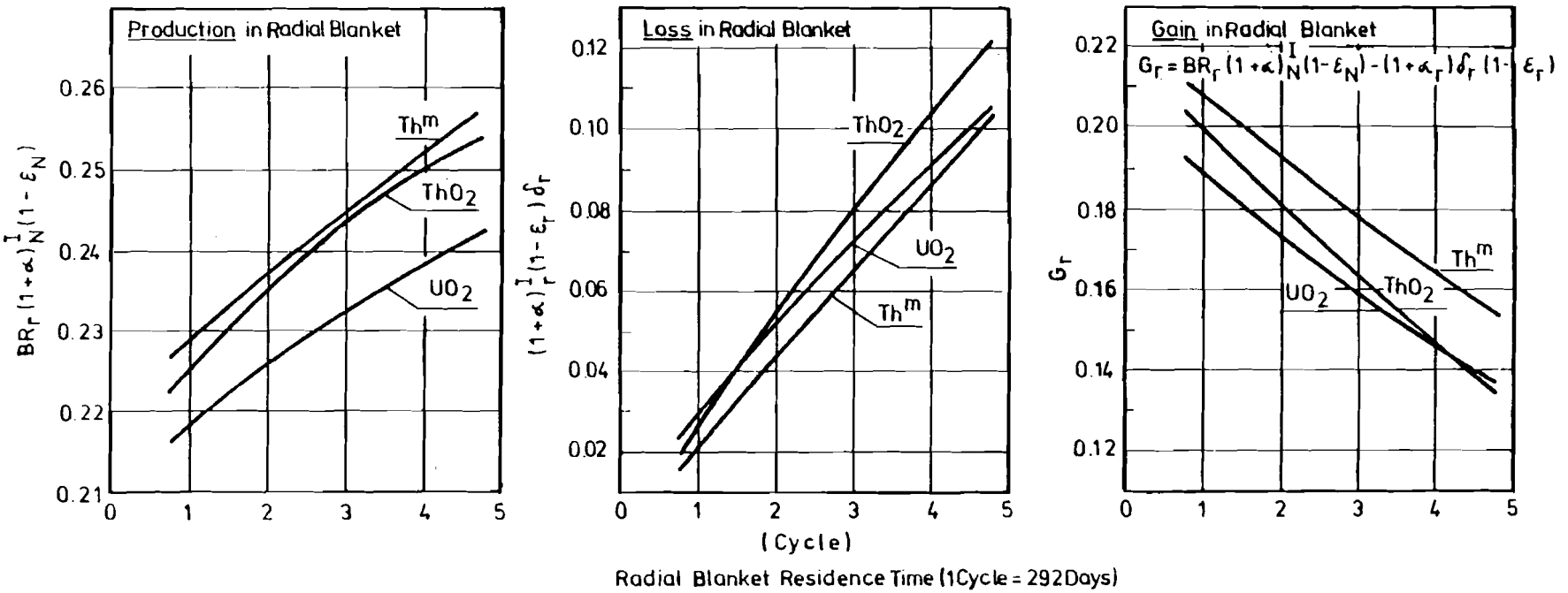

Figure II.7. Production, consumption or loss due to absorption, and surplus or breeding gain of fissile fuel in various radial blankets as a function of the radial blanket residence time.

Table II.15. Production and loss of fissile fuel and radial breeding gain for various radial blankets.

Radial blanket residence time (days)	Fissile fuel production*	Fissile fuel loss**	Radial breeding gain G_r
UO_2 blanket			
219	0.2161	0.0234	0.1927
803	0.2305	0.0669	0.1636
1387	0.2421	0.1057	0.1364
ThO_2 blanket			
219	0.2223	0.0186	0.2037
803	0.2420	0.0740	0.1680
1387	0.2541	0.1210	0.1331
Th^m blanket			
219	0.2263	0.0148	0.2115
803	0.2424	0.0602	0.1822
1387	0.2573	0.1032	0.1540

*Fissile fuel production in radial blanket: $BR_r(1+\alpha)\frac{I}{N}(1-\varepsilon_N)$.

**Fissile fuel loss in radial blanket: $(1+\alpha)\frac{I}{r}\delta_r(1-\varepsilon_r)$.

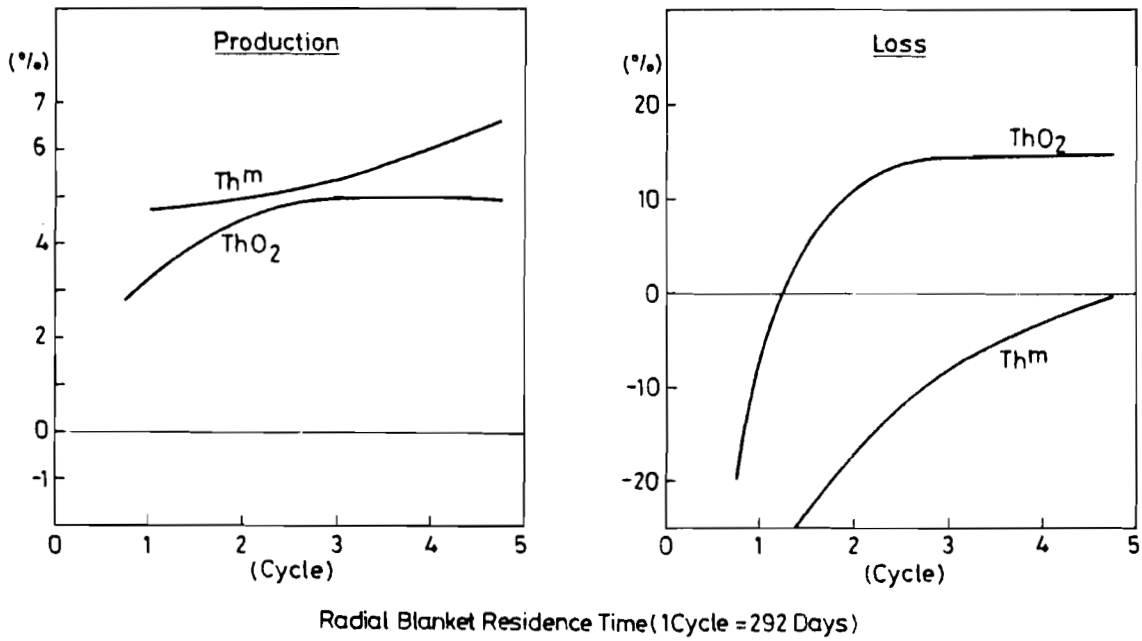

Figure II.8. Production and loss of fissile fuel in thorium blankets, given as differences in percent, with respect to the UO_2 blanket, as functions of the radial blanket residence time.

Note that the residence time of the radial blanket is determined by either the maximum permissible linear rod power achieved by the radial blanket fuel rods directly adjacent to the core region, or the maximum permissible neutron fluence of the cladding of the second blanket row, or by economic considerations. The limitations these effects may have on the blanket residence time are not specifically addressed here.

II.8.c. Influences of UO_2, ThO_2, and Th^m Blankets on BR_r, $B_{c,ax}$, BR_N, $G_{c,ax}$, and G_N

Table II.16 lists the FBR region-dependent breeding ratios and breeding gains for each different blanket configuration as a function of the radial blanket residence time. These data are depicted in Figures II.9 and II.10 as differences in percent between the thorium blankets and the reference UO_2 blanket. As previously noted, the radial breeding gains G_r of the thorium blankets are above the UO_2 blanket breeding gain, between 9.5% and 12.5% for the Th^m blanket and between 5.5% above and 2% below for ThO_2, depending on the blanket residence time (Figure II.9b).

As can be seen from Figure II.9c, the increase in the thorium blanket radial breeding gain reduces $G_{c,ax}$, the sum of the breeding gains of the core and the axial blanket. $G_{c,ax}$ of the Th^m blanket is smaller by 8-11.5% compared to $G_{c,ax}$ of the UO_2 blanket; for the ThO_2 blanket it is smaller by 3.5-7.2% than for the UO_2 blanket. The overall breeding gain G_N (Figure II.9a) in the case of a Th^m blanket then ranges from approximately 1% above to 0.5% below that of the UO_2 blanket, while for the ThO_2 blanket it is as much as 5% below that of the UO_2 blanket. This shift in region gains, favoring the radial breeding gain of the Th blankets, is explained by a redistribution in the region dependent breeding ratios. Figures II.10a, b, c show these differences in percent. BR_r for the Th blankets increases from 5% to 7% for the Th^m blanket and from 2.5% to 5.3% for the ThO_2 blanket, with respect to the UO_2 blanket. This increase in BR_r is at the expense of $BR_{c,ax}$, with the result that the global

Table II.16. Region-dependent breeding ratios BR_n and breeding gains G_n for the LMFBR with various radial blankets, as a function of the blanket residence time.

Radial blanket residence time (days)	Breeding ratio			Breeding gain		
	BR_N	BR_r	$BR_{c,ax}$	G_N	G_r	$G_{c,ax}$
UO_2 blanket						
219	1.3926	0.2180	1.1746	0.3888	0.1927	0.1961
803	1.3916	0.2310	1.1206	0.3509	0.1636	0.1873
1387	1.3162	0.2412	1.0750	0.3176	0.1365	0.1811
ThO_2 blanket						
219	1.3948	0.2235	1.1713	0.3927	0.2037	0.1890
803	1.3455	0.2421	1.1034	0.3457	0.1681	0.1776
1387	1.3004	0.2537	1.0467	0.3008	0.1331	0.1677
Th^m blanket						
219	1.3953	0.2283	1.1670	0.3920	0.2115	0.1805
803	1.3554	0.2455	1.1099	0.3512	0.1822	0.1690
1387	1.3160	0.2585	1.0575	0.3144	0.1540	0.1604

breeding ratio BR_N in the case of the Th^m blanket exhibits no significant difference from that of the UO_2 blanket (a slight increase by 0.5%), and the difference in BR_N between the ThO_2 blanket and the UO_2 blanket decreases from +0.25% to -1.25%, depending on the radial blanket residence time.

These observations serve to illustrate that the use of thorium in the FBR radial blanket causes a shift in the distribution of the region breeding ratios, in the sense that the radial breeding ratio BR_r is somewhat increased at the expense of the core and axial breeding ratios $BR_{c,ax}$. The global breeding ratio BR_N changes only insignificantly, however. Table II.17 reproduces the region-dependent discharge excess fissile fuel of the FBR investigated, averaged over five burnup cycles of the radial blanket.

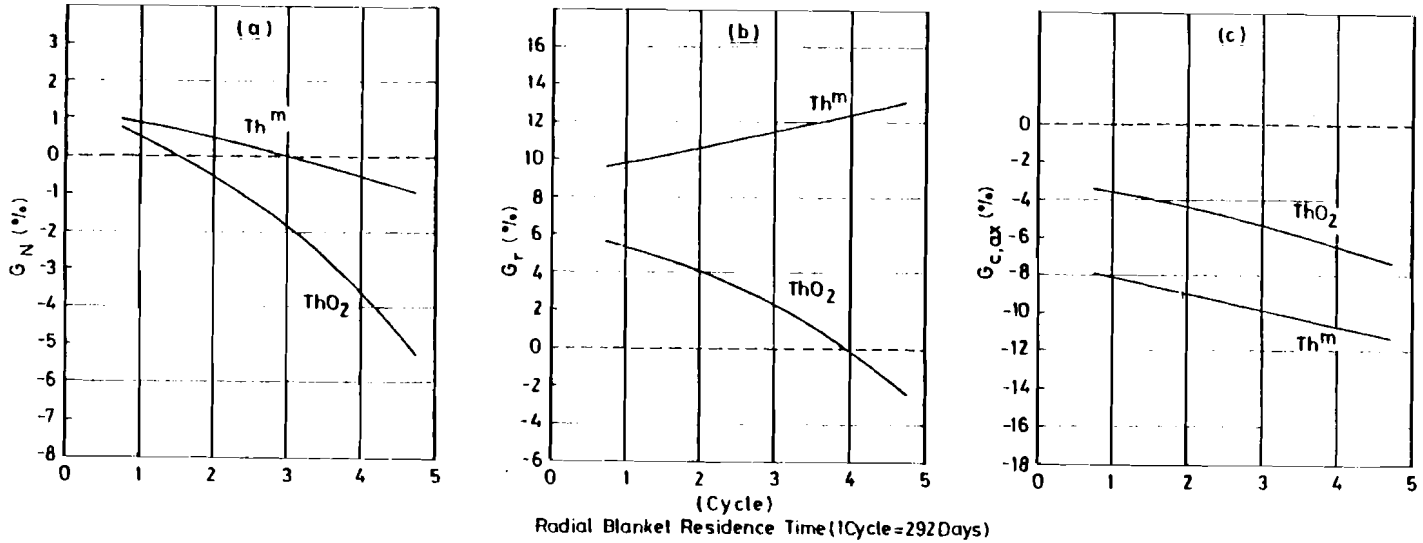

Figure II.9. Differences (%) in breeding gains G_N, G_r, and $G_{c,ax}$ of the thorium blankets compared to the UO_2 blanket, as a function of the radial blanket residence time.

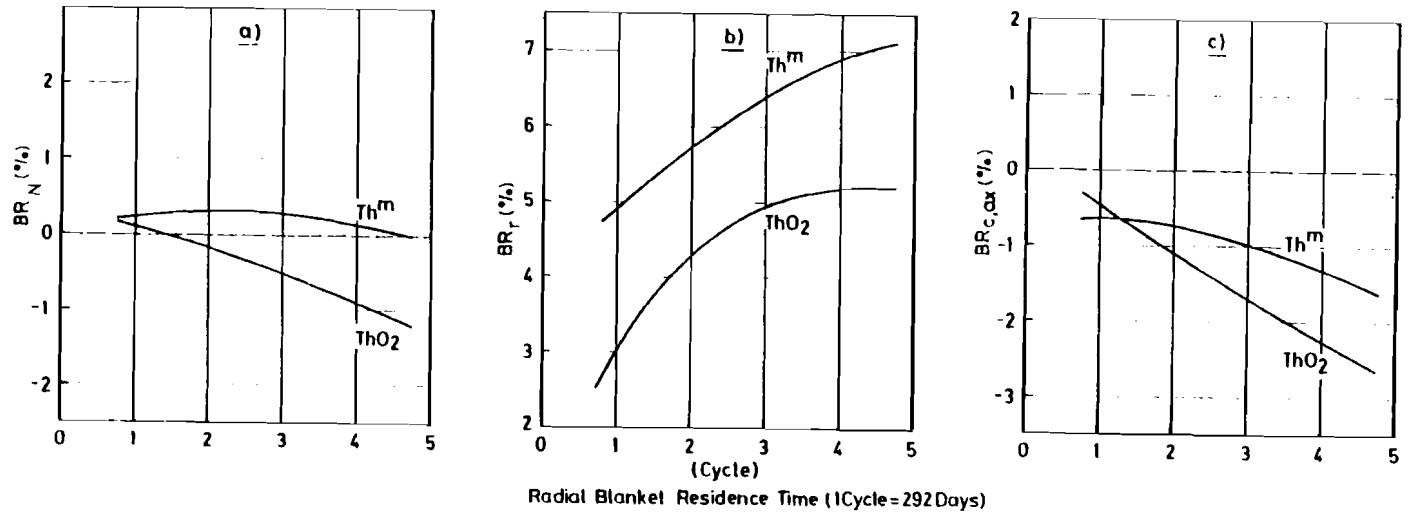

Figure II.10. Differences (%) in breeding ratios BR_N, BR_r, $BR_{c,ax}$ of the thorium blankets compared to the UO_2 blanket, as a function of the radial blanket residence time.

Table II.17. Discharged (or unloaded) excess fissile fuel averaged over five cycles, per GW(e).

Radial blanket	Discharged fissile fuel* (kg/yr)**		
	Core and axial blanket	Radial blanket	Reactor
	Pu239/Pu241	Pu239 or U233	Pu^{fiss}_{+U233}
UO_2	128.4	122.2	250.6
ThO_2	120.0	122.4	242.4
Th^m	114.4	131.6	246.4

*1 year = 292 days = 1 cycle.
**Includes unloaded U235

Here, the same characteristics are observed as for G_r, $G_{c,ax}$, and G_N. According to the first column in the table, less excess Pu239/Pu241 is unloaded from the core and axial blanket regions in the case of the thorium blankets; but more fissile fuel is at the same time discharged from the radial blankets[9]. The total excess fissile fuel discharged is slightly less for either thorium blanket: 250.6 kg/yr for the UO_2 blanket, 246.4 kg/yr for the Th^m blanket, and 242.4 kg/yr for the ThO_2 blanket (or 1.68% less for the Th^m blanket and 3.27% less for the ThO_2 blanket).

II.9. THE GLOBAL BREEDING RATIO BR_N

In connection with the above discussion on the impact of radial thorium blankets on the region-dependent breeding ratios BR_n, it is of interest to examine in more detail the effects responsible for the change in BR_N when the UO_2 blanket is replaced by thorium blankets.

[9] The reasonable assumption made here is that Pa233 decays completely to U233.

Table II.18. LMFBR global nuclear parameters for different radial blanket configurations as a function of the radial blanket residence time.

Radial blanket residence time (days)	$(\nu F)^J_N$	A^I_N	F^J_N	P_N	P_N = (L + St + FP + M + R + C)						η^I_N	$\frac{(\nu F)^J_N}{A^I_N}$	η_B	$P+F^J_N$	BR^*_N	BR^{**}_N
					L	St	FP	M	R	C						
UO_2 blanket																
0	.2145	.3398	.0725	.1093	.02636	.04265	.0129	.0055	.00422	.0177	2.3646	.6312	2.9958	.1818	1.4512	1.4515
219	.2108	.3414	.07114	.1205	.0265	.0432	.0303	.0055	.0044	.0106	2.3430	.6175	2.560	.1916	1.3927	1.3930
803	.2070	.3457	.0706	.1277	.0309	.0433	.0294	.0054	.0043	.0143	2.3358	.5988	2.9346	.1983	1.3527	1.3532
1387	.2058	.3494	.0696	.1373	.0350	.0433	.0294	.0053	.0042	.0200	2.3312	.5890	2.9202	.2069	1.3160	1.3164
ThO_2 blanket																
0	.2088	.34139	.07054	.1063	.0243	.0417	.0129	.0057	.00428	.0176	2.3700	.6117	2.9817	.1768	1.4545	1.4547
219	.2022	.34284	.0693	.11595	.02487	.0423	.0306	.00546	.0045	.0076	2.3494	.5898	2.9392	.1852	1.3947	1.3933
803	.2966	.3492	.0668	.1267	.02990	.0422	.0200	.00536	.0043	.0154	2.3455	.5630	2.9085	.1935	1.3457	1.3439
1387	.1919	.3546	.0648	.1378	.0344	.04203	.0238	.0052	.0041	.022	2.3424	.5410	2.8834	.2026	1.2992	1.2987
Th^m blanket																
0	.20946	.34077	.07077	.1108	.0308	.0402	.0126	.0052	.00427	.0176	2.3752	.6254	2.9906	.1816	1.4476	1.4479
219	.20357	.34105	.06972	.1191	.03085	.0409	.0302	.0053	.0045	.0070	2.3560	.5969	2.9529	.1888	1.3953	1.3944
803	.1993	.3459	.06776	.1288	.03603	.0406	.0286	.0051	.00432	.0138	2.3552	.5762	2.9314	.19656	1.3552	1.3543
1387	.19518	.3505	.0659	.13863	.04092	.0402	.02784	.0049	.00416	.0201	2.3549	.5567	2.9116	.2045	1.3161	1.3151

*Determined by Equation (II-5).
**Results of burnup calculations.

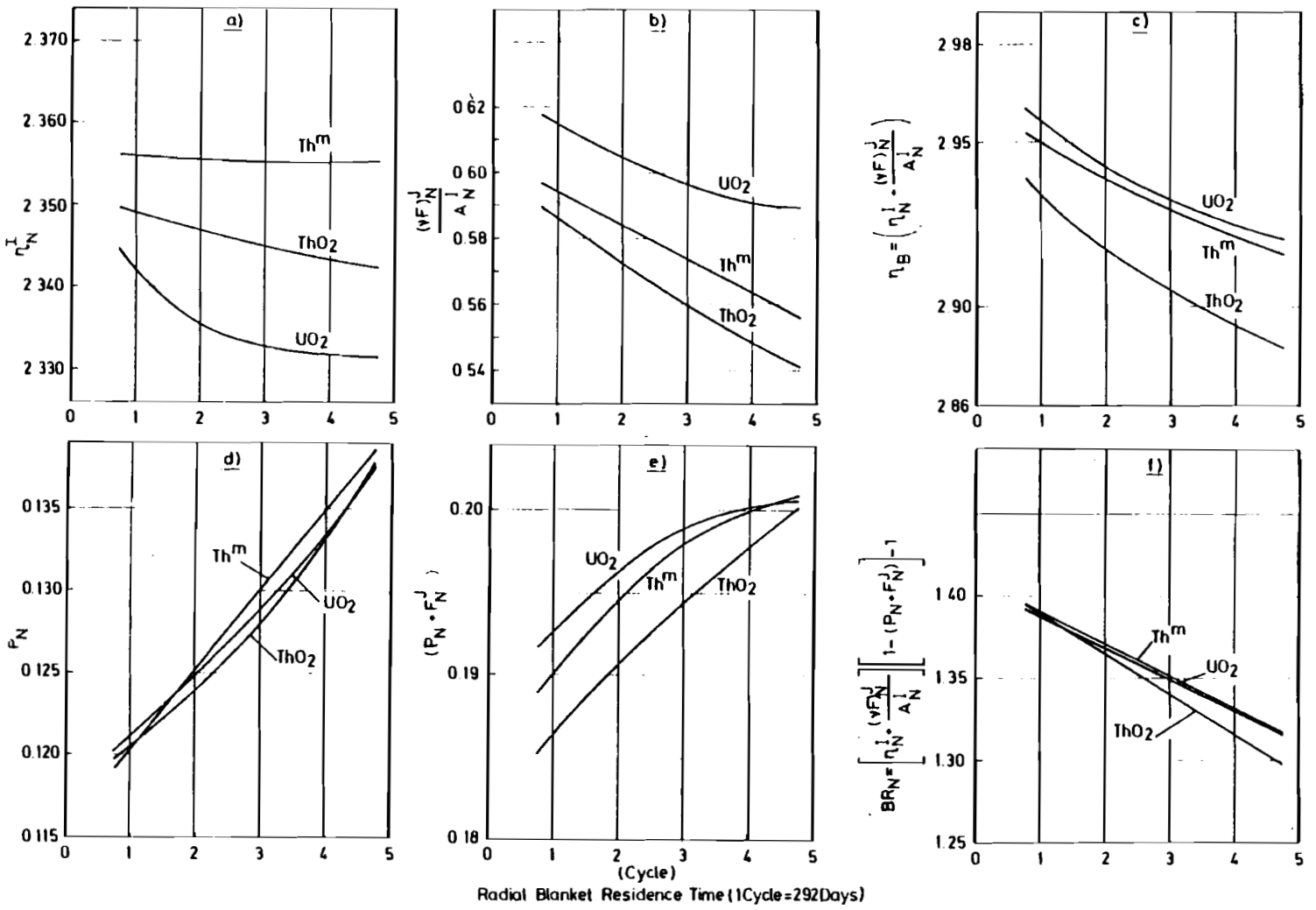

Figure II.11. LMFBR global nuclear parameters for various radial blankets as a function of the radial blanket residence time.

This can best be analyzed and illustrated by comparing the global nuclear parameters η_N^I, P_N, etc. for the various reactor configurations. Recall that these parameters have also been recommended as reference parameters for comparing different FBR designs with respect to the global breeding ratio BR_N. The relevant relation was derived in Appendix I:

$$BR_N = \left(\eta_N^I + \frac{(\nu F)_N^J}{A_N^I} \right) \left[1 - (P_N + F_N^J) \right] - 1 \quad , \qquad \text{(II-5)}$$

with

$$P_N = L + St + FP + M + C + R \quad ,$$

where $(\nu F)_N^J$ is the normalized neutron production by means of fast fission; A_N^I the normalized absorption by fissile isotopes; η_N^I is averaged over all fissile isotopes and all zones; and P_N is the sum of all fractional parasitic neutron losses due to leakage from the reactor L, absorption in the structural material St, fission products FP, sodium and oxygen M, C in the control rods, and a remainder R accounting for the absorption in Pu242, Np237, etc.

II.9.a. Influence of the Various Radial Blankets on the Global Nuclear Parameters Determining BR_N

The global nuclear parameters of Equation (II-5) are listed in Table II.18 and plotted in Figure II.11 for the three blanket configurations of the FBR investigated. The parasitic neutron losses P_N are split up into their components, showing the influence of the different blanket materials on these parameters. Compare the global breeding ratio BR_N, calculated on the basis of Equation II-5, with the results of the burnup calculations in the last two columns of Table II.18: for the burnup calculations, BR_N is determined from the ratio of the reaction rates, Equation (I-1), which is used to verify the validity of Equation (II-5).

The influence of the different blankets on the global breeding ratio BR_N is best understood by considering each term in Equation (II-5). The global η_N^I averaged over all fissile isotopes and regions is shown in Figure II.11a.

In the case of the UO_2 blanket, η_N^I decreases with the blanket residence time. This is so because as Pu239 accumulates in the radial blanket region, where the η_r^i value of Pu239 is smaller than its η_c^i in the core region, the isotope- and region-weighted η_N^I decreases. η_N^I is thus largest for a fresh UO_2 radial blanket, which contains no Pu239.

As for the thorium blankets, η_N^I does not decrease so much since η_r^i has been shown to be larger for U233 than for Pu239 (Figure II.6). This is reflected by Figure II.11a: for the Th^m blanket, η_N^I remains almost constant as U233 is being built up and consumed. This is clearly due to the fact that the η_r^i value of U233 in the Th^m blanket is almost as large as the corresponding Pu239/Pu241 value in the core zone. This is confirmed by the data in Table II.19, listing the η_n^i, ν_n^i, and $(1 + \alpha)_n^i$ values of the fissile isotopes Pu239, Pu241, U235, and U233 in the various reactor regions.

Note, first of all, the smaller η_r^i value of Pu239 in the blanket region (2.121) as compared to its η_c^i in the core region (2.327). This is reflected by the decrease in η_N^I in the case of the UO_2 blanket (Figure II.11a).

The η_r^i values of U233 in the ThO_2 and Th^m blankets (2.230 and 2.285) and that of Pu239 in the UO_2 blanket (2.121) reflect clearly the superior nuclear fuel utilization characteristics of U233 in the radial blanket region.

Comparing the core region-dependent η_c^i values of U233 and Pu239, one observes only a slightly larger value for Pu239 (2.327) than for U233 (2.297). Thus used in the FBR core region, these fissile fuels exhibit nuclear properties that do not differ significantly.

Table II.20 shows the impact of neutron flux degradation in the blanket region on $(1+\alpha)_r^i$ and η_r^i: for U233 in the oxide

Table II.19. η_n^i, ν_n^i, and $(1 + \alpha)_n^i$ values of the most important fissile isotopes in the core and in the radial oxide and metal blankets.

	U233			U235		Pu239		Pu241	
	Core	Blanket		Core	Blanket	Core	Blanket	Core	Blanket
	Oxide	Oxide	Metal	Oxide	Oxide	Oxide	Oxide	Oxide	Oxide
$(1+\alpha)_n^i$	1.108	1.132	1.109	1.270	1.330	1.254	1.374	1.171	1.192
η_n^i	2.297	2.230	2.285	1.938	1.833	2.327	2.121	2.540	2.486
ν_n^i	2.545	2.524	2.534	2.462	2.439	2.918	2.914	2.974	2.963

Table II.20. η_r^i and $(1 + \alpha)_r^i$ values of the most important fissile isotopes bred in the radial oxide and metal blankets. R1 = 1st row of blanket elements, R2 = 2nd row, R = averaged over R1 and R2.

	R1			R2			R		
	Oxide		Metal	Oxide		Metal	Oxide		Metal
	U233	Pu239	U233	U233	Pu239	U233	U233	Pu239	U233
η_r^i	2.240	2.155	2.291	2.194	2.013	2.2635	2.230	2.121	2.285
$(1+\alpha)_r^i$	1.128	1.354	1.107	1.147	1.442	1.1168	1.132	1.374	1.109

and metal fuel blankets and for Pu239 in the oxide fuel blanket, for the first and second rows of blanket fuel elements. η_r^i for Pu239 drops very rapidly by 0.142 from 2.155 in R1 to 2.013 in R2, whereas η_r^i for U233 is reduced by only 0.046 in the case of the ThO_2 blanket and by only 0.027 in the case of the Th^m blanket. This points to a relatively flatter decrease in $\eta(E)$ for U233 as compared to Pu239 (see Figure II.6).

The decrease in the *fast-fission* contribution due to Th232 in the radial blanket and its effect on the total fast fission are demonstrated in Figure II.11b, showing the fast-fission contribution $\nu F_N^J/A_N^I$. The ThO_2 blanket clearly displays the smallest share; that of the Th^m blanket lies between the contributions of the ThO_2 and UO_2 blankets. As can be seen, the harder neutron spectrum in the metal blanket can only partially compensate for the reduced fast fission in Th232.

The sum η_B of the two neutron production terms η_N^I and $\nu F_N^J/A_N^I$ is plotted in Figure II.11c. As can be seen, the advantage of the higher η_N^I values of the thorium blankets is virtually compensated for by their lower fast-fission contributions. The UO_2 blanket has the highest η_B value; it is closely followed by the Th^m blanket. The ThO_2 blanket has the smallest η_B value. This is the cause of the slightly smaller BR_N for the thorium blanket than for the UO_2 blanket.

This demonstrates that the improved fissile fuel utilization of U233 in the radial blanket is completey overshadowed by the diminished fast-fission neutron production in the thorium blankets. This negative effect of decreased fast fission is even much more dominant if the H/D ratio is larger, or if Th232 is placed in reactor regions such as the core region, whose fast-fission contributions are of significant importance for the total neutron production.

Placing Th232 in the core region will therefore drastically reduce the $\nu F_N^J/A_N^I$ component of η_B, decreasing BR_N significantly.

The parasitic losses P_N for the three blankets do not differ greatly, although the P_N of the Th^m blanket is slightly higher (Table II.18). This can be explained by the larger neutron

leakage losses L for the Th^m blanket, which are plausible because of the harder neutron spectrum of the metal blanket, which enhances neutron diffusion through the blanket region.

In Equation (II-5) the fertile fission rate F_N^J behaves the same way as the parasitic neutron loss term P_N. The sum of $(P_N+F_N^J)$ is plotted in Figure II.11e, showing that the UO_2 blanket has the largest sum because of the greater number of fast fissions. This fact partially compensates for the larger η_B value for the UO_2 blankets, with the result that the *global breeding ratios* BR_N for the various blanket configurations differ only slightly (Figure II.11f). The percentage differences in BR_N are plotted in Figure II.10a.

The above discussion has demonstrated first of all that the effects on the global breeding ratio BR_N of placing different fissile or fertile fuels in the various FBR regions can be made translucent by comparing the global nuclear parameters of Equation (II-5). Secondly--a point more relevant to the present discussion--several opposing, but largely compensating, effects have been shown to be the cause of the samll differences in the global breeding ratio BR_N between the UO_2 blanket and the thorium blankets. The net differences observed in BR_N of about 0.01, or about 1 point, are of no significance as regards the FBR investigated here.

However, the difference in BR_N must be expected to be larger for FBRs of larger H/D ratios, or for FBRs in which the contribution of the radial breeding ratio BR_r is of greater importance, i.e. where BR_r makes up more than 20% of BR_N, as is the case with SNR 300. In addition, thorium blankets have been found to cause a redistribution of the region breeding ratios and region breeding gains. BR_r and G_r both increased at the expense of $BR_{c,ax}$ and $G_{c,ax}$.

II.9.b. BR_N of Other FBR Designs in Terms of Their Global Nuclear Parameters

Before the discussion of the effects of thorium blankets on FBR performance is continued, the global breeding ratios BR_N of some other FBR designs are compared and analyzed in terms

of their global nuclear parameters. This comparison should serve, firstly, to demonstrate the usefulness of Equation (II-5) for this type of assessment, and, secondly, to explore the causes of the wide range of BR_N values obtained with FBR designs currently under discussion.

Table II.21 reproduces global nuclear parameters of some current FBR designs. The designs listed are fueled with U238 and Pu239 isotopes, except for one using Th232/U233. The table also gives the material composition in volume fractions of fuel ω, structural and cladding material β, and coolant α, to the extent such data were available.

The global breeding ratios BR_N of the PuO_2/UO_2-fueled FBRs are shown to vary over a surprisingly wide range, from 0.92 to 1.45. This large variance is due to a number of FBR design-specific characteristics, such as large structural material content, degraded neutron spectrum, or large parasitic neutron losses. A means of conveniently analyzing and explaining such differences between FBR designs is to compare their global nuclear parameters.

As discussed in the previous subsection, BR_N is primarily determined by η_B and P_N, the total number of neutrons released per fissile and fertile fuel absorption, and the fractional parasitic losses.

η_B itself depends on two parameters given in Equation II-5. Column 7 in Table II.21 reveals a variance of 25 points in η_B for the PuO_2/UO_2-fueled FBR designs, ranging from 2.96 to 2.74. This unexpectedly large variance is essentially due to the wide range of 0.41 to 0.58 of the fast-fission contribution $\nu F_N^J/A_N^I$ of the fertile isotope U238--a difference by itself of 17 points--and not so much to η_N^I, which varies only by 13 points, ranging from 2.25 to 2.38. The difference narrows down to only 8 points in the case of η_N^I for LMFBRs and GCFBRs, if the GCFBR design of Kraftwerk Union Erlangen, FRG, is excluded.

P_N, the sum of all parasitic neutron losses of the reactor, varies by a surprisingly wide margin, ranging from 0.10 to 0.25, the latter implying that 25% of all the neutrons is lost by some

Table II.21. Nuclear global parameters of some current FBR designs.

Fuel isotopes = U238/Pu

Designation	GW(e)	Core volume fractions ω	β	α	η_N^I	$(\nu F)_N^J / A_N^I$	η_B	P_N	$P_N = (L + FP + St + R)$ L	FP	St	R*	$P_N+F_N^J$	BR_N**	BR_N†
Oxide-fueled LMFBR															
(1) SNR 300	0.3	.336	.191	.473	2.331	.410	2.741	.2479	.0659	.0119	.0968	0.733*	.2987	0.9224	0.753
(2) SNR-2 (homogeneous)	2.0	.391	.230	.380	2.298	.519	2.817	.1534	.0135				.2297	1.17	0.945
(3) SNR-2 (heterogeneous)	1.0	.371	.223	.406	2.329	.577	2.906	.1291	.0212	.0197	.0590	.0292	.1944	1.341	1.028
(4) GE (1968)	1.0	.467	.149	.351	2.336	.599	2.935	.1277	.0309	.0294	.0433	.0241	.1984	1.3532	1.037
(5) CBR association	1.2	.346	.203		2.253	.458	2.711	.113	.032	.0215	.0565	.003	.1738	1.2396	0.998
Oxide-fueled GCFBR															
(6) GBR association	1.2	.273	.119		2.339	.581	2.920	.0979	.039	.018	.041		.1695	1.4248	1.110
(7) KWU	1.0				2.381	.583	2.964	.1105	.0376	.0127	.0602		.1734	1.45	1.118
Fuel isotopes = Th232/U233															
Molten salt breeder reactor															
(8) MSBR					2.195	.0255	2.2205	.0735	.0005	.015	.0281††	.0300	.0764	1.05	1.034

References

(1) Schikorr (1973).
(2) Personal communication E. Kiefhaber, Kernforschungszentrum Karlsruhe, FRG (1975).
(3) Wehmann and Stehlen (1975).
(4) General Electric (1968).
(5) Vieidier (1974).
(6) Vieidier (1974).
(7) Kraftwerksunion Erlangen (1974).
(8) Kasten et al. (1968).

*R includes absorption in the coolant, control rods, Pu242, etc. For SNR 300, the loss in the control rods = 0.670.
**Equation (II-5).
†Without fast fission, i.e. $F_N^J = 0$.
††Absorption in carrier salt.

parasitic process, instead of being utilized in the breeding process by way of capture in the fertile fuel. The largest fraction (40-50%) of P_N can be explained by the absorption losses in the structural material St, with St ranging from 0.04 to 0.10. Then follow the leakage losses L (20-30%), ranging from 0.01 to 0.06, and the relatively small (~20%) parasitic absorptions in the fission products FP, ranging from 0.01 to 0.02.

None of these FBR parasitic loss components can be significantly altered or reduced without major technological innovations. A practicable possibility would be to reduce the St component, but this would mean to use less structural material in the core, which is difficult to implement without improving the burnup characteristics of FBR fuel and cladding materials. The leakage losses L and fission product absorptions FP for large FBRs are already as low as is practicable. The parasitic losses P_N are therefore relatively fixed for the FBR, which is in contrast to present day thermal reactors, specifically the HTR, in which some of the parasitic loss components can indeed be influenced favorably without much difficulty.

The parasitic fission-product absorption component FP of the HTR reactor type can be significantly reduced by simply decreasing the fuel burnup. Since it represents the largest parasitic loss component of the reactor (~ 80% of all losses), this reduction will significantly improve the conversion ratio and thus the fissile fuel utilization (see Chapter III). At this point it suffices to recognize that none of the parasitic loss components of the FBR can be altered or reduced as conveniently as is the case with the HTR.

The only way of significantly influencing the BR_N of the FBR is by changing the neutron production term η_B in Equation (II-5). This means to change either η_N^I or $\nu F_N^J/A_N^I$, or both. Since both parameters are determined by the fissile and fertile isotopes, one can influence BR_N either by selecting the combinations of fissile and fertile fuels most favorable in the various FBR regions, in order to increase η_N^I and/or $\nu F_N^J/A_N^I$, or by increasing these values in some other ways, for example, by hardening the neutron spectrum in the core or blanket regions.

The most unfavorable neutron utilization in this respect is that of the LMFBR prototype SNR 300. It has the highest parasitic losses with P_N = 0.25; this is due to unusually high leakage losses L of 0.066, large parasitic losses in the structural material St of 0.097, and large losses due to control rod absorption of 0.067, which are included in the R term. Its low BR_N of only 0.92 is largely a result of these significant parasitic losses. The leakage losses, for example, could be reduced considerably to about 0.03 by addition of a row of radial blanket elements. This would at the same time reduce the neutron losses in the structural material, since as much as 0.035 (36% of St) is ascribed to structural material absorption losses in the neutron reflectors. A thicker radial blanket would decrease both L and St losses by altogether about 0.043, thereby increasing BR_N to 1.04. The SNR 300 control rod losses are difficult to reduce since they are an inherent feature of small FBR reactors. Small FBR cores need a large excess reactivity for the burnup swing[10], which must be compensated for by the control rods during the early burnup phase.

The average structural material losses are about 0.05, and the average leakage losses about 0.035. These values seem representative of large FBR designs in the 1000 MW(e) category. To reduce the average P_N losses of 0.13 to less than 0.10 by a major technological innovation seems justifiable if BR_N larger than 1.30 are to be attained.

The most profound effect on BR_N can be achieved with a more favorable η_B, obtained by increasing the fast-fission contribution. A comparison of the last two columns in Table II.21, giving the FBR global breeding ratio BR_N with and without fast fission, clearly reveals the importance of fast fission for FBR performance. Without the fast-fission contribution, all of the FBRs listed would have serious difficulties in attaining BR_N much above 1.0. For SNR 300, BR_N would drop from 0.92 to 0.75, for

---

[10] Small FBR cores generally have internal conversion ratios considerably less than 1.0. This feature in turn requires a large excess reactivity.

SNR-2 (homogeneous design) from 1.17 to 0.94, and for the gas-cooled fast breeder reactor (GCFBR) from 1.24 to 1.0. This illustrates the importance of the fast-fission contribution for LMFBRs.

The fissile fuel-specified η_N^I values of the various reactor designs vary within very narrow limits, i.e. from 2.30 to 2.34, provided the two extreme values of 2.38 and 2.25 are assumed to represent special cases. This narrow range is not unexpected, since all the FBRs given are fueled with the isotopes Pu239/Pu241. Being fueled with PuO_2/UO_2, all such designs can be assumed to have similar neutron spectra. GCFBRs tend toward a harder spectrum, whose influence on $\eta_{N_I}^I$ is not very signifcant. Even SNR 300 has a relatively high η_N^I of 2.33. Its large η_N^I value can partly be explained by fuel enrichment, which is higher for SNR 300 than for larger LMFBRs.

The large fluctuation in η_B, and thus in BR_N, is clearly due to the greatly varying fast-fission contribution $\nu F_N^J/A_N^I$. This parameter varies from 0.46 to 0.58, or 12 points, if the two extreme values are neglected. The reasons for this large variation cannot be extracted with certainty from the data available, but there appears to be some correlation between the structural volume fraction β and the fast-fission contribution. In addition, the ratio of $BR_{ax,r}$ to BR_N seems to have some influence on the small fast-fission contribution of 0.410 of the SNR 300 reactor.

With SNR 300, a large fraction of BR_N is ascribed to axial and radial blanket breeding. Since the fast-fission contribution in the blanket regions becomes very small as the neutron energy spectrum is degraded, the total fast fission becomes less if breeding is shifted to the blanket regions.

Gas-cooled breeders seem to achieve the highest BR_N. This is understood as being due to their hard neutron spectra, allowing both the highest η_N^I values and very large U238 fast-fission contributions. The harder neutron spectrum, in comparison to a sodium-cooled FBR, can be explained by the nature of the coolant and the apparently small volume fraction of structural

material of 11.9%, which is 23% for a sodium-cooled FBR of current design. A small volume fraction implies not only less parasitic absorption but also a harder neutron spectrum. An increase in β generally degrades the neutron spectrum, on account of the large scattering cross sections of the structural materials, thus possibly lowering η_B, as is the case with Na-cooled FBRs.

As indicated above, the fast-fission neutron contribution is very critical with respect to the breeding ratio BR_N of any FBR. This is also underlined by the differences between homogeneous and heterogeneous core designs. (See Table II.21 for the homogeneous SNR-2 and the heterogeneous SNR-2.) Besides the small decrease in P_N from 0.15 to 0.13 for the homogeneous and heterogeneous designs, the more significant difference is the gain of 6 points from 0.52 to 0.58 in the U238 fast-fission contribution and of 3 points in η_N^I from 2.30 to 2.33. This favorable combination of an increase in η_B by 9 points and a simultaneous decrease in P_N by 3 points permits a higher BR_N in the heterogeneous type by up to 20 points.

The sensitivity of the global breeding ratio BR_N to changes in the fast-fission contribution cannot be stressed often enough. One way of significantly reducing the fast-fission contribution is to replace the fertile U238 isotope by Th232 in the FBR core zones. As a result, the fast-fission contribution will decrease from 0.40-0.60 for U238 as fertile fuel to 0.05-0.15 for Th232 as fertile fuel. BR_N will decrease correspondingly. In current FBR designs, e.g. SNR-2, the global breeding ratio BR_N would certainly decrease from 1.2 to less than 1.0.

The influence of Th232/U233 as fuel in the FBR core region is demonstrated by the global nuclear parameters of the Molten Salt Breeder Reactor (MSBR), given in Table II.21. BR_N equals 1.05, although the parasitic neutron losses P_N are very small (0.073). η_N^I of 2.195 is close to the values listed in Table II.19 for U233, and about 0.13-0.20 (i.e. 13 to 20 points) below the values for the PuO_2-fueled cores. The large difference in η_B, however, is due to the almost nonexistent fast-fission contribution of only 0.026, resulting in a difference of up to 0.55 in η_B (55 points) in comparison to cores with U238 as fissile fuel.

The fuel combination Th232/Pu239 in the core zones leads to results similar to those of Th232/U233 because of the great similarity between the η_c^i values of U233 and Pu239.

Introduction of Th232 in the FBR core region will therefore significantly reduce the global breeding ratio BR_N on account of the smaller fast-fission contribution. Replacing U238 by Th232 as fertile material in current FBR designs (e.g. SNR-2) will most certainly decrease their breeding ratios below 1.0, thus making Th232 in place of U238 definitely unattractive as principal fertile fuel in the core region, especially for current sodium-cooled FBRs. The use of Th232 is thus limited to the blanket regions of the FBR, where the fast-fission contribution is less important.

II.10. ADDITIONAL COMPARISONS BETWEEN UO_2, ThO_2, AND Th^m RADIAL BLANKETS

In addition to different breeding properties, the thorium blankets exhibit burnup characteristics that are slightly different from those of the UO_2 blanket, especially with regard to blanket power fraction, linear rod power, etc. Of particular interest here is the influence of isotopes Pa233 and U233, both of which are special characteristics of the thorium cycle.

II.10.a. Power Fraction, Linear Rod Power, and Fuel Burnup of the Various Radial Blankets

Figure II.12 shows the increase in power fraction for the various radial blankets as a function of the blanket residence time. A fresh UO_2 blanket has, on account of U235 residual enrichment (0.3%) and the larger U238 fast fission, a larger power fraction than a fresh ThO_2 or Th-metal blanket. With the fissile material building up in the blankets, the power fraction of the radial blanket increases up to 10%. Between the second and third cycles (1 cycle = 292 days), the ThO_2 blanket attains the same power fraction as the UO_2 blanket. This is due to the higher fission cross section of U233 as compared to Pu239. (Compare Table II.9 for the one-group cross sections.)

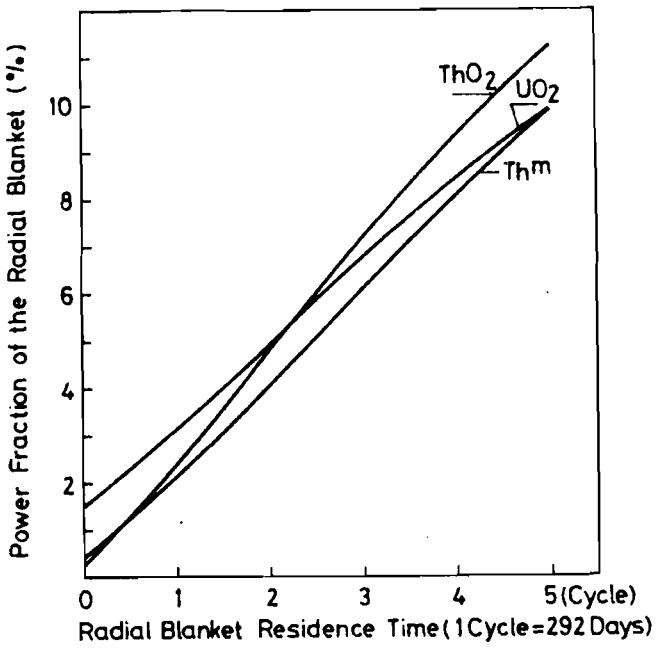

Figure II.12. Power fraction of the radial blanket as a function of its residence time (R1, R2).

Figure II.13 shows the burnups of the first and second rows of blanket elements as a function of the blanket residence time. Figure II.14 gives the maximum rod power of the blanket rods directly adjacent to core zone CZ3. The blanket rods of the UO_2-blanket element R1 attain their maximum permissible rod power of 350 W/cm within four burnup cycles, i.e. the residence time of the first row of elements of a UO_2 blanket is usually limited by the maximum permissible linear rod power. The maximum rod power of ThO_2 is 700 W/cm to 800 W/cm. This has not yet been reached within the residence time considered here, i.e. the life of the ThO_2 blanket is, unlike that of the UO_2 blanket, not limited by the maximum permissible rod power but probably by the neutron fluence. The situation is similar for a Th-metal blanket whose rod power after five cycles is 400 W/cm, well below the permissible maximum of approximately 700 W/cm.

Figures II.15 and 16 show the fissile fuel buildup in the radial blankets. For the Th blankets, unloaded Pa233 was considered, its largest fraction decaying into 233 with a half-life of 27 days.

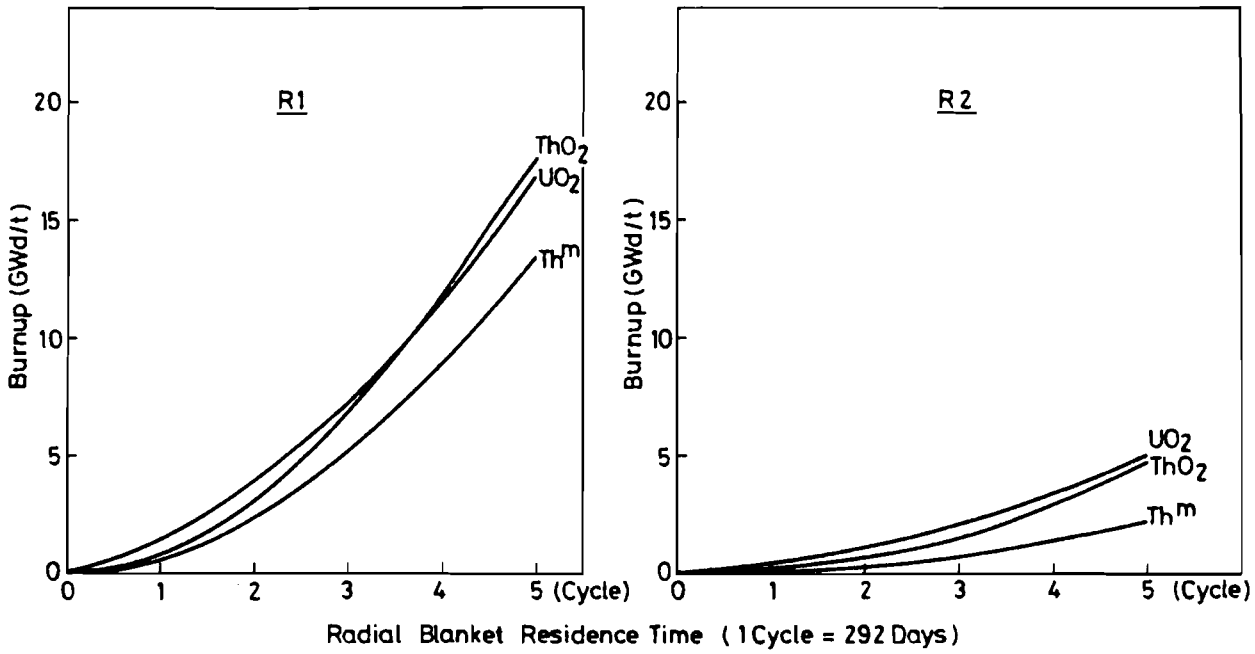

Figure II.13. Fuel burnups in the first (R1) and second (R2) rows of the radial blanket.

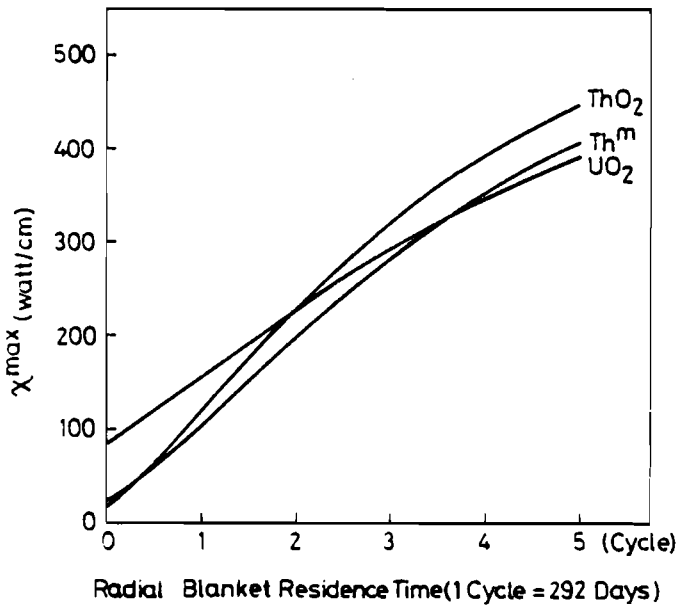

Figure II.14. Maximum linear rod power of the radial blanket pins adjacent to the core region.

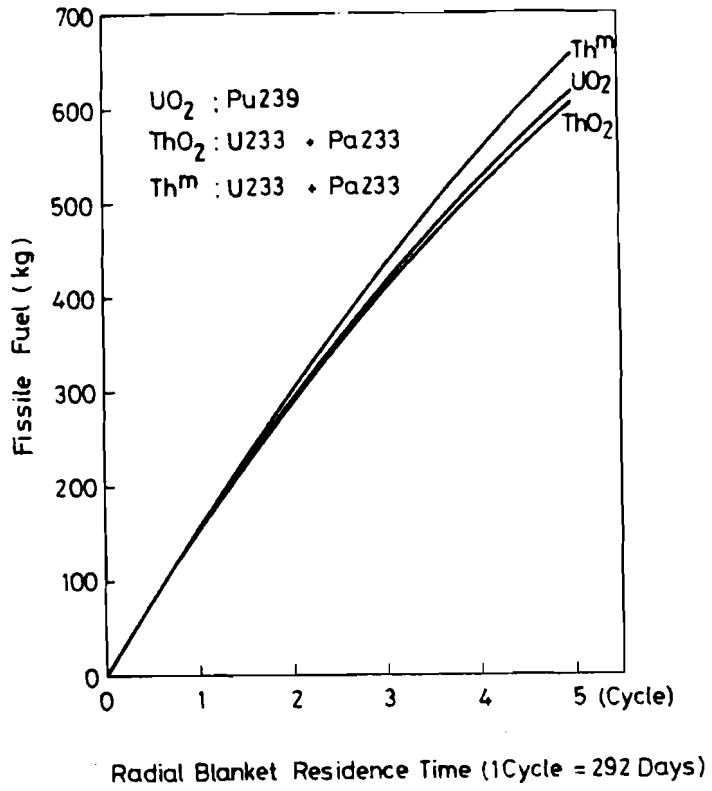

Figure II.15. Buildup of fissile fuel bred in the radial blanket.

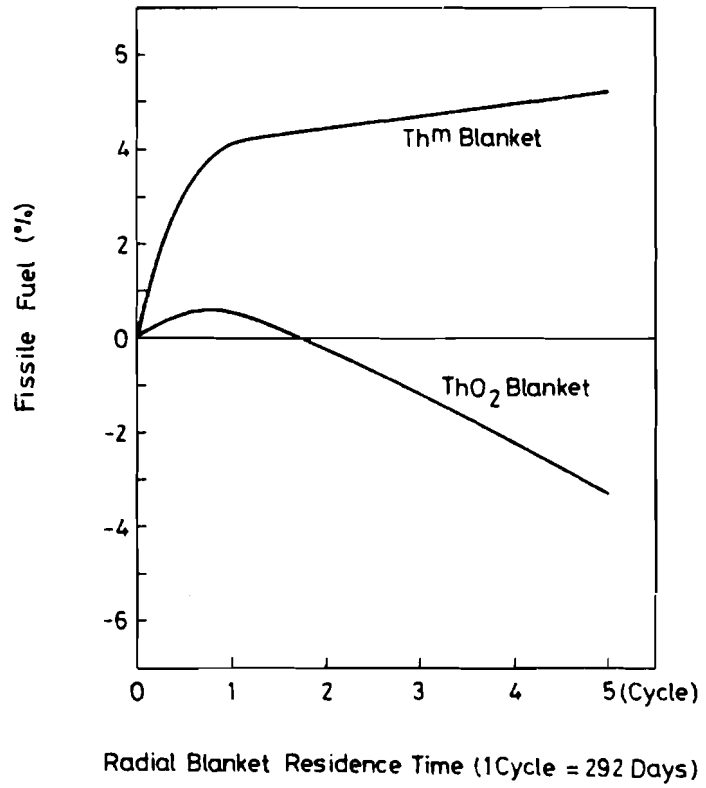

Figure II.16. Difference (%) in fissile fuel buildup in thorium blankets with respect to a UO_2 blanket.

II.10.b. Buildup of U232

One of the problems associated with the thorium cycle is the buildup of isotope U232, which leads to considerable difficulties in U233 refabrication. U232 decays into Th228, according to the diagram, with a half-life of 71.7 years. Via several alpha and beta decays, Th228 is transformed into stable Pb208. Due to the decay of intermediate products, especially due to Tl208 and Bi212, hard gammas (2.6 MeV) are generated which necessitate heavy shielding during refabrication.

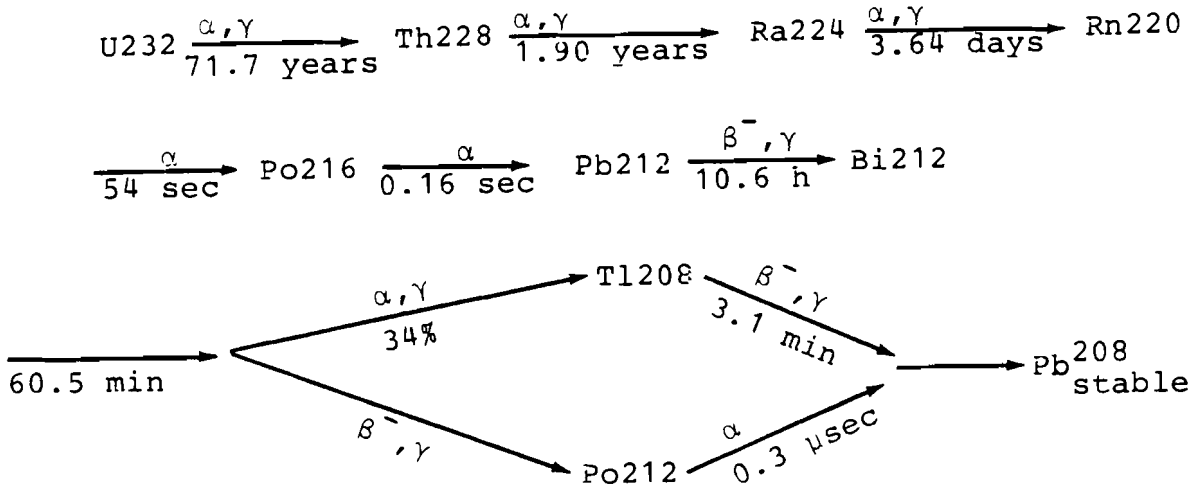

U232 concentration is linked to a financial penalty with a maximum of ₡ 2/g, according to information from AEC (U.S. ERDA). Table II.22 gives U232 concentrations and associated penalties (Eighty-Ninth Congress of the United States 1966).

During the reprocessing step, the uranium and thorium isotopes are first of all separated. The Th228 contained in the extracted thorium fuel is taken to an intermediate storage, where it remains for about 20 years to decay. Processing of thorium in hot cells before the end of this decay period is also possible.

The U232 contained in the recovered uranium, in this case in fissile fuel U233, is returned to the refabrication process after processing. Within a short time, a very high radiation

Table II.22. U232 penalty.

Parts of U232 per million parts of uranium	Penalty in dollars per gram of total uranium
0	0.40
20	0.60
45	0.80
80	1.00
130	1.20
190	1.40
250	1.50
350	1.60
500	1.70
700	1.80
1000	1.90
1500	2.00

Source: Eighty-Ninth US Congress (1966).

level builds up due to fast decay of Th228 from U232 into Ra224 (the half-life of Th228 is 1.9 years). Refabrication of larger quantities of U223 within ten days after processing would, in principle, be possible without gamma shielding, but this requires a smooth production sequence (Baier 1974).

Calculations of the U232 buildup in the HTR utilizing the thorium fuel cycle indicate U232 concentrations of up to 500 ppm in the case of repeated recycling of the fissile fuel (Baier 1974). Since this concentration level is sufficient to require shielding, this is the range of U232 concentrations shielding in HTR refabrication plants has to be designed for.

The buildup of U232 takes place by means of essentially three reactions:

(1) $\mathrm{Th232} \xrightarrow[6.34\ \mathrm{MeV}]{(n,2n)} \mathrm{Th231} \xrightarrow[25\ \mathrm{hours}]{\beta^-} \mathrm{Pa231}(n,\gamma)\ \mathrm{Pa232} \xrightarrow[1.3\ \mathrm{days}]{\beta^-} \mathrm{U232}$

(2) $\mathrm{U233} \xrightarrow[6\ \mathrm{MeV}]{(n,2n)} \mathrm{U232}$

(3) $\mathrm{Th230}\ (n,\gamma)\ \mathrm{Pa231}\ (n,\gamma)\ \mathrm{Pa232} \xrightarrow[1.3\ \mathrm{days}]{\beta^-} \mathrm{U232}$

Due to the relatively high thermal capture cross section of Th230, reaction (3) is only of significance in a thermal reactor spectrum (e.g. HTR), i.e. if the concentration of Th230 exceeds approximately 5 ppm (Baier 1974). With thresholds at approximately 6 MeV, both Th232 (n,2n) and U233 (n,2n) reactions are therefore significant, especially in very hard spectra. Although the fission spectra of the fast reactor and the thermal reactor are very similar, the fact that the neutron flux in a fast reactor is two orders of magnitude larger makes the (n,2n) reaction more important for the fast reactor than for the thermal reactor. In the fast FBR spectrum, the Th232 (n,2n) reaction clearly dominates on account of the much larger Th232 particle concentration. Approximately 95% of the U232 produced can be accounted for by this reaction.

The (n,2n) cross sections of Th232 and U233 have been determined by experiments described in Kobayashi et al. (1971 and 1973). The mean values measured for the fission spectrum were 12.5 ± 0.84 mb for Th232 (n,2n) and 4.08 ± 0.30 mb for U233 (n,2n). Absorption cross sections of U232 and Pa231 were taken from Hinkelmann (1970). The absorptions of Th231 and Pa232 were neglected because of the short half-lives of the two isotopes (of approximately one day).

Figure II.17 shows the buildup of U232 for the two rows of blanket elements in the two thorium blankets. Due to the rapid decline of the neutron flux and due to the rapid degradation of the neutron spectrum in the radial blankets, the U232 concentration in the second row is approximately four times smaller than that in the first row. With a residence time of five cycles (1460 days), the concentration is below 300 ppm. If the discharged fuel of both rows is mixed, the concentration for the ThO_2 blanket averages somewhat above 200 ppm and that for the Th-metal blanket 160 ppm. The conspicuously smaller U232 buildup (despite the harder spectrum) in a Th-metal blanket is due to the considerable fast-fission cross section of 1.2 barns of Pa231 in the upper energy group ($G = 1$). Since it has been tacitly assumed here that the U233 bred in the FBR blankets is transferred

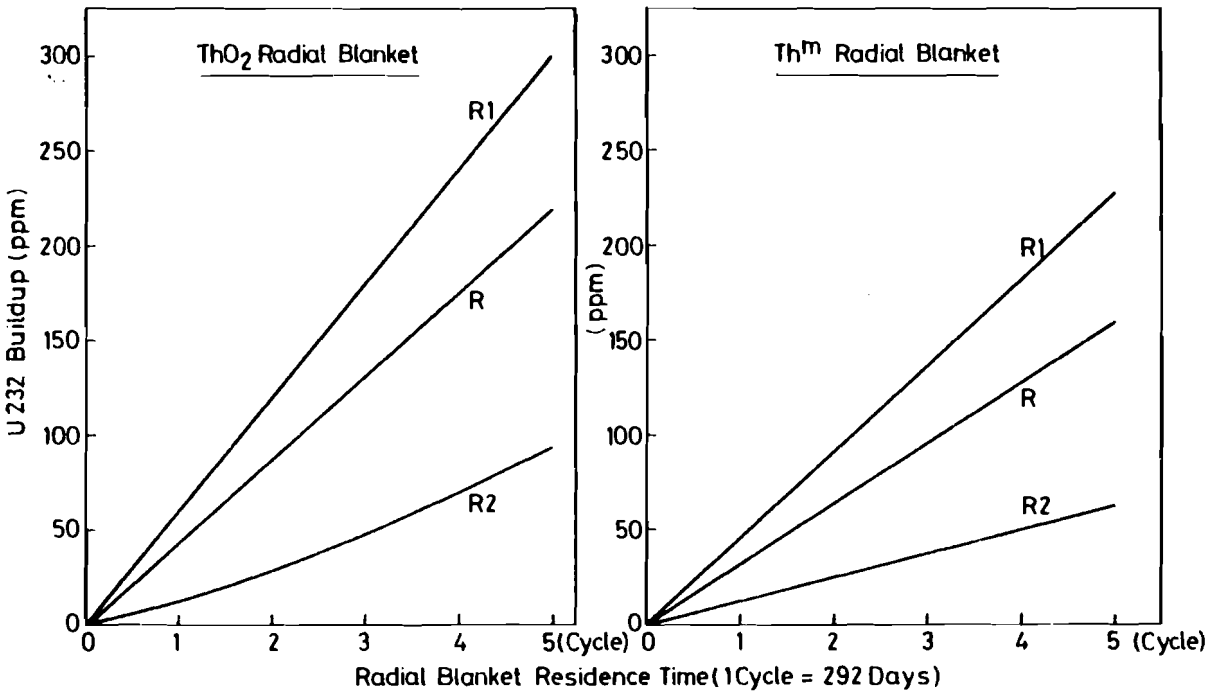

Figure II.17. Buildup of U232 in the first (R1) and second (R2) rows of blanket elements as well as for the radial blanket (R averaged over R1 and R2), in the thorium blankets.

to HTR reprocessing and refabrication plants, the U232 concentrations of both blankets remain within the range stipulated for HTR refabrication plants (500 ppm-1000 ppm).

The residence time of the radial blankets is thus not limited by the U232 buildup. The financial penalty is also kept within limits, due to the relatively low U232 concentration built up in the blanket (see Table II.22).

II.10.c. Influence of Pa233

The buildup of U233 takes place via the decay of the intermediate decay product Pa233. This process is similar to the buildup of Pu239 via the decay of the intermediate product Np239.

$$_{92}U238(n,\gamma)\ _{92}U239 \xrightarrow[23.5\ min]{\beta^-} {}_{93}Np239 \xrightarrow[2.4\ days]{\beta^-} {}_{94}Pu239$$

$$_{90}Th232(n,\gamma)\ _{90}Th233 \xrightarrow[22\ min]{\beta^-} {}_{91}Pa233 \xrightarrow[27.4\ days]{\beta^-} {}_{92}U233$$

The basic difference between these two chains is the relatively long half-life of 27.4 days for Pa233, as compared to 2.4 days for Np239. This half-life causes high equilibrium concentrations of Pa233 to build up, mainly in the case of high power densities. Considerable reactivity insertion must therefore be expected, after reactor shutdown. This reactivity insertion must be compensated for by additional control rods. If thorium is used in the core zones, this effect becomes a considerable problem (see the following section).

When thorium is used in the radial blanket, the Pa233 decay is of minor influence since, firstly, only relatively small equilibrium concentrations are built up, because of the low power density (only about 22 kg of Pa233 for the ThO_2 and Th^m blankets) and, secondly, the Pa233 is located in a reactor region of relatively small reactivity worth. The maximum reactivity worth of the above amount of Pa233 in the blankets was calculated as 3.0‰ in k_{eff}, by means of two k_{eff} calculations for

which Pa233 was assumed to be equivalent to U233. This increase in reactivity, expected to occur approximately 100 days after reactor shutdown, does not constitute any particular shutdown problems.

Another problem connected with Pa233 is the neutron capture in Pa233, resulting in the loss of one U233 atom. Due to the high absorption cross section of Pa233 in the thermal spectrum (σ_a = 45 barns), this loss of potential fissile material is of considerable significance in thermal reactors, but is small in the case of the FBR blanket spectrum ($\sigma_a \simeq 4.5$ barns). There, only 3% of the Pa233 atoms is lost due to absorption, and the remaining 97% decays into U233.

From this it may be concluded that the buildup of Pa233 in the radial blankets does not pose any significant problems.

II.10.d. The Sodium Void Coefficient

One of the most important reactivity coefficients for the sodium-cooled FBR is the sodium void coefficient. It decisively determines the course and the potential effects of a loss-of-coolant incident in the reactor. The properties of this reactivity parameter were discussed in detail by Schroeter (1970). In the present case, the difference between a UO_2 radial blanket and a ThO_2 radial blanket is considered in terms of the sodium void. 1-D perturbation calculations were performed for this purpose with the 26-ENDF/B III group set.

Figure II.18 shows the radial dependence of the void effect for a sodium-free 1-liter bubble in UO_2 and ThO_2 blankets. It can be seen that the void effect in core zone CZ1 is approximately 10% larger in the case of the ThO_2 blanket than with the UO_2 blanket. Toward the outer radius of the core, the void becomes smaller with the ThO_2 blanket than with the UO_2 blanket. This is due to the larger net leakage of neutrons into the ThO_2 blanket region (which has a higher albedo). In the case of the ThO_2 blanket, the increase in the void coefficient in the core region is to be ascribed to the larger enrichment of core zone CZ3, causing a somewhat harder spectrum.

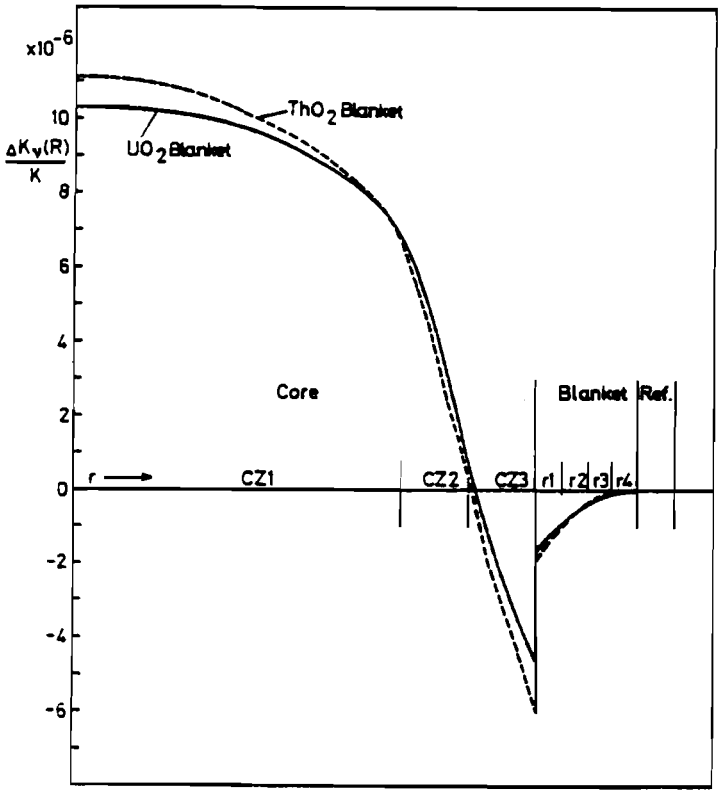

Figure II.18. Radial dependence of the sodium void effect $\Delta K_v(R)$ for UO_2 and ThO_2 radial blankets. Perturbation calculation for a sodium-free 1-liter bubble.

The 10% rise of the sodium void coefficient in core zone CZ1 is of relatively little importance, since the uncertainties in determining the sodium void effect are regarded to be within this range. The increase is therefore within the expected uncertainty limits. The Doppler coefficient could not be investigated here due to a lack of nuclear data. However, it can be deduced from Wood and Discroll (1973) that there is little difference between the Doppler coefficients of the two blanket configurations.

II.11. THORIUM IN THE FBR CORE REGION

The influence of thorium in the FBR core zones on the global breeding ratio and reactivity coefficients has been examined in detail in several studies (Loewenstein and Okrent 1958; Okrent, Cohen, and Loewenstein 1965; Hankel et al. 1962; Loewenstein and Blumenthal 1965; Allen, Stoker, and Campise 1966; Sofer et al. 1963). In this investigation, it has already been shown in Section II.9.b. that utilization of Th232 in the core region of present oxide-fueled FBRs is totally impracticable. Th232 in the core region is thus addressed only marginally.

The following problems are associated with the use of Th232 in the core region:

-- The breeding ratio is reduced significantly on account of the drastically decreased fast-fission contribution.
-- U233 bred in the core has a smaller η_c^i than Pu239 (see Table II.19), which has an additional, negative influence on BR_N (see discussion in Section II.9.a).
-- The high power density in the core region causes a high equilibrium concentration of Pa233, leading to considerable shutdown control problems after reactor shutdown.
-- The high buildup of U232 in the core zones (high neutron flux) leads to additional problems in fuel refabrication.
-- There is a mixture of U233 and Pu239 as fissile fuel in the core if Th232/Pu239 is the initial fuel; this implies mixed reprocessing of both the thorium and uranium cycles.
-- The fissile inventory increases if the power density remains unchanged.

The only attractive aspect of using thorium in the core region is limited to the distinctly lower sodium void coefficient. In the case of a U238/Pu-fueled[11] FBR, the sodium void becomes positive due to spectrum hardening during sodium voiding, which causes an

[11] Pu = Pu239/Pu240/Pu241/Pu242.

increase in the fast fission of U238 and Pu240, and a higher neutron release in Pu239 due to the steep rise of its η in the higher energy region (see Figure II.6). With the use of thorium in the core region, the positive Na-void effect is greatly reduced, due to the four times smaller fast-fission cross section of Th232 as compared to U238, the flatter η (U233) curve, and the relatively low U234 concentration as compared to the analogous Pu240 concentration. Depending on the U233/Pu239 ratio, the sodium void can even become negative (Leipunskii, Kazachkovskii et al. 1965).

To determine the influence substitution of Th232 for U238 in the core zones would have on the breeding and reactivity properties of the FBR investigated, U238 in core zone CZ1 was replaced by Th232, leaving CZ2 and CZ3 and the blankets unchanged (UO_2 as radial blanket). Thus the initial fuel of CZ1 was Th232/Pu. As the burnup of the core zones progressed U233 began to build up in CZ1, replacing the initial fissile fuel Pu239. The most relevant results of this investigation can be summarized as follows:

1. The breeding ratio BR_N decreased by 10 points.
2. The initial fissile fuel inventory of Pu increased by 7%.
3. The Pa233 equilibrium concentration of 40.6 kg corresponds to a reactivity addition of 2.94% $\Delta k/k$ 100 days after reactor shutdown. This reactivity increase must be compensated for by additional control rods.
4. U232 built up to high concentration levels of 2000-3000 ppm.
5. The Na-void coefficient in CZ1 was reduced by a factor of 3.

These results indicate that placing Th232 in the core zones of an FBR will result in significant changes in virtually all the important FBR parameters. The global breeding ratio BR_N is influenced most significantly, and is followed by the additional control problem. Complete substitution of Th232 for U238 in the core region of Na-cooled FBRs of current design, whose breeding ratios of about 1.20 are already low (homogeneous core), will

certainly decrease their breeding ratios to below 1.0, making the use of Th232 in such core regions impracticable. The use of thorium in such FBRs is therefore strictly limited to the blanket regions, preferably to the radial blanket, as has been investigated and proposed in the previous sections.

It could possibly appear feasible to use Th232 in FBR designs with inherently higher breeding ratios ($BR_N \simeq 1.3 - 1.4$), such as the heterogeneous core designs of sodium- or gas-cooled FBRs, since their BR_N would still be somewhat above unity ($BR_N \simeq 1.1$) with Th232/U233 as fuel instead of U238/Pu. In terms of their present state of technological develepment, however, gas-cooled FBRs are considered to be several years behind Na-cooled FBRs. But it is conceivable and also to be expected that their breeding ratios will gradually decrease with further research and development, as was the case with the development of Na technology for LMFBRs. On this premise, employment of thorium in these reactors is as unfeasible as in LMFBRs of current design.

II.12. SUMMARY OF CHAPTER II

It has been shown that the practical use of Th232 as fertile fuel in LMFBRs of current design ($BR_N \simeq 1.2$) is limited to the blanket regions of fast breeder reactors, preferably to the radial blanket. The use of ThO_2 or Th metal as radial blanket material can be considered a viable alternative to the conventional UO_2 blanket, whereas Th232 in the core region of present LMFBRs decreases their breeding ratio BR_N to less than 1.0. It has been shown in particular that a ThO_2 or Th-metal radial blanket in place of a UO_2 radial blanket does not have any intrinsic disadvantages as regards the FBR global breeding properties.

The most important influence of the Th blankets has been shown to be a shift in the distribution of the region breeding ratio BR_n and of the region breeding gain G_{n_m}. Due to the lower neutron reflective properties of ThO_2 and Th^m as compared to UO_2, the radial breeding ratio BR_r increased by 5% in the case of a ThO_2 blanket and by 6.5% for a Th^m blanket. At the same time the breeding ratios of the core and the axial blanket were reduced.

The radial breeding gain G_r in the case of the ThO_2 blanket was found to be approximately 2% above the G_r of a UO_2 blanket, and that of the Th^m blanket approximately 12% higher than that of a UO_2 blanket.

The global breeding ratio BR_N of the FBR was, in the case of the ThO_2 blanket, reduced by 1% as compared to a UO_2 blanket, and no noticeable difference was observed for the Th^m blanket. The global breeding gain G_N of the FBR was approximately 3% lower in the case of the ThO_2 blanket and 0.5% lower for the Th^m blanket than for a UO_2 blanket.

The superior breeding properties of the two thorium blankets were highlighted by the Th^m blanket. Its superiority can be ascribed to the neutron spectrum, which is harder in a metallic than in an oxide radial blanket. A small increase in the fissile inventory is required with Th blankets, which was 1.2% for the ThO_2 blanket and 2.37% for the Th^m blanket above the fissile inventory of a UO_2 blanket.

The buildup of Pa233 is moderate in radial Th blankets, causing no particular control problems.

The buildup of U232 was kept below 300 ppm for a residence time less than 5 cycles (1 cycle = 292 days). This concentration level is below the expected design value of HTR refabrication plants (thorium cycle).

The sodium void coefficient was approximately 10% larger for the Th blankets than for the UO_2 blanket. This is, however, within the range of uncertainty of sodium void coefficient calculations.

There is no particular incentive to recycle the radial blanket-bred U233 into the core region of the FBR since U233 is a slightly less favorable fissile fuel in the FBR core region than Pu239/Pu241.

CHAPTER III. ASSESSMENT OF THE NEUTRON AND FISSILE FUEL UTILIZATION OF THE HTR

III.1. INTRODUCTION

The HTR is a thermal reactor that requires for its operation a continuous supply of fissile fuel. The fissile isotope usually employed is U235, because the other fissile isotopes U233 and Pu239 are either not available in sufficient quantity or undesirable as fissile fuel. The uranium ore (U_3O_8) demand associated with the U235 requirement makes the HTRs of present design dependent on the continuous availability of uranium ore.

One of the most important parameters with respect to HTR fuel utilization is the actually necessary amount of uranium ore, or the fissile fuel U235 needed to sustain reactor operation. This quantity is usually directly proportional to (1-CR), with CR being defined as the HTR conversion ratio, which is normally less than 1.0. Thus little additional fissile fuel, or makeup fuel, is necessary for an HTR with a large conversion ratio of approximately 0.8 to 0.9, but considerably larger amounts in the case of a relatively small CR $\simeq$ 0.5 - 0.6.

The HTR conversion ratio CR is primarily determined by the fuel cycle employed, and to some extent by the operational mode and design of the reactor. Disregarding the latter two dependencies temporarily, one can show that CR is largely a function of the combinations of fertile and fissile isotopes used, with U238 and Th232 as fertile, and U233, U235, and Pu239 as fissile isotopes.

The results of Chapter II have shown that the breeding of U233 in the radial blanket region of the FBR is a feasible alternative to Pu239 breeding, if there is a proper incentive to do so. It has been mentioned, however, that there is no particular advantage in recycling this U233 into the FBR core region.

Therefore, the question arises as to whether transfer of the FBR-bred U233 to a thermal reactor, e.g. an HTR, would improve not only the fuel utilization of the latter but also the fuel utilization of the combined reactor system. It is indeed of interest to consider this particular fuel transfer, since the FBR can supply either Pu239 or U233 as fissile fuel, and since the HTR can in principle, utilize either isotope as makeup fissile fuel. This calls for a detailed assessment of th HTR fuel cycle economy, in order to determine the advantages and disadvantages of using U233, U235, or Pu239 as fissile HTR fuels. Such an assessment is the subject of this chapter[1].

If U233 should prove advantageous to the HTR, the breeding of U233 in the FBR radial blanket could be considered a viable alternative to the breeding of Pu239 as FBR surplus fuel.

A general assessment of the HTR fissile fuel utilization is rendered difficult by the great number of fissile fuel cycles conceivable for the HTR: both U238 and Th232 can be used as fertile isotopes, with either U233, U235, or Pu239, or a combination thereof, as fissile fuel makeup. This leads to several possible combinations of converted (self-bred) fissile fuels, makeup fissile fuels, and fertile isotopes utilized in the HTR. These combinations of fertile and fissile isotopes are referred to as *fissile fuel cycles* in the following.

Table III.1 lists the feasible fissile fuel cycles of the HTR, differentiating between uranium, thorium, and hybrid cycles. The fertile isotopes in the uranium and thorium cycles are U238 and Th232, respectively. The thorium fissile fuel cycles are called A, B, and C, and the uranium fissile fuel cycles D, E, and F. In A and F the fissile fuel makeup is U233 or Pu239, respectively, the fissile isotopes that can be supplied by the FBR; the makeup for the remaining fissile fuel cycles B, C, D, and E is U235. Fissile fuel cycles G and H are hybrid cycles, characterized by the alternative use of Th232 and Pu239 or U238 and U233. These hybrids can be shown to be insignificant from

---

[1] These results would also be applicable to LWBRs, LWRs, or any other thermal reactor using the FBR-bred U233.

Table III.1. Fissile and fertile isotopes of various thorium and uranium fissile fuel cycles of the HTR, and their designations.

Fissile fuel cycle designation	Fertile isotope	Fissile isotope (converted)	Re-cycling	Fissile isotope (makeup)	Fissile fuel inventory
Thorium cycle					
A	Th232	U233	yes	U233	U233
B	Th232	U233	yes	U235	U233, U235
C	Th232	U233	no	U235	U235, U233
Uranium cycle					
D	U238	Pu*	no	U235	U235, Pu
E	U238	Pu	yes	U235	U235, Pu
F	U238	Pu	yes	Pu	Pu
Hybrid cycle**					
G	Th232	U233	yes no	Pu	U233, Pu
H	U238	Pu	yes no	U233	Pu, U233

*Pu in this table refers to the fissile Pu vector.
**Not specifically considered.

a reactor strategic point of view, although they may be of interest in the context of proliferation. The individual fissile fuel cycles are described in more detail in Section III.2.

An assessment as to whether the feed of FBR-bred fissile isotopes generally improves the HTR fissile fuel economy can only be made on the basis of a comparison of all these fissile fuel cycles. A detailed investigation of the fuel economy of each fissile fuel cycle is made in this chapter.

Assessments of this kind usually require extensive burnup calculations, similar to those in Chapter II for the FBR blanket. Special nuclear data libraries and special computer codes would be needed. In order to avoid the considerable effort involved in preparing cross-section sets and in performing the numerous burnup calculations necessary, the fuel utilization in the various fissile fuel cycles is analyzed by means of an analytical one-group model developed here. The model is based on the availability of a few pertinent global neutron parameters that can be determined from the neutron balances of the burnup calculations already performed for some of the fissile fuel cycles.

This one-group method is attractive for its universality, transparency, and comprehensiveness: it is applicable to the HTR fuel cycles considered here, and it makes clear the relationships between the nuclear parameters and the design parameters pertinent to the fissile fuel economy of the HTR; and, most important, it allows a comprehensive overview of the HTR potential in terms of fuel utilization and design characteristics.

For example, reliable estimates of the impact of design changes on the conversion ratio, such as reduced neutron leakage of decreased fission product poisoning, can be easily obtained, without extensive burnup calculations.

The accuracy of this one-group model is verified with the results of burnup calculations performed at the nuclear research center Kernforschungsanlage (KFA) Jülich, F.R.G.

Section III.3 gives an outline of the methodology; a more extensive discussion is contained in Appendix III.A. The relevant global neutron parameters are evaluated and discussed in Section III.4, and Section III.5 summarizes the results of the fissile fuel cycle assessments performed and discussed in detail in Appendix III.B.

III.2. DESCRIPTION OF THE FISSILE AND FERTILE FUEL FLOWS IN THE VARIOUS FISSILE FUEL CYCLES

The inherent design flexibility of the HTR offers the possibility of using either the thorium cycle (fertile isotope Th232) or the uranium cycle (fertile isotope U238). Each fuel cycle requires a feed of fissile fuel as makeup, however.
Since the makeup could be U233, U235, or Pu239, there are three conceivable fissile fuel cycles to each fuel cycle. They can be reduced to two fissile fuel cycles per fuel cycle since there is no particular incentive to supply the thorium cycle, converting Th232 to U233, with Pu239 as fissile fuel. The only logical makeup fissile isotopes for the thorium cycle are either U235 or U233. A similar line of reasoning applies to the uranium cycle, for which U233 as makeup fuel is impractical.

The number of fissile fuel cycles per fuel cycle increases to three if one includes the recycling mode of the self-bred fissile fuel. Thus thorium fissile fuel cycle C assumes that the self-bred U233 cannot be recycled due to a lack of thorium reprocessing facilities (Table III.1). Should such facilities become available the self-bred U233 could be recycled into the reactor; the resulting fissile fuel cycle is designated fissile fuel cycle B. Since B and C need additional U235 as makeup in the form of highly enriched uranium (93%), they both require considerable amounts of uranium ore (U_3O_8).

A similar line of reasoning applies to the uranium cycle. Recycling of self-bred Pu239 is assumed for fissile fuel cycle E but not for D. Since both cycles require U235 in the form of low enriched uranium ($\sim$3-4%), they also have uranium ore requirements, similar to those of cycles B and C.

Should, however, an excess of fissile isotopes U233 and/or Pu239 become available through the FBR[2], the U235 makeup for B and E could be replaced by U233 or Pu239, respectively, and fissile fuel cycles A and F would become viable. In cycle A the self-bred U233 is recycled, and the makeup is also in the form of U233; cycle F assumes Pu239 recycling, and the makeup is also Pu239. Thus neither A nor F has a demand for uranium ore.

The hybrid fissile fuel cycles G and H could become relevant if the proliferation issue required denaturation of fissile fuel. They are not discussed specifically since their fuel cycle performance lies within the range of the fissile fuel cycles investigated here.

The HTR is limited to fissile fuel cycles C or D as long as there are no appropriate facilities for reprocessing the discharged fuel. Should they become available some time in the

---

[2] In an HTR system, the U233 (or Pu239) bred by some HTRs can be transferred to other HTRs utilizing fissile fuel cycle A. The HTR U233 suppliers, however, run on fissile fuel cycle C, which requires considerably larger quantities of U235. A reactor system that only relies on HTRs, therefore, always requires U235, except in the very unlikely case that the conversion ratio of the entire system becomes $\geq$ 1.0.

future, there would be a choice of operating the HTR on any one of the four fissile fuel cycles, A, B, E, or F, provided the appropriate fissile fuel makeup is available. For the following discussion of these four fissile fuel cycles, it will tacitly be assumed that such reprocessing facilities exist.

III.3. BASIC EQUATIONS RELATING TO THE FISSILE FUEL ECONOMIES OF THE VARIOUS FISSILE FUEL CYCLES

Some of the basic equations necessary for evaluating the fissile fuel economies of the various fissile fuel cycles are briefly introduced here. Additional discussions are found in Appendices III.A and III.B.

III.3.a. Fissile Fuel Demands d_z and d_z^{U5}

The *net fissile fuel demand* d_z, in kg/GW(th)d, is given by Equation (I-36), such that

$$d_z = (1 + \alpha)_z^I \, (1 - CR_z) \, W_H^I \quad . \tag{III-1}$$

$(1 + \alpha)_z^I$ is weighted over the composition of all fissile isotopes in the core. This value heavily depends on the particular fissile fuel cycle since each has a different fissile isotope composition.

In the nonrecycling fissile fuel cycles C and D, d_z represents the difference between the U235 loaded, defined as d_z^{U5}, and the self-bred fissile fuels discharged, Pu239 or U233, defined as a_z and given in Equation (III-4).

Equation (III-1) does not yield the actual U235 demand to be supplied as makeup. It can be shown that d_z^{U5}, the U235 makeup, in kg/GW(th)d, is given by

$$d_z^{U5} = (1 + \alpha)_z^{U5} \left(\frac{F_m^{U5}}{F^I} \right)_z W_H^{U5} \quad . \tag{III-2}$$

$(1 + \alpha)_z^{U5}$ is the fissile fuel cycle-weighted $(1 + \alpha)^{U5}$;
$(F_m^{U5}/F^I)_z$ is the fission fraction of the U235 makeup (see

Appendix III.A), and W_H^{U5} assumes the meaning defined in Equation (I-32); W_H^i values for the various fissile isotopes i are given below[3].

As is shown in some greater detail in Appendix III.A.1, the fission fraction of the U235 makeup can be given by

$$\frac{F_m^{U5}}{F^I} = 1 - \sum_{i \neq U5}^{I} \left(\frac{F^i}{F^I}\right) - \frac{F_b^{U5}}{F^I} \quad , \tag{III-3}$$

where (F_b^{U5}/F^I) is the fission fraction of the self-generated U235, i.e. U235 produced by successive neutron capture in U233 and U234. These fission fractions of U235 must be determined before the desired U235 feed d_z^{U5}, Equation (III-2), can be evaluated. This in particular holds for fissile fuel cycles B, C, D, and E.

If d_z and d_z^{U5}, in kg/GW(th)d, are known, then a_z, the amount of self-bred fissile fuel discharged (U233 or Pu239), can be evaluated for the nonrecycle fissile fuel cycles C and D by

$$a_z^i = d_z^{U5} - d_z \quad , \tag{III-4}$$

---

[3] If the usable energy released per fission is assumed to be 200 MeV, then:

$$W_H^{U3} = \frac{0.233 \times 864 \times 10^{13}}{200 \times 1.6 \times 10^{-13} \times 6.024 \times 10^{23}} = 1.044 \text{ kg/GW(th)d of U233}$$

$$W_H^{U5} = 1.053 \text{ kg/GW(th)d of U235,}$$

$$W_H^{Pu9} = 1.071 \text{ kg/GW(th)d of Pu239,}$$

with

$$W_H^I = \sum_i^I \left(\frac{F^i}{F^I}\right) W_H^i \quad .$$

with d_z^{U5} and d_z given by Equations (III-2) and (III-1), respectively. However, these two equations can only be determined if the fission fraction distribution (F^i/F^I) is known. It can be found if the conversion ratio CR_z for fissile fuel cycle z is known.

III.3.b. Conversion Ratio CR_z

Common to all fissile fuel cycles is the relation of the conversion ratio, which is given by Equation (I-25) and derived in Appendix I.C.1:

$$CR_z = \eta_z^I \, (1 - P) - 1 \quad ; \qquad \text{(III-5)}$$

CR_z is seen to be determined by two global nuclear parameters that will be shown to be largely independent of each other: the fractional parasitic neutron losses P, defined in Equation (I-5), will be shown to be primarily determined by reactor design and fuel burnup; and η_z^I, the number of neutrons released per fissile absorption and averaged over the fissile isotopes, will be found to depend on the respective fissile fuel cycle. If the factors and relationships determining these two parameters are known, it is possible to make a fundamental assessment of HTR fuel utilization.

η_z is given by the following set of Equations (I-26), (I-27), and (I-28), derived in Appendix I.C.1:

$$\eta_z^I = \frac{\nu_z^I}{(1 + \alpha)_z^I} \quad ,$$

$$\nu_z^I = \sum_i^I \left(\frac{F^i}{F^I}\right)_z \nu^i \quad , \qquad \text{(III-6)}$$

$$(1 + \alpha)_z^I = \sum_i^I \left(\frac{F^i}{F^I}\right)_z (1 + \alpha)_z^i \quad ;$$

$(F^i/F^I)_z$ is the fissile fuel cycle-dependent fission fraction of a particular fissile isotope i, and $(1 + \alpha)^i_z$ the corresponding $(1 + \alpha)$ value. It is seen that η^I_z strongly depends on fissile fuel cycle z, since both $(F^i/F^I)_z$ and $(1 + \alpha)^i_z$ are determined largely by the fissile fuel cycle.

In the thermal HTR neutron spectrum, the fertile isotopes U238 and Th232 have a negligible fission fraction (<0.5%). They do not appreciably contribute to η^I_z and CR, other than in the case of the FBR (see discussion II.9.b). Their contribution is felt only indirectly, i.e. in the neutron properties of the self-bred fissile isotopes U233 or Pu239. The HTR conversion ratio thus depends only on the fissile isotope composition, reflected by η^I_z, and the parasitic neutron losses P.

In order to determine the fissile fuel utilization in the fissile fuel cycles, one must know the following parameters:

-- P = fraction of parasitic losses;
-- ν^i = neutron release per fission of individual fissile isotopes i;
-- $(1 + \alpha)^i_z$ = HTR spectrum-weighted $(1 + \alpha)^i$ values of each fissile isotope i;
-- $(F^i/F^I)_z$ = fission fraction distribution of the individual isotopes.

P, ν^i, and $(1 + \alpha)^i_z$ are nuclear parameters; they are discussed in the following section on the basis of the burnup calculations available. The fissile fuel cycle-dependent fission fraction distribution $(F^i/F^I)_z$ can then be evaluated with the help of analytical relations, derived and discussed in detail in Appendix III.A.

III.4. GLOBAL HTR NEUTRON DATA FOR THE VARIOUS FISSILE FUEL CYCLES

In order to determine CR, parameters P, ν^i, and $(1 + \alpha)^i_z$ must be obtained for each fissile fuel cycle. Representative parameter values can be extracted from the neutron balance distributions of the burnup calculations performed at KFA Jülich.

III.4.a. Parasitic Neutron Losses P in the HTR

As is the case in the FBR, a considerable fraction of the neutrons available is lost in the HTR by parasitic absorption and leakage. These parasitic losses are given in Equation (I-5) as

$$P = L + FP + St + M + C + R \quad , \qquad \text{(III-7)}$$

where the right hand terms represent the fractional neutron losses: L is due to leakage, FP is losses due to absorption in fission products, St in structural material, M in the moderator, C in the control rods, and R in parasitic actinides[4].

Table III.2 lists the contributions of these terms to parasitic absorption P for several HTR reference designs; they are extracted from the neutron balances of burnup calculations performed at KFA (Teuchert et al. 1972, 1974a and b; Schulten et al. 1977). The relevant fuel cycles of the HTR investigated are given in the sequence of the nomenclature [5] of Table III.1.

---

[4] P can also be determined as

$$P = 1 - A^{I} - A^{J} + A^{J+1} \quad ,$$

with

$$R = \sum_{i}^{I} A^{i+1} + 2A^{j+1} \quad .$$

A^{j+1} is the parasitic absorption in each of the intermediate actinides Pa233, Np239, etc; A^{i+1} is the parasitic absorption in actinides such as U236, Pu242, Np237. Absorption of a neutron in Pa233 or Np239 means loss of the neutron and the loss of fissile isotope U233 or Pu239, constituting a double entry in the neutron balance.

[5] e.g. cases A-1, A-2, etc, represent burnup calculations for fissile fuel cycle A.

Table III.2. Distribution of the parasitic loss fractions of the HTR for various fissile fuel cycles and designs (burnup and reactor size), taken from available burnup calculations.

Fissile fuel cycle†	Reactor power GW(th)	Fuel burnup GWd/t	Fission products			P = L + FP + (St + M) + R			P	Reference	
			Xe	S	FP	L	St + M	R			
Thorium cycle:											
A-1	3	36.4	.0147	.0520	.0667	.0426		.0134	.1227	Case 4022/L2	Teuchert 1974c*
A-2	1	28.6	.0176	.0445	.0621	.0658		.0173	.1452	Case 14907	Teuchert 1974c*
A-3	3	24	.014	.0387	.0525	.0405		.0111	.1041	Case 3212	Teuchert 1976
B-1	1	113	.0216	.0988	.1204	.0893		.0325	.2422	Case B	Teuchert 1974a
B-2	1	92	.0208	.0849	.1057	.0747	.0157	.0279	.2246	Case XI	Teuchert 1974a
C-1	2.7	106	.0217	.0995	.1212	.0673	.0177	.0228	.2290	Ref. Case 1	Teuchert 1974b
C-2	1	110	.0221	.1036	.1257	.0930		.0369	.2556	Case 48200	Lohnert 1973**
C-3	1	111	.0219	.103	.1248	.0906		.0379	.2524	Case A	Teuchert 1974a
C-4	1	91	.0215	.0916	.1131	.0763	.0175	.0224	.2240	Ref. Case I	Teuchert 1974a
C-5	3	23	.021	.0495	.0705	.0484		.0326	.1515	Case 323-B	Teuchert 1976*
Uranium cycle:											
D-1	3	101	.0202	.0831	.1033	.0750		.0084	.1867	Case 23502	Lohnert 1974**
D-2	1	108	.0226	.0941	.1167	.1038		.0109	.2314	Case 18200	Lohnert 1973**
D-3	1	90	.0200	.072	.0930	.0847	.0124	.009	.1830	LOTTO III	Teuchert 1974a
D-4	0.5	78	.021	.077	.098	.096				Case IV	Teuchert 1972
D-5	0.5	63	.021	.071	.092	.095				Case V	Teuchert 1972
D-6	0.5	44	.021	.062	.083	.089				Case I	Teuchert 1972
D-7	0.5	25	.020	.050	.070	.090				Case VI	Teuchert 1972

P = L + FP + (St + M) + R, FP = S + Xe.

†For fissile fuel cycle designations see Table II.1.

*Personal communication, KFA Jülich, F.R.G.

**Personal communication, Gesellschaft für Hochtemperatur, Bensberg, F.R.G.

Also indicated in column 2 is the respective reactor power, reflecting the size of the core and hence the leakage term L. The fuel burnup is tabulated in column 3. FP, the absorption losses in the fission products, is separated into a xenon fraction Xe and a remaining S fraction:

$$FP = (Xe + S) \quad . \qquad \text{(III-8)}$$

Examining the distribution of the parasitic losses more closely reveals that

- -- The largest fraction of parasitic losses is due to absorptions in the fission products.
- -- The second largest losses occur as a result of leakage.
- -- The parasitic losses in the structural materials and in the moderator are insignificant.
- -- The total parasitic losses P range from 0.18 to 0.25 for burnups larger than 80 GWd/t.
- -- The parasitic xenon fraction appears to reach an equilibrium value of Xe = 0.02 for all burnups.
- -- The parasitic losses in the actinides are larger in the thorium cycle than in the uranium cycle.

These observations, which are now discussed in more detail, are in some cases related to the corresponding values observed in FBRs (Table II.21).

The most important parasitic losses in the HTR are the losses in the fission products, FP. In the thermal HTR spectrum, a clear correlation should be observable between the S fraction, which excludes the Xe losses, and fuel burnup. This is illustrated by Figure III.1, in which S is plotted as a function of fuel burnup. This loss fraction clearly increases as the burnups increases; for high burnups, the uranium cycle with $S \simeq 0.08$ exhibits a smaller S fraction than the thorium cycle with $S \simeq 0.16$.[6] At low burnups of 20-30 GWd/t, S reduces to

[6] The fission products of U233 have larger absorption cross sections, which explains the larger losses in the thorium cycle.

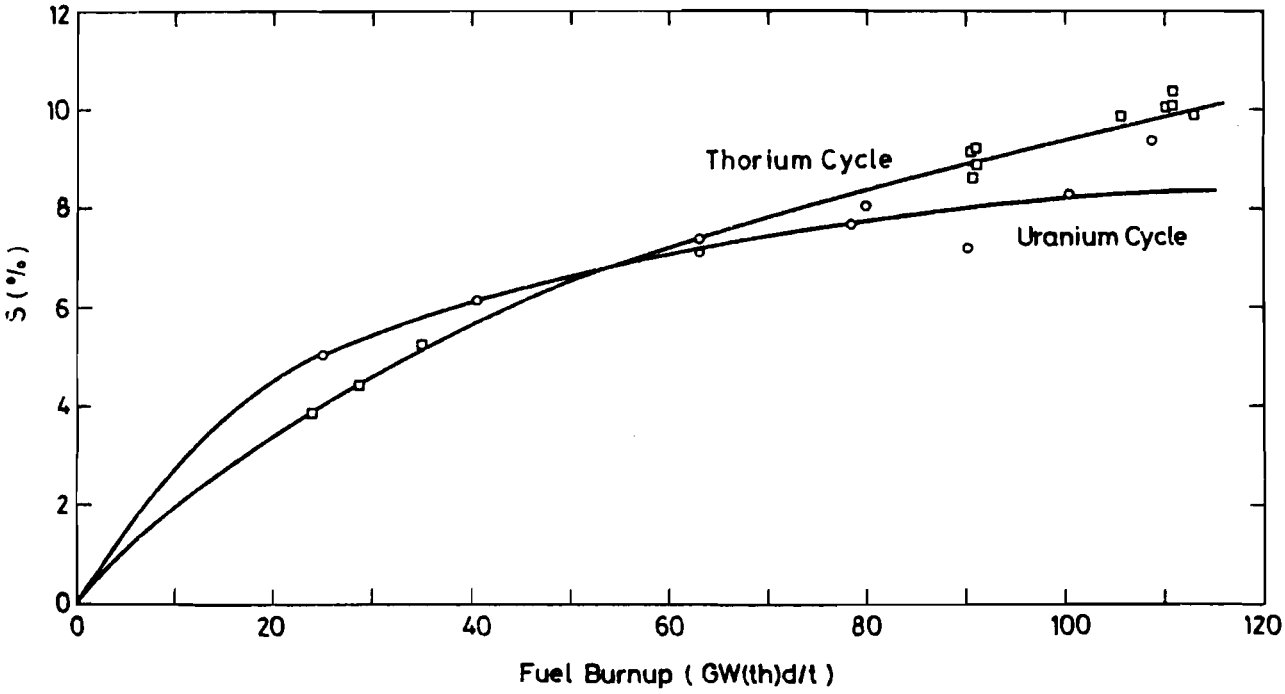

Figure III.1. Fractions of neutron absorption in the fission products (excluding Xe absorptions) of the HTR thorium and uranium cycles, as a function of fuel burnup (data from Table III.2).

values between 0.05 and 0.04. A decrease in fuel burnup thus leads to a significant reduction of S by about 0.05 to 0.07, or 5 to 7 points. Comparing these values with the FP fraction of the FBR in Table II.21, one observes that in the FBR the fission product losses are relatively significant for the total P_N losses. The impact of the burnup on P and thus on CR or BR_N is therefore much larger in the HTR than in the FBR.

The second largest parasitic loss fraction in the HTR, leakage losses L, is seen to vary between 0.04 and 0.10. L losses are found to be larger with HTR designs of power output less than 1 GW(th), whereas an increase in plant size to 3 GW(th) decreases L to 0.04. The L range in the FBR is between 0.065 and 0.02. SNR 300, with a plant size of 0.3 GW(e), clearly shows the largest L of 0.066, whereas FBRs of 1-2 GW(e) size show L losses of about 0.015. Therefore, leakage losses L are influenced by reactor size in both FBRs and HTRs, with FBRs exhibiting a tendency to generally lower values.

The losses in the structural materials, St, are unimportant for the HTR. In the FBR, St represents the largest loss contribution of 0.04-0.10. Decreasing this loss fraction in the FBR requires a redesign or possibly a technological innovation in FBR fuel and/or cladding material properties. St in the FBR generally cannot be influenced to the extent the S fraction in the HTR can be adjusted.

The above arguments lead one to infer that the FP and L fractions of the HTR can be influenced by variation of fuel burnup and/or reactor size. By contrast, loss fractions Xe and R seem to be less influenced by these factors. Xe seems to approach an equilibrium value of approximately 0.021 at a fairly wide range of burnups for all fissile fuel cycles from B to D. As the xenon concentration in the reactor attains an equilibrium within the first few days of reactor operation, Xe can thus be assumed to be largely independent of fuel burnup. Xe should decrease, however, as the average neutron flux Φ decreases. This has been observed for the HTR designs designated A-1, A-2, and A-3 in Table III.2--cases where the higher fissile enrichment required for these cycles reduces neutron flux Φ. In general, Xe and R take on greater importance only in the case of $P < 0.10$.

The above observations about the distribution of the parasitic neutron losses among the various HTR losses are summarized in Table III.3. The relatively large P fraction of 0.24 for HTRs of small size (1-GW(th) unit) and high fuel burnup is assumed to decrease with larger plant sizes (3-GW(th) units) and with reduced fuel burnup. P values as low as 0.09 appear to be achievable if the fuel burnup is held at 20-30 GWd/t.

According to Table III.2, there is no significant difference in P between the thorium and uranium cycles. Accounting for the slightly smaller R losses in the thorium cycle, however, Table III.3 lists somewhat different P values for the thorium and uranium cycles. These P values serve as reference values for the fuel cycle assessments discussed in the following sections.

Table III.3. Estimated influence of fuel burnup and reactor size on the neutron loss fractions FP (fission products and xenon), L (leakage), R (parasitic actinides), and P (total parasitic neutron losses) for the HTR thorium and uranium cycles.

Fuel cycle Fissile fuel cycle	Thorium cycle A, B, C				Uranium cycle D, E, F			
Loss fractions	P	L	FP	R	P	L	FP	R
Reactor size: 1 GW(th) Fuel burnup: 100 GWd/t	.24	.09	.12	.03	.23	.10	.11	.01
Reactor size: 3 GW(th)								
Fuel burnup: ~100 GWd/t	.20	.05	.12	.03	.19	.06	.11	.01
~50 GWd/t	.15	.05	.08	.02	.14	.06	.07	.01
~30 GWd/t	.12	.05	.06	.01	.11	.06	.05	-
~20 GWd/t	.10	.05	.04	.01	.09	.06	.03	-

$P = L + FP + R + (St + M)$, $FP = S + Xe$.

III.4.b. HTR Spectrum-Weighted $(1 + \alpha)_z^i$ and Fissile Isotope-Dependent ν^i Values

The neutron parameters that remain to be determined are the fissile isotope- and fissile fuel cycle-dependent $(1 + \alpha)_z^i$ values and the fissile isotope-dependent ν^i values. The $(1 + \alpha)_z^i$ values have to be extracted from the burnup calculations, whereas the ν_z^i values are shown to be independent of the fissile fuel cycle.

In the HTR most neutrons are absorbed in the thermal or epithermal neutron energy range. The distribution between the thermal and epithermal absorptions depends on the prevailing neutron energy spectrum, which in turn is determined by the moderation ratio. Since different moderation ratios are expected for the various fissile fuel cycles, the values of the energy-dependent global neutron parameters are also expected to differ for each fissile fuel cycle. The ν^i values are energy dependent

Table III.4. Fissile isotope data for the various fissile fuel cycles.

Fissile fuel cycle	Parameters	U233	U235	Pu239	Pu241
Thorium cycle: Fissile fuel cycle A	$(1+\alpha)^i$*	1.125	1.298	-	-
	ν^i**	2.50	2.43		
	η^i	2.222	1.872		
Thorium cycle: Fissile fuel cycles B, C	$(1+\alpha)^i$†	1.104	1.248	1.356	1.159
	ν^i**	2.50	2.43	2.89	2.97
	η^i	2.264	1.947	2.131	2.562
Uranium cycle: Fissile fuel cycles D, E, F	$(1+\alpha)^i$††		1.362	1.590	1.410
	ν^i**		2.43	2.89	2.97
	η^i		1.784	1.818	2.106

* These values are mean values of cases A-1, A-2, and A-3 listed in Table III.5 (references are given in Table III.2).

** Personal communciation by E. Teuchert, Kernforschungsanlage Jülich, FRG (1974); good agreement with BNL-5800 and ENDF/B-III.

† These values are mean values of cases B-1 to C-5 listed in Table III.5. The Pu values appear somewhat low, but have only an insignificant influence on the neutron balances of these cases.

†† The U235 value represents the mean value of cases D-1 to D-4. Since the Pu239 and Pu 241 values of 1.460 and 1.265, respectively, as they were determined from these cases, seem somewhat too low, the values from Teuchert and Brandes (1975, p. 139) were used for these isotopes. The corresponding Pu value of 1.627 from the program system ORIGIN agrees well with these values.

in the upper energy range of > 100 keV. In the thermal and epithermal energy ranges, however, they remain constant for all practical purposes, since absorption in the high energy region is of little importance in the HTR. Unaffected by change in the distribution of thermal and epithermal absorptions due to a changing moderation ratio, the ν^i values are therefore independent of the fissile fuel cycle. This is reflected by Table III.4, where the isotope-dependent ν^i values are the same for all fissile fuel cycles. These values were taken from the

modified GAM nuclear data set (30 thermal and 68 epithermal energy groups used at KFA Jülich, which show good agreement with the values in BNL-5800, in the ENDF/B-III (Kidman and Scheuter 1971), and in the HAMMER group constant set (Suich and Honeck 1967)).

The by far most critical parameters among the global neutron parameters, and also the most difficult to determine accurately, are the fissile isotope- and fissile fuel cycle-dependent $(1 + \alpha)_z^i$ values. They must be extracted from the neutron balance distribution of the burnup calculations, since they are highly energy dependent and thus fissile fuel cycle specific. Table III.5 lists these values as they were extracted from the burnup calculations referred to in Table III.2, for fissile fuel cycles A, B, C, and D. No burnup calculations were available for cycles E and F.

The $(1 + \alpha)_z^i$ values of a particular isotope and of a particular fissile fuel cycle are observed to fall within a relatively narrow band, as is the case, for example, with U235 in cycle C. The moderation ratios are also listed. The isotope-specific $(1 + \alpha)_z^i$ values of Table III.5 were averaged over all the values available for a given fissile fuel cycle. These mean $(1 + \alpha)_z^i$ values are listed in Table III.4, together with the corresponding η_z^i values, which can now be evaluated since ν^i and $(1 + \alpha)_z^i$ are known.

The influence of the moderation ratio or of the neutron spectrum on $(1 + \alpha)^i$ is seen in particular for U235. The moderation ratio of fissile fuel cycle C centers around an average value of 230, but that of cycle D around 420. A larger moderation ratio implies a softer neutron spectrum, placing more emphasis on thermal rather than on epithermal absorptions. $(1 + \alpha)^{U5}$ is known to be a very sensitive function of the neutron energy, increasing to generally higher values as the neutron spectrum softens. This is reflected by the average $(1 + \alpha)^{U5}$ value of 1.362 in fissile fuel cycle D compared to 1.248 in cycle C. The sensitivity of the neutron energy to $(1 + \alpha)^i$ is illustrated by Figure III.2, where $(1 + \alpha)^i$ is plotted for isotopes U233, U235, Pu239, and Pu241 in the thermal and in part of the epithermal energy regions, from 0 to 5 eV. It must be emphasized at this point that heterogeneity and fuel temperature

Table III.5. HTR spectrum-averaged $(1 + \alpha)^i$ values* of fissile isotopes for various fissile fuel cycles and their moderation ratios N_C/N_{HM} from the burnup calculations available.

Fissile Fuel Cycle**	U233	U235	Pu239	Pu241	Moderation ratio N_C/N_{HM}
Thorium cycle					
A-1	1.126	1.289			110
A-2	1.125	1.308			
A-3	1.123	1.299			110
B-1	1.107	1.254	1.346	1.131	230/280
B-2					230
C-1					180
C-2	1.102	1.253	1.350	1.178	280/240
C-3	1.099	1.248	1.364	1.197	230/280
C-4	1.105	1.250			230
C-5	1.109	1.237	1.365	1.1307	200
Uranium cycle					
D-1		1.360	1.473	1.268	500
D-2		1.337	1.455	1.257	420/460
D-3		1.354	1.408***		350
D-4		1.397	1.405***		

* Fissile fractions (F^i/F^I) and absorptions A^i are extracted from the neutron balances. $(1 + \alpha)^i$ can be determined by using ν^i from Table III.4 and the equation:

$$(1+\alpha)^i = \frac{A^i}{(F^i/F^I)} \sum_i^I \left(\frac{F^i}{F^I}\right) \nu^i$$

** See Table III.2. for references.

*** Mean values for Pu239/241.

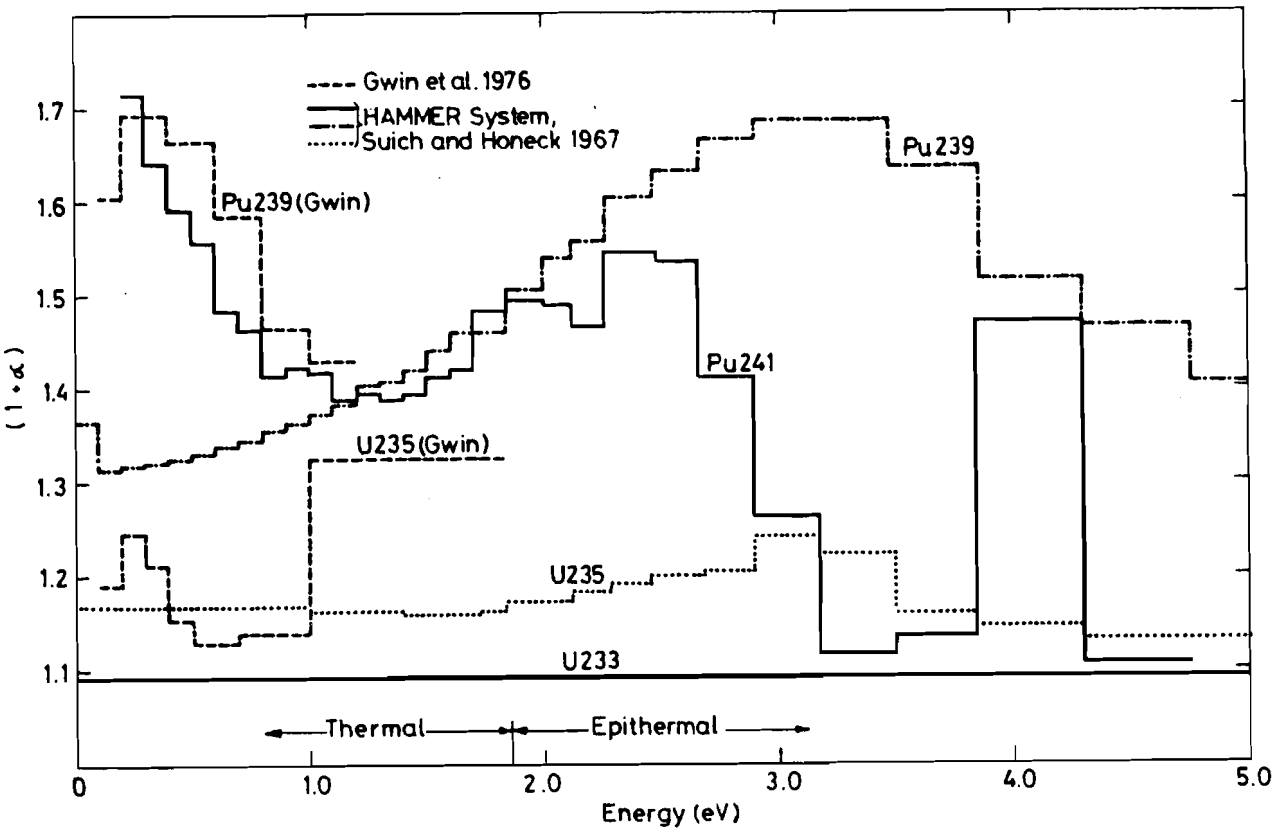

Figure III.2. $(1 + \alpha)$ energy group data for Pu239, U235, and U233 from 0 to 5 eV.

have a very important influence on the fissile fuel cycle-specific $(1 + \alpha)^i$ values, so that a comparison between the data listed in Tables III.4 and III.5 and those plotted in Figure III.2 is not directly applicable. However, the general trend of $(1 + \alpha)^i$ as a function of neutron energy or moderation ratio is clearly demonstrated.

Some of the data in Figure III.2 are taken from the data set of the HAMMER system (Suich and Honeck 1967), and some from measurements performed by Gwin et al. (1976). Gwin gives the ratios of the absorption and fission cross sections measured.

A smaller moderation ratio N_C/N_{HM} shifts the neutron spectrum from the thermal into the epithermal energy range, where the $(1 + \alpha)^i$ values for Pu239 and U235 are higher. U233, by contrast, remains largely constant over the entire thermal and epithermal energy ranges.

It can be inferred from the energy dependence of the $(1 + \alpha)^i$ values of U235 and U233 in Figure III.2 that the moderation ratio in the thorium cycle has relatively little influence on the HTR spectrum-averaged $(1 + \alpha)^i$ values, since $(1 + \alpha)^{U3}$ is relatively flat. The moderation ratio in the uranium cycle, on the other hand, is considerably more significant due to the steep rise of $(1 + \alpha)^i$ of Pu239.

The $(1 + \alpha)^i$ values of the Pu isotopes, which were determined from the neutron balances available, still seem somewhat uncertain. As regards thorium fissile fuel cycle C, however, Pu is only of minor significance; the Pu239 and Pu241 values, which seem quite low, may be fairly uncertain for all thorium fissile fuel cycles since they do not significantly influence fissile fuel utilization. By contrast, the U235 and U233 values determined for the thorium cycles must be highly reliable.

As regards fissile fuel cycles D, E, and F, i.e. the uranium cycle, burnup calculations were available only for cycle D. The $(1 + \alpha)^i$ values for the Pu isotopes (1.460 and 1.265 for Pu239 and Pu241, respectively) taken from these calculations probably require some revision. In the meantime, values of 1.59 and 1.41 have been published without accompanying neutron balances (Teuchert and Brandes 1975), which show closer agreement with the global HTR data of $(1 + \alpha)^{Pu9} = 1.627$ and $(1 + \alpha)^{Pu41} = 1.373$ contained in the ORIGEN code system (Bell 1973) and the data measured by Gwin et al. 1976 (Figure III.2). For cases D to F, the values proposed in Teuchert and Brandes (1975) were accepted with the reservation that they might require revision. A comparison of $(1 + \alpha)^i$ for the Pu isotopes in the D_2O reactor (N. Pieroni, recalculations for Atucha, Argentina, personal communication, Gesellschaft für Kernforschung, Karlsruhe, 1974) yields values of 1.526 for Pu239, 1.439 for Pu241, and 1.180 for U235. This is as far as the problem of accurary of such $(1 + \alpha)^i_z$ data can be discussed here; a more detailed examination would exceed the scope of the present investigation.

III.5. DESCRIPTION OF THE ONE-GROUP CALCULATIONS PERFORMED

The relevant global neutron parameters P, ν^i, and $(1 + \alpha)_z^i$ were evaluated in the preceding sections. In order to obtain the conversion ratio CR, Equation (III-5), we still have to determine the fissile fission fraction distribution $(F^i/F^I)_z$, for which analytical relations are developed in Appendix III.A. According to these equations, the distribution of $(F^i/F^I)_z$ can be determined for all fissile fuel cycles, once the respective $(1 + \alpha)_z^i$ values are available and the conversion ratio CR_z is known. Since CR_z is the parameter to be obtained, an iterative process is needed for determining CR_z and $(F^i/F^I)_z$.

Briefly, this iterative process is the following: ν^i and fissile fuel cycle-specific $(1 + \alpha)_z^i$ values are taken from Table III.4, and an HTR design- and fuel burnup-specific P value from Table III.3. These parameters remain constant throughout the iteration. First one makes a zero order approximation of the conversion ratio $CR_{l=0}$ (l = iterative step) using Equation (III-5), after having chosen a plausible $\eta^I_{l=0}$ value from the η^i_z values of the pertinent fissile isotopes in Table III.4 (see example in Appendix III.A). With $CR_{l=0}$ available, an $(F^i/F^I)_{l=1}$ distribution can be determined by means of the appropriate equations in Appendix III.A. With $(F^i/F^I)_{l=1}$ available, one obtains a revised $\eta^I_{l=1}$ value with Equation (III-6), using the specified $(1+\alpha)_z^i$ and ν^i values. Thus one calculates a revised $CR_{l=1}$, which again can be used to determine a new $(F^i/F^I)_{l=2}$ distribution. This iterative process is repeated until $CR_{l=n}$ converges. Convergence is usually attained after three or four iterative steps. Having specified $CR_{l=n}$, one can proceed to calculate the U235 fission fractions, the U235 demand d_z^{U5}, and the discharged fissile fuel a_z^i, with the help of Equations (III-2), (III-4), and (III-1).

Comparison of the results obtained with this analytical method to the results of exact burnup calculations shows a consistently good agreement. More details are given in Appendix III.B, where the calculations for each fissile fuel cycle are

Table III.6. Accuracy of the one-group model for fissile fuel cycle parameters in comparison to exact burnup calculations (P values taken from exact calculations, $(1 + \alpha)^i$ values from Table III.4).

	CR_z	η_z^I	$\frac{F^{U3(Pu)}}{F^I}$	$(\frac{F_t^{U5}}{F^I})_z$	d_z^{U5}	a_z
Accuracy	$\pm.01$	$\pm.01$	$\pm.01$	$\pm.01$	3%	10%

discussed separately. Tables III.B.1 to III.B.4 compare the method on the basis of the results of the reference burnup calculations listed in Table III.2. The accuracy of prediction that can be obtained for the relevant fuel utilization parameters CR_z and d_z^{U5} and for some other important parameters is summarized in Table III.6: CR_z can be predicted up to 1 point (0.01), and d_z^{U5} up to 3%.

The accuracy of the results largely depends on the availability of reliable $(1 + \alpha)_z^i$ and P values. The P values were shown to be well predictable for all fissile fuel cycles, but the $(1 + \alpha)_z^i$ values varied significantly among the individual fissile fuel cycles. Based on ten reference burnup calculations, the $(1 + \alpha)_z^i$ values in Table III.4 for the thorium cycle can be regarded as quite reliable. $(1 + \alpha)_z^i$ for the uranium cycle, on the other hand, specifically for fissile fuel cycles E and F, are estimates, based on the burnup calculations for fissile fuel cycle D. A relatively small error ($\sim$5%) in these values will affect the results quite considerably. It is felt, however, that the $(1 + \alpha)_z^i$ values adopted here for the uranium cycle, and especially those considered for Pu239 and Pu241, represent reasonable estimates that conform to the values observed for other thermal reactors.

III.6. RESULTS PERTAINING TO THE FISSILE FUEL UTILIZATION IN FISSILE FUEL CYCLES A TO F

It has been shown above that the HTR conversion ratio CR can be represented by the two nuclear parameters η_z^I and P; η_z^I has been shown to primarily depend on the respective fissile fuel cycle, and P on design and fuel burnup.

Realizing that η_z^I and P can be considered separately, one may carry out an investigation scanning the complete spectrum of HTR fuel utilization by assessing firstly, the influence of the different fissile fuel cycles on η_z^I and, secondly, the impact of fuel burnup on P, employing to this end the analytical procedure described above. Within the context of this investigation, it is of particular interest to assess U233 and/or Pu239 as fissile fuel makeup, since these isotopes can be supplied by the FBR.

The influence of the fissile fuel feed was analyzed by selecting from Table III.4 the $(1 + \alpha)_z^i$ values of a fissile fuel cycle under consideration and a certain P value, depending on HTR design characteristics and fuel burnup, from Table III.3. The influence of decreased burnup was simulated for each fissile fuel cycle, by reduction of the parasitic neutron losses P in accordance with the data in Table III.3, the $(1 + \alpha)_z^i$ values being held constant[7].

The data assumed for these calculations are summarized in Table III.7. Tables III.8 and III.9 reproduce the calculation results for each fissile fuel cycle, which are discussed in greater detail in Appendix III.B. Table III.8 shows the fissile composition-averaged $(1 + \alpha)_z^I$, ν_z^I, and η_z^I values obtained, and Table III.9 gives the relevant fissile fuel cycle parameters CR_z, U235 feed demand d_z^{U5}, net fissile demand d_z, and discharged

---

[7] Analysis of the neutron balances of various HTR designs shows that $(1 + \alpha)_z^i$ values are independent of P values. The fissile isotope composition-averaged $(1 + \alpha)_z^I$ value, Equation (III.6), however, slightly changes with P.

Table III.7. Fissile fuel cycle-dependent nuclear parameters and parasitic loss fractions P (for 3-GW(th) units) assumed for analytical calculations.

Fissile fuel cycle (z)	$(1+\alpha)_z^i$				ν_z^i				P for burnup (GWd/t)		
	U233	U235	Pu239	Pu241	U233	U235	Pu239	Pu241	30	50	100
A	1.125	1.298	--	--	2.50	2.43	--	--	0.12	0.15	0.20
B	1.104	1.248	1.356	1.159	2.50	2.43	2.89	2.97	0.12	0.15	0.20
C	1.104	1.248	1.356	1.159	2.50	2.43	2.89	2.97	0.12	0.15	0.20
D	--	1.362	1.590	1.410	--	2.43	2.89	2.97	0.11	0.14	0.19
E	--	1.362	1.590	1.410	--	2.43	2.89	2.97	0.11	0.14	0.19
F	--	1.362	1.590	1.410	--	2.43	2.89	2.97	0.11	0.14	0.19

Table III.8. Global HTR fissile fuel cycle-averaged nuclear parameters as determined by analytical calculations for various fissile fuel cycles as a function of fuel burnup.*

Fissile fuel cycle (z)	Fuel burnup (GWd/t) 30			50			100		
	$(1+\alpha)_z^I$	η_z^I	CR_z	$(1+\alpha)_z^I$	η_z^I	CR_z	$(1+\alpha)_z^I$	η_z^I	CR_z
A	1.140	2.183	0.92	1.140	2.187	0.86	1.140	2.187	0.75
B	1.164	2.188	0.88	1.176	2.108	0.79	1.157	2.138	0.71
C	1.198	2.049	0.80	1.190	2.065	0.75	1.183	2.080	0.66
D	1.451	1.814	0.62	1.448	1.819	0.56	1.438	1.824	0.48
E	1.467	1.859	0.65	1.458	1.849	0.59	1.443	1.839	0.49
F	1.537	1.896	0.69	1.537	1.896	0.63	1.537	1.896	0.54

*See tables in Appendix III.B for comparing these results with those of exact burnup calculations.

Tabele III.9. Evaluated HTR fissile fuel cycle parameters: conversion ratio CR_z, U235 demand d_z^{U5}, fissile fuel demand d_z, and fissile fuel discharged a_z for various fissile fuel cycles as a function of fuel burnup.

Fissile fuel cycle (z)	Re-cycle	Fissile isotope makeup	Fuel burnup (GWd/t)											
			30				50				100			
			CR_z	d_z^{U5}*	d_z*†	a_z*	CR_z	d_z^{U5}*	d_z*†	a_z*	CR_z	d_z^{U5}*	d_z*†	a_z*
A	yes	U233	0.92	0	90**	0	0.86	0	168**	0	0.75	0	300**	0
B	yes	U235	0.88	182	182	0	0.79	290	290	0	0.71	390	390	0
C	no	U235	0.80	788	248	540**	0.75	707	306	401**	0.66	640	442	198**
D	no	U235	0.62	804	586	218††	0.56	810	662	148††	0.48	848	789	59††
E	yes	U235	0.65	565	539	26††	0.59	637	628	9††	0.49	758	743	15††
F	yes	Pu239	0.69	0	505††	0	0.63	0	597††	0	0.54	0	750††	0

*Measured in g/GW(th)d
**U233
†$d_z = d_z^{U5} - a_z$
††Pu^{fiss}

fissile fuel a_z, for different fuel burnups and fissile fuel cycles z. The latter are shown in Figures III.3, III.4, and III.5.

Figure III.3 shows the conversion ratio for each fissile fuel cycle listed in Table III.1 as a function of fuel burnup. The following observations can be made:

-- CR increases considerably as the fuel burnup decreases. This holds true for all fissile fuel cycles. The increase is primarily due to the smaller parasitic losses P.
-- The thorium cycle permits considerably higher conversion ratios than the uranium cycle. The difference between the comparable fissile fuel cycles is about 20 points[8] at a burnup A of about 100 GW(th)d/t, and about 20-30 points at A ≃ 20-30.
-- The nonrecycling fissile fuel cycles C and D show the lowest conversion ratios.
-- Recycling the self-bred fissile isotopes, i.e. changing from cycle C to cycle B in the thorium cycle and from cycle D to E in the uranium cycle, leads to higher conversion ratios. Recycling U233 in the thorium cycle, however, results in a larger increase in CR (~ 5 points at A ≃ 100) than recycling Pu239 in the uranium cycle (~ 1 point at A ≃ 100).
-- The optimal fissile feed isotope is U233 (fissile fuel cycle A). This feed allows conversion ratios close to 1.0 for very low fuel burnups, i.e. CR ≃ 0.95 for A ≃ 20-30. For comparison, a Pu239 feed allows conversion ratios of only CR = 0.71 for low burnups, i.e. A ≃ 20-30.

The large difference between the thorium and uranium cycles in the HTR[9] is explained by the large difference in the $(1 + \alpha)_z^i$ values of U233 and Pu239 in the thermal neutron spectrum. This is most clearly seen for fissile fuel cycles A and F with $\eta^{U3} \simeq 2.22$ and $\eta^{Pu9} \simeq 1.82$, or $(1 + \alpha)^{U3} = 1.125$ and $(1 + \alpha)^{Pu9} = 1.590$.

---

[8] 1 point = 0.01 in CR, A = fuel burnup (GW(th)d/t).

[9] like in any other thermal reactors relying only on fissile fission.

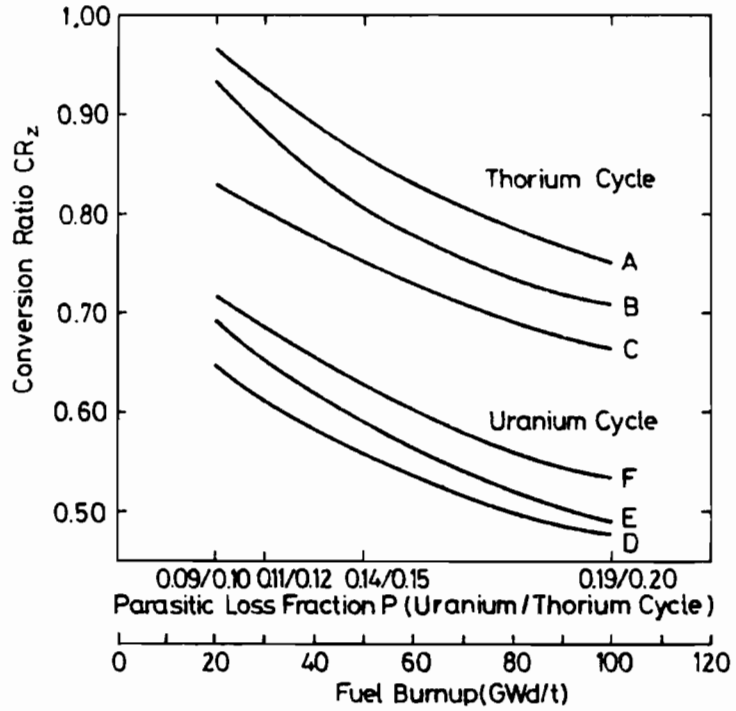

Figure III.3. HTR conversion ratios CR_z for various fissile fuel cycles (Table III.1) as a function of fuel burnup (for 3-GW(th) units).

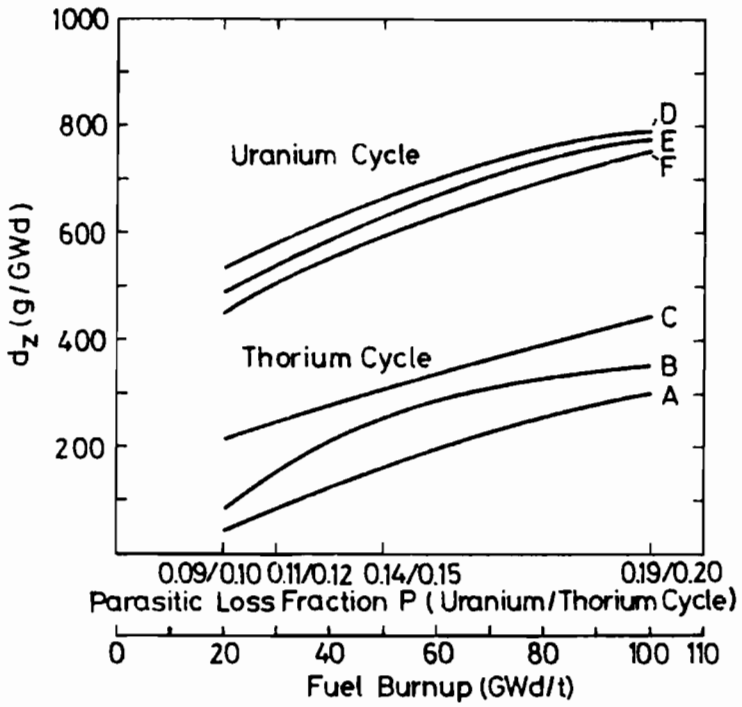

Figure III.4. Fissile fuel demand d_z for various fissile fuel cycles (Table III.1) of the HTR as a function of burnup (for 3-GW(th) units).

Figure III.4 shows the fissile fuel demands d_z, Equation (III-1), of the six cycles. For the nonrecycle fissile fuel cycles C and D, d_z represents the difference between the U235 loaded and the self-bred fuel discharged, i.e. U233 in C and Pu 239 in D. For cycles B and E, d_z represents the actual U235 requirements.

For cycles A and F, the respective U233 and Pu239 demands are given by d_z. d_z is directly proportional to (1 - CR), and the cycles with the highest conversion ratios consequently have the lowest net fissile fuel demands d_z. This comparison is of particular interest.

Figure III.5 shows the uranium ore-dependent U235 makeup d_z^{U5} for fissile fuel cycles B, C, D, and E. For the recycling cyles B and E, for which availability of reprocessing facilities is assumed, there is a definite incentive to decrease the fuel burnup since considerable U235 savings result.

This is not the case with the nonrecycling cycles C and D, where lower burnups have the opposite effect. As the burnup decreases, more self-bred fissile fuel is discharged at the expense of a higher U235 demand, in spite of the increased conversion ratio. Since the discharged self-bred fuel is stored and not recycled, there is no incentive to decrease the burnup of the HTR in these nonrecycling fissile fuel cycles. This implies that, without reprocessing facilities, the U235 demand of the HTR is lowest at high fuel burnups and with conversion ratios of CR = 0.55-0.65. Increasing CR by decreasing the fuel burnup thus results in a higher U235 demand for the nonrecycle fissile fuel cycles C and D.

Figure III.6 shows the influence on the U235 demand d_z^{U5} when operation is shifted from the nonrecycle to the recycle mode; the ratios of the recycle to the nonrecycle fissile fuel cycles for the thorium and uranium cycles are plotted as functions of fuel burnup. Shifting from the nonrecycle to the recycle mode results in a significant decrease in U235 demand, i.e. the recycle U235 demand in thorium cycle B at A ≈ 100 is only about 60% of the nonrecycle demand, and decreases with lower burnups to about

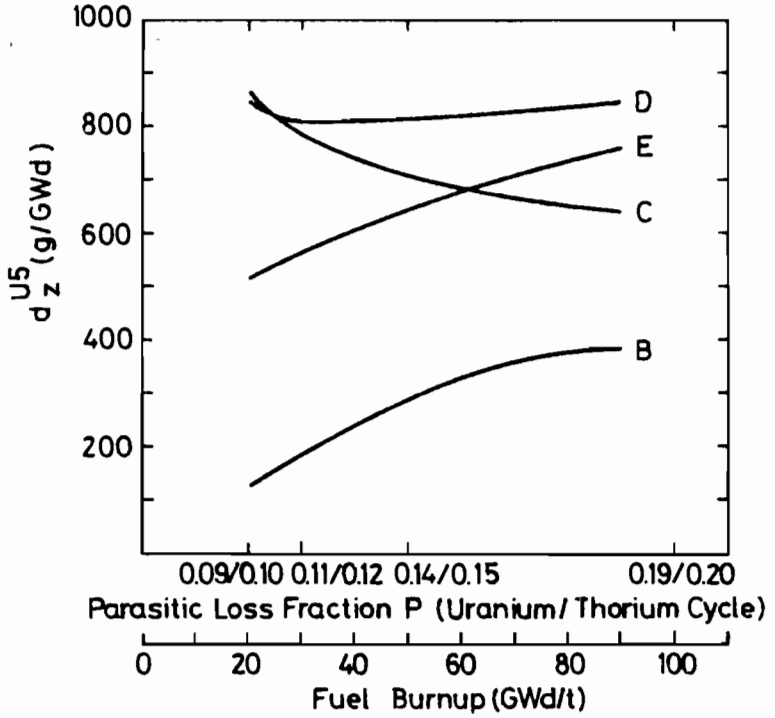

Figure III.5. U235 makeup d_z^{U5} for various HTR fissile fuel cycles as a function of fuel burnup (for 3-GW(th) units).

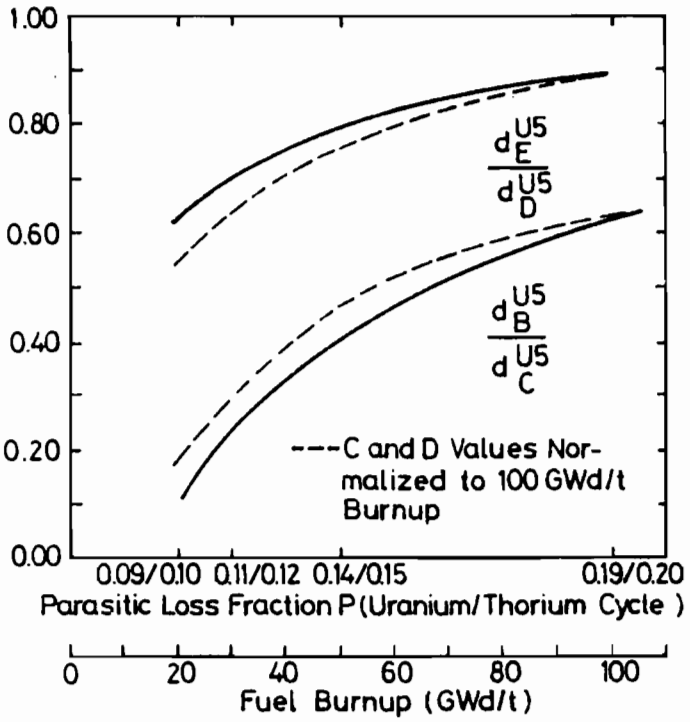

Figure III.6. Ratio of U235 makeup d_z^{U5} of the recycle to the nonrecycle fissile fuel cycles for the thorium (d_B^{U5}/d_c^{U5}) and uranium cycles (d_E^{U5}/d_D^{U5}).

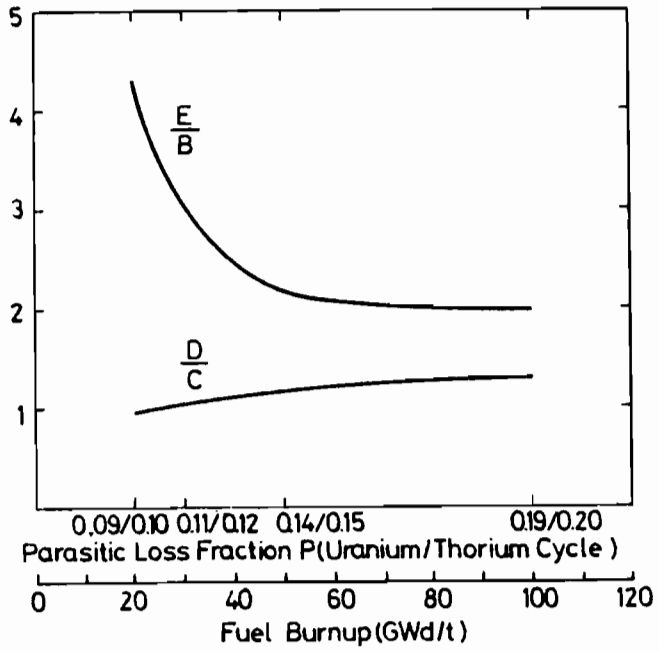

Figure III.7. Ratio of U235 makeup d_z^{U5} of the uranium to the thorium cycle for the nonrecycling fissile fuel cycles D and C and the recycling fissile fuel cycles E and B, as a function of fuel burnup (for 3-GW(th) units).

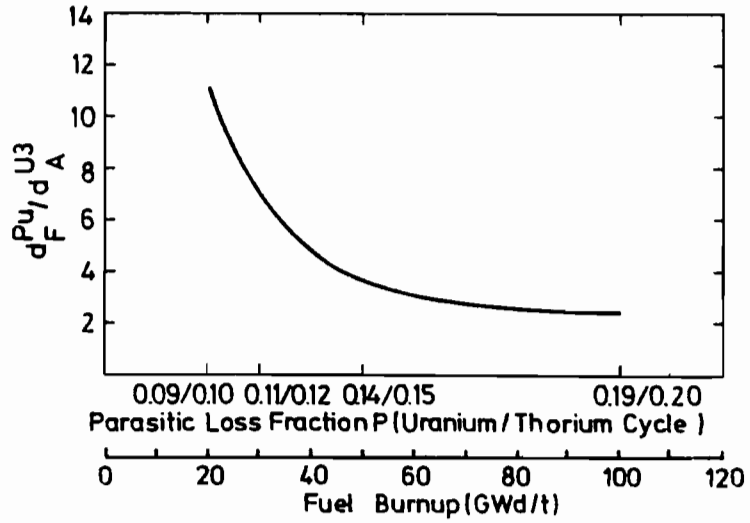

Figure III.8. Ratio of Pu^{fiss} demand d_F^{Pu} for fissile fuel cycle F to U233 demand d_A^{U3} for fissile fuel cycle A, as a function of fuel burnup (for 3-GW(th) units).

15%. In the uranium cycle the savings are not as large, i.e. still about 90% of the nonrecycle U235 is needed for the recycle cycle E at A ≈ 100 GWd/t.

Figure III.7 shows the ratio of U235 demands d_z^{U5} of the recycle fissile fuel cycles E (uranium cycle) to B (thorium cycle) and of the respective nonrecycle cycles D to C. Relative to the big difference in U235 demand between the two recycle fissile fuel cycles, especially at low burnups, there is little difference between the two nonrecycle fissile fuel cycles. This implies that the thorium and uranium cycles do not differ much with respect to their U235 demand as long as no reprocessing facilities are available.

Figure III.8 shows the relative amounts of Pu239 feed in cycle F and U233 feed in cycle A. At high burnups of A ≈ 100, cycle F needs about twice as much Pu239 as U233 is needed in cycle A, the difference or ratio increasing steeply as the burnup decreases. This fact will be of significance for the considerations of Chapter IV.

III.7. SUMMARY OF CHAPTER III

It has been shown that the analytical method developed here for studying the fissile fuel utilization of different HTR fissile fuel cycles is of sufficient accuracy as compared to detailed burnup calculations, provided the global nuclear parameters $(1 + \alpha)_z^i$ are reliably known. By analysis of the neutron balances of detailed burnup calculations, it was deduced that the HTR conversion ratio can be significantly influenced in two different ways:

-- changing the fissile isotope composition in the HTR by supplying it with different fissile isotopes;
-- manipulating the parasitic neutron losses due to absorption in fission products by way of changing the fuel burnup.

An assessment of these effects has shown that

-- The fuel burnup has a significant effect on the fissile fuel utilization in the HTR for all the fissile fuel cycles considered.
-- The thorium cycle allows considerably higher conversion ratios than the uranium cycle if reprocessing facilities are available.
-- If the self-bred fissile fuels, i.e. U233 in the thorium cycle and Pu239 in the uranium cycle, are not recycled (for lack of reprocessing facilities), there is little difference in U235 demand between the thorium and uranium cycles.
-- In the nonrecycle mode, there is no advantage in lowering the HTR burnup since the U235 demand increases as the burnup decreases, in spite of an increase in CR. The lowest U235 demand is achieved with conversion ratios CR $\simeq$ 0.50-0.60.
-- Decreasing burnups to obtain higher conversion ratios and lower U235 demands is only reasonable if HTR reprocessing facilities are available.
-- Decreasing the burnup in the recycle mode allows significant U235 savings.
-- Recycling the self-bred fissile fuel is more advantageous in the throium cycle than in the uranium cycle, i.e., the U235 savings are larger.
-- If the feed fissile isotope is not U235 but U233 or Pu239, the thorium cycle with U233 as feed is superior by several factors to the uranium cycle with Pu239 feed.
-- The fullest potential of the HTR is thus achieved if
  a. the thorium cycle is utilized, i.e. Th232 is used as fertile fuel;
  b. the self-bred U233 is recycled, i.e. on the assumption that thorium reprocessing facilities are available;
  c. the feed fissile isotope is U233.

If only condition a. is fulfilled, the thorium cycle has no definite advantage over the uranium cycle, at least not as far as its U235 demand is concerned.

If conditions a. and b. are met, the advantage of the thorium cycle over the uranium cycle can be considerable, depending on the design and the fuel burnup of the HTR.

And, if a transfer of fissile fuel from the FBR to the HTR were ever contemplated, the HTR should definitely utilize the thorium cycle.

CHAPTER IV. FISSILE FUEL ECONOMY IN A SYMBIOTIC FBR/HTR REACTOR SYSTEM

IV.1. THE STYLIZED FBR/HTR SYSTEM

The influence of the various fuel cycles on the fissile fuel utilization in the FBR and the HTR has so far been assessed in quantitative and qualitative terms: in Chapter II this was done for the FBR, and in Chapter III for the HTR. The results of these assessments are now being combined in order to determine the fuel cycle of a symbiotic FBR/HTR system with the most favorable fissile fuel utilization.

Even though a fully deployed reactor system consisting only of FBRs and HTRs cannot be expected to be operative within the next few decades, an assessment of the fuel cycle characteristics of such a symbiotic reactor system appears to be of relevance already today: it permits a timely recognition of the potential and the constraints of such a system, and focuses attention on the pertinent system parameters at a time when the two reactor types in question are still under development.

The period in which such an assumed symbiotic FBR/HTR system will be operative is referrred to as the asymptotic phase. It is basically characterized by the absence of a further large-scale expansion of nuclear energy, yet does not foreclose the possibility of a continued but limited growth of the FBR/HTR system.

The asymptotic phase is preceded by a transition phase, which is basically characterized by the substitution of nuclear energy for fossil fuels. This phase is initially dominated by the deployment of other reactor types, such as the LWR, in conjunction with the commercial introduction of FBRs and HTRs. The fuel logistics of the transition phase are more closely investigated in Chapter V. This chapter addresses the fuel logistics of the asymptotic FBR/HTR system.

The assessment of the fuel cycle performance of an FBR/HTR system is stimulated by the prospect of obtaining a self-sustaining system with a closed fissile fuel balance between the FBRs and the HTRs. Two questions arise immediately: What is the fissile fuel logistics between FBRs and HTRs in the case of optimum fissile fuel utilization? How many HTRs can one FBR supply with fissile fuel?

If, for example, it can be demonstrated that an FBR/HTR system is self-sufficient in terms of fissile fuel--i.e. fissile fuel isotopes, such as U235, U233, or Pu239, need not be supplied from external sources--then it can be shown that such a system could meet the energy needs for several centuries, for the fertile fuel isotopes Th232 and U238 necessary to sustain the system are available in abundant quantities. Such a symbiotic FBR/HTR system would offer the following long-range advantages:

-- independence of the uranium ore (U_3O_8) requirement once the asymptotic phase has been reached;
-- a self-sustaining energy system independent of finite fissile fuel resources (U235);
-- an energy system with a practically inexhaustible fuel supply base (U238, Th232);
-- an energy system based on already stockpiled fuels, i.e. depleted uranium (U238), accumulated in very large quantities during the transition phase, as the byproduct of LWR and HTR fuel enrichment.

These characteristics, especially the practical inexhaustibility and the accessibility of the fuel resource base, place the FBR/HTR system in the same category as the two other energy systems of virtually inexhaustible fuel supply: solar energy and fusion energy. Such features are of particular interest to nuclear fuel resource-deficient countries that must increasingly rely on the continued development of nuclear energy. If the development of the present advanced reactor types (FBRs and HTRs) is continued, and if their full-scale deployment is implemented at a relatively vigorous pace in the coming decade, the goal of reaching such a practically fuel resource-independent (U_3O_8) reactor system could be realized within the next few decades.

This chapter assesses the requirements of a self-sustaining FBR/HTR system with a closed fissile fuel balance between the two reactor types. Differentiation is made between two FBR/HTR systems, a nonexpanding system in a steady-state condition and an expanding system assumed to undergo a limited growth. The relations developed for the steady-state case lend themselves to determining the optimal fuel logistics between FBRs and HTRs on the premise that FBRs are indeed self-sufficient with respect to their own fissile fuel needs.

In the following, the total, time-dependent thermal power of such an FBR/HTR system is assumed to be

$$P_S(t) = P_F(t) + P_H(t) \quad , \qquad \text{(IV-1)}$$

where $P_S(t)$ is the total thermal power of the FBR/HTR reactor system, $P_F(t)$ the total thermal power of the FBRs, and $P_H(t)$ the total thermal power of the HTRs.

IV.2. THE NONEXPANDING FBR/HTR REACTOR SYSTEM

The fissile fuel logistic of a nonexpanding, i.e. stationary, FBR/HTR power system is addressed. The system is assumed to be governed by the following conditions:

-- $P_S(t) = \text{constant} = P_S^o$,

-- $\frac{P_H}{P_F} = \text{constant}$[1],

-- $BR_N > 1.0$, or $g_N^V > 0$ for the FBRs,

-- $CR < 1.0$, or $d^V > 0$ for the HTRs.

The first two conditions state that

$$P_S^o = P_F^o + P_H^o \quad . \qquad \text{(IV-2)}$$

---

[1] The case of a nonconstant power ratio is not explicitly treated in this section since the influence of the FBR and HTR fissile fuel inventories on the fuel balance of the system is described in Section IV.4.

This implies that no additional FBRs or HTRs are deployed except for replacements. As a result, the total fissile fuel inventory of the system ($P_H^o I_Z^H + P_F^o I_Z^F$) remains constant, requiring no additional fissile fuel for first core inventories. Thus the entire breeding gain g_N^V of the FBRs can be utilized to meet the fissile fuel demand of the HTRs. A closed fissile fuel balance between FBRs and HTRs is then assured if

-- the entire fissile fuel requirements of the HTRs are met by the excess fissile fuel bred by the FBRs, and
-- fissile fuel self-supply of the FBRs is guaranteed.

Even though not completely independent of one another, the two conditions can be discussed separately.

IV.2.a. The Fissile Mass Balance Between FBRs and HTRs

For the FBR/HTR system in a steady-state condition, a closed fissile mass balance between FBRs and HTRs is assured if

$$P_F^o \cdot g_N^V = P_H^o \cdot d^V \quad , \qquad \text{(IV-3)}$$

where g_N^V is the surplus of fissile fuel of the FBR, defined by Equation (I-33), and d^V the continuous fissile fuel demand of the HTR, defined by Equation (I-37). The HTR-FBR thermal power ratio attainable with a closed fissile fuel balance can be written

$$\frac{P_H^o}{P_F^o} = \frac{g_N^V}{d_z^V} = \frac{\left[(BR_N - 1)(1 - \varepsilon_N)(1 + \alpha)\frac{I}{N}(1 - V^F)W_N^F - V^F \sum_n^N \frac{I_n}{T_n}\right]^{FBR}}{\left[(1 - CR_z)(1 + \alpha)\frac{I}{z}W_I^H + \frac{I^H V^H}{T^H}\right]^{HTR}} \qquad \text{(IV-4)}$$

If the fissile fuel losses in the external fuel cycles of both the HTR and the FBR can be neglected, i.e., $V^F = V^H = 0$, then the above equation can reduced to

$$\frac{P_H^O}{P_F^O} = \frac{(BR_N - 1)}{(1 - CR_z)} \cdot f_N^S \quad ; \qquad \text{(IV-5)}$$

f_N^S is defined as the *global fuel cycle factor* of the FBR/HTR system.

$$f_N^S = \frac{f_N^F}{f_z^H} = \frac{\left[(1 - \varepsilon_N)(1 + \alpha)_N^I \cdot W_N^F\right]^{FBR}}{\left[(1 + \alpha)^I \cdot W_I^H\right]^{HTR}} \quad , \qquad \text{(IV-6)}$$

where f_H^F and f_z^H are defined by the global reactor parameters. W_N^F and W_I^H are found in Chapters II and III. Both f_N^F and f_z^H depend on parameters determined only by the fuel cycles in the respective reactor types. Table III.8 lists $(1 + \alpha)_z^I$ for the HTR for the various feasible fissile fuel cycles; and representative $(1 + \varepsilon_N)$ and $(1 + \alpha)_N^I$ values of the FBR are given in Table II.14. f_N^S of the system is thus essentially determined by the fuel cycles employed in the FBR and in the HTR.

The derivations of the above relations assume transfer of the entire FBR global breeding gain g_N^V to the HTR. If on account of the FBR design only g_n^V, the breeding gain of a specified FBR region n, e.g., the radial blanket, is used for the breeding of HTR fissile fuel, Equations (IV-3) to (IV-6) are rewritten:

$$\frac{P_H^O}{P_F^O} = \frac{g_n^V}{d_z^V}$$

$$= \frac{\left\{\left[BR_n(1 - \varepsilon_N)(1 + \alpha)_N^I - (1 - \varepsilon_n)\,\delta_n\,(1 + \alpha)_n^I\right](1 - V^F)\,W_N^F - \frac{I_n}{T_n}V^F\right\}^{FBR}}{\left\{(1 - CR_z)(1 + \alpha)_z^I \cdot W_H^I + \frac{I^H V^H}{T^H}\right\}^{HTR}} \qquad \text{(IV-7)}$$

where g_n^V, Equation (I-34), has replaced g_N^V. If the external fuel cycle losses are again neglected, the above equation reduces to

$$\frac{P_H^O}{P_F^O} = \frac{g_n}{d_z} = \frac{BR_n}{(1 - CR_z)} f_N^S - \frac{f_n^S}{(1 - CR_z)} \quad ; \qquad \text{(IV-8)}$$

there the new factor f_n^S, defined as the *FBR region-dependent fuel cycle factor of the FBR/HTR system*, is given as

$$f_n^S = \frac{f_n^F}{f_z^H} = \frac{\left[(1 - \varepsilon_n)\,\delta_n\,(1 + \alpha)_n^I \cdot W_N^F\right]^{FBR}}{\left[(1 + \alpha)_z^I \cdot W_H^I\right]^{HTR}} \quad . \qquad \text{(IV-9)}$$

The region-dependent FBR reactor parameters $(1 - \varepsilon_n)$, δ_n, and $(1 + \alpha)_n^I$ specifying f_n^F are listed in Table II.14; they appear to be determined by the fuel cycle employed in the FBR region n. In the case of the radial blanket being region n, f_n^S is governed by the fuel cycle in the radial blanket of the FBR and the finite fuel cycle of the HTR.

IV.2.b. The Fissile Fuel Requirements of the FBR

The requirements of a closed fissile fuel balance within the steady-state FBR/HTR system presuppose fissile fuel self-supply of the FBR. This was indirectly assumed for the derivations of Equations (IV-3) to (IV-6) since g_N^V, the FBR global breeding gain, was derived on this condition. However, the condition of FBR fissile fuel self-supply must be reascertained if not g_N^V but only the breeding gain of one particular region n is transferred to the HTR. Assume this region to be the radial blanket; then we know from Equation (I-23) that $g_N^V = g_{c,ax}^V + g_r^V$, where $g_{c,ax}^V$ is the sum of the breeding gains of the core and the axial blanket, and g_r^V the gain of the radial blanket. For the condition of FBR self-supply to be satisfied, $g_{c,ax}^V \geq 0$, implying that $g_r^V \leq g_N^V$. This in turn places certain requirements on $BR_{c,ax}$ which are to be addressed briefly.

If the U238/Pu239 cycle is selected as fuel cycle of the core and axial blanket regions and the Th232/U233 cycle for the radial blanket (see Table IV.1), the FBR fissile fuel self-supply is assured if enough Pu239 is bred in the core and the axial blanket. This requires that the following relationship is satisfied:

Table IV.1. Fuel cycles in the FBR reactor zones.

Reactor region	For FBR self-supply Core, axial blanket	For fuel transfer to HTR Radial blanket
Fuel cycle	U238/Pu	Th232/U233

$$KR^{Pu} = \frac{(\text{Pu produced})_{c,ax}}{(\text{Pu consumed})_{c,ax}} = 1.0 \quad . \qquad \text{(IV-10)}$$

Here KR^{Pu} is defined as the *plutonium conversion ratio*, i.e. the ratio of the plutonium produced in the core and the axial blanket to that consumed in the two regions. In terms of reaction rates, this can be written as

$$KR^{Pu} = KR_{c,ax} = \frac{C_c^J + C_{ax}^J}{A_c^I + A_{ax}^I} = \frac{C_{c,ax}^J}{A_{c,ax}^I} = 1.0 \quad . \qquad \text{(IV-11)}$$

The FBR region conversion ratio KR_n has been defined by Equation (I-11). Using the definition of the region breeding ratio BR_n, Equation (I-9), one can easily show that the relationship between $KR_{c,ax}$ and $BR_{c,ax}$ is given by

$$KR_{c,ax} = BR_{c,ax} \left\{ 1 + \frac{A_r^I}{A_{c,ax}^I} \right\} = KR^{Pu} \quad , \qquad \text{(IV-12)}$$

A_r^I and $A_{c,ax}^I$ being the respective reaction rates of fissile absorption in the radial blanket region and the sum of the core and axial blanket regions. Since $KR_{c,ax} = KR^{Pu}$ then $KR_{c,ax} = 1.0$. This latter condition, reflecting Pu self-supply, can be assured even if $BR_{c,ax}$ is less than 1.0, provided the ratio of the absorption rates in Equation (IV-12) is larger than zero.

Table IV.2. Ratio of fissile absorption rates in the radial blanket A_r^I and in the core and axial blanket $A_{c,ax}^I$, as a function of the radial blanket residence time.

$A_r^I/A_{c,ax}^I$ *	Radial blanket residence time (days)				
	0	292	511	876	1186
UO_2 blanket	0.006	0.029	0.048	0.075	0.098
ThO_2 blanket	0	0.026	0.049	0.085	0.113
Th^m blanket	0	0.020	0.040	0.069	0.094

*See Table III.A.1.

This is usually the case since $A_r^I > 0$, except for fresh blankets, having accumulated no fissile fuel.

Table IV.2 lists the ratio of the fissile absorption rates[2] $A_r^I/A_{c,ax}^I$ for the FBR assessed in Chapter II, for the UO_2, ThO_2, and Th^m blankets, as a function of the blanket residence time. Varying between 0.05 and 0.07 in equilibrium burnup condition, the ratio of 0.06 is taken as representative and substituted into Equation (IV-12). Plutonium self-supply, i.e., $KR^{Pu} = 1.0 = KR_{c,ax}$, is thus assured if $BR_{c,ax} = 0.94$.

The above considerations neglect the fissile fuel losses incurred in the FBR external fuel cycle. If $V^F \neq 0$, the fissile fuel inventory and the residence time of the fuel in the core and the axial blanket take on importance. Compensation of these losses requires an increase in $BR_{c,ax}$. The relevant equation for $BR_{c,ax}$, derived in Appendix IV.A, is given as

$$BR_{c,ax} = \frac{\left[\frac{V^F}{(1 - V^F)W_N^F} \sum_n^{c,ax} \frac{I_n V^F}{T_n} + \sum_n^{c,ax} (1 - \varepsilon_n)\delta_n (1 + \alpha)_n^I\right]}{(1 - \varepsilon_N)(1 + \alpha)_N^I} \quad \text{(IV-13)}$$

[2] $A_r^I/A_{c,ax}^I$ depends on the H/D ratio of the FBR core design. The absorption rate ratio is smaller for flat cores with small H/D than for cores with high H/D (e.g. gas-cooled breeders).

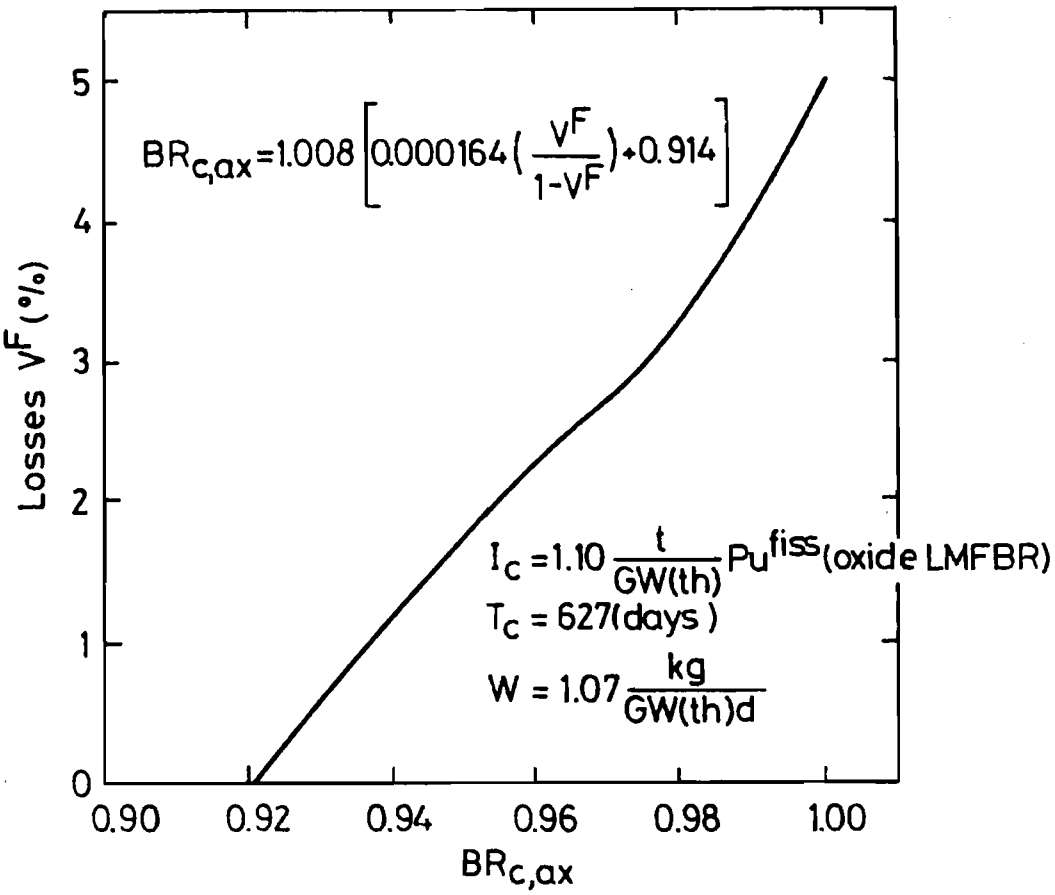

Figure IV.1. $BR_{c,ax}$ as a function of fissile plutonium losses in the excore cycle (reprocessing and fabrication), sustaining KR^{Pu} = 1.0 in the absence of fissile fuel from the FBR radial blanket. See Equation (IV-13).

The sensitivity of the loss rate V^F to $BR_{c,ax}$ becomes evident (Figure IV.1) if one substitutes into the equation I_c and T_c values typical of a current oxide-fueled LMFBR (Schröder and Wagner 1975). For V^F = 0, $BR_{c,ax}$ = 0.92. However, if V^F = 5%, $BR_{c,ax}$ must be increased to 1.0 in order to assure fissile self-supply of the FBR. Self-sufficiency of the FBRs in an FBR/HTR system can therefore be assured with FBRs whose $BR_{c,ax}$ is less than 1.0, provided the losses in the external fuel cycle are correspondingly small.

IV.3. DETERMINATION OF THE FUEL CYCLE LOGISTICS OF A SYMBIOTIC FBR/HTR REACTOR SYSTEM

The relations developed in the previous section are particularly suitable for determining the optimal fuel cycle logistics of a symbiotic FBR/HTR system.

A self-sufficient FBR/HTR system must generate or breed its own fissile fuel. This requirement limits the system, if implemented on a large scale, to the two fissile isotopes U233 and Pu239, since they are the only ones for which sufficient fertile fuel--Th232 and U238--is available[3].

Table IV.3 lists the four possible combinations of U233 and Pu239 fissile fuel utilization in the two reactor types. In two cases the HTR is supplied with Pu239 and in two with U233, employing either fissile fuel cycles F or A, as discussed in Chapter III. It is assumed for all four cases that the fissile fuel for the HTR is bred as surplus in the radial blanket region of the FBR, whose core and axial blanket regions are self-sufficient.

In the FBR/HTR system using the fuel cycle designated *uranium cycle* /U/ in Table IV.3, both FBR and HTR utilize exclusively U238/Pu239 as fuel. The HTR obtains its fissile fuel in the form of Pu239 from the FBR, where all regions are fueled with fertile isotope U238. U238 is also the fertile fuel of the HTR.

Thorium cycle /Th/ relies exclusively on Th232/U233 as fuel. The FBR transfers U233 to the HTR, and the fertile fuel of either reactor is Th232.

In the case of the *mixed cycle* /U-Th/, both Th232/U233 and U238/Pu239 are utilized. There are two possible combinations of fuel transfer, mixed cycles A and B (Table IV.3). In A, U238/Pu239 is utilized in the core and axial blanket regions of the FBR, breeding U233 as surplus in the radial blanket, which in turn is transferred to the HTR. The fertile fuel in the FBR

---

[3] U235 cannot be considered as a fissile isotope for the closed system since the fertile fuel U234 needed is not available in nature in abundant quantities.

Table IV.3. Utilization of fertile and fissile isotopes in a self-sustaining FBR/HTR system.

Nomenclature of fuel cycles of the symbiotic FBR/HTR system	FBR				HTR			HTR fissile fuel cycle*
	Self-supply		Surplus to HTR		Demand from FBR	Self-conversion		
Reactor region	*Core, axial bl.*		*Radial blanket*		*Core*	*Core*		
Isotope	*Fissile*	*Fertile*	*Fissile*	*Fertile*	*Fissile*	*Fissile*	*Fertile*	
/U/ uranium cycle	Pu239	U238	Pu239	U238	Pu239	Pu239	U238	F
/Th/ thorium cycle	U233	Th232	U233	Th232	U233	U233	Th232	A
/U-Th/mixed cycle A	Pu239	U238	U233	Th232	U233	U233	Th232	A
/U-Th/mixed cycle B	U233	Th232	Pu239	U238	Pu239	Pu239	U238	F

*See Table III.1.

radial blanket and in the HTR is Th232. In the case of mixed cycle B, Th232/U233 is the fuel employed in the core and axial blanket regions of the FBR. The radial blanket breeds excess Pu239 that is transferred to the HTR. The fertile fuel in the FBR radial blanket and in the HTR is U238.

Two of the four possible combinations can be eliminated for the reasons put forward in Chapter II against Th232 utilization in the FBR core region. This leaves *uranium cycle* /U/ and /Th-U/ *mixed cycle* A as the only viable fuel cycle options for the symbiotic FBR/HTR system. (Mixed cycle A will from now on simply be referred to as mixed cycle /U-Th/.)

Which of the two cycles, /U/ or /U-Th/, is then to be preferred as fuel cycle of the FBR/HTR system?

The fuel cycle with the most favorable fissile fuel utilization for the FBR/HTR system can be determined with Equations (IV-5) or (IV-8), describing the HTR-to-FBR thermal power ratio. A large ratio implies that a relatively small number of FBRs can supply many HTRs with fissile fuel; in the case of a smaller ratio more FBRs are needed. A large power ratio is therefore indicative of good fuel utilization.

Equation (IV-5) assumes no excore fuel cycle losses, i.e. $V^F = 0 = V^H$, as well as transfer of the entire FBR breeding gain g_N to the HTR. If, for the time being, one assumes that the global breeding gain can be ascribed to the FBR radial blanket region, i.e. $g_N = g_r$, then the HTR-FBR power ratio achievable is determined by f_N^S, CR_z, and BR_N, with f_N^S being the ratio of f_N^F to f_z^H.

f_N^S is solely determined by the fuel cyles employed in the two types of reactors. The values of f_N^S, f_N^F, and f_z^H for the two viable fuel cycles of the FBR/HTR system are listed in Table IV.4. The evaluation of f_N^F and f_z^H is based on the assessments in Chapters II and III[4]. As can be observed, f_N^F of the FBR differs

---

[4] For the FBR investigated in Chapter II, condition $g_N = g_r$ is not met (Table II.14). Thus the f_N^F values given for the thorium blanket cases do not exactly correspond to the f_N^S values needed for Equation (IV-5). Since the f_N^S values differ only insignificantly between the UO_2 blanket case and the thorium blanket cases, the error introduced is negligible, however.

Table IV.4. Fuel cycle factors f_N^F and f_z^H of FBR and HTR, and FBR/HTR system fuel cycle factor f_N^S.

Symbiotic FBR/HTR system fuel cycle	FBR*					HTR			f_N^S
	Rad. bl. fuel mat.	f_N^F	$(1-\varepsilon_N)$	$(1+\alpha)_N^I$	W_N^F	f_z^H	$(1+\alpha)_z^I$	W_z^I	
Uranium /U/	UO_2	1.0676	0.793	1.257	1.071	1.646	1.537**	1.071	0.649
Mixed cycle A /U-Th/	ThO_2	1.0694	0.806	1.240	1.070	1.190	1.140***	1.044	0.899
	Th^m	1.0564	0.804	1.228	1.070	1.190	1.140***	1.044	0.888

*Data from Table II.14.
**Data from Table III.7, fissile fuel cycle F.
***Data from Table III.7, fissile fuel cycle A.

only negligibly between the two thorium blanket cases (/U-Th/ system cycle) and the UO_2 blanket case (/U/ system cycle): it is larger by 0.17% for the ThO_2 blanket, and smaller by 1.05% for the Th^m blanket, than in the /U/ cycle. On the other hand, f_z^H of the HTR decreases from 1.646 for the /U/ cycle to 1.190 for the /U-Th/ cycle, or by 27.7%. The primary impact on f_N^S (0.649 for the /U/ cycle and 0.899 or 0.888 for the /U-Th/ cycle) can therefore be ascribed to the large change in f_z^H from the uranium to the thorium cycle in the HTR. This is reflected by the large difference in the $(1 + \alpha)_z$ values of U233 and Pu239 in the thermal neutron spectrum of the HTR.

The other two parameters to be determined are BR_N and CR_z. The conversion ratio CR_z of the HTR has been shown (Chapter III) to be determined by essentially two parameters, the fissile fuel cycle and the fuel burnup. The conversion ratios of the relevant fissile fuel cycles A and F (Table III.1) have been shown conclusively to range between 0.55 and 0.93, depending on the burnup of discharged fuel.

The range of BR_N of the FBR and the determining parameters are more difficult to quantify. The fuel cycle in the FBR core must be U238/Pu239, as was rationalized in Section II.9.b; the discussion also indicated that the fuel burnup does not have any significant influence on BR_N, compared with its effect on CR_z in the HTR. The parameters largely affecting BR_N are reactor design (e.g. homogeneous or heterogeneous FBR), type of fuel material employed (e.g. oxide or carbide fuel), type of coolant (i.e. Na or He), and the behavior of the fuel under burnup condition (i.e. large structural steel volume fraction and/or low linear rod power). The range of BR and its parametric dependence on these various parameters cannot be stated as comprehensively and conclusively as for CR of the HTR. Table IV.5 therefore lists BR_N and BR_r of several current 1-GW(e) FBRs. The global breeding ratio varies between 1.20-1.40, and the radial breeding ratio between 0.20-0.32. These values can be assumed to represent BR_N and BR_r ranges of typical FBR designs.

The HTR-FBR power ratio for the /U/ and /U-Th/ cycles can now be estimated by substituting the appropriate f_N^S values in Table IV.4 into Equation (IV-5), yielding the following set of equations:

Table IV.5. Conversion ratios and feasible breeding ratios of HTRs and FBRs in the FBR/HTR system.

HTR		
Fissile fuel cycle*	CR	Burnup range (GWd/t)
A	0.71 - 0.93	110 - 20
F	0.55 - 0.75	110 - 20
FBR		
LMFBR**	BR_N	BR_r
Oxide, homogeneous	1.20	0.25
Oxide, heterogeneous	1.35	0.25
Carbide, homogeneous	1.35	0.25
GCFBR**		
Oxide, homogeneous	1.40	0.32

*See Table III.1 for nomenclature.
**1000 MW(e) class, U238/Pu239 fuel cycle in the core region.

For the *uranium cycle* /U/:

$$(BR_N - 1) = 1.55 \frac{P_H^O}{P_F^O} (1 - CR_F) \quad , \qquad \text{(IV-14)}$$

for $0.55 \leq CR_F \leq 0.75$.

For the *mixed cycle* /U-Th/:

$$(BR_N - 1) = 1.118 \frac{P_H^O}{P_F^O} (1 - CR_A) \quad ,$$

for $0.75 \leq CR_A \leq 0.95$ and $g_N \simeq g_r$.

Figures IV.2 and IV.3 are graphical representations of these equation, the abscissa being given in terms of the conversion ratio CR and the corresponding fuel burnup of the HTR. Comparison of the two figures allows one to conclude that

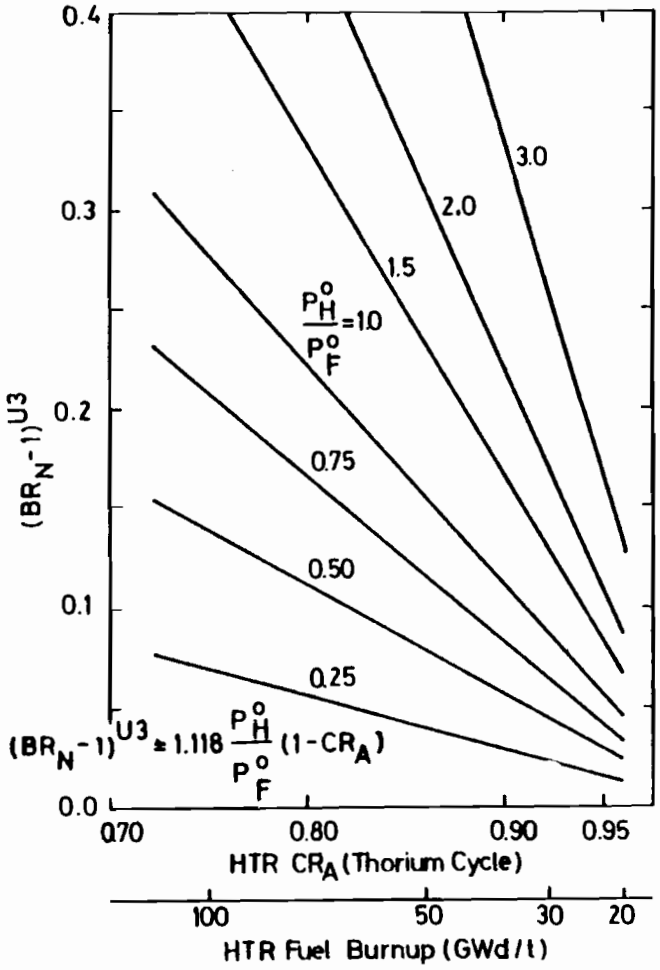

Figure IV.2

Correlation between FBR breeding ratio (BR_N - 1), HTR conversion ratio CR_A (or fuel burnup), and attainable power ratio P_H^o/P_F^o of a steady-state FBR/HTR system for the *mixed* fuel cycle /U-Th/. (HTR uses fissile fuel cycle A; FBR breeding gain is U233.)

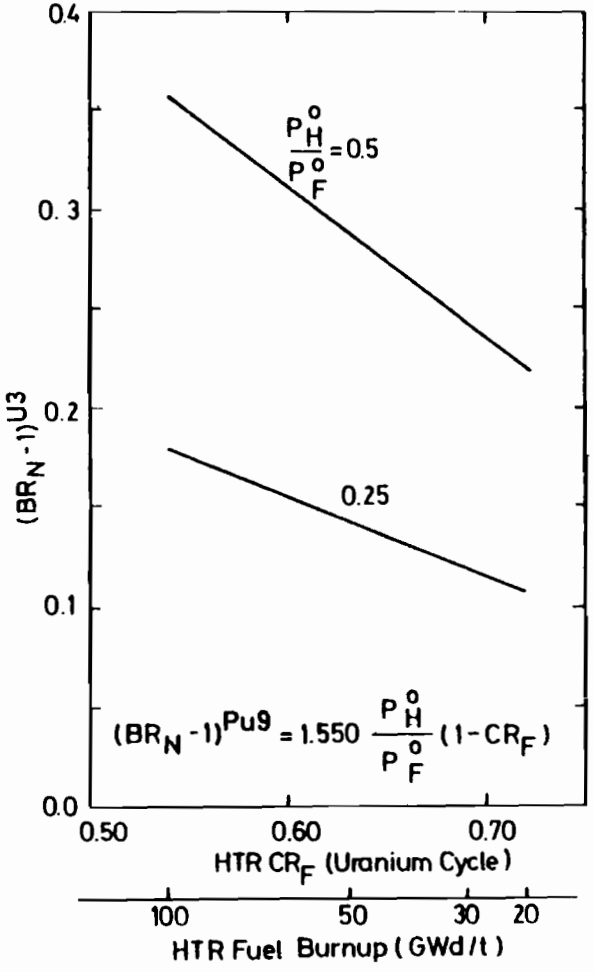

Figure IV.3.

Correlation between FBR breeding ratio (BR_N - 1), HTR conversion ratio CR_F (or fuel burnup), and attainable power ratio P_H^o/P_F^o of a steady-state FBR/HTR system for the *uranium* fuel cycle /U/. (HTR uses fissile fuel cycle F; FBR breeding gain is in the form of Pu239.)

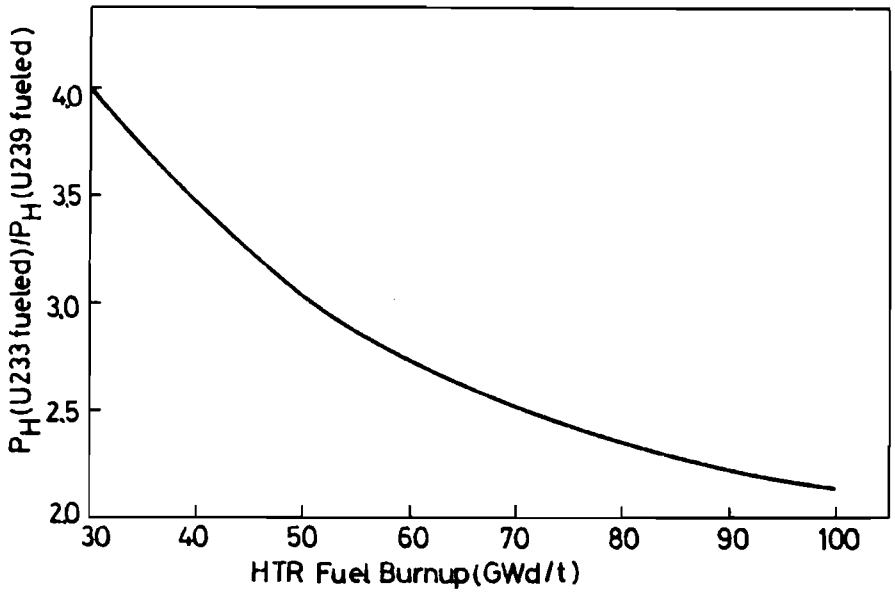

Figure IV.4. Power ratio of HTRs supplied with U233 as fissile fuel to HTRs supplied with Pu239 in a symbiotic FBR/HTR system.

-- Considerably higher HTR-to-FBR power ratios can be attained if the FBR/HTR system uses mixed cycle /U-Th/ instead of the /U/ cycle, i.e., fewer FBRs are necessary to maintain a certain HTR power base.

-- The HTR burnup is the most viable means of controlling the power ratio, or the fuel utilization in the FBR/HTR system.

The question of the relative advantage of the mixed cycle over the uranium cycle is resolved conclusively in Figure IV.4. It compares the HTR-FBR power ratio in the /U-Th/ cycle to that of the /U/ cycle as a function of HTR fuel burnup. At high HTR burnups of 100 GWd/t, about 2.2 times more HTRs can be supplied with fissile fuel if the /U-Th/ system fuel cycle is used instead of the /U/ cycle; the factor increases to 4 as the HTR burnup decreases to about 30,000 MWd/t. This large differential in the HTR-FBR power ratios attainable clearly demonstrates the superiority of the mixed /U-Th/ cycle over the /U/ cycle for an FBR/HTR reactor system.

For a given ratio of HTRs to FBRs in the asymptotic phase, determined, for example, by specified process heat and electricity demands, any set of (BR_N, CR) values along the fixed parametric lines of P_H^o/P_F^o (Figure IV.2) assures a closed fissile fuel balance between the two types of reactors. In the case of an HTR-FBR power ratio of 1.0 and an FBR with a BR_N of 1.15, a closed fissile fuel balance is obtained if the HTR fuel burnup is about 40 GWd/t, corresponding to a conversion ratio CR_A of 0.89. For a more recent FBR design with BR_N = 1.33, HTRs with CR_A = 0.79 would be adequate. The criteria for an appropriate set of (BR_N, CR) in the asymptotic phase most likely depend on the fast breeder reactor types available at the time and on the prevailing economic conditions. The maximum HTR-FBR power ratio attainable is estimated to lie between 4 and 5, given an FBR with BR_N = 1.40 and an HTR burnup of less than 30 GWd/t. This, of course, assumes utilization of the /U-Th/ cycle. The corresponding maximum HTR-FBR ratio of the /U/ cycle would be 0.9.

The above considerations assume that the global breeding gain g_N is transferred to the HTR and that Equation (IV-5) is applicable, based on the assumption that $g_N = g_r$ for the /U-Th/ cycle. Let us now assume transfer of only the radial breeding gain g_r and an FBR with $g_r < g_N$. In this case $g_{c,ax} > 0$, and an excess of Pu239 is bred in the core and the axial blanket (as in the FBR in Chapter II). Then Equation (IV-8) applies. Representative f_r^F values from Chapter II are reproduced in Table IV.6. Comparing them one can deduce that f_r^F is largely determined by a given FBR design, i.e. the relative importance of the radial blanket, and only marginally by the fuel cycle used in the radial blanket.

Substituting these f_r^F and the f_N^F values (Table IV.4) for the thorium blanket cases into Equation (IV-8), one obtains for the FBR analysed in Chapter II HTR-FBR power ratios of 0.924 for the ThO_2 and 1.030 for the Th^m blanket, assuming CR_A = 0.85.[5] The transfer of radial-blanket Pu239 leads to a ratio of 0.222 for the UO_2 blanket, given CR_F = 0.65. Thus the Th^m blanket supports a 11% larger HTR power base than the UO_2 blanket, while the HTR power base in the case of the UO_2 blanket is only about 20-25% of that provided by FBRs with thorium blankets.

Table IV.6. The radial blanket fuel cycle factor f_r^F of the FBR.

Symbiotic FBR system fuel cycle	Radial blanket fuel material	FBR*					
		f_r^F	$(1-\varepsilon_r)$	$(1+\alpha)_r^I$	δ_r	W_N^F	BR_r
Uranium /U/	UO_2	0.072	0.755	1.370	0.0647	1.071	0.231
Mixed cycle /U-Th/	ThO_2	0.079	0.937	1.132	0.0697	1.070	0.242
	Th^m	0.064	0.917	1.107	0.0593	1.070	0.246

*See Table II.14

This again shows that the mized /U-Th/ cycle as specified in Table IV.3 is the optimal fuel cycle for the symbiotic FBR/HTR system.

Small amounts of fertile fuel are required to sustain the system. The amounts of U238 and Th232 needed are about equivalent to the amounts converted to fissile fuel in the reactors. This is approximately one ton each of U238 and Th232 per GW(e)yr, e.g. ~ 100 t/yr of each for either reactor type in an FBR/HTR system consisting of a 100-GW(e) FBR and a 250-GW(th) HTR.

---

[5] For a UO_2 blanket and $CR_F \simeq 0.65$:

$$\frac{P_H^O}{P_F^O} = \frac{0.231}{1-0.65}\,0.649 - \frac{0.072}{1-0.65} = 0.222$$

For ThO_2 blanket and $CR_A \simeq 0.85$:

$$\frac{P_H^O}{P_F^O} = \frac{0.242}{1-0.85}\,0.899 - \frac{0.079}{1-0.85} = 0.924$$

For Th^m blanket and $CR_A \simeq 0.85$:

$$\frac{P_H^O}{P_F^O} = \frac{0.246}{1-0.85}\,0.888 - \frac{0.064}{1-0.85} = 1.030$$

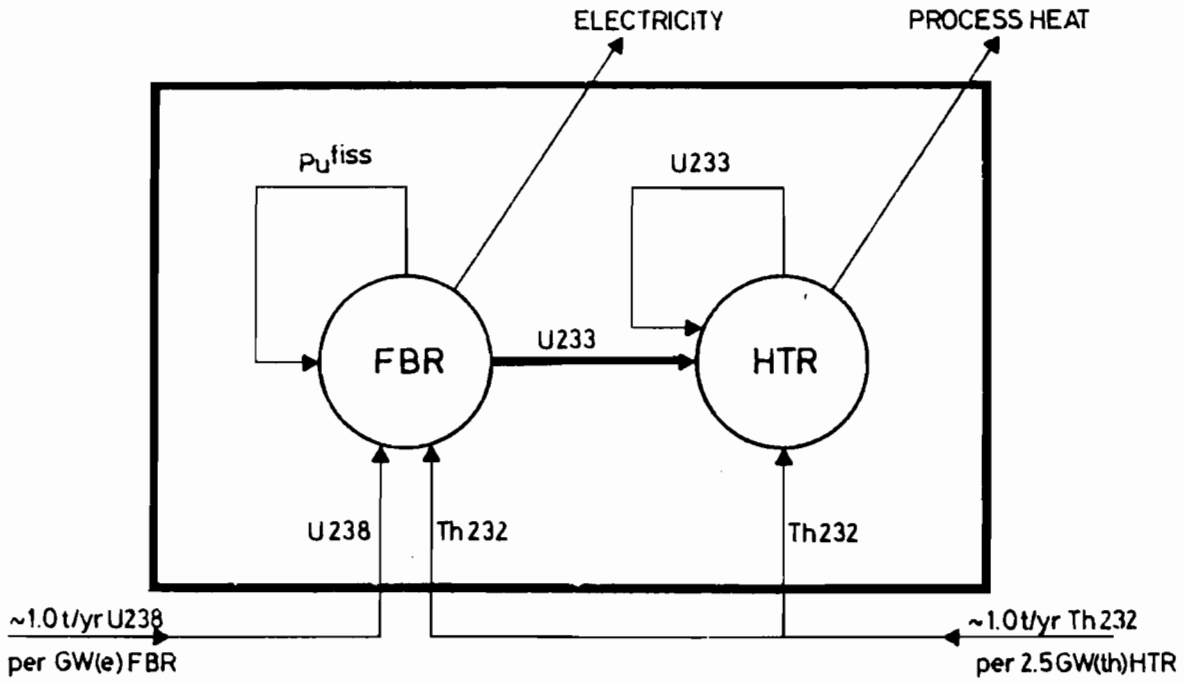

Figure IV.5. Fissile and fertile isotope flows between FBRs and HTRs of a symbiotic FBR/HTR system.

Assuming Th232 and U238 resources to be on the order of ten million tons each, this particular FBR/HTR system would have sufficient fuel for 10 x 10^6 tons/100 tons per year, or for 10^5 years.

The fissile and fertile fuel flows within such a *self-sustaining* reactor system of FBRs and HTRs are schematized in Figure IV.5.

Inclusion of excore fissile fuel losses, neglected above, will not significantly alter the above conclusions.

IV.4. THE EXPANDING FBR/HTR REACTOR SYSTEM

The relations developed in Section IV.3 apply to a nonexpanding FBR/HTR system in the steady state. This restriction is now relaxed in that the total power of the system $P_S(t)$ is allowed to increase while the distribution between FBR and HTR remains unchanged, that is, the power ratio of HTR to FBR, remains constant. The system is assumed to utilize the mixed cycle /U-Th/ described above.

In an expanding FBR/HTR system, the FBR must, in addition to the continuous fissile fuel demand d_A^V of the HTR, supply the first core inventories of newly added FBRs and HTRs. Since the fissile inventory of the FBR in the /U-Th/ cycle is Pu239 and that of the HTR U233, the FBR breeding gain g_N^V must in this case provide both fissile isotopes. g_N^V is therefore separated into a Pu and U233 breeding gain components, such that

$$g_N^V = g^{Pu} + g^{U3} \quad . \tag{IV-15}$$

Of interest here is the rate of expansion or growth rate α_S of the FBR/HTR system. α_S is derived in Appendix IV.C.

$$\alpha_S = \frac{\left[g_N^V \cdot L_F \frac{P_F^O}{P_H^O} - d_A^V \cdot L_H \right]}{\left[I_Z^H + I_Z^F \frac{P_F^O}{P_H^O} \right]} \quad , \tag{IV-16}$$

where I_Z^H and I_Z^F represent the respective HTR and FBR fissile fuel cycle inventories, L_H and L_F the corresponding load factors, and P_F^O/P_H^O the constant FBR-to-HTR power fraction. g_N and d_A are given by Equations (I-33) and (I-37). The distribution between g^{U3} and g^{Pu} can be determined by the relation

$$g^{Pu} = \frac{\alpha_S I_Z^F}{L_F} \quad . \tag{IV-17}$$

If the losses $V^H = V^F = 0$, and the appropriate parameters for g_N and d_A from Chapters II and III (Tables II.14 and III.8) are substituted into Equation (IV-16), the growth rate α_S of the FBR/HTR system can be written as

$$\alpha_S = \frac{\left[1.06(BR_N - 1)L_F \frac{P_F^o}{P_H^o} - 1.19(1 - CR_A)\right]}{\left[I_Z^H + I_Z^F \frac{P_F^o}{P_H^o}\right]} \quad . \qquad \text{(IV-18)}$$

α_S is plotted in Figures IV.6 and IV.7 as a function of $(BR_N - 1)$; the parameters are the P_F^o/P_H^o ratio and the FBR fuel cycle inventory I_Z^F, or the P_F^o/P_H^o ratio and the HTR conversion ratio CR_A. The doubling time of the FBR/HTR system was assumed to be represented by $T_S = \ln 2/\alpha_S$.

Figure IV.6 illustrates the influence of the FBR fuel cycle inventory I_Z^F on α_S of T_S. The HTR parameters I_Z^H and CR_A are fixed at 3.0 t of U233 per GW(e) and 0.85. The power ratios P_F^o/P_H^o of interest were chosen to be 1.0 and 2.0, and the ranges of FBR inventory as 5.0 t, 3.75 t, and 2.5 t of Pu^{fiss} per GW(e).

If $(BR_N - 1)$ is assumed to be predetermined, the influence of I_Z^F on α_S for a fixed power ratio is clearly noticeable. Large I_Z^F imply small growth rates or long system doubling times. For $(BR_N - 1) = 0.30$ and $P_F^o/P_H^o = 1.0$, α_S increases from 1.75%/yr to 2.5%/yr for a transition from a large inventory I_Z^F = 5.0 to 2.5 t/GW(e) Pu^{fiss}, an increase of 43% in α_S. Doubling time T_S decreases correspondingly, from 39.6 years to 27.7 years. For the larger P_F^o/P_H^o ratio of 2.0, α_S increases from 3.5%/yr to 5.7%/yr for the corresponding I_Z^F values.

The respective influence of BR_N and I_Z^F on α_S can be illustrated if α_S is held constant. Thus, if α_S is assumed 3%/yr and $P_F^o/P_H^o = 1.0$, an FBR with $BR_N = 1.40$ and $I_Z^F = 5.0$ has the same rate of expansion as an FBR with $BR_N = 1.33$ and $I_Z^F = 2.5$.

The significant influence of the HTR conversion ratio CR_A or of the HTR fuel burnup is demonstrated by Figure IV.7. If, e.g., the FBR and HTR inventories are fixed at 3.75 t/GW(e) Pu^{fiss} and 3.0 t/GW(e) U233, respectively, given an FBR breeding ratio BR_N of 1.30, doubling time T_S of the system can be shortened from

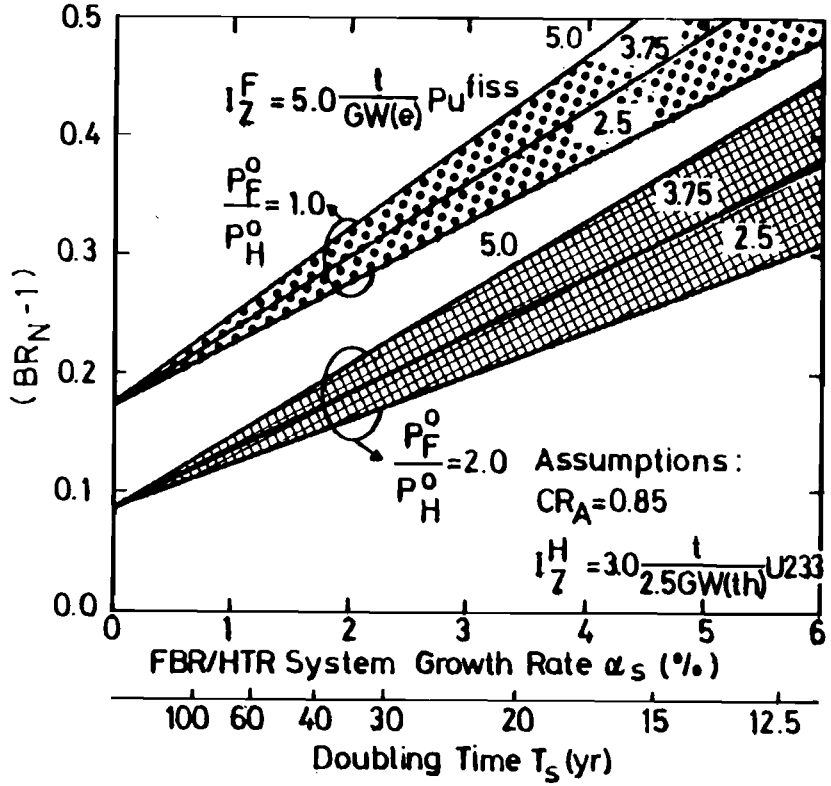

Figure IV.6.

Influence of FBR breeding ratio BR_N and fissile fuel inventory I_Z^F on growth rate α_S and doubling time T_S of the FBR/HTR system for various FBR-HTR power ratios and V = 0 (mixed fuel cycle /U-Th/).

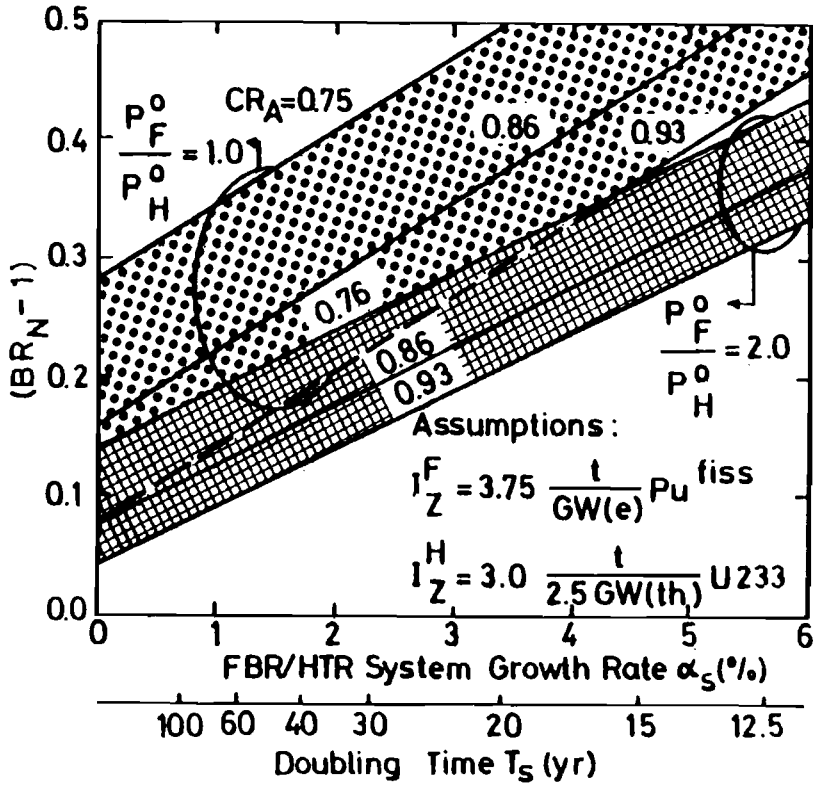

Figure IV.7.

Influence of FBR breeding ratio BR_N and HTR conversion ratio CR on growth rate α_S and doubling time T_S of the FBR/HTR system for various FBR-HTR power ratios and V = 0 (mixed fuel cycle /U-Th/.

140 to 24 years if CR_A is increased from 0.76 to 0.92 by reduction of the burnup from 100 to about 20 GWd/t. The influence of CR_A slightly decreases with a larger FBR-HTR power ratio.

These results illustrate that an FBR of appropriate design can, in conjunction with the more flexible operational mode of the HTR, assure a sustained expansion of the FBR/HTR system. For the currently designed oxide LMFBRs with $BR_N \simeq 1.18$ and $I_Z^F \simeq 3.75$ t/GW(e) Pu^{fiss}, a doubling time T_S of less than 30 years can only be achieved if the FBR-HTR power ratio is no less than 2.0 and the HTR conversion ratio CR_A at least 0.85.

IV.5. SUMMARY OF CHAPTER IV

It has been shown in this chapter that the fissile fuel cycle most favorable to a symbiotic FBR/HTR reactor system is a combination utilizing both the uranium and the thorium fuel cycles. *A mixed FBR/HTR system fuel cycle* /U-Th/ has been shown to have a significantly superior fissile fuel utilization (by a factor 2 to 4, determined by the HTR fuel burnup) than the uranium cycle /U/.

In the uranium cycle /U/, FBR and HTR would exclusively rely on the U238/Pu239 fertile/fissile fuel cycle. In the mixed cycle /U-Th/, on the other hand, the U238/Pu239 cycle is used in the core and axial blanket regions of the FBR, and the Th232/U233 cycle in the HTR and in the FBR radial blanket. Exclusive reliance on the Th232/U233 cycle in both the FBR and the HTR is not a viable option since the FBR must utilize the U238/Pu239 cycle in the core region in order to maintain a breeding ratio BR_N above 1.0 (see discussion in Chapter II).

In a symbiotic FBR/HTR system with no growth, i.e. in steady-state condition, the fissile inventories of FBR and HTR have no particular impact. On the basis of either a high FBR breeding ratio or a relatively low HTR burnup, one FBR can supply up to three HTRs of equal thermal power with sufficient fissile fuel (U233).

In an expanding FBR/HTR system, growth rates of up to 5%/yr are achievable if both reactor types are designed appropriately,

i.e. for a relatively low fissile inventory and a relatively low medium breeding ratio of the FBR, and/or for a low HTR burnup. The size of the fissile inventories is of considerable importance in an expanding system. Reactor strategically speaking, however, FBRs with low inventories and medium breeding ratios are preferable over FBRs with high breeding ratios and high inventories.

The Th232 and U238 fertile isotopes necessary to fuel the symbiotic FBR/HTR system are available in abundant quantities, in order to sustain such a reactor system for many centuries. For example, a system consisting of one hundred GW(e) FBRs and two hundred and fifty GW(th) HTRs could be sustained for about 100,000 years, or a system ten times as large for about 10,000 years, under the assumption that Th232 and U238 resources in the order of ten million tons each are available.

What values or set of values will ultimately be selected for the parameter set (BR_N, BR_r, CR, I_Z^H, and I_Z^F) depends, first of all, on the technological evolution of FBRs and HTRs and, secondly, on the optimization criteria relevant at the time when the asymtotic phase is reached and FBRs and HTRs begin to function as a symbiotic, self-sustaining, reactor system. The constraints imposed on the set of values will most likely be a combination of technological limitations as well as economic and political considerations impossible to foresee today.

All the above considerations intrinsically assume the availability of both thorium and uranium fuel reprocessing and fabrication facilities. Without these facilities, the proposed FBR/HTR system could not be self-sustaining.

CHAPTER V. THE U_3O_8 DEMAND OF VARIOUS REACTOR STRATEGY SCENARIOS

V.1. Introduction

Chapters II to IV have shown that the use of thorium in the FBR is motivated primarily by fuel logistic considerations, relevant to a symbiotic FBR/HTR reactor system, rather than by breeder-specific reasons. It was demonstrated in Chapter IV that, for this particular reactor system, breeding U233 as surplus fissile fuel in the FBR radial blanket is clearly advantageous over the breeding of Pu239.

The assessment in that chapter concentrated on the fuel logistics of an asymptotic, basically nonexpanding, reactor system. This chapter deals with the fuel logistics of the transition period, a time phase of 40-60 years in which nuclear power replaces fossil fuels, serving as a major energy source. This transition period is assumed to be characterized by the deployment of three reactor types, namely LWRs, HTRs, and FBRs. The focus is on the question of optimal fuel logistics of this reactor system, with minimum uranium resource (U_3O_8) demands as optimization criterion. Of primary interest is an assessment of the most important parameters governing this uranium ore demand. One such parameter is the point in time at which it will become advantageous to employ thorium in the FBR radial blanket breeding excess U233 instead of plutonium.

Relevant statements in this context can only be made on the basis of hypothetical scenarios extending over a time horizon that covers the introduction as well as the market penetration of both FBRs and HTRs. Such an assessment requires a reactor strategy model reflecting the most likely development of reactor technology in the coming decades, and the expansion and establishment of nuclear energy over a period of approximately 40-60 years.

Before the model is discussed, some qualitative remarks regarding such analyses are in order.

Any assessment extending over several decades into the future is necessarily based on a number of underlying assumptions that inherently influence the results of the analysis.

On the one hand, there are assumptions reflecting fairly accurately the present state of the art; then there are conjectures, which are considered reasonable, about the most likely technological evolution of certain advanced reactor types and their time of large-scale commercial introduction.

On the other hand, there are assumptions that extend so far into the future and that, by their very nature, are so uncertain that their influence must be reassessed periodically. One such assumption, for example, is the future energy demand.

The results of such analyses are, therefore, determined by the plausibility of the model chosen and the underlying assumptions. This makes it seem prudent to discuss the results more in qualitative rather than quantitative terms. Placing the proper emphasis is sometimes difficult, however, especially if the results of such an assessment must serve as the basis of recommendations for long-term policies.

Since, like in this case, no other methodology is available for assessing the long-term influence of certain reactor types and the interrelationship between relevant parameters determining the future uranium demand, the judgments and recommendations that are based on such results should be carefully balanced in the light of both qualitative and quantitative arguments, especially as regards the continued development of advanced FBR and HTR reactor types.

The following considerations are based on the reactor strategy model initially proposed by Häfele and Schikorr (1973). Its underlying reactor strategy is the LWR/FBR//HTR scenario discussed in more detail later in this chapter. An extended version of this model has been used as a basis for reactor strategy calculations, performed in particular to assess the impact of the time of introduction and large-scale deployment

of various fast breeder reactor designs on future uranium demand in the F.R.G. and the DeBeNeLux countries (Schröder and Wagner 1975; Schikorr 1974, 1975a, 1975b).

In the present investigation alternative reactor strategy scenarios are also considered, providing a basis of comparison for the reference LWR/FBR//HTR scenario. Two different scenarios are of particular interest: in one the future development of nuclear power relies primarily on today's LWR technology; the other assumes heavy reliance on a future large-scale deployment of HTRs. FBR deployment is assumed for neither scenario. The parameter of interest in this comparison is the total uranium ore requirement or commitment associated with a given scenario, since the world's economically viable uranium resources seem to be finite, limited to amounts below the anticipated needs, and confined to a few geographic regions.[1]

The first few sections of this chapter concentrate on the fissile fuel logistics and the main parameters of the LWR/FBR//HTR scenario in the transition phase. A comparison of U_3O_8 demands for the various strategy scenarios follows in Section V.6.

In general, a number of parameters are of significance for reactor strategy analyses of this kind. Accordingly, it is not the aim of this assessment to examine each parameter in detail but to concentrate on the most important variables. The question of breeding U233 or Pu in the FBR is assessed within this context. Numerical sample calculations in Section V.5 illustrate these breeding alternatives for a given nuclear energy demand forecast for the DeBeNeLux countries.

For the purposes of this investigation, an extensive reactor strategy computer code has been developed (Jansen, Schikorr, and Seele 1976) taking detailed account of the fissile fuel flows,

---

[1] Costs are not discussed in this assessment; they were considered in the investigations by Häfele and Manne (1974) and Schikorr and Rogner (1975).

mass balances, delay times, etc., of the in- and excore fuel cycles of all the reactor types considered.

V.2. The Reactor Strategy Model for an LWR/FBR//HTR Scenario

The reactor strategy model proposed by Schikorr and Häfele attempts to account for the current state of technological development and the probable future evolution of nuclear energy on the basis of the growing scarcity of petroleum and natural gas and the restricted geographic availability of limited uranium ore (U_3O_8) resources.

V.2.a. Assumptions Underlying the LWR/FBR//HTR Scenario

The reactor strategy model for an LWR/FBR//HTR scenario is based on the following set of assumptions:

- -- Nuclear power undergoes a phase of reasonable growth in the next few decades, i.e. transition phase.
- -- Within the next 40-60 years, this transition phase merges into a saturation or asymptotic phase, in which the further growth of nuclear power is restrained.
- -- The reactor types employed initially in the transition phase are LWRs, being gradually replaced by FBRs and HTRs.
- -- Commercial FBRs and HTRs are introduced approximately 20-30 years after commercialization of LWRs.
- -- FBRs and HTRs are both introduced at about the same time.

It appears reasonable to partition the future nuclear energy requirement into sectors of nuclear electricity demand and process heat demand. The reactor types considered are assumed to be utilized in a given sector, depending on their best potential and most suitable application:

- -- LWRs and FBRs meet future nuclear electricity demands, and HTRs process heat requirements[2].

---

[2] HTRs can, in principle, also be used in the electricity sector; this would not alter the results described in this chapter.

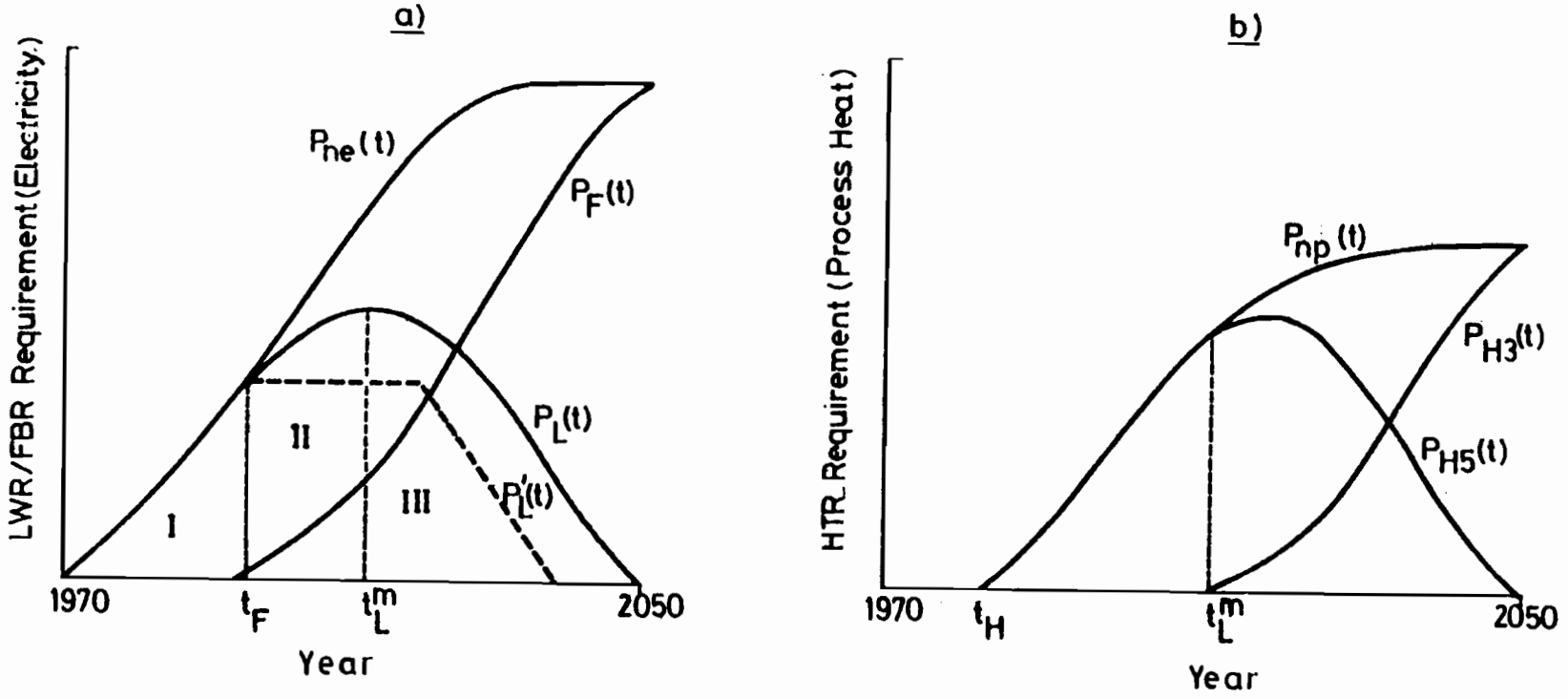

Figure V.1. Schematic of nuclear energy forecasts P_{ne} and P_{np} and reactor capacities P_F, P_L, P_{H5} and P_{H3} in the (a) electricity and (b) process heat sectors. (F stands for FBR, L for LWR, H5 for U235-consuming HTRs, and H3 for U233-supplied HTRs; P_L corresponds to minimum LWR capacity.)

-- Deployment of LWR/FBRs and HTRs is governed by specified forecasts of nuclear electricity and nuclear process heat demands.

These concepts are schematically illustrated in Figure V.1. The introduction dates of FBRs and HTRs are designated t_F and t_H. $P_{ne}(t)$ and $P_{np}(t)$ are specified nuclear electricity and process heat demand forecast curves; $P_L(t)$ and $P_F(t)$ are the respective installed capacities of LWRs and FBRs. Process heat demand is met by two types of HTRs, designated H5-HTRs and H3-HTRs, utilizing either U235 or FBR-supplied U233 as fissile fuel makeup. The installed HTR capacities are given as $P_{H5}(t)$ and $P_{H3}(t)$, respectively, such that

$$P_{np}(t) = P_L(t) + P_F(t) \quad , \tag{V-1}$$

$$P_{np}(t) = P_{H3}(t) + P_{H5}(t) \quad . \tag{V-2}$$

V.2.b. Uranium Ore as Optimization Criterion

Given a minimum demand for U_3O_8 as optimization criterion, the LWR/FBR//HTR system of the transition phase converges into an FBR/HTR reactor system, since the FBR/HTR system has been shown to require no U_3O_8, as discussed in Chapter IV. The total uranium ore demand in this reactor scenario is thus limited to the transition phase. In analogy to the critical mass of a reactor, this finite U_3O_8 demand of the transition phase can be referred to as the *critical U_3O_8 requirement* associated with the establishment of the asymptotic FBR/HTR reactor system. This requirement is determined by a number of parameters, among which is the point in time when FBRs begin to breed U233 fissile fuel surplus in the radial blanket.

In Figure V.1a, the transition phase is divided into three distinct time phases for the nuclear electrical energy sector. Phase I is described solely by an increase in LWR capacity from time 0 (1970) to t_F, the introduction of the FBR. Phase II is considered the time interval between t_F and t_L^m, the point in time of maximum LWR capacity. Phase III is characterized by a

decreasing LWR capacity. Among them, Phase II, the breeder introduction phase, is of particular significance since the demand for uranium over the entire transition phase is, to a large extent, predetermined during Phase II.

The uranium demand is determined by the LWRs and the H5-HTRs both requiring U235 (and thus U_3O_8) as fissile fuel makeup. The total U_3O_8 requirements for the transition phase are finite, since LWRs are replaced by FBRs for electricity production and H5-HTRs by U233-consuming H3-HTRs for process heat. The total uranium ore requirement E_T is therefore given by

$$E_T = E_L + E_{H5} = e_L \int_{1970}^{\infty} P_L(t)dt + e_{H5} \int_{t_H}^{\infty} P_{H5}(t)dt \quad , \quad (V-3)$$

where e_L and e_{H5} are the annual U_3O_8 requirements of LWRs and H5-HTRs, respectively[3]. Being relatively fixed by the reactor design, e_L and e_{H5} can be influenced only marginally (this holds true especially for H5-HTRs in the case of the nonrecycle thorium cycle--fissile fuel cycle C, Table III.1--see discussion in Chapter III). Therefore, the total uranium demand E_T can only be influenced effectively by the two power integrals in Equation (V-3), i.e. the LWR capacity $P_T(t)$ after FBR introduction, governed by $P_F(t)$, and HTR capacity $P_{H5}(t)$, governed by $P_{H3}(t)$. Both $P_F(t)$ and $P_{H3}(t)$ in turn depend on the fissile fuel logistics between LWR and FBR and between FBR and HTR.

Since, in general, $e_L > e_{H5}$ ($e_L/e_{H5} \simeq 2 - 3$ for the HTR thorium cycle, fissile fuel cycle B), the LWR power integral assumes considerably greater importance than the P_{H5} integral.

---

[3]Since integration is over the entire time span of LWR and H5 capacity, the first-core inventory requirements of LWR and HTR can be neglected here. The LWRs and H5s newly constructed in the growth phase have such ore requirements. The LWRs and H5s being phased out in Phase III, however, release a large portion of their first-core requirements (approximately 60% in the case of the LWR, 50-80% in the case of the H5, depending on burnup). In addition, the first-core requirement is only approximately 10-20% of the total requirement calculated over the lifetime of an LWR.

(This changes as the ratio e_L/e_{H5} approaches unity). The priority is thus clearly to optimize first the LWR/FBR fuel logistic and thereafter the FBR/HTR fuel logistic.

V.3. The Fissile Fuel Logistics Between LWRs, FBRs, and HTRs During the Transition Phase of the LWR/FBR//HTR Scenario

As indicated earlier, the total uranium demand of the LWR/FBR//HTR scenario is largely determined by the fissile fuel logistics between LWR, FBR, and HTR.

Regarding the LWR and FBR fuel cycles, the following assumptions are made:

- -- The LWR utilizes the low enriched U235/U238 fuel cycle, i.e. it requires U235 as fissile makeup and thus U_3O_8.
- -- The FBR employs the U238/Pu239 fuel cycle in the core and axial blanket regions to assure breeding ratios above 1.0. The fertile fuel in the radial blanket is either U238 or Th232, depending on the particular fissile fuel requirements of the LWR/FBR and FBR/HTR fissile fuel logistics.
- -- The Pu generated in the LWRs is transferred to the FBRs to be utilized as first core inventory. This assumes reprocessing of the spent LWR fuel.
- -- The HTR utilizes the higly enriched thorium cycle (see Chapter III). As long as no U233 is supplied by the FBRs, the HTR employs either fissile fuel cycle C (no U233 reprocessing) or fissile fuel cycle B (U233 reprocessing), as discussed in Chapter III. Each of the two cycles has a demand for U235 makeup. When excess U233 from the FBRs becomes available, fissile fuel cycle A is used in the HTRs. In this case the HTRs need no more U235, or U_3O_8.

Utilization of the uranium cycle in the HTR is not considered for these assessments since it was shown in Chapter IV that, in the case of fissile fuel transfer from the FBR to the HTR, the HTR should utilize the thorium cycle. In addition, there is no incentive to employ the uranium cycle in the HTR

since the uranium ore requirement of this cycle--comparable to that of LWRs--is considerably higher than for thorium fissile fuel cycle B.

V.3.a. The Fissile Fuel Logistics Between LWRs and FBRs

It is assumed here that the increase in FBR capacity after commercial introduction of the FBR at t_F is determined by two constraints:

-- availability of plutonium,

and/or

-- a maximum attainable FBR construction rate that is determined by an industrial capacity constraint.

With the increase in FBR capacity after t_F, which is in the following assumed to be limited only by the availability of Pu[4], the rate of introduction of additional FBRs after t_F is determined by the fissile plutonium balance between LWRs and FBRs, given by

$$I_Z^F \frac{dP_F(t)}{dt} = a_L P_L(t) + g_N^{Pu} P_F(t) \quad , \qquad (V\text{-}4)$$

for $t \geq t_F$, with

$$P_F(t) + P_L(t) = P_{ne}(t) \quad ;$$

I_Z^F is the FBR fissile fuel cycle inventory, and a_L the annual LWR fissile plutonium production. The analytical solution for $P_L(t)$ is given in Appendix V.A. The parameters of importance are I_Z^F and g_N^{Pu} as well as the LWR capacity after t_F. In the phase of FBR introduction, Phase II, the predominant parameters

[4] Considering the present delay in the development of LWR reprocessing, it can easily be argued that Pu availability will most likely be the determining constraint. This will be so, in particular, if LWR capacities are relatively low at the time of FBR introduction, i.e. when the forecasts of nuclear electricity demand are low.

are I_Z^F and the LWR capacity at and after t_F. The breeding gain takes on importance with increasing FBR capacity. Under the assumption of Pu transfer from the existing LWRs to FBRs, the most important design parameter for the FBR during Phase II clearly is the fissile fuel inventory (and not the doubling time), as will become evident in Section V.6.

V.3.b. The Fissile Fuel Logistics Between FBRs and HTRs

As long as the FBR breeds Pu239 as fissile fuel surplus there is no link between FBR and HTR fuel cycles. FBRs can begin to supply U233 to HTRs as soon as Pu is no longer needed in the LWR/FBR sector, which is expected to happen sometime after $t = t_L^m$ (see below). The construction of U233-fueled H3-HTRs is then governed by the fissile fuel balance between FBRs and H3-HTRs as given by

$$I_Z^{H3} \frac{dP_{H3}(t)}{dt} + d_A P_{H3}(t) = g_r^{U3} P_F(t) \quad , \qquad \text{(V-5)}$$

where $P_F(t)$ is obtained from Equation (V-4), I_Z^{H3} is the fissile fuel cycle inventory of H3-HTRs utilizing fissile fuel cycle A, d_A is the HTR fuel burnup-dependent annual U233 demand given in Table III.8, and g_r^{U3} is the radial breeding gain of the FBR supplying U233 (see Table II.14 for the FBR investigated in Chapter II). By solving Equation (V-5) for $P_{H3}(t)$ one can determine $P_{H5}(t)$ since

$$P_{H5}(t) = P_{np}(t) - P_{H3}(t) \quad .$$

With $P_L(t)$ and $P_{H5}(t)$ being known, one can use Equation (V-3) to evaluate the total uranium demand E_T. This system of differential equations is solved numerically in the reactor strategy computer code referred to below.

V.3.c. U233 Surplus Breeding in the FBR

As discussed in Appendix V.A, FBRs should breed Pu239 as surplus fissile fuel up to the point in time when no more new LWRs have to be introduced since enough plutonium is available in the LWR/FBR sector (Equation V-4). According to Figure V.1, this will be the case at the earliest when maximum LWR capacity has been attained at $t = t_L^m$. Thus FBRs should breed Pu239 during Phase II. After t_L^m, some FBRs can be converted to breed U233 as surplus since the then existing FBRs and LWRs will produce sufficient plutonium ensuring a continued expansion of FBR capacity.

Reactor-strategically speaking, TH232 should therefore be used as fertile blanket fuel in the FBR no sooner than t_L^m.

In Appendix V.A, the duration of Phase II, i.e. the time interval between t_F and t_L^m, is derived for a linear approximation of $P_{ne}(t) = \omega t$ such that

$$t_L^m - t_F = \frac{\left[I_Z^F . \omega - a_L . P_L(t_F) \right]}{\left[a_L . \omega + \left(\frac{g^{Pu} - a_L}{I_Z^F} \right) a_L . P_L(t_F) \right]} \qquad (V\text{-}6)$$

for $t > t_F$ and $t_L^m - t_F < 20$ years. The start of thorium use in the FBR, therefore, depends on a number of parameters, most of which cannot be specified with certainty as of today. $P_L(t_F)$ is the LWR capacity at the time of FBR introduction, and ω is the expansion rate (construction rate) of nuclear power in the electricity sector. Under the assumption of $P_L(t_F) \simeq 45$ GW(e) and $\omega = 4$ GW(e)/yr, Figure V.2 shows the interrelationship between the duration of Phase II, $t_L^m - t_F$, and fissile fuel cycle inventory I_Z^F and breeding gain g_N^V of the FBR. This leads one to observe the following:

-- The most important parameter in Phase II, the FBR introduction phase, is the FBR fissile fuel cycle inventory I_Z^F given a reasonably large value for $P_L(t_F)$.

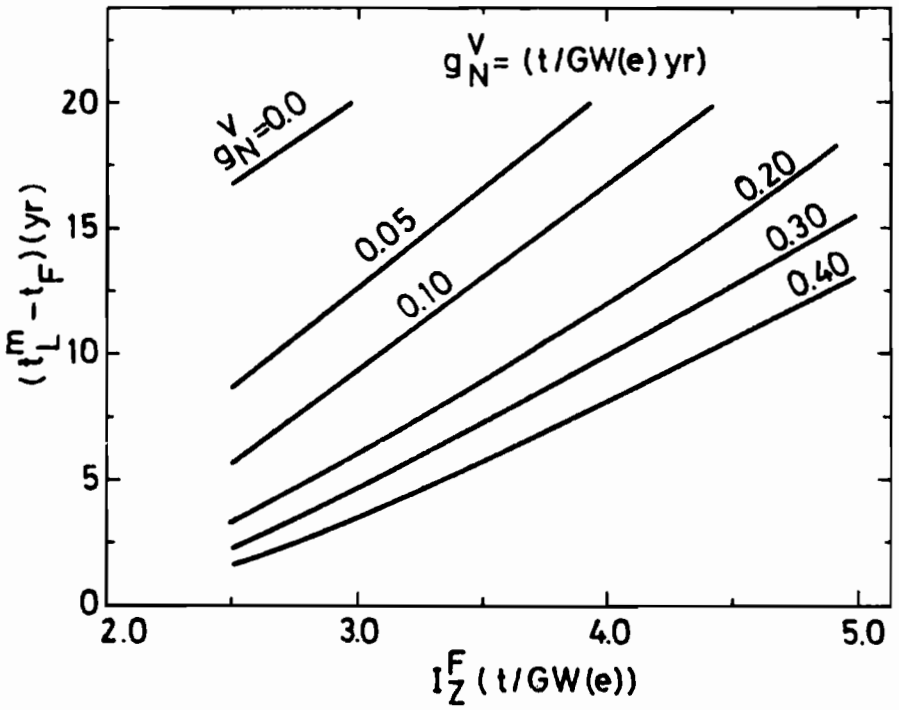

Figure V.2. Influence of FBR breeding gain g_N^V and I_Z^F on the time interval $(t_L^m - t_F)$; t_L^m corresponds to maximum LWR capacity and t_F to time of FBR introduction.

-- In Phase II, breeding gain g_N^V has comparatively little influence compared to that of the fuel cycle inventory, provided $g_N^V > 0.15$.
-- For large cycle inventories I_Z^F, the LWR capacity reaches its maximum 10-20 years after t_F.
-- For small I_Z^F the LWR capacity reaches its maximum in less than 10 years after t_F.

Regarding the use of thorium in the FBR radial blanket one can thus deduce the following:

-- Small I_Z^F values generally permit an early substitution of Th232 for U238 as radial blanket material.
-- The exact time of substitution depends upon a number of parameters, see Equation (V-6), most of which cannot be precisely specified as of today. The exact

Table V.1. Relevant FBR parameters and their time dependent significance after FBR introduction time t_F.

Time interval after FBR introduction t_F *	Most important parameter in LWR/FBR//HTR scenario	FBR fissile fuel surplus in the form of:
$t_F < t < t_L^m$ +	I_Z^F**	Pu
$t \geq t_L^m$	I_Z^F, g_N^V ++	Pu/U233
$t >> t_L^m$	g_N^V	U233

*See Figure V.1.

**I_Z^F = FBR fuel cycle inventory (incore and excore).

+ t_L^m = time of maximum LWR capacity.

++ g_N^V = FBR breeding gain, Equation (I-33).

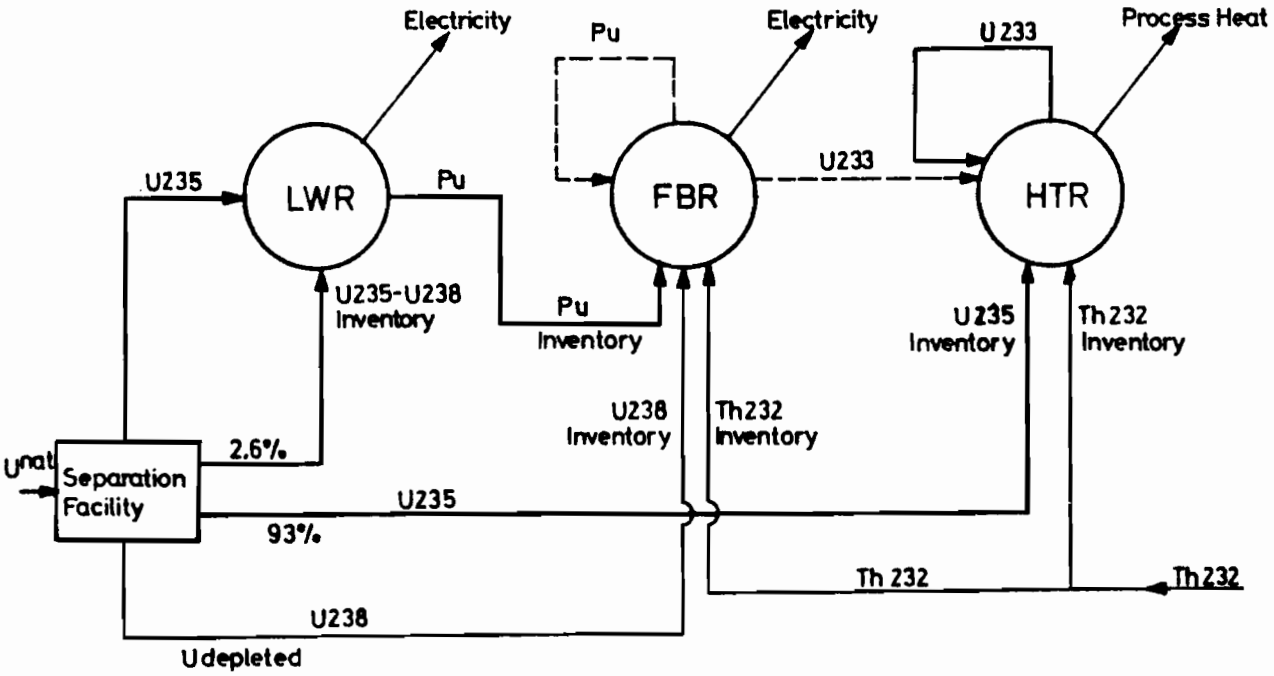

Figure V.3. Fertile and fissile fuel cycle logistics of the LWR/FBR//HTR reactor system in the transition phase after t_L^m.

point in time will have to be determined around time t_L^m, when the then prevailing conditions are known[5].

These observations are summarized in Table V.1. Figure V.3 shows the fertile and fissile fuel flows between LWRs, FBRs, and HTRs after the time of maximum LWR capacity t_L^m.

V.4. Long-Range Reactor Strategy Calculations

For assessing the viability of the LWR/FBR//HTR strategy scenario described, the uranium resource requirement of this scenario should be compared to the requirements of other possible reactor strategy scenarios. One scenario should rely predominantly on present LWR technology, and another be based on large-scale HTR deployment. Neither of these two scenarios assume any FBR deployment. A comparison of the U_3O demand of these three scenarios will thus allow an effective comparison of the long-range potential of the three reactor types: LWR, HTR, and FBR.

The uranium requirements of the three reactor strategy scenarios are evaluated for three different nuclear energy forecasts for the DeBeNeLux countries, covering a broad spectrum of possible future nuclear energy developments.

V.4.a. The Reactor Strategy Scenarios Considered: LWR/FBR//HTR, LWR/LWR//HTR, and LWR/HTR//HTR

The following reactor strategy scenarios describe possible nuclear power developments over the next decades. For each scenario, process heat requirements are assumed to be supplied exclusively by HTRs.

---

[5] These arguments apply if plutonium availability rather than construction rate capacity is the limiting constraint. In the latter case, U233 breeding by FBRs could start already earlier, possibly even at the time of FBR introduction t_F.

S1: LWR/FBR//HTR. This scenario corresponds to that discussed in detail in the previous section. LWRs and FBRs supply nuclear electricity, and HTRs provide process heat. The reactor type emphasized in this scenario is the FBR.

S2: LWR/LWR//HTR. This scenario involves no FBRs. Nuclear electricity demand is met exclusively by LWRs, and HTRs supply process heat. The focus is on the LWR.

S3: LWR/HTR//HTR. FBRs are not deployed. Nuclear electricity demand is met initially by LWRs, and these are gradually replaced by HTRs introduced commercially in the 1990s. Supply of process heat is by HTRs. The reactor type clearly central to this scenario is the HTR.

V.4.b. The Reactor Strategy Computer Code

The computer code developed takes detailed account of the fissile and fertile fuel logistics between the various reactor types considered within a given scenario.

The code allows introduction of different designs of a given reactor type at any specified point in time. Thus one can either gradually replace all of the older types by newer ones, or simply assume a mix of different types. The delay times in the excore and incore fuel cycles as well as the corresponding mass flow data are reproduced in detail. This code is extensively described in Jansen, Schikorr, and Seele (1976).

V.4.c. Nuclear Energy Demand Forecasts for the DeBeNeLux Countries

The most uncertain parameter in assessments of this kind is the long-range nuclear energy demand forecast. For this reason three widely differing forecasts of nuclear electricity demand have been considered here, together with two forecasts of nuclear process heat (see Table V.2). The three nuclear electricity demands $P_{ne}(t)$ are designated /H/, /M/, and /L/. /H/ represents a very optimistic, /M/ a more realistic, and

Table V.2. Nuclear energy demand projections for LWRs/FBRs (electricity demand) and HTRs (process heat demand). for the DeBeNeLux countries.

$P_{ne}(t)$ *for LWR/FBR (GW(e))*

Forecast	Year 1970	1980	1990	2000	2010	2020	2030	2040
/H/	0	28	118	240	406	560	684	755
/M/	0	28	91	174	227	227	309	337
/L/	0	28	60	80	91	98	103	107

$P_{np}(t)$ *for HTR (GW(th))*

Forecast	Year 1970	1980	1990	2000	2010	2020	2030	2040
/P1/	0	0	10	47	92	142	165	182
/P2/	0	0	13	75	145	215	260	290

/L/ a low demand. The HTR process heat forecasts $P_{np}(t)$ given as /P1/ and /P2/ represent estimates of future high-temperature process heat requirements (Schröder and Wagner 1975).

V.4.d. Reactor Data for LWR, FBR, and HTR

Since it is not yet possible to specify all the design characteristics of the reactor types under consideration, especially those of FBRs and HTRs, some of the relevant data are parameterized over a wide range of possible reactor designs.

FBR Data. The designs of present oxide-fueled LMFBRs are rather conservative, with breeding ratios of about $BR_N \simeq 1.2$, or breeding gains of $g_N^V \simeq 0.15$, and fissile fuel cycle inventories of $I_Z^F \simeq 4\text{-}5$ tons of Pu per GW(e). Both parameters are expected to change, however, as more practical experience in LMFBR operation and design becomes available. Both g_N^V and I_Z^F are therefore varied over a broad range of values encompassing also those of other possible FBR types, such as the GCFBR. Figure V.4 shows the

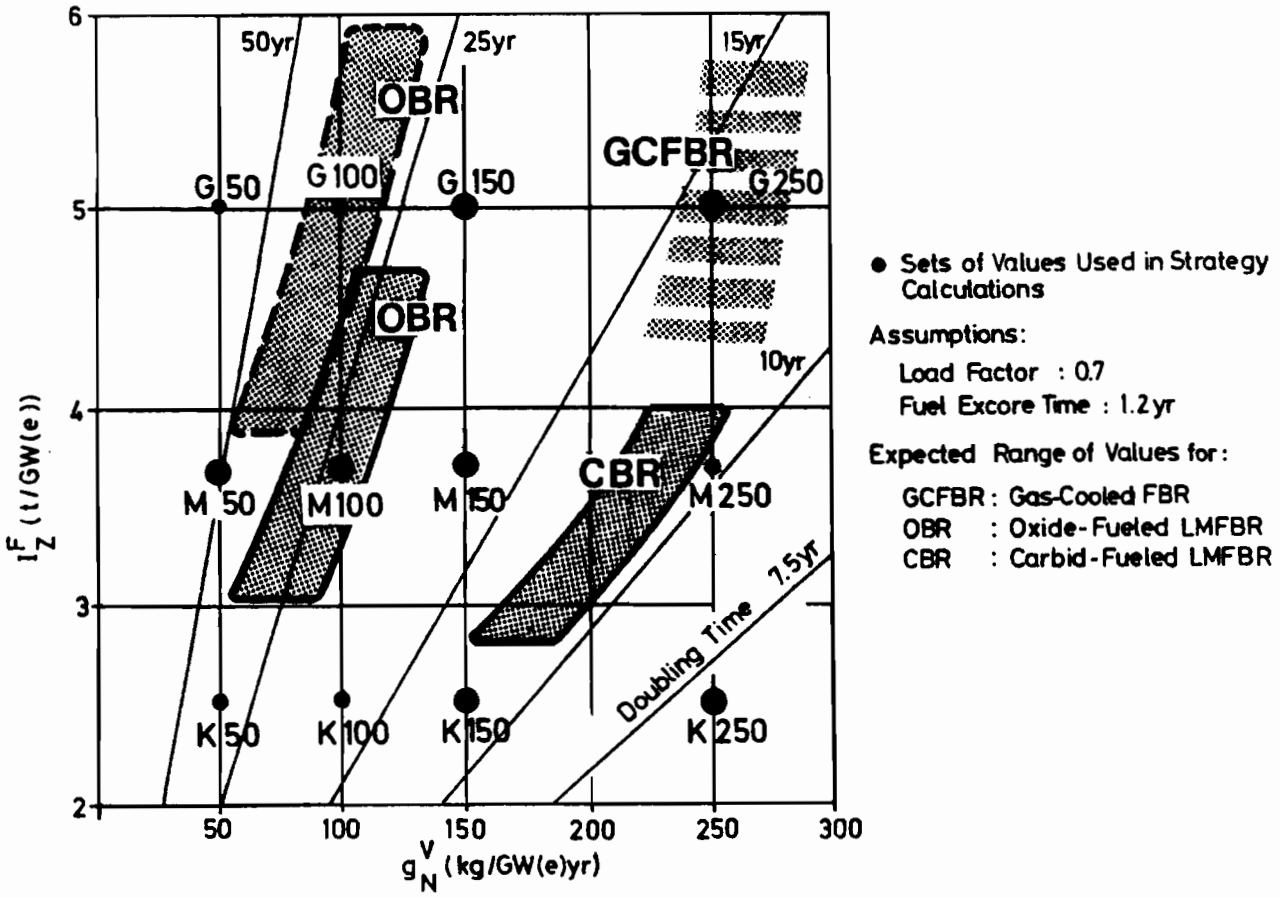

Figure V.4. Considered parameter range of fissile fuel cycle inventory I_Z^F and Pu^{fiss} breeding gain g_N^V of the FBR.

parameter range of present FBR designs. OBR represents current oxide-fueled LMFBR designs, CBR LMFBRs with carbide fuel, and GBR GCFBRs with oxide fuel. Also shown is the doubling time for each combination of g_N^V and I_Z^F. The dots indicate the parameter sets of g_N^V and I_Z^F considered in this assessment. The designations of these g_N^V and I_Z^F parameter sets are summarized in Table V.3. G represents a high inventory I_Z^F of 5.0, M a medium I_Z^F of 3.75, and K a low I_Z^F of 2.5 tons Pu/GW(e). Breeding gain g_N^V in this case represents the Pu surplus after losses in the excore fuel cycle, with the respective fissile surpluses of g_N^V = 50, 100, 150, 200, and 250 given in kg Pu^{fiss} per GW(e) yr.

LWR Data. The LWR data in Table V.4 are mean values of current PWR and BWR light-water reactors (Schneider and Wagner 1975).

Table V.3. FBR designations used in scenario S1 (LWR/FBR//HTR) of FBR designs investigated, as a function of fissile fuel inventory I_Z^F and breeding gain g_N^V

Fuel cycle inventory I_Z^F Pu^{fiss} t/GW(e)	Designation	Breeding gain g_N^V kg/GW(e)yr				
		50	100	150	200	250
2.50	K	K50	K100	K150	K200	K250
3.75	M	M50	M100	M150		
5.0	G		G100	G150	G200	G250

Table V.4. LWR data.

First core			No Pu recycle	Pu recycle
		*Annual demand**		
Tail assay (%)	0.25	U_3O_8 (t/GW(e)yr)	212**	172**
Enrichment (%)	2.25	Enrichment (%)	2.98	2.98
U_3O_8 (t/GW(e))	485**	Separative work (SW) (t/GW(e))	136	108
Uranium (t/GW(e))	94.5	Tail assay** (%)	0.25	0.25
		Annual discharge		
		Fissile Plutonium (t/GW(e)yr	0.214	0.25

*1 year = 8760 hours.

**Value of e_L in Equation (V-1).

Table V.5. HTR data for the thorium cycle.

First-core demand		HTR (block elements)	HTR (pebbles)	
Uranium	(t/GW(e))†	1.54	1.03	--
Enrichment	(%)	93	93	--
Tail assay	(%)	0.25	0.25	--
Thorium	(t/GW(e))†	32.3	23.7	83
U_3O_8	(t/GW(e))†	368	243	3.0 (U233)

*Annual demand***

Fissile fuel cycle*		C no U233 recycle U233 makeup		B U233 recycle U235 makeup		A*** U233 recycle U233 makeup	
Fuel burnup A	(GWd/t)	100	30	100	30	100	30
Conversion rate	CR_z	0.62	0.79	0.66	0.85	0.76	0.92
Tail assay	(%)	0.25	0.25	0.25	0.25	0	0
U_3O_8 ††	(t/GW(e)yr)†	188	231	115	65	0	0
SW	(t/GW(e)yr)†	170	209	105	59	0	0
U233	(t/GW(e)yr)†	0	0	0	0	0.265	0.100

*See Tables III.1 and III.9.
**1 year = 8760 hours.
***This cycle can be realized in conjunction with FBRs providing U233 makeup.
†Electric equivalent where efficiency was assumed to be $\varepsilon = 0.40$.
††Corresponds to e_{H5} in Equation (V-1).

Table V.6. Designations used in scenario S3 (LWR/HTR//HTR) of HTR designs investigated, as a function of fissile fuel cycle and fuel burnup.

Burnup (GWd/t)	HTR fissile fuel cycle* A	B	C
100	HA10	HB10	HC10
30	HA03	HB03	HC03

*See Tables III.1 and V.5.

HTR Data. The data in Table V.5 for the thorium cycle are taken from the literature (Teuchert et al. 1974, 1972, 1974, and Schulten et al. 1977), especially the first core inventories, and from Table III.9. In Table V.6 showing HTR designations, HA10 signifies fissile fuel cycle A from Table III.1 with a burnup of 100 GWd/t, and HB03 fissile fuel cycle B with a burnup of 30 GWd/t. Only these two burnup states are considered here since they are assumed to represent the span of economically feasible burnups of HTRs.

V.4.e. Introduction Dates of the Reactor Types Considered

It is assumed in the following that LWRs are deployed starting 1970; they meet the nuclear electricity demand forecasts given in Table V.2. Commercial introduction of both oxide-fueled LMFBRs and HTRs is assumed for around 1990. In all LWR/FBR//HTR cases considered, the LMFBRs deployed until 1995 are of the conservative design M100, to be replaced thereafter by one of the FBR types listed in Table V.3.

V.4.f. Construction Rate Constraints

Another important parameter is the constraint on the rate of both FBR and HTR expansion during Phase II. This constraint is determined by a number of arguments (for details see Schröder and Wagner 1975). Here it suffices to say that the

HTR construction rate in scenario S3, where HTRs supply both nuclear electricity and process heat, is assumed to correspond to the most optimistic FBR expansion rate in scenario S1[6].

V.5. Sample Calculations of the LWR/FBR//HTR Scenario

Some typical results of LWR/FBR//HTR scenario S1 are now discussed, demonstrating the influence of some of the important parameters on U_3O_8 demand. These calculations underlie the combination /M,P1/ of nuclear energy demand forecasts. (Table V.2)

V.5.a. Influence of Parameters I_Z^F and g_N^V of the FBR and of CR of the HTR

Figure V.5 shows the power distributions of LWRs and FBRs in the nuclear electricity sector and of U235-fueled H5-HTRs and U233-fueled H3-HTRs in the process heat sector for two different FBR designs (M150 and K250, see Table V.3). H3-HTRs that are assumed to utilize fissile fuel cycle A with a burnup of 100,000 MWd/t are designated HA10; H5-HTRs utilizing fissile fuel cycle B with a burnup of 100,000 MWd/t are designated HB10 (see Table V.6).

The influence of I_Z^F and g_N^V is evident from the different distributions of LWR and FBR power capacity in Figure V.5a; there the K250-FBR permits a larger addition of FBR capacity with a correspondingly lower LWR capacity demand, compared to the FBR of type M150. Since the LWR power demand is smaller for K250 than for M150, uranium demand E_L in Equation (V-3) will be lower accordingly.

The influence of breeding gain g_N^V on the H3-HTR and H5-HTR power distribution can be inferred from Figure V.5b. An FBR with a higher breeding gain permits a faster H3-HTR buildup than an FBR with a lower gain. With a faster H3-HTR buildup fewer U235-consuming H5-HTRs are needed, as is seen from the different power capacity curves H5(K250) and H5(M150). This in turn leads to a lower uranium demand E_{H5} in Equation (V-3).

---

[6] This implies that the LWR capacity demand in S3 corresponds to the LWR capacity demand in S1 for the most optimistic FBR capacity expansion.

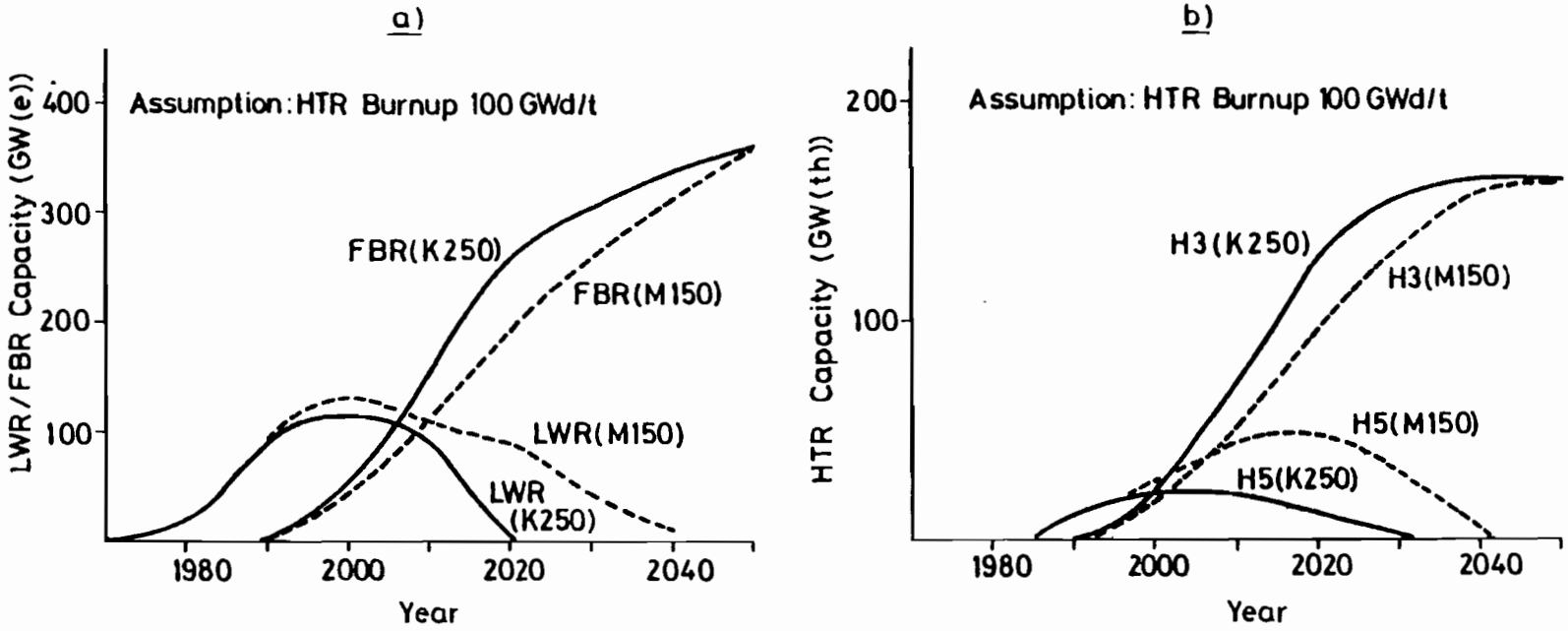

Figure V.5. LWR/FBR capacity distribution in the electric sector (a), and M3-HTR/HT-HTR distribution in the process heat sector (b), both for FBR designs M150 and K250, given nuclear energy demand forecast /M,P1/.

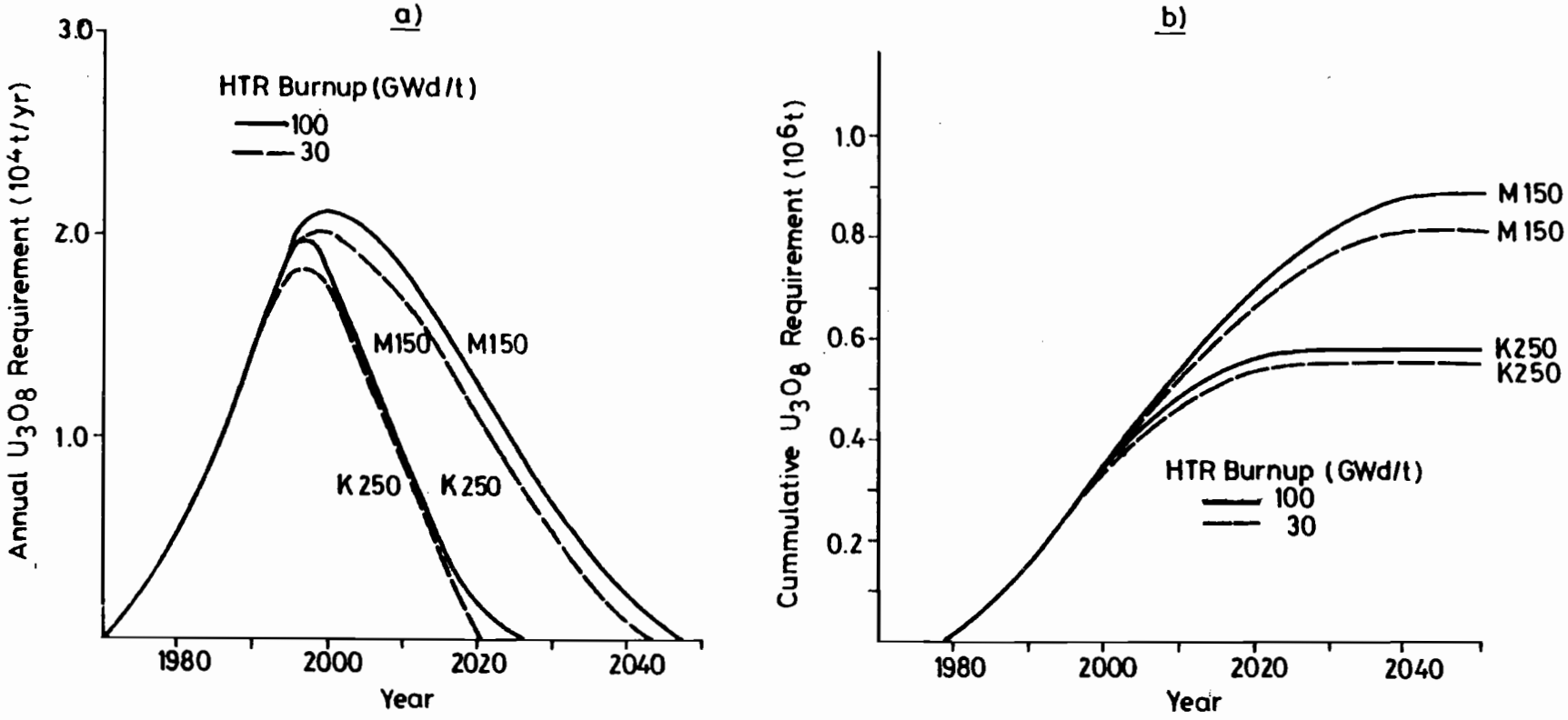

Figure V.6. Annual (a) and cumulative (b) U_3O_8 requirements for FBR designs M150 and K250 and for two different HTR fuel burnups, given nuclear energy demand forecast /M,P1/.

Figure V.6 demonstrates the influence of HTR burnup on the annual and cumulative uranium demands for the two different FBR types. E_T is the sum of the uranium demands E_L of LWRs and E_{H5} of H5-HTRs, Equation (V-3). The dotted lines describe an HTR fuel burnup of 30 GWd/t, and the solid lines of 100 GWd/t.

Foremost, the annual demand for U_3O_8 becomes zero much sooner with FBRs of type K250 than with M150--the difference is about 20 years--so that the LWR/FBR//HTR scenario reaches independence from U_3O_8 supply faster with K250 than with M150 (Figure V.6a). The total uranium requirement E_T for the K250 design is correspondingly smaller by about 30%.

The influence of reduced HTR burnup is less striking for K250 than for M150 (Figure V.6b). This is in accordance with the results obtained in Chapter IV, where a reduction in HTR burnup was shown to be less significant for FBRs with very good breeding properties. For this energy forecast, the breeding gain g_N^V of K250 is large enough for a very rapid H3-HTR buildup, irrespective of the HTR fuel burnup. Lowering the HTR fuel burnup will in this case not allow much U_3O_8 saving. With the lower g_N^V for M150, however, the difference in H3-HTR buildup between the high and low burnups is considerably larger, leading to larger U_3O_8 savings if the HTR fuel burnup is decreased.

V.5.b. Influence of FBR Surplus Breeding of U233 or Pu239

In the LWR/FBR//HTR scenario a surplus of Pu is expected for the LWR/FBR strategy at some time after t_L^m (Figure V.1). After accumulation of a specified quantity of excess Pu (e.g. 5 tons), the FBR breeding gain is changed from Pu to U233, i.e. thorium is used in the radial blankets of the FBRs. In the event that an excess of U233 is produced, FBRs again switch to the breeding of Pu, which is subsequently recycled into the disappearing LWRs, reducing their U_3O_8 demand. In this manner optimal utilization of the bred fissile fuel is assured.

Figure V.7 shows the difference in annual U_3O_8 requirements when the FBRs breed only Pu (V.7a) and when they instead produce U233 after $t = t_L^m$ (V.7b). The spectrum of curves il-

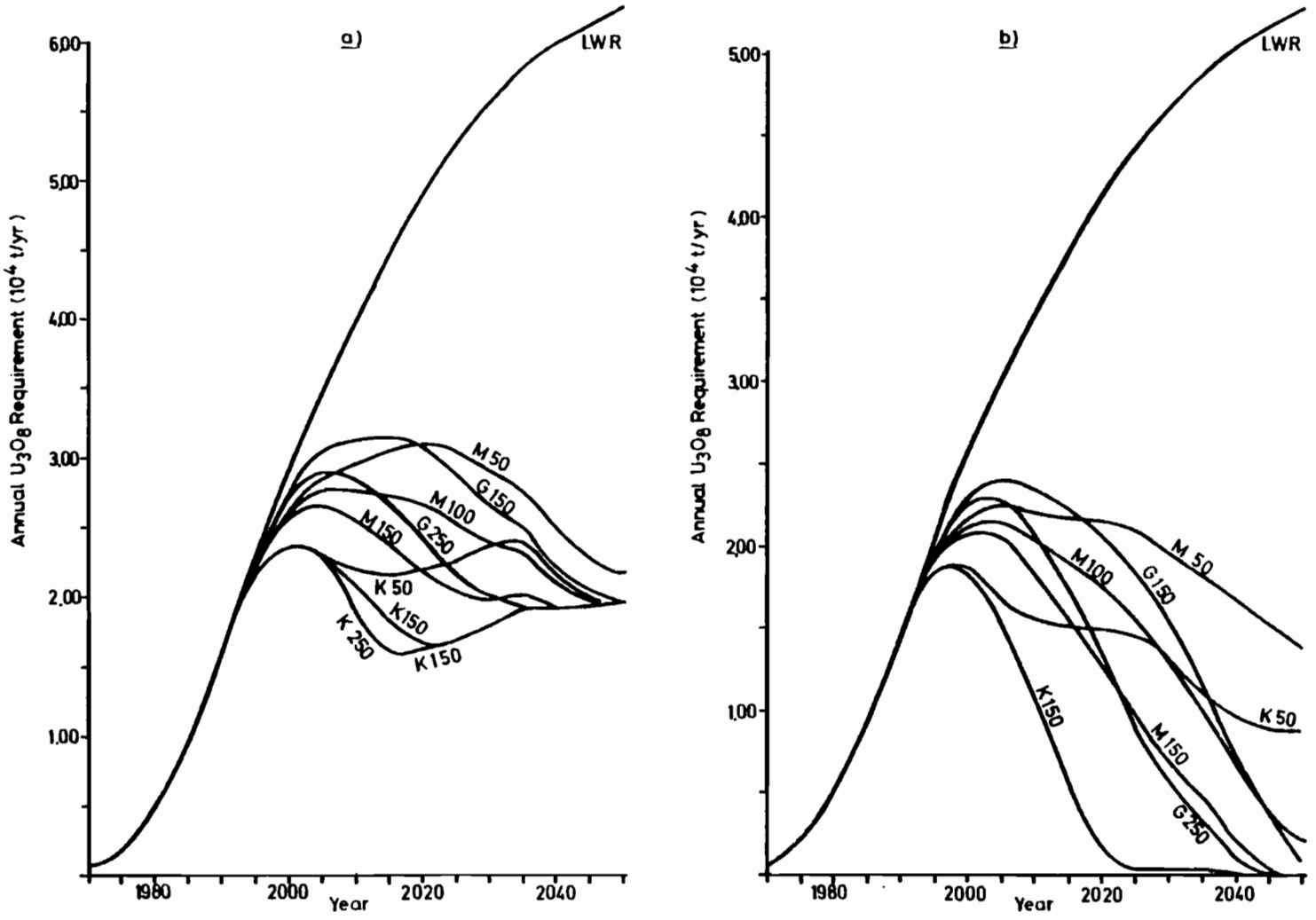

Figure V.7. Annual U_3O_8 requirement for (a) FBRs and HTRs not in symbiosis (no fissile fuel transfer), and (b) FBR/HTR symbiosis (U233 transfer), given demand forecast /M,P2/.

lustrates the influence of different FBR designs deployed after the year 2000 in the LWR/FBR//HTR scenario. The annual U_3O_8 demand for LWR/LWR//HTR scenario S2 (called LWR in the figure), where nuclear electricity is only supplied by LWRs, is shown for reference purposes. /M,P2/ is the combination of nuclear electricity and nuclear process heat demand assumed.

In Figure V.7b, FBRs breed U233 some time after $t = t_L^m$, and the annual U_3O_8 demand obviously approaches zero around the middle of the 21st century, the exact time depending on the type of FBR deployed. In the case where FBRs do not breed U233 but continue to breed Pu as surplus (Figure V.7a), the annual U_3O_8 demand approaches a constant value due to the continuous demand of H5-HTRs. Thus the annual demand will not approach zero, and there will always be a continuous U_3O_8 demand thereafter[7]. The HTR burnup assumed for these calculations was 100 GWd/t, and the fuel cycles employed correspond to HA10 and HB10 (see Table V.6).

V.6. Annual and Cumulative U_3O_8 Demands of the Three Reactor Strategy Scenarios

This is a discussion of the numerical results pertaining to the three reactor strategy scenarios discussed in Section V.4.a., which are based on the nuclear energy demand forecasts in Section V.4.c.

Figures V.8 to V.10 show the annual U_3O_8 requirements of these scenarios for nuclear energy demand forecasts /H,P2/, /M,P1/, and /N,P1/; the corresponding cumulative U_3O_8 demands E_T are depicted in Figures V.11 to V.13. The uranium ore demands of scenarios S1, S2, and S3 are evaluated for each forecast: the curve designated LWR represents the result of one strategy considered in scenario S2 (LWR/LWR//HTR); curves HB10 and HB03 are the results of the two strategies considered in scenario S3 (LWR/HTR//HTR) for the two different HTR fuel burnups, 100 GWd/t

---

[7] This is the case if the P_H/P_F ratio is larger than 0.5, see Figure IV.3.

and 30 GWd/t, and fissile fuel cycle B (U233 recycled); and the set of curves M50 to K250 are the results of the eight strategies in scenario S1 (LWR/FBR//HTR), reflecting different FBR designs deployed after the year 1995.

In scenario S2 (LWR scenario for short), LWRs recycle self-generated Pu, and HTRs utilize fissile fuel cycle C (without U233 recycling).

In scenario S3 (abbreviated HTR scenario), the use of HTRs with high conversion ratios (CR $\simeq$ 0.85) is depicted by curve HBO3, where the HTRs utilize thorium fissile fuel cycle B recycling self-bred U233. This fuel logistic closely corresponds to the optimal fissile fuel utilization HTRs can achieve without external U233 supply. HTR strategy HBO3 therefore shows the least U_3O_8 requirements to expect if reliance should be only on HTRs in the coming decades. HB10 corresponds to a more realistic HTR case, also assuming recycling of self-generated U233 but with an economically more viable burnup of 100 GWd/t.

The family of curves for the LWR/FBR//HTR scenario (called FBR scenario) demonstrates the influence of different breeding gains g_N^V and fissile fuel inventories I_Z^F of FBRs on the U_3O_8 requirements. I_Z^F is seen to be the most important FBR parameter in the initial 15-20 years of FBR introduction characterized by the increase in annual U_3O_8 demand. The influence of g_N^V is reflected by the gradients of decreasing annual U_3O_8 demand.

Among the three scenarios, LWR scenario S2 has by far the largest annual U_3O_8 requirement, followed by the HTR scenario S3. This pattern is observed for all cases irrespective of the energy demand forecast considered. For the HBO3 strategy, the annual U_3O_8 requirements after the year 2010 are considerably less than those for the LWR and HB10 scenarios. All three strategies: LWR, HB10, and HBO3 eventually approach a constant annual U_3O_8 demand in the 21st century, which reflects a continuous reliance on U_3O_8 even after the year 2050. The total U_3O_8 demand E_T will thus be *unlimited* for both LWR and HTR scenarios.

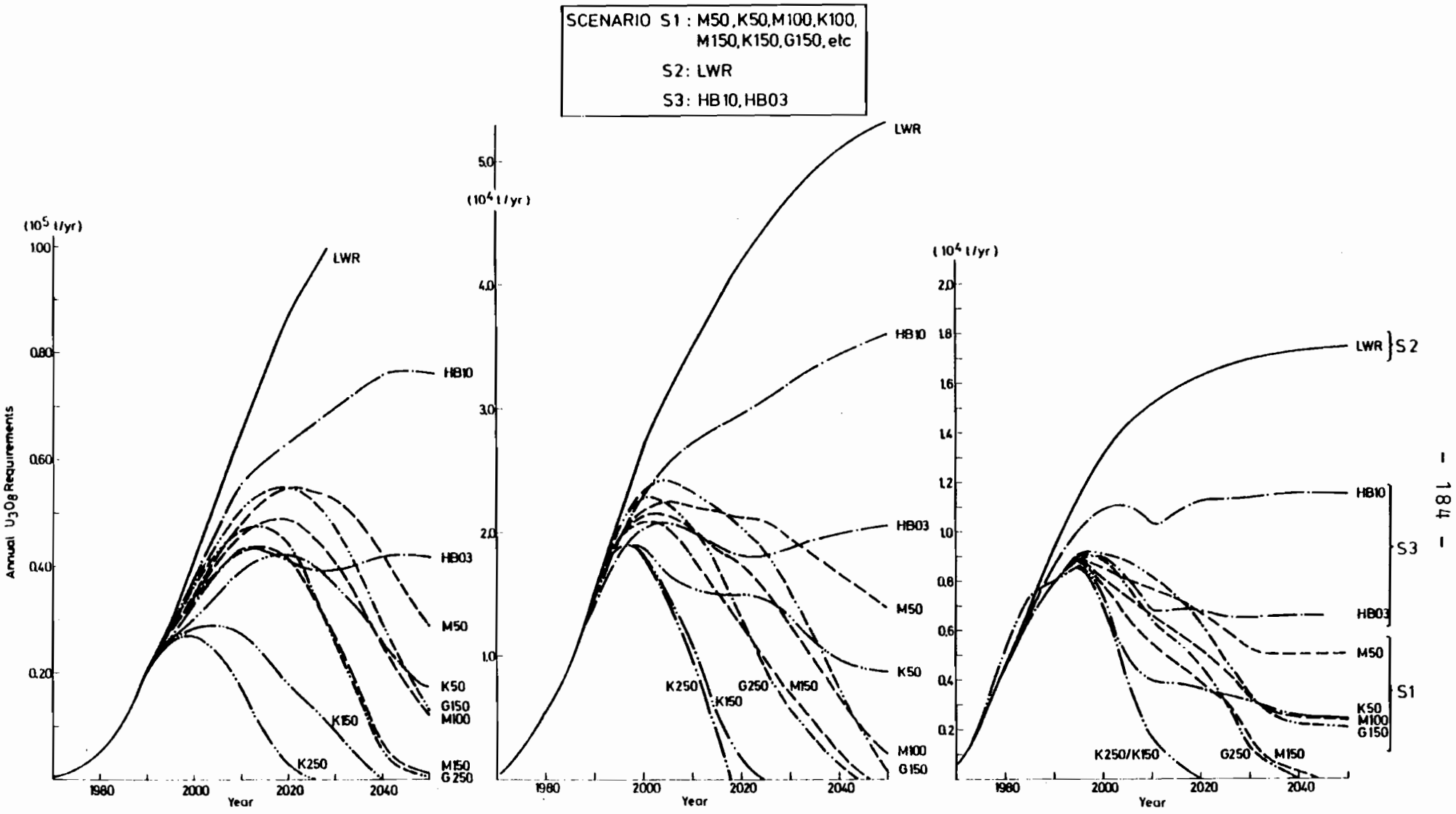

Figure V.8.

Annual U_3O_8 requirements (t/yr) for various scenarios; forecast /H,P2/.

Figure V.9.

Annual U_3O_8 requirements (t/yr) for various scenarios; forecast /M,P1/.

Figure V.10.

Annual U_3O_8 requirements (t/yr) for various scenarios; forecast /N,P1/.

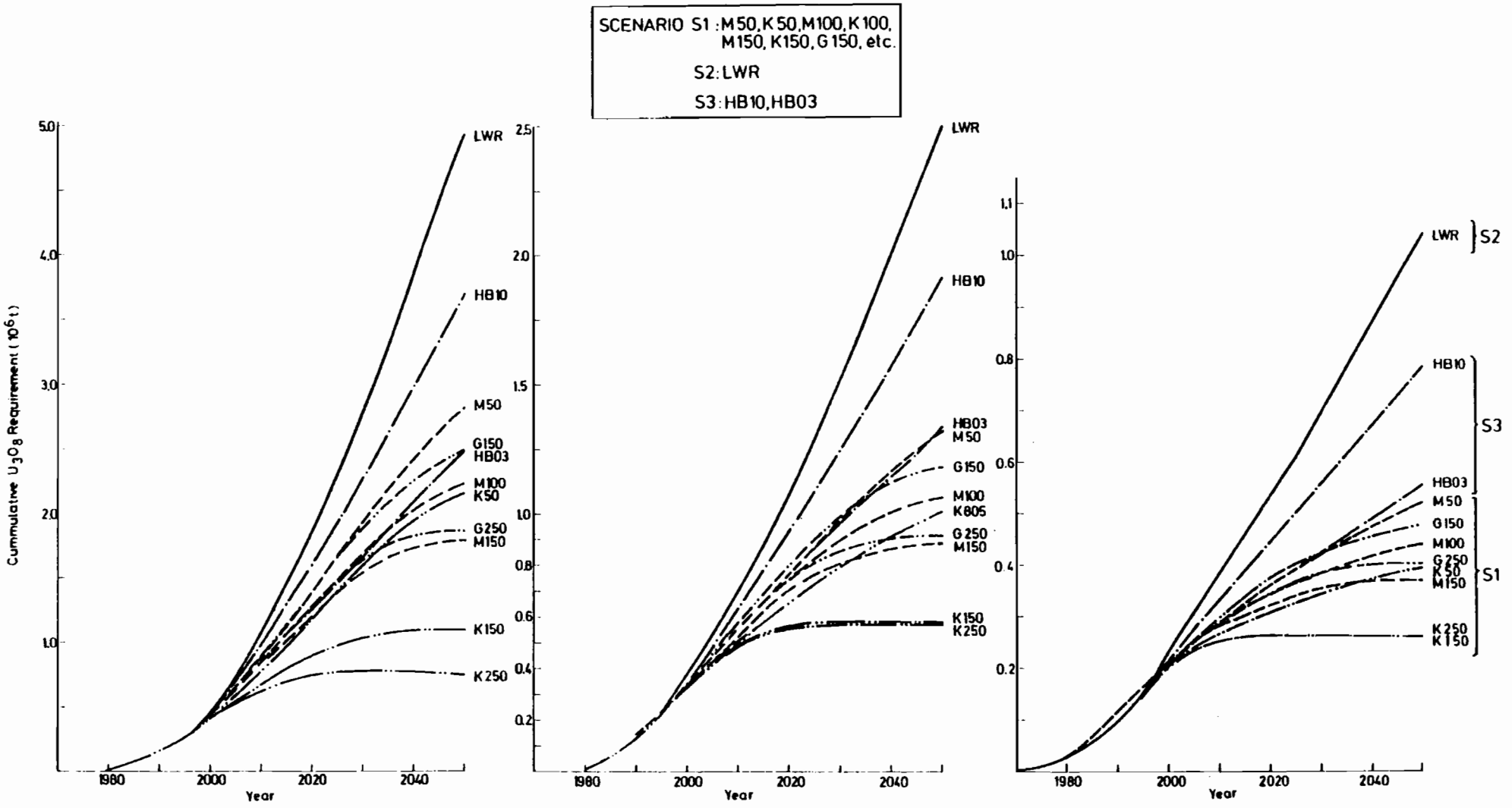

Figure V.11.

Total U_3O_8 requirements (t) for various scenarios; forecast /H,P2/.

Figure V.12.

Total U_3O_8 requirements (t) for various scenarios; forecast /M,P1/.

Figure V.13.

Total U_3O_8 requirements (t) for various scenarios; forecast /N,P1/.

The only reactor scenario approaching zero annual U_3O_8 demand some time about 2050 is LWR/FBR//HTR, scenario S1, or FBR scenario. With FBR designs of excellent reactor strategic characteristics, zero annual U_3O_8 demand can be reached approximately 25-35 years after FBR introduction, i.e. in about 2025-2050, depending on I_Z^F and g_N^V. The K250-FBR strategy is the fastest to approach this point in all three nuclear demand forecasts (2020-2030). Then follow KB150, G250, M150, etc. The FBRs with the lowest fissile fuel inventories, designated by K, clearly have the best strategic properties, since the increase in annual U_3O_8 demand after their introduction in 1995 is considerably lower than that of any other FBRs with high (M and G) inventories, even if the breeding gain of the latter should be higher. This becomes evident from a comparison of the annual U_3O_8 demand curves K150 and G250. Breeding gain g_N^V becomes more important after the annual U_3O_8 demand has reached its maximum, as is illustrated by the rate of decrease in the annual U_3O_8 demand. Here the G250-FBR surpasses the M150-FBR although I_Z^F of M150 is lower. Total U_3O_8 demand E_T is finite for all FBR strategies, in contrast to the LWR or HTR scenarios.

As has been shown, the annual U_3O_8 demand of strategy HBO3 in HTR scenario S2 is lower for a few decades still in the 21st century than for several of the FBR strategies. Reactor-strategically unfavorable FBRs, such as M50 and M100, show lower annual demands than the HBO3 strategy no sooner than in 2040, for forecasts /H,P2/ and /M,P1/. K250, K150, and M150 are the only FBR strategies with lower annual U_3O_8 demands over the entire period. For an interval of 20-40 years, a higher annual U_3O_8 demand must be therefore anticipated for all other FBR designs than for the most favorable HTR strategy HBO3. The salient difference between this HTR strategy and the FBR scenario, however, lies in the fact that all FBR strategies will eventually reach zero annual U_3O_8 demand, but the HBO3 strategy never will. For the HBO3 strategy, there will always remain an annual U_3O_8 demand as long as exclusive reliance is on HTRs. The total U_3O_8 demand will thus steadily increase for this HTR strategy, requiring more and more U_3O_8.

Total or cumulative U_3O_8 demands, the integral of annual U_3O_8 demand curves, are depicted in Figures V.11 to V.13 for the LWR, HTR, and FBR scenarios for the three nuclear energy demand forecasts. Reactor strategies not having reached zero annual U_3O_8 demand level by 2050 will exhibit a positive total U_3O_8 demand gradient. This is particularly evident for the LWR scenario, the HB10 and HBO3 strategies of the HTR scenario, and some FBR strategies, such as M50. While the total U_3O_8 demand curves of all FBR strategies will eventually level off, indicating a finite total demand, the curves for the LWR and HTR scenarios will never reach a plateau, indicating an unlimited U_3O_8 demand. The difference in total demand between the LWR and HTR scenarios and the FBR scenarios increases progressively as integration extends over longer periods of time.

The total U_3O_8 demand for establishing and sustaining a reactor system over a wide time horizon (several centuries) can be regarded as the total U_3O_8 *commitment* associated with that system. This commitment is infinite for the LWR scenario and the HTR scenarios in the long run. For the FBR scenario, however, this commitment is finite. It was referred to as the *critical U_3O_8 demand* of the FBR/HTR reactor system (see Section V.2.b.)[8].

The total U_3O_8 demands in metric tons of the various scenarios up to the year 2050 are given in Table V.7. It is clearly lowest for the K250-FBR strategy, which is 0.68 million tons of U_3O_8 for the /H,P1/ forecast, and 0.57 and 0.26 million tons for the /M,P2/ and /N,P1/ demands, respectively. The difference in total demand of the different FBR designs indicates possible U_3O_8 savings due to favorable FBR designs. It is interesting to observe that an FBR with both a high breeding gain g_N^V and a high

---

[8] Comparatively small quantities of U238 and Th232 are necessary for sustaining the FBR/HTR system in the asymptotic phase. The U238 accumulated in the transition phase (approximately 80% of the cumulative U_3O_8 requirement is retained as unused U238) will last for several centuries. If the K250-FBR is taken as a basis, U238 will be available for the /H,P2/ forecast for at least 700 years, for the /M,P1/ forecast for at least 1300 years, and for /N,P1/ for at least 2000 years. This period is relatively longer for FBR types with larger U_3O_8 requirements. The remaining Th232 reqirement is limited to approximately 115 t/yr for /H,P2/, and to approximately 50 t/yr for /M,P1/ and /N,P1/.

Table V.7. U_3O_8 requirements, in million tons, accumulated up to 2050 for three reactor strategy scenarios S1, S2, and S3, and three nuclear energy forecasts.

FBR Scenario S1 (LWR/FBR//HTR)* Forecasts	FBR design							
	K250	K150	K50	M150	M100	M50	G250	G150
/H,P2/	0.68	1.10	2.15	1.80	2.24	2.82	1.88	2.50
/M,P1/	0.57	0.75	1.00	0.88	1.07	1.33	0.92	1.18
/L,P1/	0.26	0.26	0.40	0.37	0.44	0.52	0.40	0.48

*An FBR of design M100 is used until the year 1995.

LWR Scenario S2 (LWR/LWR//HTR) Forecasts	LWR (Pu recycled)
/H,P2/	4.95
/M,P1/	2.50
/L,P1/	1.04

HTR Scenario S3 (LWR/HTR//HTR) Forecasts	HTR Cycle** HB10	HB03
/H,P2/	3.72	2.50
/M,P1/	1.93	1.35
/L,P1/	0.79	0.55

**See Table V.5

inventory I_Z^F, such as G250, has a slightly higher U_3O_8 commitment than an FBR with medium gain and inventory, such as M150.

Comparing (Table V.7) HTR strategy HBO3 with the various FBR strategies in terms of overall U_3O_8 demand up to the year 2050 shows no significant difference with respect to FBR designs M50, G150, M100, and K50. Thus the U_3O_8 demands until 2050 of the HTR scenario utilizing HTRs of advanced design (HBO3) and of the FBR scenario with fairly conservative FBR design, e.g., M150, are quite similar.

However, comparing the advanced HBO3 strategy with a comparably advanced FBR strategy such as the K250 design, yields very signigicant differences in U_3O_8 demand, favoring the FBR scenario by a factor of 2 to 3 as the nuclear energy demand increases (see Table V.7).

Qualitatively speaking, all reactor strategies exhibit very similar annual and total U_3O_8 demand characteristics irrespective of the nuclear energy forecast. They primarily differ in quantitative terms. This is manifested by the total U_3O_8 demand differences between scenarios S1, S2, and S3, and between the various FBR designs in FBR scenario S1. These differences increase decisively as the forecasts increase. This is of particular significance since any reactor strategy adopted must take into consideration the rather limited world uranium ore resources.

Current estimates of assured U_3O_8 reserves in the OECD countries run from one to four million tons, with estimated additional reserves up to 30 million tons. If the U_3O_8 available is indeed limited to quantities in this range, the employment of FBRs seems practically mandatory if nuclear energy is to serve as a long-term energy supply system--even more so since these reserves appear to be confined to a few geographic regions. Countries with practically no U_3O_8 reserves are thus required to deploy FBRs should they not wish to replace their current commitment to fossil fuels, i.e. their dependence on oil, by a long-term dependence on uranium ore beyond the transition phase. The U_3O_8 reserves available must, therefore, be treated as a one-time endowment that is to be used expediently by investing it

establishment of a reactor system that can offer U_3O_8 independence at some time. Any other strategy could prematurely foreclose nuclear power as a long-range energy option. The future availability of uranium must even then be seriously questioned since the expected worldwide U_3O_8 needs fall short of the proven reserves. Simply compare the absolute minimum U_3O_8 demands anticipated for the small DeBeNeLux region ($\sim$ 0.5 million tons) with the currently proven world resources (< 4 million tons). The severe situation is compounded by the fact that there are no uranium resources indigenous to this region.

V.7. Summary of Chapter V

In this chapter the demand of U_3O_8 has been analyzed for three, basically very different, reactor strategy scenarios. Scenario S1 relies primarily on the large-scale deployment of FBRs in conjunction with HTRs; scenario S2 assumes reliance on LWRs with some HTRs; and the third scenario S3 focuses on large-scale HTR deployment. No FBR deployment is assumed for S2 and S3. The future U_3O_8 demands of these scenarios have been evaluated for three different nuclear energy demand forecasts for the DeBeNeLux countries, representing a wide range of possible developments.

The calculations have first of all shown that only through the deployment of FBRs can the long-term U_3O_8 demand be kept within the limits of estimates of present world U_3O_8 resources. LWR scenario S2 clearly requires the largest U_3O_8 demand, with no prospect of ever becoming independent of U_3O_8 requirements. The same conclusion applies to HTR scenario S3, except that its demand is somewhat lower if the HTRs utilize the thorium cycle and have conversion ratios of approximately 0.72. Increasing the HTR conversion ratio to about 0.85 by reducing the fuel burn-up to 30 GWd/t will result in significant U_3O_8 savings, but long-term reliance on continuous U_3O_8 supply remains. There will be similar U_3O_8 demands for FBR scenario S1 in the first few decades of the 21st century, if the most favorable HTR strategy HBO3 is compared to reactor strategically unfavorable FBR designs. A

comparison of this optimistic HTR strategy to an equally optimistic FBR strategy, however, shows a clear advantage of the FBR scenario over the HTR scenario, by a factor of 2 to 3, depending on the nuclear energy demand forecast.

FBRs of different designs have quite dissimilar U_3O_8 demands, differing by up to a factor of 3. It has further been shown that the FBR fissile fuel inventory is by far the most important parameter during the introductory phase of FBRs--and not the doubling time--with the breeding gain becoming more important 10 to 20 years after FBR introduction. The design parameter for optimization of the first FBR generation should therefore be the fissile fuel inventory rather than the doubling time. An FBR with an average breeding gain and an average inventory, such as M150, has a U_3O_8 demand comparable to that of FBRs with very high gains but high inventories (G250). As the transition phase merges into the asymptotic phase, the importance of the breeding ratio and the fissile fuel cycle inventory is reversed.

It has also been shown that the differences in U_3O_8 demand between the various scenarios and the reactor designs within a given scenario increase with rising nuclear energy demand. The differences between the scenarios can be within a range of one to three million tons of U_3O_8 (in the year 2050) for high nuclear energy demand forecasts, and in the range of 100,000 to 500,000 tons of U_3O_8 for relatively low forecasts.

Of primary importance in this assessment is the observation that the LWR/FBR//HTR scenario does converge into a symbiotic and fissile fuel self-sufficient FBR/HTR reactor system in the asymptotic phase. It is easy to show that the amounts of fertile isotopes U238 and Th232 needed to sustain the symbiotic FBR/HTR system will be available worldwide in sufficient quantities, lasting for several centuries. These U238 requirements will have already been accumulated in the transition phase, in the form of depleted uranium.

The *critical U_3O_8 demand* of the FBR/HTR system is basically characterized by the design and type of FBRs deployed in the transition phase (i.e. GCFBRs and LMFBRs with oxide or carbide

fuels) and by the fissile fuel cycle in HTRs (thorium or uranium cycles, recycling or nonrecycling of the self-generated fissile fuel).

Designs of both HTRs and FBRs that are reactor strategically favorable can save considerable quantities of uranium ore. In any event, deployment of FBRs and HTRs assures optimum utilization of the uranium and thorium reserves available if both reactor types are combined in a symbiotic reactor system, as was suggested in Chapter IV.

Furthermore, it has been shown on the premise of limited U_3O_8 reserves that nuclear energy can only serve as a long-range energy supply system if the reactor system of the transition phase merges into a U_3O_8-independent reactor system in the asymptotic phase. This under all circumstances requires the deployment of the FBR.

The use of thorium as breeding material in the radial blanket of the FBR has been shown to be practical after the plutonium requirements of FBR first-core inventories have been satisfied. This can be as early as at the time of commercial introduction of fast breeder reactors, or 10-20 years thereafter, depending primarily on the LWR capacity existing at the time of FBR introduction and on the FBR fissile fuel cycle inventory.

REFERENCES

Abagjan, L.P., et al. (1964) Gruppenkonstanten schneller und intermediärer Neutronen für die Berechnung von Kernreaktoren. KFK-tr.-144. Karlsruhe, F.R.G.: Gesellschaft für Kernforschung.

Adkins, C.R. (1972) The breeding ratio with correlation to doubling time and fuel cycle reactivity variation. Nuclear Technology 13:114.

Allen, W.O., D.J. Stoker, and A.V. Campise (1966) Fast breeder reactors with mixed fuel cycles. Proceedings of the Second International Thorium-Fuel Cycle Symposium, Gatlinburg, Te., May 3-6, 1966. Symposium Series 12. Washington, D.C.: U.S. Atomic Energy Commission.

Baier, J. (1974) Herstellung von HTR-Brennelementen aus wiederaufgearbeitetem Brennstoff. HTRB-IB-1/74. Mannheim, F.R.G.: Hochtemperaturreaktorbau.

Batyrebekov, G.A., et al. (1964) Some characteristics of a fast reactor with a thorium shield. Atomnaia energia. English translation in Soviet Atomic Energy 17(4).

Bell, M.J. (1973) ORIGEN - The ORNL Isotope Generation and Depletion Code. ORNL-4628. Oak Ridge, Te.: Oak Ridge National Laboratory.

Brogli, R.H., and K.R. Schultz (1974) Thorium utilization in an FBR/HTGR power system. Vol. 36, p. 247, Proceedings of the American Power Conference. Chicago: Illinois Institute of Technology.

Bundschuh, V. (1972) Brennelemente mit Thorium als Strukturmaterial und verschiedenen Spaltstoffarten. IPC-B-4/72. Jülich, F.R.G.: Kernforschungsanlage.

Congress of the United States (1966) Uranium Enrichment Services Criteria and Related Matters, Hearings before the Joint Committee on Atomic Energy. Pages 411-416, Eighty-Ninth Congress, Second Session, August 2, 3, 4, 16, and 17.

Dahlberg, R.C., et al. (1974) HTGR fuel and fuel cycle. Nuclear Engineering and Design 26:58-77.

Fowler, T.B., et al. (1971) Nuclear Reactor Core Analysis Code: CITATION. ORNL-TM-2496. Oak Ridge, Te.: Oak Ridge National Laboratory.

General Electric (1968) Conceptual Plant Design for a 1000 MWe Sodium-Cooled Fast Reactor, Follow On Study. GEAP-5678. San Jose, Ca.: General Electric.

Gwin, R., et al. (1976) Measurement of the neutron capture and fission cross section Pu239 and U235, 0.02 eV to 200 keV, the neutron capture cross sections of An197, and neutron fission cross sections of U233, 5 to 200 keV. Nuclear Science Engineering 59:79-105.

Gesellschaft für Kernforschung (1971) Gasbrüter-Memorandum, Ergebnisse einer Untersuchung über die Realisierbarkeit und Wirtschaftlichkeit eines gasgekühlten schnellen Brüters. KFK 1375, EUR4575d, JÜL-744RG. Karlsruhe.

Hankel, R., et al. (1962) An Evaluation of U233/Thorium Fast Breeder Power Reactors. NDA-2164-3, Elmsford, N.Y.: United Nuclear Corporation.

Häfele, W., and A.S. Manne (1974) Strategies for a Transition from Fossil to Nuclear Fuels RR-74-7 Laxenburg, Austria: International Institute for Applied Systems Analysis. Also in Energy Policy 2:3-23, 1975.

Häfele, W., and W.M. Schikorr (1973) Reactor strategies and the energy crisis. Proceedings of a Study Group Meeting on Reactor Strategies Calculations, Vienna, November 5-9, 1973. IAEA-167. Vienna, International Atomic Energy Agency. Paper also appeared as RR-73-13. Laxenburg, Austria: International Institute for Applied Systems Analysis.

Hinkelmann, B. (1970) Evaluation of neutron nuclear data for several actinides in the energy range from thermal to 10 MWe. p. 720, Proceedings on Nuclear Data for Reactors - 1970, Helsinki, June 15-19, 1970. STI/Pub/259. Vienna: International Atomic Energy Agency.

Höbel, W., H. Huschke, et al. (1966) Das Karlsruher Nuklear-Programm-System NUSYS. Karlsruhe, F.R.G.: Gesellschaft für Kernforschung, unpublished.

Jansen, P., U. Seele, and W.M. Schikorr (1976) Beschreibung des Rechnerprogrammes zur Simulation von Strategien zur Kernkrafteinführung. IAS-Nr.14/76. Karlsruhe, F.R.G.: Gesellschaft für Kernforschung.

Kasten, P.R., E.S. Bettis, H.F. Baumann, et al. (1968) Summary of molten-salt breeder reactor design studies. Thorium Fuel Cycle, Proceedings of the Second International Thorium Fuel Cycle Symposium, Gatlinburg, Te., May 3-6, 1966. Symposium Series 12. Washington, D.C.: U.S. Atomic Energy Commission.

Kidman, R.B., and R.E. Scheuter (1971) Group Constants for Fast Reactor Calculations. HEDL-TME-71-36. Richland, Wash.: Hanford Engineering Development Laboratory.

Kiefhaber, E. (1972) The KFK-INR Set of Group Constants. Nuclear Data Basis and First Results of Its Application to the Realization of Fast Zero Power Reactors. KFK 1572. Karlsruhe, F.R.G.: Gesellschaft für Kernforschung.

Kobayashi, K., et al. (1971) Measurement of average cross section for Th232(n,2n) Th231 reaction to neutrons with fission-type reactor spectrum, and gamma-ray intensities of Th231. Nuclear Science and Technology 8(9):492.

Kobayashi, K., et al. (1973) Measurement of average cross section for U233 (n,2n) U232 reaction. Nuclear Science and Technology 10(11):668.

Kraftwerksunion (1974) 1000 MWe-Gasgekühlter Schneller Brüter, Referenz- und Sicherheitsstudie, Annual Report. KWU-AG RZR2. Erlangen, F.R.G.

Lang, L.W. (1968) Thorium can reduce power costs for thermal and fast reactors. ANS Transactions 11:38.

Lang, L.W. (1969) Dependence of fast reactor startups on the thorium fuel cycle. ANS Transactions 12:443.

Leipunskii, A.I., O.D. Kazachkovskii, S.M. Shikhov, and V.M. Murogov (1965) An investigation of the possibility of using thorium in high energy reactors. Atomnaia energia. English translation in Soviet Atomic Energy 18(4).

Leipunskii, A.I., et al. (1971) Improved physical characteristics of fast plutonium reactors using U233 and thorium. Atomnaia energia. English translation in Soviet Atomic Energy 30(6).

Loewenstein, W.B., and D. Okrent (1958) The physics of fast power reactors: a status report. Vol. 12, Proceedings of the Second U.N. International Conference on the Peaceful Uses of Atomic Energy, New York. Vienna: International Atomic Energy Agency.

Loewenstein, W.B., and B. Blumenthal (1965) Mixed fuel cycle fast breeder reactors: nuclear safety, and material considerations. Proceedings of the Conference on Safety, Fuels, and Core Design in Large Fast Power Reactors. ANL-7120. Argonne, Ill.: Argonne National Laboratory.

Okrent, D. (1964) Neutron physics considerations in large fast reactors. Power Reactor Technology 7(2):107.

Okrent, D., K.P. Cohen, and W.B. Loewenstein (1965) Some nuclear and safety considerations in the design of large fast power reactors. Vol. 6, Proceedings of the Third U.N. International Conference on the Peaceful Uses of Atomic Energy, New York, 1964. Vienna: International Atomic Energy Agency.

Olsen, A.R., et al. (1966) Irradiation behaviour of thorium-uranium alloys and compounds, utilization of thorium in power reactors. Technical Reports Series No. 52:246. Vienna: International Atomic Energy Agency.

Schikorr, W.M. (1973) SNR 300, Mark I-a, burnup calculations with cross-section set MOXTOT. Karlsruhe: Gesellschaft für Kernforschung, unpublished.

Schikorr, W.M. (1974a) Der geschlossene Spaltstoffkreislauf einer SBR-HTR Symbiose, draft, August 1974. Karlsruhe: Gesellschaft für Kernforschung, limited distribution.

Schikorr, W.M. (1974b) Langfristige Reaktorstrategien und deren Einfluß auf den Uranerzbedarf der BRD. Reaktortagung Nürnberg 1974. Bonn: Deutsches Atomforum, Kerntechnische Gesellschaft im Deutschen Atomforum.

Schikorr, W.M. (1975a) Optimal reactor strategy toward long-range energy independence. Nuclear Energy Maturity, First European Conference, Paris, April 21-25, 1975. ANS Transactions 20.

Schikorr, W.M. (1975b) Implications of fuel logistics for utilizing thorium in FBRs and HTRs, submitted to ANS Winter Meeting, San Francisco, November 1975.

Schikorr, W.M., and H.H. Rogner (1975) Übergang von Öl und Kohle zur Kernenergie unter wirtschaftlichen und rohstoffpolitischen Aspekten. Reaktortagung Düsseldorf 1975. Bonn: Deutsches Atomforum, Kerntechnische Gesellschaft im Deutschen Atomforum.

Schroeter, K.E. (1970) Einfluß von Berechnungsmethoden auf den Multiplikationsfaktor k_{eff} und den Voideffekt k_v für einen großen schnellen natriumgekühlten Brutreaktor. KFK 1180. Karlsruhe, F.R.G.: Gesellschaft für Kernforschung.

Schröder, R., and J. Wagner (1975) Überlegungen zur Einführung schneller Brutreaktoren im DeBeNeLux-Bereich. KFK-Ext. 25/75-1. Karlsruhe, F.R.G.: Gesellschaft für Kernforschung.

Schulten, R., et al. (1977) HTR Nahebrüterkonzept zur Spaltstoffersparnis. Atomwirtschaft-Atomtechnik 22(2).

Sofer, G.A., et al. (1963) Economics and Safety Aspects of Large Ceramic U-Th Fast Breeder Reactors. ANL-6792. Argonne, Ill.: Argonne National Laboratory.

Suich, J.E., and H.C. Honeck (1967) The HAMMER System. DP-1064. Aiken, S.C.: Du Pont de Nemours, Savannah River Lab.

Teuchert, E., et al. (1972) Basisstudie zum Kugelhaufenreaktor in OTTO-Beschickung. JÜL-858-RG. Jülich, F.R.G.: Kernforschungsanlage.

Teuchert, E., et al. (1974a) OTTO-Kugelhaufenreaktor im Thorium-Brennstoffzyklus. JÜL-1059-RG Jülich, F.R.G.: Kernforschungsanlage.

Teuchert, E., et al. (1974b) OTTO-Kugelhaufenreaktor für eine 1000 MWe Heliumturbinenanlage. JÜL-1070-RG Jülich, F.R.G.: Kernforschungsanlage.

Teuchert, E., and S. Brandes (1975) Verhalten des Hochtemperaturreaktors bei verschiedenen Brennstoffzyklen. Atomkernenergie 25:137.

Vieidir, G., et al. (1974) Comparison of the fuel cycle performance of Na- and He-cooled fast breeders utilizing stainless steel clad pin fuel. Reaktortagung Berlin 1974. Bonn: Deutsches Atomforum, Kerntechnische Gesellschaft im Deutschen Atomforum.

Wenzel, P. (1971) Crossed uranium-plutonium and thorium-uranium fuel cycles for a developing nuclear power system with thermal converters and fast breeder reactors. Kernenergie 14 (7/8):231-235.

Wood, P.J., and M.J. Discroll (1973) Assessment of Thorium Blankets for Fast Breeder Reactors. COO-2250-2, MITNE-148. Springfield, Va.: National Technical Information Service.

Wehmann, U., and U. Stehlen (1975) Leistungs- und Abbrandrechnungen für einen Natriumbrüter von 1200 MWe mit internen Brutzonen. Internal Report. Bergisch Gladbach, F.R.G.: Interatom.

APPENDIX I.A. DERIVATION OF THE BREEDING RATIOS OF A MULTIREGION REACTOR WITH FAST FISSION (e.g. FBR)

I.A.1. Derivation of the Breeding Ratio of a Multiregion Reactor with Fast Fission

Equation (I-15) has to be derived. The starting point is the neutron balance of a critical multiregion reactor (FBR) with

$$(\nu F)_N^I + (\nu F)_N^J = A_N^I + A_N^J + P_N = 1.0 \quad . \tag{I.A-1}$$

If the absorption rate is expanded by $A_N^J = C_N^J + F_N^J$, and if both sides are divided by A_N^I and the following relations are used:

$$\eta_N^I \overset{\alpha}{=} \frac{(\nu F)_N^I}{A_N^I} \quad , \quad BR_N = \frac{C_N^J}{A_N^I} \quad , \tag{I.A-2}$$

(I.A-1) can be rewritten as

$$BR_N = (\eta_N^I + \frac{(\nu F)_N^J}{A_N^I}) - \frac{F_N^J}{A_N^I} - \frac{P_N}{A_N^I} - 1 \quad . \tag{I.A-3}$$

The terms $\frac{F_N^J}{A_N^I}$ and $\frac{P_N}{A_N^I}$ can each be expanded by

$$[(\nu F)_N^I + (\nu F)_N^J]$$

so that

$$\frac{F_N^J}{A_N^I} - \frac{P_N}{A_N^I} = F_N^J \left(\eta_N^I + \frac{(\nu F)_N^J}{A_N^I}\right) - P_N\left(\eta_N^I + \frac{(\nu F)_N^J}{A_N^I}\right) ,$$

and (I.A-3) can be written as

$$BR_N = \left[\eta_N^I + \frac{(\nu F)_N^J}{A_N^I}\right] (1-P_N-F_N^J) - 1 . \qquad \text{(I.A-4)}$$

This can be rewritten as

$$BR_N = \left(\eta_N^I + \frac{(\nu F)_N^J}{A_N^I}\right) \left[1 - (P_N + F_N^J)\right] - 1 , \qquad \text{(I.A-5)}$$

or

$$BR_N = \eta_B \left[1 - (P_N + F_N^J)\right] - 1 , \qquad \text{(I.A-6)}$$

where η_B represents the sum of neutron productions in the fissile and fertile fuels.

I.A.2. Derivation of the Breeding Ratio of Individual Regions of a Multiregion Reactor with Fast Fission

Equation (I.A-5) can be rewritten as follows:

$$BR_N = \left\{\frac{1}{A_N^I} \sum_n^N A_n^I \left[\left(\eta_n^I + \frac{(\nu F)_n^I}{A_n^I}\right) (1-P_n-F_n^J) - 1\right]\right\} . \qquad \text{(I.A-7)}$$

On the basis of Equation (I-12)

$$BR_N = \sum_n^N \left\{\frac{A_n^I}{A_N^I} KR_n\right\} , \qquad \text{(I.A-8)}$$

so that

$$KR_n = \left(\eta_n^I + \frac{(\nu F)_n^I}{A_n^I} \right) \left[1 - (P_n + F_n^J) \right] - 1 \quad . \qquad \text{(I.A-9)}$$

The form of this equation is identical with that of (I.A-5), except that (I.A-9) contains the values averaged over region n, and (I.A-5) those averaged over the entire reactor.

APPENDIX I.B. DERIVATION OF THE BREEDING GAINS G_N, G_m, AND G_n OF A MULTIREGION REACTOR (e.g. FBR)

I.B.1. The Global Breeding Gain G_N

In Section I.2, the global breeding gain G_N of an N zone reactor, normalized to the overall fission rate F_N^{IJ} of the reactor, is given as

$$G_N = \frac{C_N^J - A_N^I}{F_N^{IJ}} \quad , \tag{I.B-1}$$

where

$$F_N^{IJ} = F_N^I + F_N^J = \sum_n^N \sum_i^I F_n^i + \sum_n^N \sum_j^J F_n^j \quad . \tag{I.B-2}$$

Using $BR_N = \frac{C_N^J}{A_N^I}$, Equation (I.B-1) can be written as

$$G_N = \frac{A_N^I}{F_N^{IJ}} (BR_N - 1) \quad . \tag{I.B-3}$$

Since

$$\frac{A_n^i}{F_n^i} = \frac{a_n^i}{f_n^i} = (1+\alpha)_n^i \quad , \tag{I.B-4}$$

$$A_N^I = \sum_n^N \sum_i^I A_n^i = \sum_n^N \sum_i^I F_n^i \, (1+\alpha)_n^i \quad . \qquad \text{(I.B-5)}$$

By substitution of (I.B-5), (I.B-3) can then be written as

$$G_N = (BR_N - 1) \sum_n^N \sum_i^I \left(\frac{F_n^i}{F_N^{IJ}}\right) (1+\alpha)_n^i \quad . \qquad \text{(I.B-6)}$$

The somewhat more customary form of G_N (Equation (I.20)) is obtained by rewriting (I.B-6) as

$$G_N = (BR_N - 1) \left[\sum_n^N \sum_i^I \left(\frac{F_n^i}{F_N^{IJ}}\right) \cdot \sum_n^N \sum_i^I \left(\frac{F_n^i}{F_N^{I}}\right) (1+\alpha)_n^i \right] \quad . \qquad \text{(I.B-7)}$$

If ε_N is defined as the fast fission fraction of the overall fission fraction $(F_N^I + F_N^J)$ of all N zones with

$$\varepsilon_N = \frac{F_N^J}{F_N^{IJ}} = \sum_n^N \sum_j^J \frac{F_n^j}{F_N^{IJ}} \quad , \qquad \text{(I.B-8)}$$

it can be shown that

$$(1-\varepsilon_N) = \frac{F_N^I}{F_N^{IJ}} = \sum_n^N \sum_i^I \frac{F_n^i}{F_N^{IJ}} \quad . \qquad \text{(I.B-9)}$$

In addition, we define

$$(1+\alpha)_N^I = \sum_n^N \sum_i^I \left(\frac{F_n^i}{F_N^{I}}\right) (1+\alpha)_n^i \quad , \qquad \text{(I.B-10)}$$

which also leads to

$$\frac{A_N^I}{F_N^I} = (1+\alpha)_N^I \quad . \qquad \text{(I.B-11)}$$

Thus (I.B-7) can be transformed to the general and customary form

$$G_N = (BR_N - 1) \, (1-\varepsilon_N) \, (1+\alpha)_N^I \quad . \qquad \text{(I.B-12)}$$

I.B.2. The Breeding Gain G_m of Several Regions m

The breeding gain of one region n or several regions m is of interest where m < N. For the general case with m zones, the following relations can be derived:

$$G_m = \frac{C_m^J - A_M^J}{F_N^{IJ}} \quad , \tag{I.B-13a}$$

and

$$BR_m = \frac{C_m^J}{A_N^I} - \frac{\sum_n^m C_n^J}{A_N^I} \quad . \tag{I.B-13b}$$

Thus Equation (I.B-13a) can be rewritten as

$$G_m = BR_m \frac{A_N^I}{F_N^{IJ}} - \frac{A_m^I}{F_N^{IJ}} \quad , \tag{I.B-14}$$

where $\frac{A_N^I}{F_N^{IJ}}$ can be substituted by means of Equation (I.B-3) together with (I.B-7) or (I.B-12). On the other hand,

$$\frac{A_m^I}{F_N^{IJ}} = \sum_n^m \sum_i^I \frac{A_n^i}{F_N^{IJ}} = \sum_n^m \sum_i^I \frac{F_n^i}{F_N^{IJ}} (1+\alpha)_n^i \quad . \tag{I.B-15}$$

Thus Equation (I.B-14) can be changed to

$$G_m = BR_m \sum_n^N \sum_i^I \left(\frac{F_n^i}{F_N^{IJ}}\right) (1+\alpha)_n^i - \sum_n^m \sum_i^I \left(\frac{F_n^1}{F_N^{IJ}}\right) (1+\alpha)_n^i \quad . \tag{I.B-16}$$

In the more useful global form, (I.B-16) can be written as

$$G_m = BR_m(1-\varepsilon_N) (1+\alpha)_N^I - \sum_n^m (1-\varepsilon_n) \delta_n (1+\alpha)_n^I \quad . \tag{I.B-17}$$

To this end (I.B-15) has been expanded to

$$\frac{A_m^I}{F_N^{IJ}} = \sum_n^m \frac{F_n^I}{F_N^{IJ}} \sum_i^I \left(\frac{F_n^i}{F_n^I}\right) (1+\alpha)_n^i \qquad \text{(I.B-18)}$$

$$= \sum_n^m \left(\frac{F_n^{IJ}}{F_N^{IJ}}\right) \left(\sum_i^I \frac{F_n^i}{F_n^{IJ}}\right) \left[\sum_i^I \left(\frac{F_n^i}{F_n^I}\right) (1+\alpha)_n^i\right] .$$

If ε_n represents the fast fission fraction of the overall fission in region n (and not N, as in Equation (I.B-8)),

$$\varepsilon_n = \frac{F_n^J}{F_n^{IJ}} = \sum_j^J \frac{F_n^j}{F_n^{IJ}} , \qquad \text{(I.B-19)}$$

then

$$(1-\varepsilon_n) = \frac{F_n^I}{F_n^{IJ}} = \sum_i^I \frac{F_n^i}{F_n^{IJ}} , \qquad \text{(I.B-20)}$$

since

$$F_n^{IJ} = F_n^I + F_n^J .$$

If δ_n is defined as the fissile fraction of region n per fission in all regions N (or power fraction of region n)

$$\delta_n = \frac{F_n^{IJ}}{F_N^{IJ}} \quad \text{with} \quad \delta_N = \sum_n^N \delta_n = 1 , \qquad \text{(I.B-21)}$$

and

$$\sum_i^I \left(\frac{F_n^i}{F_n^I}\right) (1+\alpha)_n^i = (1+\alpha)_n^I = \frac{A_n^I}{F_n^I} , \qquad \text{(I.B-22)}$$

then Equation (I.B-17) can be written.

I.B.3. The Breeding Gain G_n of One Region

The breeding gain per fission G_n of one region n can be derived from (I.B-16) and (I.B-17) for m = 1 as follows:

$$G_n = BR_n \sum_{n}^{N} \sum_{i}^{I} \left(\frac{F_n^i}{F_N^{IJ}}\right) (1+\alpha)_n^i - \sum_{i}^{I} \left(\frac{F_n^i}{F_N^{IJ}}\right) (1+\alpha)_n^i \quad , \qquad \text{(I.B-23)}$$

or as

$$G_n = BR_n \ (1-\varepsilon_N) \ (1+\alpha)_N^I - (1-\varepsilon_n) \ \delta_n (1+\alpha)_n^I \quad . \qquad \text{(I.B-24)}$$

These two equations are often used in Chapters III and V. In additon, it can be shown that

$$G_N = \sum_{n}^{N} G_n \quad , \qquad \text{(I.B-25)}$$

such that

$$G_N = \sum_{n}^{N} \left(\frac{C_n^J - A_n^I}{F_N^{IJ}}\right) = \frac{C_N^J - A_N^I}{F_N^{IJ}} \quad .$$

APPENDIX I.C. DERIVATION OF THE CONVERSION RATIO AND FISSILE FUEL REQUIREMENT OF A SINGLE-REGION REACTOR WITHOUT FAST FISSION (e.g. HTR)

I.C.1. Derivation of the Conversion Ratio of a Single-Region Reactor without Fast Fission

For a single-region reactor, i.e. N = 1, with a minor fast fission fraction, i.e., $\nu F^J \simeq 0$, (this would correspond to an HTR or LWR), Equation (I.A-1) can be rewritten as follows:

$$(\nu F)^I = A^I + C^J + P = 1.0 \text{ for } \begin{cases} N = 1 \\ F^J = 0 \end{cases} . \qquad \text{(I.C-1)}$$

If both sides are divided by A^I and the following relations used,

$$\eta^I = \frac{(\nu F)^I}{A^I}$$

$$CR = \frac{C^J}{A^I} \qquad \text{(I.C-2)}$$

then Equation (I.C-1) yields

$$CR = \eta^I - 1 - \frac{P}{A^I} \quad ;$$

since $(\nu F)^I = 1$, $\frac{P}{A^I}$ can be rewritten as

$$\frac{P}{A^I} = \frac{P}{(\nu F)^I} \quad \frac{(\nu F)^I}{A^I} = \eta^I \, P \quad .$$

Thus

$$CR = \eta^I (1-P) - 1 \quad . \qquad \text{(I.C-3)}$$

This form corresponds to Equations (I.A-5) and (I.A-6), differing only by the etas. The eta referred to in Equation (I.C-3) is that of the fissile isotopes. The eta referred to in Equation (I.A-6) is modified to include the contribution of fast fission.

$$\eta^I = \frac{(\nu F)^I}{A^I} = \frac{\sum_i^I (\nu F)^i}{\sum_i^I A^i} = \frac{\sum_i^I \frac{(\nu F)^i}{F^I}}{\sum_i^I \frac{A^i}{F^I}} = \frac{\sum_i^I (\frac{F^i}{F^I}) \nu^i}{\sum_i^I (\frac{F^i}{F^I}) (1+\alpha)^i} \quad , \qquad \text{(I.C-4)}$$

so that

$$\eta^I = \frac{\sum_i^I (\frac{F^i}{F^I}) \nu^i}{(1+\alpha)^I} \quad , \qquad \text{(I.C-5)}$$

where

$$(1+\alpha)^I = \sum_i^I (\frac{F^i}{F^I}) (1+\alpha)^i \quad . \qquad \text{(I.C-6)}$$

I.C.2. Derivation of the Fissile Fuel Requirement of a Single-Region Reactor without Fast Fission and CR < 1.0

The conversion ratio is defined as

$$CR = \frac{C^J}{A^I} \quad . \qquad \text{(I.C-7)}$$

Reference is only made to a breeding gain if $C^J > A^I$. In the HTR or LWR, $C^J < A^I$ in general, i.e. the conversion ratio CR is smaller than 1.0. This means that these reactor types exhibit a *negative* breeding gain or positive demand D of fissile fuel.

Equation (I.C-1) can be written as follows:

$$\frac{A^I - C^J}{A^I} = (1-CR) \quad . \tag{I.C-8}$$

If $A^I > C^J$, then (1-CR) is positive, and thus synonymous with a positive demand D.

The requirements of fissile fuel per fission is to be found by

$$D = \frac{A^I - C^J}{F^I} \quad , \; (F^J = 0) \quad . \tag{I.C-9}$$

Equation (I.C-9) can be rewritten as:

$$D = (1-CR) \; \frac{A^I}{F^I} \quad ,$$

but

$$\frac{A^I}{F^I} = \sum_i^I \frac{A^i}{F^I} = \sum_i^I \left(\frac{F^i}{F^I}\right) \; (1+\alpha)^1 = (1+\alpha)^I \quad , \tag{I.C-10}$$

so that

$$D = (1-CR) \; (1+\alpha)^I \quad .$$

APPENDIX II.A. REGION-DEPENDENT NORMALIZED REACTION RATES OF AN FBR WITH VARIOUS RADIAL BLANKETS (TABLE)

Table II.A.1. Region-dependent normalized reaction rates, averaged over fissile (I) and fertile (J) isotopes, of an FBR with different radial blankets, as a function of the radial blanket residence time.

Radial blanket residence time (days)	Core						Axial blanket					
	A_c^I	C_c^I	F_c^I	A_c^J	C_c^I	F_c^J	A_{ax}^I	C_{ax}^I	F_{ax}^I	A_{ax}^J	C_{ax}^J	F_{ax}^I
UO_2 blanket												
0	.3252	.06269	.2625	.35318	.28987	.0634	.01243	.00331	.00912	.13267	.1259	.00678
219	.3068	.0599	.2469	.3345	.2739	.0606	.02654	.00694	.01960	.1347	.1271	.00755
803	.2976	.0580	.2396	.3236	.2649	.0587	.02492	.00654	.01838	.1302	.1228	.00735
1387	,28898	.05625	.2327	.3136	.2567	.05691	.02360	.00632	.01728	.12607	.1189	.00710
ThO_2 blanket												
0	.3289	.06324	.2656	.3542	.2901	.06411	.01242	.00332	.00910	.13277	.1260	.00682
219	.30979	.06035	.24944	.3355	.2742	.06125	.02665	.00697	.01968	.13499	.1273	.00769
803	.29867	.05803	.24064	.3223	.2633	.05897	.02456	.00645	.01820	.12937	.1220	.00735
1387	.2888	.05599	.23282	.3106	.2536	.05707	.02304	.00603	.01701	.12462	.1176	.00705
Th^m blanket												
0	.32808	.06415	.2655	.35005	.2859	.06415	.01230	.00326	.00904	.1316	.1248	.00678
219	.30952	.05984	.24968	.3328	.2714	.0614	.02646	.00689	.01957	.13428	.1266	.00768
803	.30002	.05783	.24220	.3213	.2618	.05956	.02475	.00644	.01831	.1295	.1221	.00743
1387	.2909	.05592	.23498	.31051	.25276	.05775	.02324	.00605	.01719	.1251	.1179	.00717

Radial blanket						Reactor							
A_r^I	C_r^I	F_r^I	A_r^J	C_r^J	F_r^J	A_N^I	A_N^J	F_N^I	F_N^J	F_N^{IJ}	νF_N^I	νF_N^J	k_{eff}
.00217	.00055	.00162	.08108	.07745	.00363	.3398	.5669	.27324	.0738	.34705	.80349	.2145	1.0180
.00805	.00207	.00598	.07823	.07441	.00382	.3414	.5475	.2725	.0719	.3444	.7999	.21079	1.0107
.02316	.00625	.01691	.08542	.07987	.00555	.3457	.5393	.2749	.0716	.3465	.8075	.2070	1.01452
.03683	.00968	.02715	.09128	.08427	.00701	.3494	.5309	.2771	.0710	.3481	.8145	.2058	1.02038
0	0	0	.08135	.08048	.00087	.34139	.56835	.2747	.0718	.3465	.80909	.2088	1.01792
.00641	.00078	.00563	.07753	.07662	.00091	.34284	.5480	.27475	.06985	.3446	.80548	.2022	1.00768
.02585	.00302	.02283	.08609	.08456	.00154	.3492	.53775	.2816	.06785	.3494	.81906	.1966	1.01565
.04281	.00488	.03793	.09214	.08998	.00216	.35465	.5274	.28776	.06628	.35405	.83074	.19186	1.0226
0	0	0	.08312	.08202	.00111	.34037	.56478	.27454	.07204	.34658	.80846	.20946	1.01792
.00507	.00052	.00456	.07901	.07787	.00114	.34105	.54607	.2738	.07022	.3440	.80353	.20357	1.0071
.02115	.00208	.01907	.08664	.08492	.00172	.3459	.53748	.2816	.06871	.3503	.81467	.1993	1.01397
.03635	.00349	.03286	.09292	.0906	.00232	.3505	.52854	.2850	.06724	.3522	.82539	.19513	1.02052

APPENDIX III.A. DETERMINATION OF THE FISSILE FISSION FRACTION DISTRIBUTION (F^i/F^I) IN THE HTR

In order to determine the conversion ratio, Equation (III-5), and the U235 feed demand d_z^{U5}, Equation (III-2), of the HTR, the fissile fission fraction distribution $(F^i/F^I)_z$ for the equilibrium burnup conditions must be known[1]. In the following, analytical equations are derived to show how this distribution was determined, which is normally calculated by means of detailed burnup calculations.

Each of the three fissile fuel cycles of the uranium and thorium cycles has characteristics of its own with regard to the buildup and loss of each fissile isotope, to be accounted for by the analytical equations. In order to derive them, one must therefore consider each fissile fuel cycle separately, since the correlations between the corresponding recycling or nonrecycling fissile fuel cycles among the uranium and thorium cycles are only limited in extent.

---

[1] In the HTR, the fertile fission (fast fission) in the thorium cycle plays an insignificant role. In the following, fission fraction (distribution) is being used interchangeably with fissile fission fraction (distribution).

III.A.1. THE THORIUM CYCLE

In this fuel cycle U233 is bred from Th232. In all three fissile fuel cycles C, B, and A, the major portion of the fissions (98.5%) is due to fissile isotopes U233 and U235; treatment of the small remaining fissile fission fractions ascribed to Pu239 and other isotopes (1.5%) can be neglected within the scope of these investigations.

In the thorium cycle, part of the U235 in the core is not U235 feed but self-bred, obtained by successive neutron capture in U233 and U234. This is especially the case in fissile fuel cycles B and C. The following fission fraction distribution therefore applies to all three fissile fuel cycles.

$$\frac{F^{U3}}{F^{I}} + \frac{F_t^{U5}}{F^{I}} = \frac{F^{U3}}{F^{I}} + \frac{F_b^{U5}}{F^{I}} + \frac{F_m^{U5}}{F^{I}} = 1.0 \quad , \qquad \text{(III.A-1)}$$

F_I is the total fission usually normalized to unity. F_t^{U5} represents the sum of F_b^{U5} and F_m^{U5}; F_m^{U5} represents the fissions in the U235 makeup or feed designated by subscript m, and F_b^{U5} the fissions in the self-bred U235, designated by subscript b.

The U233 fission fraction (F^{U3}/F^{I}) in the equilibrium burnup condition can be given as follows:

$$\frac{F^{U3}}{F^{I}} = \frac{F^{U3}}{F^{U3} + F_t^{U5}} = \left\{ 1 + \frac{\sigma_f^{U5} N_t^{U5}}{\sigma_f^{U3} N^{U3}} \right\}^{-1} \quad ; \qquad \text{(III.A-2)}$$

σ_f is the HTR spectrum- and flux-weighted one-group fission cross sections and N the particle densities. When determining the particle densitiy ratio N_t^{U5}/N^{U3}, a distinction must be made between the differing fissile feeds of fissile fuel cycles B, C, and A.

III.A.1.a. Fissile Fuel Cycles B and C

For the burnup equilibrium condition, the particle density ratio N_t^{U5}/N^{U3} of fissile fuel cycles B and C can be determined with the help of the definition of the conversion ratio for U233 and the equation governing the buildup of U233, such that

$$CR^{U3} = \frac{C^{Th2}}{A^{U3} + A^{U5}} = \frac{\sum_c^{Th2}}{\sum_a^{U3} + \sum_a^{U5}} \quad , \qquad \text{(III.A-3)}$$

c is the capture rates, and a represents the absorption rates; and $\sum_x^i = \sigma_x^i \cdot N^i$. The U233 buildup can be given by

$$N^3(t) = \frac{\sum_c^{Th2}}{\sigma_a^{U3}} \left\{1 - \exp(-\sigma_a^{U3}\phi t)\right\} \quad . \qquad \text{(III.A-4)}$$

ϕ is the one-group neutron flux, and t the fuel residence time. If γ_z is defined by $(1 - \exp(-\sigma_a^{U3}\phi t)$ and Equation (III.A-4) solved for $\sum_c^{Th2}$, then the particle ratio N_t^{U5}/N^{U3} can be determined by means of Equation (III.A-3). If the ratio is introduced in Equation (III.A-2), the U233 fission fraction can be written as follows:

$$\frac{F^{U3}}{F^I} = \left\{1 + \frac{(1+\alpha)^{U3}}{(1+\alpha)^{U5}} \left(\frac{1}{\gamma_z CR^{U3}} - 1\right)\right\}^{-1} \quad . \qquad \text{(III.A-5)}$$

$\alpha = \sigma_c/\sigma_f$. With (F^{U3}/F^I) known, (F_t^{U5}/F^I) can be determined by Equation (III.A-1).

The self-bred U235 fission fraction (F_b^{U5}/F^I) can be determined as follows: if the concentrations of U233 and U235 are in equilibrium, $\sum_c^{U3} = (\sum_a^{U5})_b$, or $N_b^5/N^3 = \sigma_c^3/\sigma_a^5$. Then

$$\frac{F^{U3}}{F^{U3} + F_b^{U5}} = \left\{1 + \frac{\alpha^{U3}}{(1+\alpha)^{U5}}\right\}^{-1} \quad , \qquad \text{(III.A-6)}$$

so that

$$\frac{F_b^{U5}}{F^I} = \frac{\alpha^{U3}}{(1+\alpha)^{U5}} \left[\left(\frac{F^{U3}}{F^I}\right)\right] \quad , \qquad \text{(III.A-7)}$$

where (F^{U3}/F^I) is given by Equation (III.A-5). By means of Equation (III.A-1), one can then determine the fission fraction of the U235 feed (F_m^{U5}/F^I).

Determination of the fission fractions (F^i/F^I) requires knowledge of CR^{U3}, γ_z, and $(1+\alpha)^i$. For fissile fuel cycle C, in which the isotopic concentration of U233 and self-bred U235 are not in equilibrium, γ_C depends on the fuel burnup, on account of factor ϕt in Equation (III.A-4). (This also applies to fissile fuel cycle D.)

For all recycling fissile fuel cycles A, B, E, and F, $\gamma_z = 1.0$, since it can be assumed that $t \to \infty$. For the nonrecycle fissile fuel cycles C and D, $\gamma_z \neq 1.0$ since t is finite. The burnup dependence of γ_C and γ_D is shown in Figure III.A.1. (The burnup calculations from Teuchert et al. (1974, 1972) and Schulten et al. (1977) have been used to determine these curves.) $(1+\alpha)^i$ are given in Table III.4 for the corresponding fissile fuel cycles.

The relations between CR^{U3} and CR can be given by

$$CR_z^{U3} = k_z \cdot CR_z \quad , \qquad \text{(III.A-8)}$$

where the term $k_z \leq 1.0$. k_z depends on the neutron captures in U234 or Pu240 in the uranium cycle. Table III.A.1 lists representative k_z values for the various fissile fuel cycles and burnup conditions. Some of these values could be determined from the burnup calculations available.

Table III.A.1. $k_z = CR_z^i/CR_z$ (i = U233, Pu239) for various HTR fissile fuel cycles as a function of fuel burnup.

Fissile fuel cycle (z)	Fuel burnup (GWd/t)		
	100	50	30
A	0.90	0.90	0.90
B	0.85	0.85	0.85
C	0.92	0.95	0.97
D	0.86	0.89	0.93
E	0.85	0.85	0.85
F	0.92	0.92	0.92

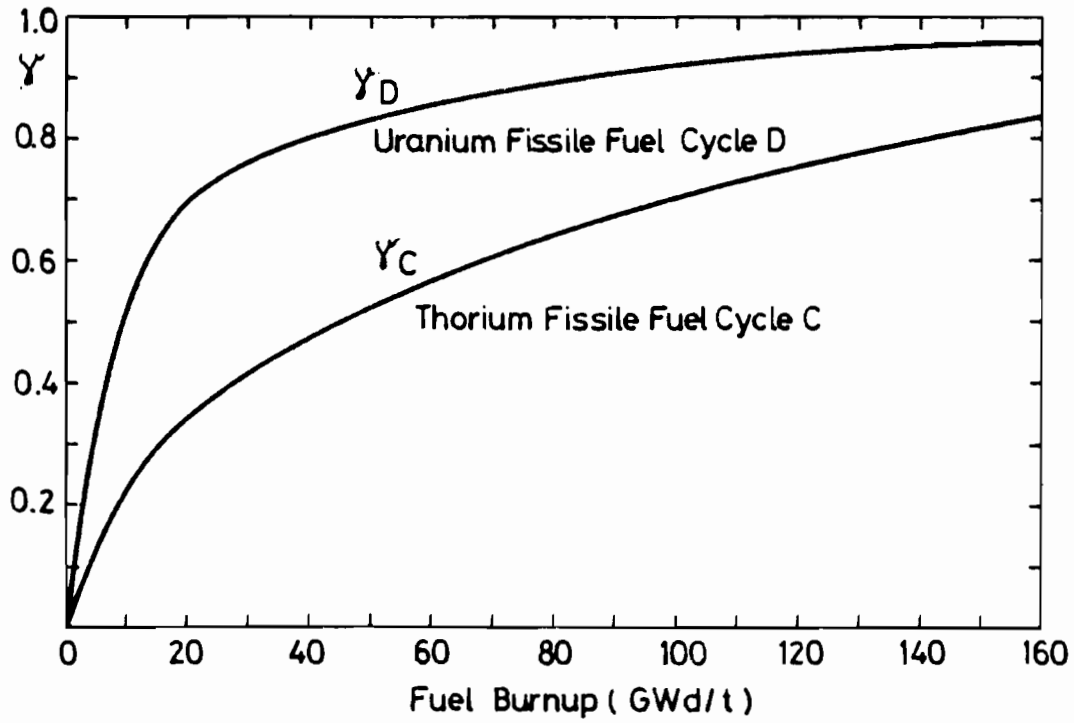

Figure III.A.1. Factor $\gamma_z = (1 - e^{-\sigma_a^i \phi t})$ as a function of fuel burnup for HTR fissile fuel cycles C (i = Pu239) and D (i = U233).

III.A.1.b. The Iterative Method

By coupling CR^{U3} with CR, the fission fractions given by the above equations and thus also CR, Equation (III-5), can be determined for fissile fuel cycles B and C by the following iterative method.

1. The initial values selected are burnup- and reactor-size-specific value P from Table III.3 and an $\eta^{I}_{l=0}$ value of the number of neutrons released per fissile absorption from Table III.4. The estimated $\eta^{I}_{l=0}$ should be selected, for example, to lie between η^{U5} and η^{U3} for fissile fuel cycles B and C, i.e. at approximately $\eta^{I}_{l=0} \approx 2.0$. P is fixed throughout the entire iteration.
2. Fissile fuel cycle-specific $(1 + \alpha)^{i}$ and isotope-specific ν^{i} values are taken from Table III.4.
3. One then evaluates an initial $CR_{l=0}$ (l is the iteration step) by using Equation (III-5).
4. $CR^{U3}_{l=0}$ is determined on the basis of the appropriate k_z value in Table III.A.1 and Equation (III.A-8).
5. For fissile fuel cycle C, γ_C is taken from Figure III.A.1; for fissile fuel cycle B, $\gamma_B = 1.0$.
6. The fission fractions $(F^{U3}/F^{I})_{l=0}$ and $(F^{U5}_{t}/F^{I})_{l=0}$ can be determined by Equations (III.A-5) and (III.A-1).
7. With these fission fractions available, one can evaluate a $\nu^{I}_{l=0}$ value and a $(1 + \alpha)^{I}_{l=0}$ value, in order to determine an iterated $\eta^{I}_{l=1}$ by way of Equation (III-6).
8. With $\eta^{I}_{l=1}$ available, an iterated $CR_{l=1}$ can be determined, Equation (III-5), in order to evaluate an iterated $CR^{U3}_{l=1}$.

Steps (4) to (8) are iterated to convergence of $CR_{l=n}$. It can be shown to be reached very rapidly, i.e. after three or four steps.

9. With $CR_{l=n}$ converged, the U235 feed fission fraction $(F^{U5}_{m}/F^{I})_{l=n}$ can be calculated with the help of Equations (III.A-7) and (III.A-1). On this basis one can determine U235 demand d^{U5}_{z}, Equation (III-2), net fissile fuel demand d_z, Equation (III-1), and the self-bred fissile fuel discharged a^{i}_{z}, Equation (III-4).

The following example illustrates how to use this method.

III.A.1.c. Example of How to Determine CR_B and d_B^{U5}

A numerical example for fissile fuel cycle B serves to exemplify application of the iterative method. In cycle B, the self-bred U233 is recycled several times, i.e. $\sigma_a^{U3}\phi t \to \infty$ in Equation (III.A-4) and $\gamma_B = 1.0$. k_B is given as 0.85 in Table III.A.1 for burnup A ≃ 100 GWd/t.

For this fissile fuel cycle, the $(1 + \alpha)^i$ values for U233 and U235 are taken from Table III.4. The initial values chosen are $\eta^I_{l=0} = 2.0$ and P = 0.24 (burnup = 100, reactor size = 1 GW(th)). Thus

$$CR_{l=0} = 2.0(1 - 0.24) - 1 = 0.52 \quad ,$$

and

$$CR^{U3}_{l=0} = 0.85 \cdot CR_{l=0} = 0.44 \quad .$$

Fission fraction (F^{U3}/F^I) then is

$$\frac{F^{U3}}{F^I} = \left\{1 + \frac{1.104}{1.248}\,\frac{(1 - 0.44)}{0.44}\right\}^{-1} = 0.470 \quad ,$$

and

$$\frac{F^{U5}_t}{F^I} = 1 - 0.470 = 0.530 \quad .$$

Thus one obtains

$$\nu^I_{l=0} = (2.50)(0.470) + (2.43)(0.530) = 2.463$$

and

$$(1 + \alpha)^I_{l=0} = (1.107)(0.470) + (1.248)(0.530) = 1.182 \quad ,$$

which leads to $\eta^I_{l=1} = 2.084$. By further iteration

Table III.A.2. Comparison of conversion ratios CR, $(1 + \alpha)^i$, and fission fractions F^i/F^I obtained with the iterative method, with results from exact burnup caclulations (B-1, Table III.2, and case b3, Table III.B.2).

	Iteration step l	η_l^I	CR_l	CR_l^{U3}	$(F^{U3}/F^I)_l$	$(F_t^{U5}/F^I)_l$	ν_l^I	$(1+\alpha)_l^I$
b3	0	2.0	0.52	0.44	0.470	0.530	2.463	1.182
	1	2.084	0.584	0.496	0.526	0.474	2.467	1.174
	2	2.102	0.597	0.508	0.537	0.462	2.465	1.171
	3	2.105	0.599	0.510	0.539	0.461	2.468	1.172
	4	2.106	0.600	0.510	0.540	0.460	2.468	1.172
	5	2.106	0.600	0.510	0.540	0.460	2.468	1.172
B-1		2.109	0.598	0.515	0.546	0.443	2.468	1.171

$$CR_{l=1} = 2.084(1-0.24) - 1.0 = 0.584,$$

and

$$CR_{l=1}^{U3} = 0.496 \quad .$$

Table III.A.2 gives the values obtained by further iteration and compares the converged values with the results of detailed burnup calculations.

Very good agreement is shown by comparison between the iteratively determined values for l = 4, and the exact results from burnup calculations, case B-1, Table III.2, and case b3, Table III.B.2[2]. If the small fission fractions (1.5%) of isotopes not included by the analytical method are assumed to be 0.015 on an average, for all cycles considered, and deducted from the U235 fission fraction determined by iteration, one obtains $F_t^{U5}/F^I = 0.445$, which agrees very well with the exact value of 0.443. If $F_b^{U5}/F^I = 0.046$, Equation (III.A-7), is deducted from

[2] e.g. cases A-1, A-2, etc. represent burnup calculations for fissile fuel cycles, e.g. cases a1, a2, etc. in these tables refer to the numerical calculations performed here.

0.445, F_m^{U5}/F^I is 0.399. The U235 makeup in kg/GW(th)d can then be determined by Equation (III-2), such that

$$d_B^{U5} = 1.248 \times 0.399 \times 1.053 = 0.524 \quad .$$

This agrees quite well with the value for U235 of 504 g/GW(th)d obtained from the burnup calculations (B-1). In this fissile fuel cycle, the self-bred fissile fuel unloaded is recycled into the reactor; thus $a_B^{U3} = 0$.

III.A.1.d. Fissile Fuel Cycle A

Only U233 is supplied as makeup in fissile fuel cycle A. The U235 fissile fraction therefore only consists of self-bred U235. It is given as

$$\frac{F_b^{U5}}{F^I} = \frac{F_b^{U5}}{F^{U3} + F_b^{U5}} = 1 - \left\{1 + \frac{\alpha^{U3}}{(1 + \alpha)^{U5}}\right\}^{-1} \quad , \qquad \text{(III.A-9)}$$

on the basis of Equation (III.A-6). In cycle A, the distribution of the U233 and U235 fissile fission fractions for different burn-up conditions remains constant with $F_b^{U5}/F^I = 0.088$ and $F^{U3}/F^I = 0.912$ for the $(1 + \alpha)^i$ values in Table III.4. Due to the structure of the determining equation system, no iteration is necessary for this cycle. The U233 makeup is determined by Equation (III-1), such that

$$d_A^{U3} = (1 + \alpha)_A^I (1 - CR_A) W_H^{U3} \quad , \qquad \text{(III.A-10)}$$

with $(1 + \alpha)_A^I \simeq (1 + \alpha)_A^{U3}$ given.

III.A.2. THE URANIUM CYCLE

In a discussion of the fissile fuel cycles of the uranium cycle, the self-bred fissile isotope Pu241 must be considered explicitely.

III.A.2.a. Fissile Fuel Cycles D and E

Similarly as for fissile fuel cycles B and C, the following relations can be derived for D and E:

$$\mu \equiv \frac{F^{Pu9}}{F^{Pu9} + F_t^{U5}} = \left\{ 1 + \frac{(1+\alpha)^{Pu9}}{(1+\alpha)^{U5}} \left(\frac{1}{\gamma_z CR_z^{Pu9}} - 1 \right) \right\}^{-1} \quad \text{(III.A-11)}$$

and

$$q \equiv \frac{F^{Pu41}}{F^{Pu9} + F^{Pu41}} = \left\{ 1 + \frac{(1+\alpha)^{Pu41}}{\alpha^{Pu9}} \right\}^{-1} , \quad \text{(III.A-12)}$$

where Equation (III.A-12) assumes Pu241 equilibrium concentration that only applies to the recycle fissile fuel cycles E and F. For cycle D, Pu241 is not in equilibrium for burnups below 120 GWd/t, and Figure III.A.2 plots q as a function of fuel burnup.

Given the above equations, the following fissile fission fractions can be written:

$$\frac{F^{Pu9}}{F^I} = \left\{ \left(\frac{q}{1-q} \right) + \frac{1}{u} \right\}^{-1} , \quad \text{(III.A-13)}$$

$$\frac{F^{Pu41}}{F^I} = \left\{ 1 + \left(\frac{1-q}{q} \right) \frac{1}{u} \right\}^{-1} , \quad \text{(III.A-14)}$$

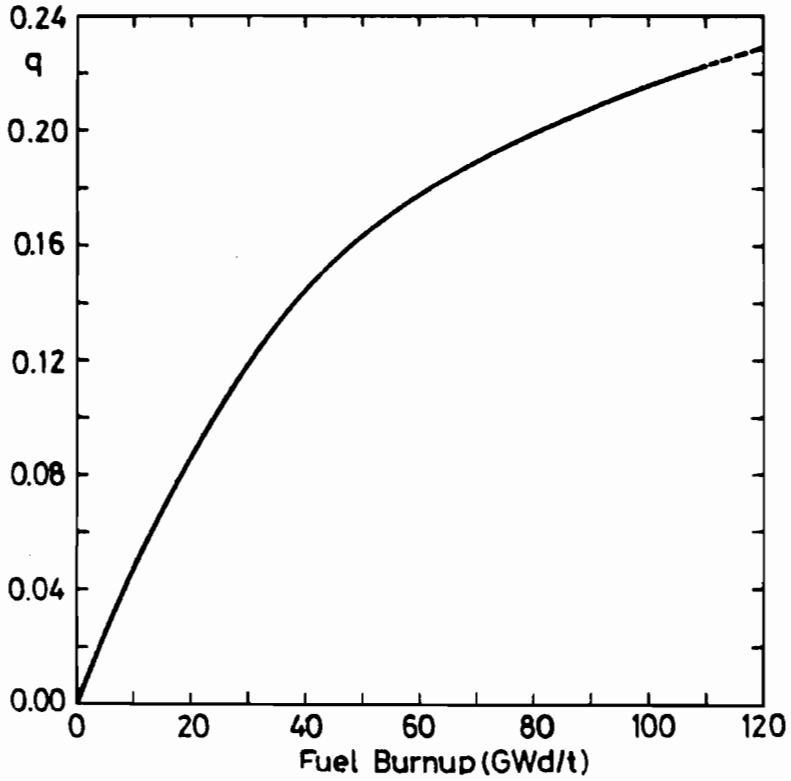

Figure III.A.2. $q = \frac{F^{Pu41}}{F^{Pu9} + F^{Pu41}}$ as a function of fuel burnup for HTR fissile fuel cycle D (data from Teuchert 1972).

and, in the case of the uranium cycle,

$$\frac{F_m^{U5}}{F^I} = \frac{F_t^{U5}}{F^I} = 1 - \frac{F^{Pu9}}{F^I} - \frac{F^{Pu41}}{F^I} \quad . \qquad \text{(III.A-15)}$$

In order to determine the fissile fission fractions, it is necessary to apply the iterative method with the corresponding values of k_z (Table III.A.1) and γ_z (Figure III.A.1), as was done for fissile fuel cycles B and C in the thorium cycle. For fissile fuel cycle E, $\gamma_E = 1.0$; for fissile fuel cycle D, γ_D is given in Figure III.A.1.

III.A.2.b. Fissile Fuel Cycle F

In this cycle, only Pu239 and Pu241 are available as fissile isotopes. Their respective concentrations are in equilibrium, and the Pu241 fissile fraction is given by Equation (III.A-12).

This yields $F^{Pu41}/F^{I} = 0.295$ and $F^{Pu9}/F^{I} = 0.705$ for the $(1 + \alpha)^{i}$ values in Table III.4. Like in cycle A, this distribution remains constant for all burnup conditions. (The iterative method need not be applied.) Pu makeup is given by Equation (III-1).

APPENDIX III.B. ANALYSIS OF FISSILE FUEL UTILIZATION IN FISSILE FUEL CYCLES A TO F

The results of the calculations on HTR fissile fuel utilization are described here for each fissile fuel cycle listed in Table III.1. The calculations are based on an HTR design of 3 GW(th), with the burnup-dependent loss fractions P given in Table III.3. The ν^i and fissile fuel cycle-specific $(1 + \alpha)^i$ values are given in Table III.4.

In order to verify the methodology of the iterative method described in Appendix III.A, the author reconstructed the exact results of the burnup calculations with the help of the iterative method, taking the exact P values from the burnup calculations (Table III.2) and the $(1 + \alpha)^i$ values from Table III.4. These comparisons are given in Tables III.B.1 to III.B.4.

As was discussed in Section III.3, the conversion ratio CR_Z can be described by two parameters that are largely independent of one another: the loss fraction P and the fissile isotope composition-dependent η_Z^I. While P is almost completely independent of η_Z^I, the latter is not completely independent of P. The dependence of P on η_Z^I is briefly discussed here.

In the case of low burnups, P is almost equally reduced for all fissile fuel cycles. On the other hand, η_Z^I is primarily determined by the fissile fuel cycle-dependent fissile isotopic

composition, as is reflected by the fissile fission fraction distribution. However, since this distribution depends on CR_z, Equations (III.A-5) and (III.A-11), which in turn depends on P by Equation (III-5), the fissile fraction distribution exhibits a moderate P dependence. Thus, η_z^I slightly changes with P. This is true for fissile fuel cycles B, C, D, and F. Fissile fuel cycles A and F are not influenced in this way.

This effect is observed to be largest in the nonrecycle fissile fuel cycles C and D, where the isotopic composition of the self-bred fissile isotopes U233/U235 and Pu239/Pu241 is not in equilibrium for burnups below 120 GWd/t. The effect is smaller in the recycle fissile fuel cycles B and E, where the bred fissile isotopes are in equilibrium concentration. Accordingly, the burnup dependence of CR is reflected to a large extent by P and to a lesser extent by η^I, the former having most and the latter much less influence.

III.B.1. THE THORIUM CYCLE

A significant difference in η_z^I must be expected between the recycling fissile fuel cycles A and B and the nonrecycling cycle C, since the η^{U3} of the self-bred fissile isotope is much larger than the η^{U5} of the fissile isotope supplied.

III.B.1.a. Fissile Fuel Cycle A

In this *recycling* thorium cycle

-- the self-bred U233 is recycled, and
-- the fissile fuel supplied is U233.

In fissile fuel cycle A, the HTR fissile inventory consists of U233 and a small fraction of self-bred U235. The isotopic composition of these isotopes is in equilibrium, so that the equilibrium fission fraction distribution is given by Equation (III.A-9). With the $(1 + \alpha)^i$ values from Table III.4, this yields F^{U3}/F^I = 0.912, i.e. approximately 9% of the fissions are due to the self-bred U235.

The iterative method need not be applied with this fissile fuel cycle. Accordingly, η_A^I is independent of P, and the burnup dependence of CR_A is solely due to P. As is the case in fissile fuel cycles B and C, the P values are taken from Table III.3 for the results of cases a1, a2, a3, and a5 listed in Table III.B.1, and the $(1 + \alpha)^i$ values are taken from Table III.4.

In the cases of (a4, a5), (a6, a7) and (a8, a9), the results of the exact burnup calculations, referred to in Table III.B.1 in the nomenclature adopted in Table III.2, are compared to the results of the iterative method. As has been noted, good agreement is found for all the parameters. Reference cases A-1 and A-2 are listed separately because they do not correspond to realistic fuel cycles. In cases A-1 and A-2, the U233 fission fraction is 99%, constituting an almost pure U233 inventory. This does not correspond to the equilibrium concentration of fissile isotopes U233 and U235.

Table III.B.1. Conversion ratio CR_A, U233 requirement d_A^{U3}, and other parameters of HTR fissile fuel cycle A, as a function of fuel burnup and reactor size (for 3- and 1-GW(th) units).

Case	Burnup (GWd/t)	P 3GW(th)	P 1GW(th)	Reference*	CR_A	η_A^I	$(1+\alpha)_A^I$	$\frac{F^{U3}}{F^I}$	d_A^{U3} (g/GWd)
Burnup ≃ 100									
a1		.20		analyt.	.75	2.187	1.140	.912	300
Burnup ≃ 50									
a2		.15		analyt.	.86	2.187	1.140	.912	168
Burnup ≃ 30									
a3		.12		analyt.	.925	2.187	1.140	.912	90
a4	24	.104		A-3*	.97	2.207	1.131	.928	41
a5		.104		analyt.	.968	2.187	1.140	.912	38
Burnup ≃ 30									
a6**	28		.145	A-2*	.902	2.228	1.122	.990	171
a7**			.145	analyt.	.896	2.218	1.127	.99	122
a8**	36	.123		A-1*	.947	2.225	1.123	.987	85
a9**		.123		analyt.	.945	2.218	1.127	.99	65

*A-1, A-2, and A-3 are exact burnup calculations (for references see Table III.2); all other cases are results of the analytical calculations performed here.

**Cases a6 to a9, where U233/U235 is not in equilibrium (F^{U3}/F^I is too high), are not representative; they serve comparative purposes.

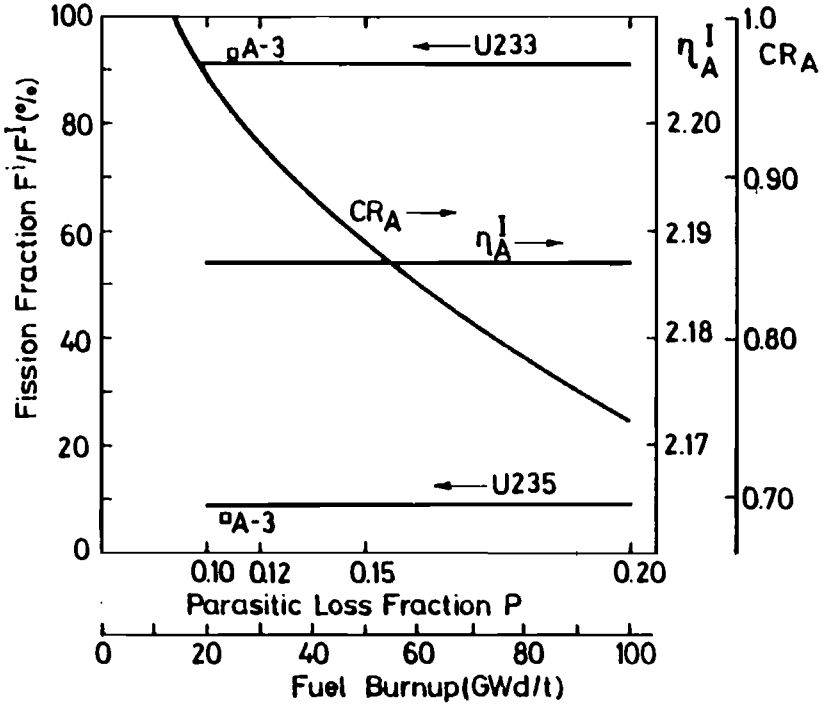

Figure III.B.1.

Fission fractions, eta, and conversion ratio for HTR fissile fuel cycle A as a function of fuel burnup (for 3-GW(th) units).

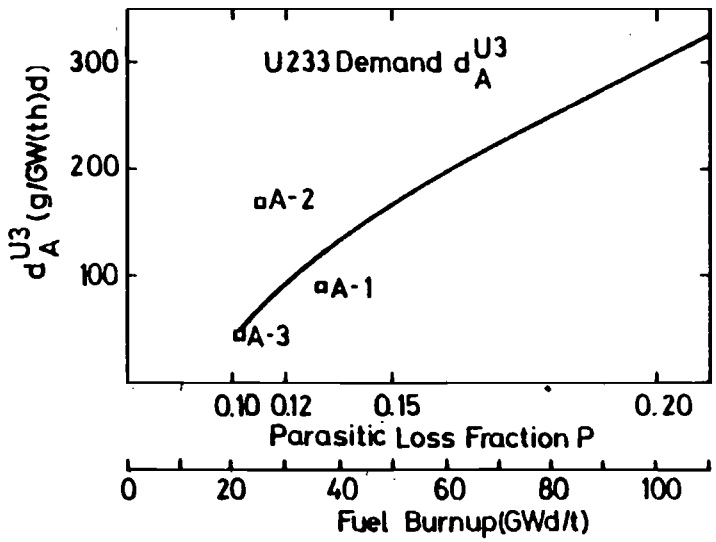

Figure III.B.2.

U233 makeup d_A^{U3} for HTR fissile fuel cycle A as a function of fuel burnup (for 3-GW(th) units).

Figure III.B.1 illustrates the burnup dependence of CR_A, η_A^I, and the fission fractions. In this cycle, the increasing CR_A is only due to the reduction in P. Fissile fuel cycle A attains the highest conversion ratios among all fissile fuel cycles, due to the high η_A^{U3} = 2.22 and the very high U233 fission fraction. CR_A lies between 0.75 for high burnups (A ≈ 100 GWd/t) and 0.97 for very low burnups (A ≈ 20). At this point, therefore, it should again be stressed that the HTR can attain high conversion ratios under the following conditions only:

-- Th232 is used as fertile material,
-- the self-bred U233 is recycled, which implies the need for thorium reprocessing facilities,
-- the makeup consists of U233 coming from an external source, e.g. FBR,
-- the burnup is very low, so that FP and R and thus P are kept small (A ≈ 20-30 GWd/t).
-- HTR units are large, so that L and thus P are kept small (~3 GW(th)).

For a high CR to be attained, the loss fraction P must not become much larger than 0.10-0.11. This calls for an extremely careful neutron utilization.

Figure III.B.2 shows the U233 makeup d_A^{U3} as a function of fuel burnup. To be mentioned here is the very low U233 requirement at low burnups in comparison to the fissile fuel demand of all the remaining fissile fuel cycles.

III.B.1.b. Fissile Fuel Cycle B

In this *recycling* thorium cycle

-- the self-bred U233 is recycled, and
-- the fissile fuel supplied is U235.

The U233 concentration is in equilibrium for all fuel burnup conditions due to constant recycling. Factor $\gamma_B = \{1 - \exp(-\sigma_a^{U3}\phi t)\} = 1.0$ since $t \to \infty$, Equation (III.A-4).

As in fissile fuel cycle C, the iterative method is applied. The results are listed in Table III.B.2. Cases b1, b5, and b6 are evaluated by means of the P values in Table III.5 for a 3-GW(th) unit and the $(1 + \alpha)^i$ and ν^i values listed in Table III.4.

Cases b2 and b3 are used for checking the iterative method. As in cycles A and C, good agreement is found between the analytical and the exact results for all the essential parameters. The P values assumed were those of the burnup calculations, and $(1 + \alpha)^i$ and ν^i are given in Table III.4.

Figure III.B.3 plots the burnup dependence of CR_B and fission fractions for a 3-GW(th) unit. In contrast to the non-recycling cycle C, the U233 fission fraction rises with decreasing burnups. Since $\eta^{U3} > \eta^{U5}$, this leads to higher values of η_B^I.

In fissile fuel cycle B, the increase in the conversion ratio in the case of low burnups is due to the increase in η_B^I and the reduction in P. The conversion ratio for cycle B is between 0.71 for high burnups (A ≃ 100 GWd/t), and up to 0.9 for very low burnups (A < 20).

Figure III.B.4 shows the U235 makeup d_B^{U5}. The results of the exact burnup calculations for B-1 and B-2 are larger than the analytical results, since B-1 and B-2 were calculated for a 1-GW(th) and not for a 3-GW(th) unit.

Table III.B.2. Conversion ratio CR_B, U235 requirement d_B^{U5}, and other parameters of HTR fissile fuel cyle B, as a function of fuel burnup and reactor size (for 3- and 1-GW(th) units).

Case	Burnup (GWd/t)	P 3GW(th)	P 1GW(th)	Reference*	CR_B	η_B^I	$(1+\alpha)_B^I$	$\frac{F^{U3}}{F^I}$	$\frac{F_m^{U5}}{F^I}$	d_B^{U5} (g/GWd)
Burnup ≃ 100										
b1		.20		analyt.	0.71	2.138	1.157	.633	.298	390
b2			.24	analyt.	0.600	2.106	1.172	.540	.398	521
b3**	113		.2422	B-1*	0.598	2.109	1.170	.546		503
b4	91		.224	B-2*	0.636	2.108	1.172	.592		460
Burnup ≃ 50										
b5***		.15		analyt.	0.79	2.108	1.176	.703	.213	290
Burnup ≃ 30										
b6***		.12		analyt.	0.88	2.133	1.164	.771	.139	182

*B-1 and B-2 are exact burnup calculations (for references see Table III.2); all other cases are results of the analytical calculations performed here.
**Example from Table III.A.2 in Appendix III.A.
***Because of the high U233 fission fraction, the $(1+\alpha)^i$ values of cycle A in Table III.4 were used for these burnups.

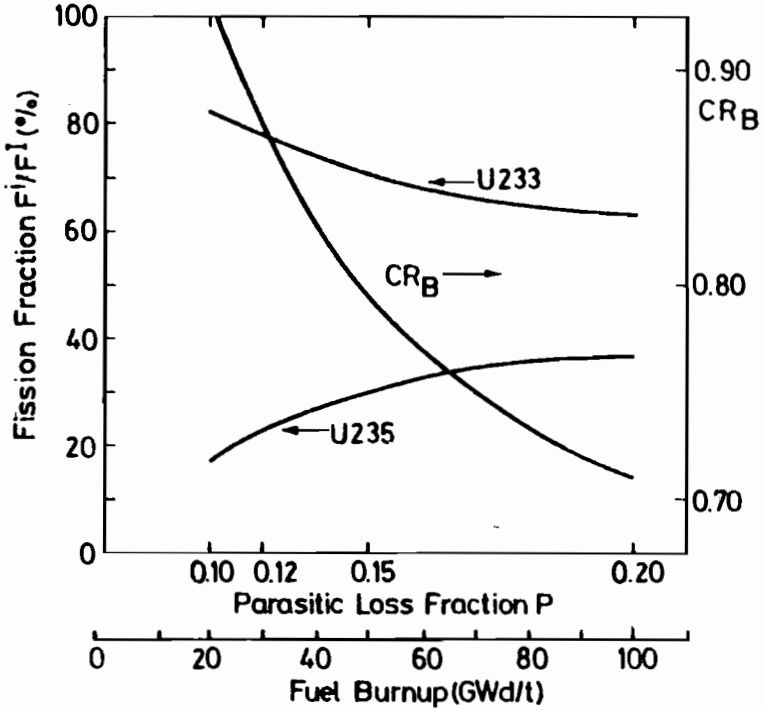

Figure III.B.3.

Fission fractions and conversion ratio for HTR fissile fuel cycle B as a function of fuel burnup (for 3-GW(th) units).

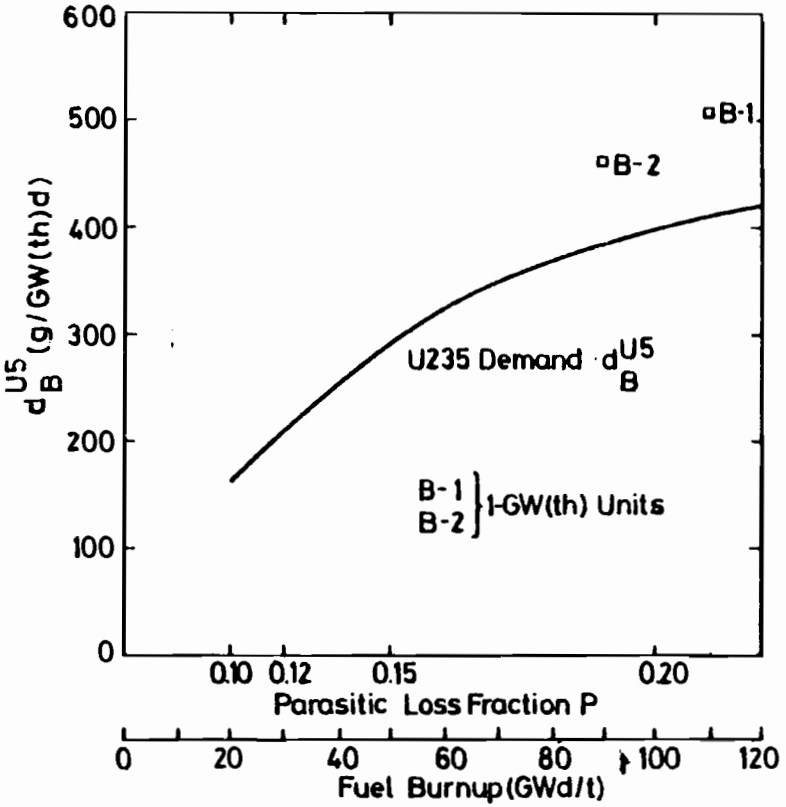

Figure III.B.4.

U235 makeup d_B^{U5} for HTR fissile fuel cycle B as a function of fuel burnup (for 3-GW(th) units).

III.B.1.c. Fissile Fuel Cycle C

In the *nonrecycling* thorium cycle

-- the self-bred U233 is *not* recycled, and

-- the fissile fuel supplied is U235.

Of all the fissile fuel cycles, cycle C (as well as uranium cycle D) is the most difficult to simulate by analytical methods. In this cycle, the U233 concentration and thus also the U233 fission fraction is not in equilibrium for burnups of less than 150 GWd/t, i.e. $\gamma_C = (1 = e^{-\sigma_a^{U3}\phi t}) \leq 1.0$ in Equation (III.A-4). $\sigma_a^{U3}\phi t$, a function of fuel burnup, can only be determined indirectly because of the asymmetrical neutron flux distribution ϕ in the HTR. By using the burnup calculations available, it was possible to determine a correlation between $\sigma_a^{U3}\phi t$ and fuel burnup. The corresponding γ_C is reproduced in Figure III.A.1.

Cases c1, c6, c7, and c10 in Table III.B.3 were determined by using the P values given in Table III.3 for a 3-GW(th) HTR unit and the $(1 + \alpha)^i$ and ν^i values suggested in Table III.4.

Cases (c2, c3), (c4, c5), (c8, c9) were used for checking the iterative method. A comparison of these results and the results from the exact burnup calculations (Table III.2, P values from burnup calculations, $(1 + \alpha)^i$ and ν^i from Table III.4) shows very good agreement for all parameters.

Figure III.B.5 illustrates the burnup dependence of η_C^I, the fission fractions, and conversion ratio CR_C for a 3-GW(th) unit. In the case of fissile fuel cycle C, the decrease in η_C^I for low burnups is due to the decrease in the U233 fission fraction. The increase in CR thus only depends on the reduction of P. The conversion ratio lies between 0.66 for high burnups (A ≈ 100 GWd/t) and 0.80 for low burnups (A ≈ 30 GWd/t).

Figure III.B.6 shows the fissile fuel flow of the U235 demand d_C^{U5} and the discharged U233 a_C^{U3} as functions of burnup for a 3-GW(th) unit. A rising U235 demand is to be expected, due to the increase in the U235 fission fraction in the case of low burnups. On the other hand, more U233 is produced. However, the

net fissile fuel demand d_C, Equation (III-1), is lower in the case of low burnups.

Figure III.B.6 also shows results from the exact burnup calculations. C-2 and C-3 are results for 1-GW(th) units and thus not directly comparable with the analytically determined results for 3 GW(th). The U235 requirement is therefore distinctly higher for those units; note, however, the agreement of their U233 outputs with the analytical results for the 3-GW(th) unit. This appears to indicate that the U233 output is independent of reactor size; the difference between 1- and 3-GW(th) units appears to be expressed by the U235 makeup d_C^{U5}.

Fissile fuel cycle C is of interest only in the absence of thorium reprocessing facilities. Unloaded fuel elements with U233 content are stored. Because of the larger U235 requirement for low burnups (despite the better net fissile fuel demand d_C), it is less desirable to reduce the burnup in this cycle.

Table III.B.3. Conversion ratio CR_C, U235 requirement d_C^{U5}, discharged U233 a_C^{U3}, and other parameters of HTR fissile fuel cycle C, as a function of fuel burnup and reactor size (for 3- and 1-GW(th) units).

Case	Burnup (GWd/t)	P 3GW(th)	P 1GW(th)	Reference†	CR_C	η_C^I	$(1+\alpha)_C^I$	$\frac{F^{U3}}{F^I}$	$\frac{F_m^{U5}}{F^I}$	d_C^{U5} (g/GWd)	a_C^{U3} (g/GWd)
Burnup ≃ 100											
c1		.20		analyt.	.664	2.080	1.183	.457	.488	640	198
c2	110		.2556	C-2*	.540	2.069	1.192	.390		750	162
c3			.2556	analyt.	.532	2.058	1.194	.385	.566	742	155
c4**	106	.229		C-1*	.592	2.065	1.190	.415		723	195
c5		.229		analyt.	.594	2.069	1.189	.420	.547	718	211
Burnup ≃ 50											
c6		.15		analyt.	.755	2.065	1.190	.409	.540	707	401
Burnup ≃ 20-30											
c7		.12		analyt.	.803	2.049	1.198	.354	.601	788	540
c8***	23	.1515		C-5*	.739	2.053	1.193	.299		896	564
c9		.1515		analyt.	.738	2.048	1.196	.289	.674	874	545
c10		.10		analyt.	.830	2.033	1.205	.302	.657	861	646

*C-2, C-1, and C-5 are exact burnup calculations (for references see Table III.2); all other cases are results of the analytical calculations performed here.
**The HTR unit size of C-1 is 2.7 GW(th).
***Case c8 is listed here although P corresponds to the losses of burnup ≃50 GWd/t. This high P value is due to the mixture of fuel pebbles with extremely different burnups.

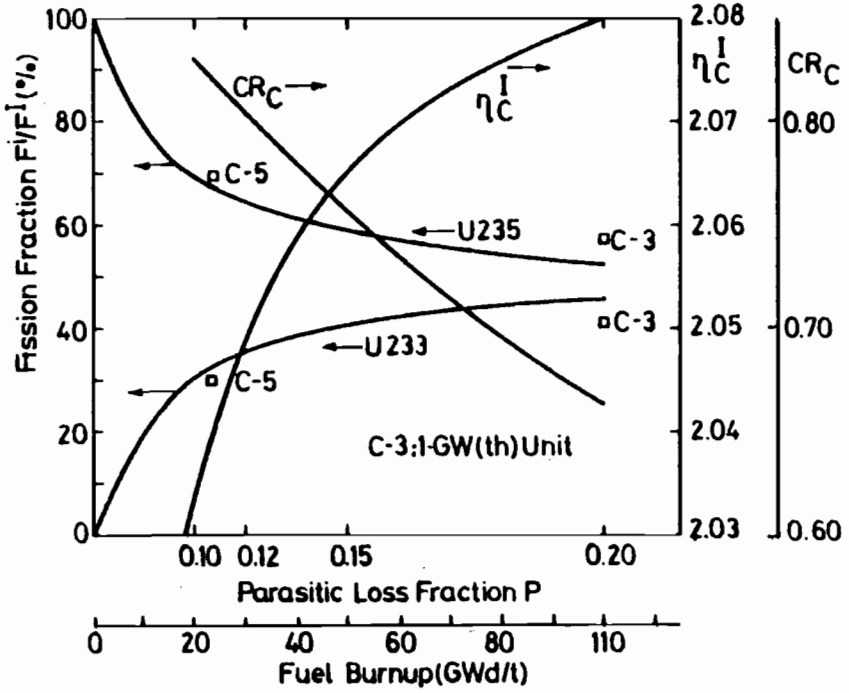

Figure III.B.5.

Fission fractions, eta, and conversion ratio for HTR fissile fuel cycle C as a function of fuel burnup (for 3-GW(th) units).

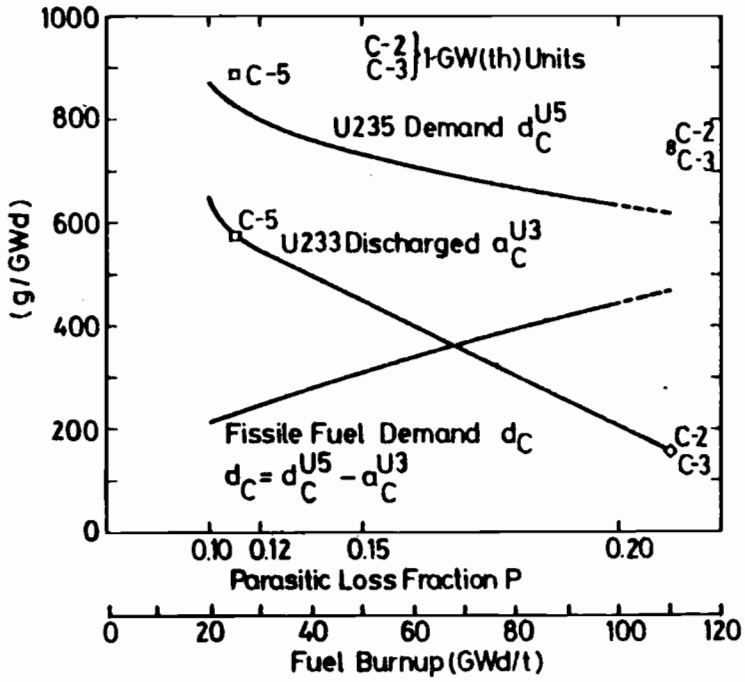

Figure III.B.6.

U235 makeup, U233 discharged, and fissile fuel demand for HTR fissile fuel cycle C as a function of fuel burnup (for 3-GW(th) units).

III.B.2. THE URANIUM CYCLE

The conversion ratio in the uranium cycle is primarily determined by the $(1 + \alpha)^i$ values of fissile isotopes Pu239 and Pu241. These values are not known with the same reliability as the corresponding values in the thorium cycle. The following results should therefore be seen only as indicative of the fuel utilization in the uranium cycle.

III.B.2.a. Fissile Fuel Cycle D

In the *nonrecycling* uranium cycle

-- the self-bred Pu239/Pu241 is not recycled, and
-- the fissile fuel supplied is U235.

Since the self-bred fissile isotopes Pu239 and Pu241 are not recycled, their isotopic compositions are not in equilibrium in the case of low burnups, i.e. $\gamma_D < 1.0$. The dependence of γ_D on the burnup is plotted in Figure III.A.1. The difference between γ_C (thorium cycle) and γ_D (uranium cycle) can be explained by the larger Pu239 thermal absorption cross section σ_a^{Pu9} = 1200 barns in contrast to U233, where σ_a^{U3} = 270 barns. This implies that Pu239 attains equilibrium concentration faster than U233.

Table III.B.4 lists comparative calculations with respect to the exact burnup calculations available for cases d1 and d3. Good agreement was obtained between the analytical and the exact results if the $(1 + \alpha)_D^i$ values were taken directly from the burnup calculations for D-1 and D-2 rather than from Table III.4. As mentioned initially, the values in the burnup calculations appear too low. Comparing d1 and d5 shows the impact of a change to the higher $(1 + \alpha)^i$ values suggested in Table III.4. Here the conversion ratio is reduced from 0.557 to 0.483, corresponding to a 14.3% higher U235 demand d_D^{U5}. The Pu^{fiss} discharged is reduced by 35.2%. These differences illustrate the great influence of the $(1 + \alpha)^i$ values.

The results of cases d6 to d9 are shown as functions of fuel burnup in Figures III.B.7 and III.B.8. The curves of η_D^I, CR_D, and F^i/F^I are subject to arguments similar to those for fissile fuel cycle C. Despite the decreasing η_D^I values with decreasing burnup, CR_D increases due to the smaller parasitic losses P. The isotopic equilibrium concentration of Pu239 and Pu241 is attained at much lower burnups than with the corresponding U233 equilibrium concentration in fissile fuel cycle C (compare Figures III.B.7 and III.B.5).

The U235 requirement in Figure III.B.8 increases only very slightly with reduced fuel burnup, compared to cycle C. Due to the somewhat higher output of fissile plutonium, a smaller net fissile fuel demand d_D is obtained with decreasing fuel burnup.

Table III.B.4. Conversion ratio CR_D, U235 requirement d_D^{U5}, discharged Pu^{fiss} a_D^{Pu}, and other parameters of HTR fissile fuel cycle D, as a function of fuel burnup and reactor size (for 3- and 1-GW(th) units).

Case	Burnup (GWd/t)	P 3GW(th)	P 1GW(th)	Reference*	CR_D	η_D^I	$(1+\alpha)_D^I$	$\frac{F^{Pu9}}{F^I}$	$\frac{F^{Pu41}}{F^I}$	$\frac{F_m^{U5}}{F^I}$	d_D^{U5} (g/GWd)	a_D^{Pu} (g/GWd)
Burnup ≃ 100												
d1	100	.1867		D-1*	.557	1.919	1.386	.3758	.1044	.5148	736	94
d2**		.1867		analyt.	.552	1.908	1.393	.3758	.1047	.5144	735	80
d3	108		.2314	D-2*	.490	1.942	1.360	.3368	.1010	.558	782	57.8
d4**			.2314	analyt.	.485	1.932	1.365	.3340	.1003	.560	786	48.4
Burnup ≃ 100												
d1	101	.1867		D-1*	.557	1.919	1.386	.3758	.1044	.5148	736	94
d5†		.1867		analyt.	.483	1.824	1.439	.3178	.0885	.5886	841	61
Burnup ≃ 100												
d6††		.19		analyt.	.477	1.824	1.438	.3136	.0885	.593	848	59
Burnup ≃ 50												
d7††		.14		analyt.	.564	1.819	1.448	.3611	.0674	.5665	810	148
Burnup ≃ 20-30												
d8††	~30	.11		analyt.	.615	1.814	1.451	.3809	.0513	.5662	804	218
d9††	~20	.09		analyt.	.646	1.808	1.448	.3706	.0342	.590	843	305

*D-1, D-2 are exact burnup calculations (Table III.2); all others result from analytical calculations performed.
**Cases d2, d4 assume the $(1+\alpha)^i$ values from the exact burnup calculations (see Table III.5).
†Comparison (d1,d5) shows the change of Pu $(1+\alpha)^i$ values from Table III.5 to Table III.4.
††For cases d6 to d9, the $(1+\alpha)^i$ values in Table III.4 were used.

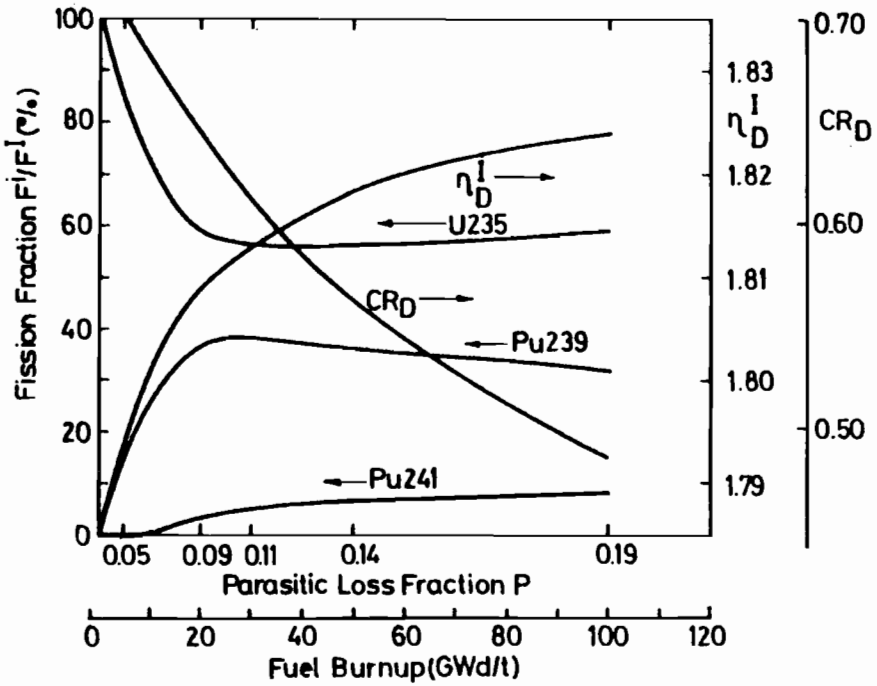

Figure III.B.7.

Fission fractions, eta, and conversion ratio for HTR fissile fuel cycle D as a function of fuel burnup (for 3-GW(th) units).

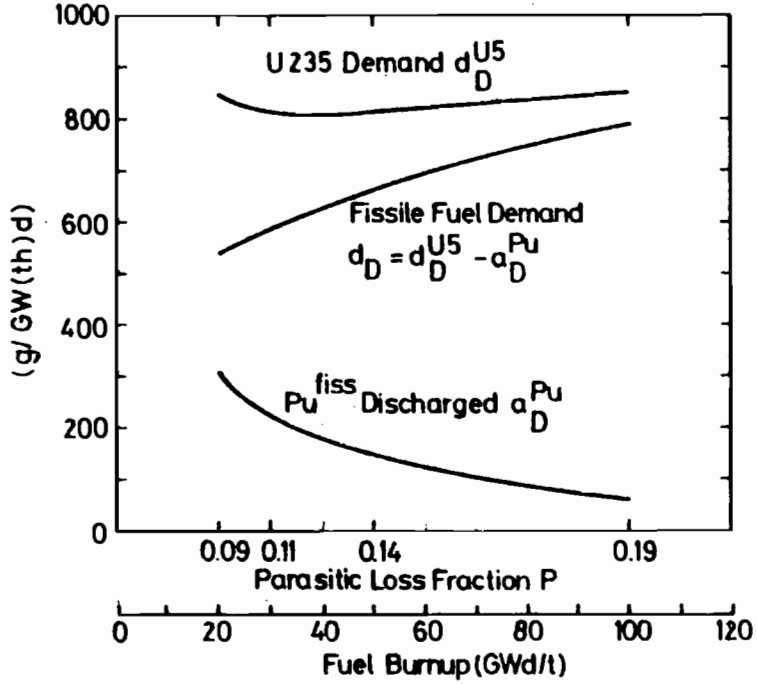

Figure III.B.8.

U235 makeup, Pu^{fiss} discharged, and fissile fuel demand for HTR fissile fuel cycle D as a function of fuel burnup (for 3-GW(th) units).

Table III.B.5. Conversion ratio CR_E, U235 requirement d_E^{U5}, discharged Pu^{fiss} a_E^{Pu}, and other parameters of HTR fissile fuel cycle E as a function of fuel burnup (for 3-GW(th) units).

Case	Burnup (GWd/t)	P / 3GW(th)	Reference*	CR_E	η_E^I	$(1+\alpha)_E^I$	$\frac{F^{Pu9}}{F^I}$	$\frac{F^{Pu41}}{F^I}$	$\frac{F_m^{U5}}{F^I}$	d_E^{U5} (g/GWd)	a_E^{Pu}
Burnup ≃ 100											
e1**		.19	analyt.	.490	1.839	1.443	.3274	.1369	.530	758	15
Burnup ≃ 50											
e2**		.14	analyt.	.590	1.849	1.458	.3878	.1622	.4450	637	9
Burnup ≃ 20-30											
e3**	~30	.11	analyt.	.650	1.854	1.467	.4231	.1770	.395	565	26
e4**	~20	.09	analyt.	.691	1.858	1.473	.4467	.1869	.361	517	39

*No burnup calculations were available for fissile fuel cycle E; all cases are results of the analytical calculations performed here.
**Table III.4 gives the $(1+\alpha)^i$ values assumed.

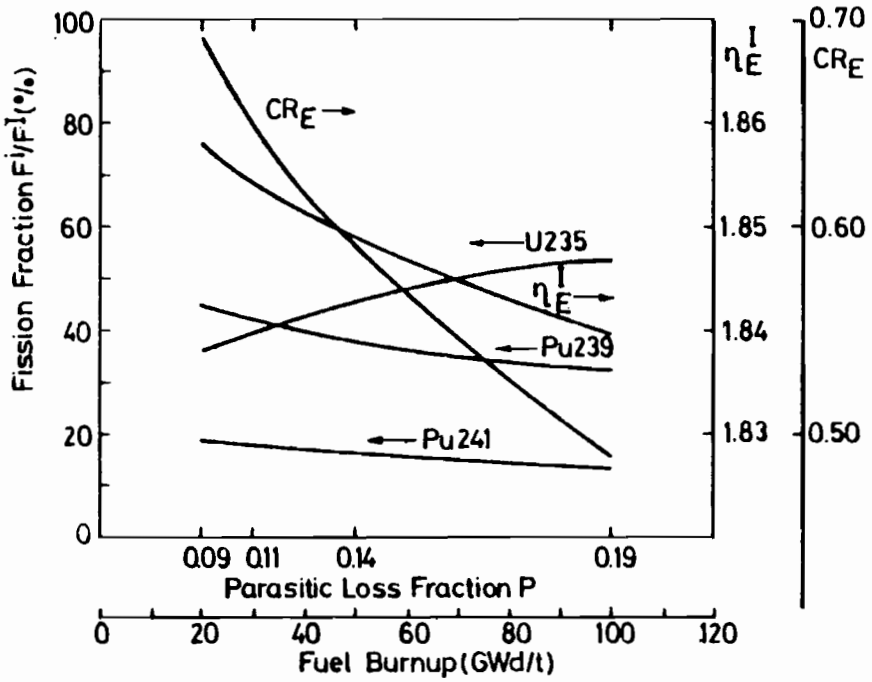

Figure III.B.9.

Fission fractions, eta, and conversion ratio for HTR fissile fuel cycle E as a function of fuel burnup (for 3-GW(th) units).

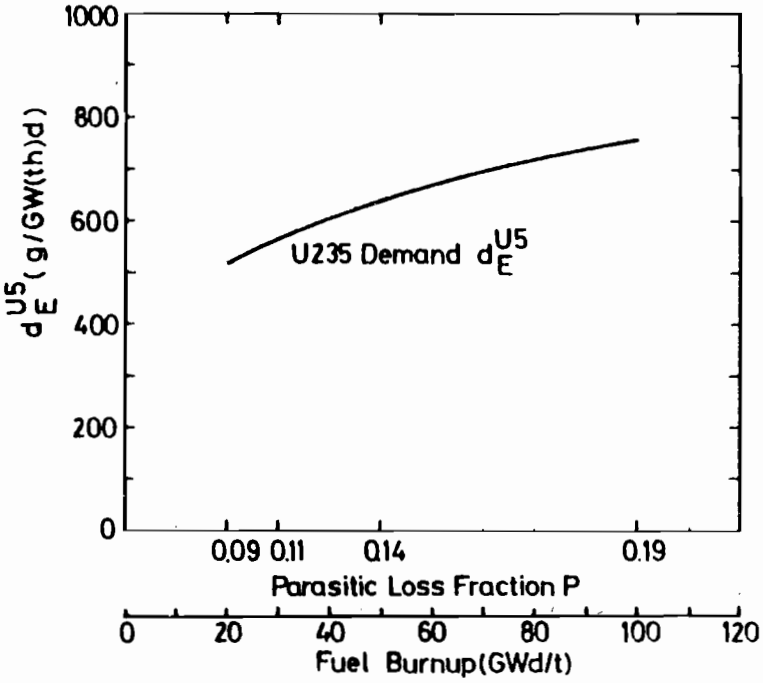

Figure III.B.10.

U235 makeup d_E^{U5} for HTR fissile fuel cycle E as a function of fuel burnup (for 3-GW(th) units).

III.B.2.b. Fissile Fuel Cycle E

In the *recycling* uranium cycle

-- the self-bred Pu239/Pu241 is recycled, and
-- the fissile fuel supplied is U235.

In cycle E, the Pu fissile isotopes are in equilibrium concentration, and thus $\gamma_E = 1.0$. No exact burnup calculations are available for this fissile fuel cycle, and the results indicated in Table III.B.5 have been obtained by using the $(1 + \alpha)^i$ values suggested in Table III.4.

The results of the analytical calculations are illustrated in Figures III.B.9 and III.B.10. In contrast to fissile fuel cycle D, η_E^I in fissile fuel cycle E increases with decreasing fuel burnup. This is partly due to the increasing Pu241 fission fraction, which increases up to 0.20 on account of the high value of $\eta^{Pu241} = 2.106$. Apart from that, the curves of CR_E, η_E^I, and the fissile fission fractions are governed by arguments similar to those that apply to fissile fuel cycle B.

As is the case in all the other fissile fuel cycles, conversion ratio CR_E increases with reduced fuel burnup. This is expressed by a lower U235 demand d_E^{U5} (see Figure III.B.10).

III.B.2.c. Fissile Fuel Cycle F

In this *recycling* uranium cycle

-- the self-bred Pu239/Pu241 is recycled, and
-- the fissile fuel supplied is Pu239, coming from an external source, e.g. FBR.

In this fissile fuel cycle, the fissile inventory consists only of Pu239 and Pu241. This isotopic composition is in equilibrium, so that the equilibrium fission fraction distribution of Pu239 and Pu241 is given by Equations (III.A-13) and (III.A-14), respectively. The distribution is 0.705 for Pu239 and 0.295 for Pu241 (Table III.B.6), assuming the $(1 + \alpha)^i$ values listed in Table III.4. This compares to 0.912 for U233 and 0.088 for U235 in the corresponding fissile fuel cycle A.

Since the fission fraction distribution remains constant as a function of the burnup in fissile fuel cycle F, η_F^I also remains constant (see Figure III.B.11). The increasing conversion ratio CR_F is consequently only due to the reduced parasitic losses P. The corresponding fissile Pu demand $d_F^{Pu^{fiss}}$ is plotted in Figure III.B.12 for a 3-GW(th) HTR unit. This Pu^{fiss} demand is seen to be significantly larger than the U233 demand d_A^{U3} in fissile fuel cycle A (Figure III.B.2).

Table III.B.6. Conversion ratio CR_F, Pu^{fiss} demand d_F^{Pu}, and other parameters of HTR fissile fuel cycle F as a function of fuel burnup (for 3-GW(th) units).

Case	Burnup (GWd/t)	$\frac{P}{3GW(th)}$	Reference*	CR_F	η_F^I	$(1+\alpha)_F^I$	$\frac{F^{Pu9}}{F^I}$	$\frac{F^{Pu41}}{F^I}$	d_F^{Pu} (g/GWd)
Burnup ≃ 100									
f1**	100	.19	analyt.	.535	1.896	1.537	.705	.295	750
Burnup ≃ 50									
f2**	50	.14	analyt.	.630	1.896	1.537	.705	.295	597
Burnup ≃ 20-30									
f3**	30	.11	analyt.	.687	1.896	1.537	.705	.295	505
f4**	20	.09	analyt.	.725	1.896	1.537	.705	.295	404

*No burnup calculations were available for fissile fuel cycle F; all cases are results of the analytical calculations performed here.
**Table III.4 gives the $(1+\alpha)^i$ values assumed.

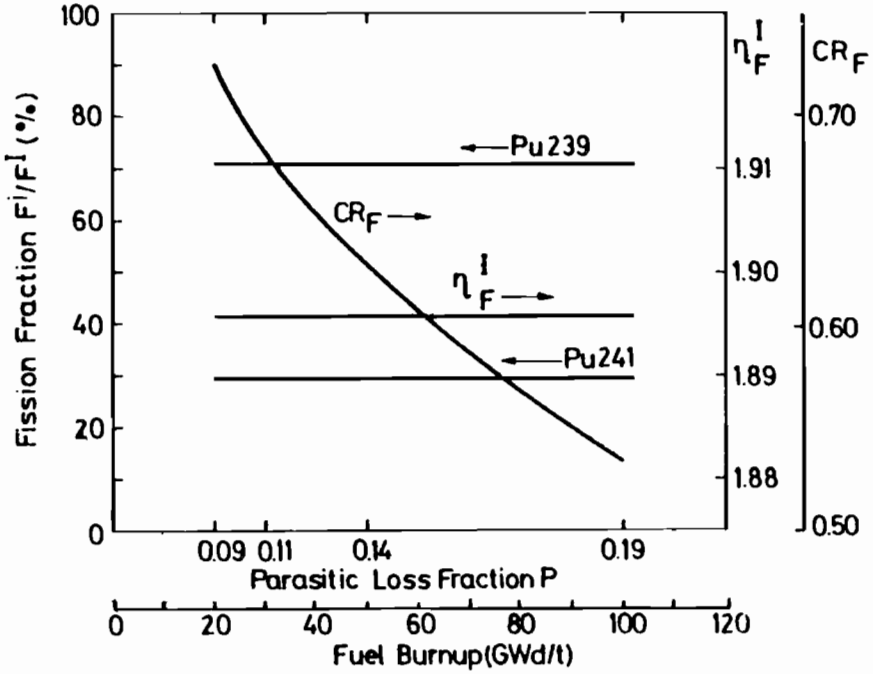

Figure III.B.11.

Fission fractions, eta, and conversion ratio for HTR fissile fuel cycle F as a function of fuel burnup (for 3-GW(th) units).

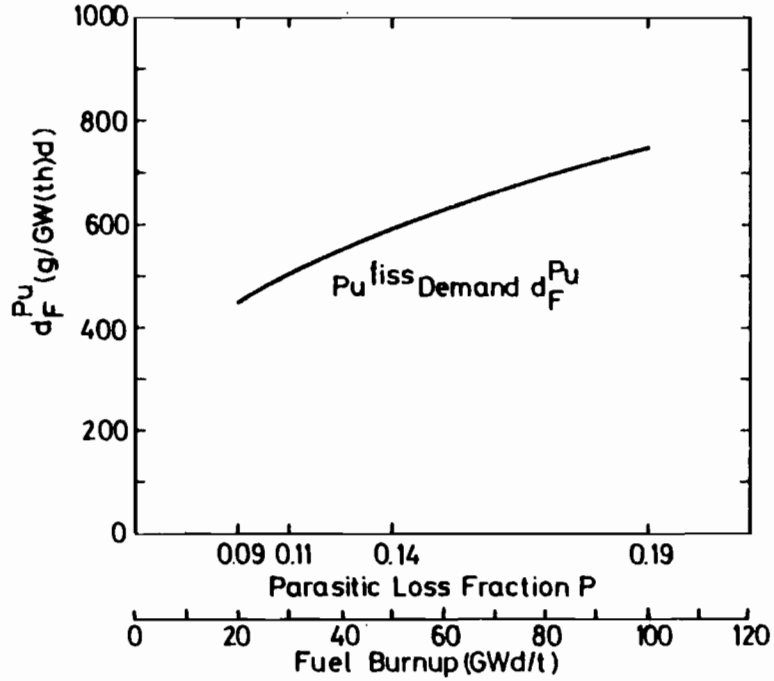

Figure III.B.12.

Fissile plutonium makeup d_F^{Pu} for HTR fissile fuel cycle F as a function of fuel burnup (for 3-GW(th) units).

APPENDIX IV.A. SELF-SUPPLY OF FBRs IN THE STEADY-STATE FBR/HTR SYSTEM

The condition

$$\frac{Pu^{fiss}\ produced}{Pu^{fiss}\ consumed} = 1.0 = KR^{Pu^{fiss}} \qquad (IV.\ -1)$$

for the core and the axial blanket is synonymous with the statement that the breeding gain of the two regions *after* losses

$$g_m = g_{c,ax} = 0 \quad , \qquad (IV.A-2)$$

where $g_{c,ax}$ refers to the breeding gain of the core and axial blanket regions *after* losses. In accordance with Equation (I-35), therefore,

$$g_{c,ax} = g_{c,ax}(1 - V^F)W_N^F - \sum_n^{c,ax} \frac{I_n V^F}{T_n} = 0 \quad . \qquad (IV.A-3)$$

$BR_{c,ax}$, the breeding ratio of the core and axial blanket regions, which is necessary to meet condition (IV.A-1), is obtained by

substitution of Equation (I.B-17) into Equation (IV.A-3), and by solving the latter for $BR_{c,ax}$:

$$BR_{c,ax} = \frac{\left[\frac{V^F}{(1 - V^F) W_N^F} \sum_n^{c,ax} \frac{I_n V^F}{T_n} + \sum_n^{c,ax} (1 - \varepsilon_n) \delta_n (1 + \alpha) I_n\right]}{(1 - \varepsilon_N)(1 + \alpha) I_N} . \quad \text{(IV.A-4)}$$

APPENDIX IV.B. GROWTH RATE OF THE EXPANDING FBR/HTR SYSTEM

The thermal power $P_S(t)$ of an FBR/HTR system is given as

$$P_S(t) = P_F(t) + P_H(t) \quad . \tag{IV.B-1}$$

The growth rate α_S of the system is determined such that

$$P_S(t) = P_S^o \, e^{\alpha t} \quad . \tag{IV.B-2}$$

If the ratio $\frac{P_H(t)}{P_F(t)}$ is assumed to remain constant, i.e.

$$\frac{P_H(t)}{P_F(t)} = \text{constant} = \frac{P_H^o}{P_F^o} \quad , \tag{IV.B-3}$$

then it can be shown that

$$\alpha_S = \frac{1}{P_S} \frac{dP_S}{dt} = \frac{1}{P_F} \frac{dP_F}{dt} = \frac{1}{P_H} \frac{dP_H}{dt} \quad . \tag{IV.B-4}$$

If the breeding gain g_N is divided into

$$g_N = g^{U3} + g^{Pu} \quad , \tag{IV.B-5}$$

the following set of differential equations apply:

$$\text{FBR:} \quad I_Z^F \frac{dP_F}{dt} = g^{Pu} P_F L_F \quad ; \tag{IV.B-6}$$

$$\text{HTR:} \quad I_Z^H \frac{dP_H}{dt} + d_A P_H L_H = g^{U3} P_F L_F \quad ; \tag{IV.B-7}$$

L_F and L_H are load factors, and I_Z^F and I_Z^H the fuel cycle fissile inventories. Using (IV.B-4), Equations (IV.B-6) and (IV.B-7) can be rewritten as

$$\frac{1}{P_F} \frac{dP_F}{dt} = \frac{g^{Pu} L_F}{I_Z^F} = \alpha_S \tag{IV.B-8}$$

and

$$\alpha_S + \frac{d L_H}{I_Z^H} = \frac{g^{U^3} L_F}{I_Z^H} \frac{P_F(t)}{P_H(t)} \tag{IV.B-9}$$

According to (IV.B-8), $g^{Pu} = \frac{\alpha_S I_Z^F}{L_F}$. If this term is introduced in Equation (IV.B-5), solved for g^{U^3}, and used as a substitute in (IV.B-9), one obtains for the FBR/HTR system growth rate

$$\alpha_S = \frac{\left[g_N^V L_F \frac{P_F^o}{P_H^o} - d_A^V L_H \right]}{\left[I_Z^H + I_Z^F \frac{P_F^o}{P_H^o} \right]} , \qquad \text{(IV.B-10)}$$

where g_N^V and d_A^V, which include the losses in the excore fuel cycle, are given by Equations (I-33) and (I-37). The separation of g_N into g^{U3} ang g^{Pu} can be determined from Equations (IV.B-6) and (IV.B-7).

APPENDIX V.A. THE LWR/FBR FISSILE FUEL BALANCE IN THE TRANSITION PHASE

A specified nuclear electricity demand forecast $P_{ne}(t)$ is assumed initially (cf. Figure V.1). From the time of FBR introduction, t_F, the following relation must be satisfied:

$$P_{ne}(t) = P_L(t) + P_F(t) \quad . \qquad \text{(V.A-1)}$$

The distribution between $P_L(t)$ and $P_F(t)$ is here assumed to be determined by the availability of plutonium, i.e. LWR Pu production a_L and FBR breeding gain g_N^{Pu} supply the first core inventories for additional FBRs to be constructed, such that

$$I_Z^F \frac{dP_F}{dt} = a_L P_L(t) + g_N^{Pu} P_F(t) \quad . \qquad \text{(V.A-2)}$$

$P_L(t)$ is to be determined for this inhomogeneous differential equation system. By differentiation of Equation (V.A-1) with respect to t and substitution in Equation (V.A-2), this equation can be written as

$$\frac{dP_L}{dt} + \left(\frac{a_L - g^{Pu}}{I_Z^F}\right) P_L(t) = \frac{dP_{ne}}{dt} - \frac{g^{Pu}}{I_Z^F} P_{ne}(t) \quad . \text{(V.A-3)}$$

By using the method of variable coefficients, one obtains the solution

$$P_L(t) = P_{ne}(t) - \frac{a}{I} e^{-(\frac{a-g}{I})} \int P_{ne}(t)\, e^{(\frac{a-g}{I})t} dt + S_o e^{-(\frac{a-g}{I})t} \quad \text{(V.A-4)}$$

for t after FBR introduction, i.e. $t > t_F$. If the specified forecast $P_{ne}(t)$ can be approximated by a linear function, such that

$$P_{ne}(t) = \omega t \quad , \qquad \text{(V.A-5)}$$

then the solution of Equation (V.A-4) can be found to be

$$P_L(t) = P_{ne}^o + \left(\frac{g}{g-a}\right)\omega t - \left(\frac{g}{g-a}\right)\left(\frac{\omega I}{g-a} + P_{ne}^o\right)\left[e^{\frac{g-a}{I} t} - 1\right] \quad \text{(V.A-6)}$$

where P_{ne}^o is the LWR power capacity at the time of FBR introduction, i.e. $P_L(t_F)$. Equation (V.A-6) thus describes the LWR power capacity as a function of the time after FBR introduction.

The time t_L^m at which $P_L(t)$ attains its maximum, $P_L(t_L^m)$, can be obtained by differentiation of Equation (V.A-6). As a first approximation for $t_L^m - t_F \leq 20$ years it can be shown that

$$t_L^m - t_F = \frac{\left[I_Z^F \omega - a_L P_L(t_F)\right]}{\left[a_L \omega + \left(\frac{g_N^{Pu} - a_L}{I_Z^F}\right) a_L P_L(t_F)\right]} \quad . \qquad \text{(V.A-7)}$$

Here it has been assumed firstly that the plutonium generated in the LWRs is recycled in the LWRs themselves during Phase I (Figure V.1), and thus is not available for FBRs;[1] secondly, that the time-dependent decrease in LWR power in Phase III is given only by the Pu fissile fuel balance between FBRs and LWRs. (LWR plant life is not taken into consideration in this analytical description.)

The power integral $\int_0^{t_F} P_L(t)dt$ in Equation (V-1)

is determined by the given demand curve $P_{ne}(t)$ up to the point in time t_F of FBR introduction. The LWR power integral $\int_{t_F}^{t_L^m} P_L(t)dt$ of Phase II can, however, be considerably influenced by $P_L(t)$, which in itself depends on the FBR deployment described by Equation (V.A-2). For example, the total integral has its minimum (exhibiting the minimum ore requirement) when, after t_F, no more LWRs are added, and from then on $P_L(t)$ is determined solely by the LWR plant life. This ideal case is marked as $P_L'(t)$ in Figure V.1. A further addition of LWRs after t_F must be expected, however, which depends, among other things, on the FBR construction rate. If this is the case, $P_L(t)$ in Phase II is directly linked to the FBR construction rate.

The following can be said about the time-dependent LWR power curve during the FBR introduction phase: every LWR newly constructed in Phase II (be it because of Pu shortage or due to an FBR construction capacity constraint) will, for economic reasons, have to be operated throughout one plant life of approximately 25-30 years. That is to say, the time-dependent decrease in LWR

---

[1] This assumption is realistic for two reasons: firstly, for reasons of proper plutonium technology management, the technological know-how must be collected prior to the use of breeders. This implies Pu-recycling in the LWR. Secondly, it is easy to show numerically that the plutonium accumulated in Phase I could cover the breeder addition for at most two or three years after t_F ($\sim$20 years), and therefore does not contribute significantly to the overall plutonium aggregation.

power capacity is influenced not only by the fissile fuel balance between FBRs and LWRs as in Equation (V.A-3), but also by the LWR plant life. If the LWR capacity decline in Phase III is due to the LWR plant life, then an excess of Pu can be expected. Accordingly, with regard to a low LWR power integral, the further addition of LWRs after t_F should be as small as possible in order to prevent such an LWR generated Pu surplus at a later time. High values for $t_L^m - t_F$ generally imply a higher LWR power integral, which again has direct effects on the uranium ore requirements of the LWRs. For this reason, $t_L^m - t_F$ should be kept as small as possible as was discussed in more detail in Section V.3.c.